ANALYTICA CHIMICA ACTA

International monthly devoted to all branches of analytical chemistry
Revue mensuelle internationale consacrée à tous les domaines de la chimie analytique
Internationale Monatsschrift für alle Gebiete der analytischen Chemie

ELSEVIER SCIENTIFIC PUBLISHING COMPANY

AMSTERDAM

Anal. Chim. Acta, Vol. 65, No. 1, 1–252, June 1973

Published monthly

Publication Schedule for 1973

Vol. 63, No. 1	January 1973	
Vol. 63, No. 2	February 1973	**(completing Vol. 63)**
Vol. 64, No. 1	March 1973	
Vol. 64, No. 2	April 1973	
Vol. 64, No. 3	May 1973	**(completing Vol. 64)**
Vol. 65, No. 1	June 1973	
Vol. 65, No. 2	July 1973	**(completing Vol. 65)**
Vol. 66, No. 1	August 1973	
Vol. 66, No. 2	September 1973	
Vol. 66, No. 3	October 1973	**(completing Vol. 66)**
Vol. 67, No. 1	November 1973	
Vol. 67, No. 2	December 1973	**(completing Vol. 67)**

Subscription price: Dfl. 410.00 plus Dfl. 30.00 postage. Subscribers in the U.S.A. and Canada receive their copies by airmail. Additional charges for airmail to other countries are available on request. For advertising rates apply to the publishers.

GENERAL INFORMATION

Languages

Papers will be published in English, French or German.

Submission of papers

Papers should be sent to:

PROF. PHILIP W. WEST,
Coates Chemical Laboratories,
College of Chemistry and Physics,
Louisiana State University,
Baton Rouge 3,
La. 70803 (U.S.A.)

or to:

DR. A. M. G. MACDONALD,
Department of Chemistry,
The University,
P.O. Box 363
Birmingham B15 2TT (Great Britain)

Reprints

Fifty reprints will be supplied free of charge. Additional reprints (minimum 100) can be ordered at quoted prices. They must be ordered on order forms which are sent together with the proofs.

PRINTED IN THE NETHERLANDS

ANALYTICA CHIMICA ACTA
Vol. 65 (1973)

ANALYTICA CHIMICA ACTA

International monthly devoted to all branches of analytical chemistry
Revue mensuelle internationale consacrée à tous les domaines de la chimie analytique
Internationale Monatsschrift für alle Gebiete der analytischen Chemie

ELSEVIER SCIENTIFIC PUBLISHING COMPANY
AMSTERDAM

Anal. Chim. Acta, Vol. 65 (1973)

PRINTED IN THE NETHERLANDS

Analytica Chimica Acta, 65 (1973) 1–17

SYSTEMATIC ERRORS IN 14-MeV NEUTRON ACTIVATION ANALYSIS FOR OXYGEN

PART II*. A GENERAL STANDARDIZATION METHOD FOR THE DETERMINATION OF OXYGEN

C. VANDECASTEELE**, R. VAN GRIEKEN***, R. GIJBELS**** and A. SPEECKE
Institute for Nuclear Sciences, Ghent University, Ghent (Belgium)
(Received 20th November 1972)

Several authors have described standardization methods for the determination of oxygen in steel[1–3], aluminium[4], organic and inorganic compounds[5,6] by 14-MeV neutron activation analysis. They all considered systematic errors introduced by the neutron and γ-ray attenuation differences in the sample and the standard. The present work extends the standardization method described by Gijbels *et al.*[1–3] to solid samples of any composition.

GENERAL PRINCIPLES

The equipment and experimental set-up of the complete analytical system have been described in detail elsewhere[3,7]. Cylindrical samples (9 mm thick, 26 mm diam.) and oxygen standards are pneumatically conveyed to the Sames Jγ neutron generator through a pair of rectangular aluminium transfer tubes (internal section 9.5 mm × 26.5 mm). At the irradiation station, the sample and oxygen standard are irradiated simultaneously behind each other as is schematically represented in Fig. 1. The oxygen standard consists of a mixture of Fe_2O_3 graphite (containing 412 mg of oxygen), compressed into a steel capsule with the same external dimensions as the samples (see Fig. 1) and with internal dimensions 7 mm thick and 22 mm diameter.

In order to correct for the neutron flux gradient (the sample in position 1 will receive a neutron dose approximately 3 times higher than the standard in position 2), one can irradiate two identical oxygen standards and determine the ratio K of the ^{16}N activities (from $^{16}O(n,p)^{16}N$). K includes the possible differences in counting geometry for the two standards and in the single channel setting for the two detection systems with which the simultaneous countings are performed. For an actual analysis, however, the determination of K is not sufficient for the following reasons: (*a*) during the determination of K, the standard in position 2 is shielded from the target by a different material than during the actual analysis; (*b*) in position 1, the sample (during the analysis) and standard (during the

* Part I: *Anal. Chim. Acta*, 64 (1973) 187.
** Aspirant of the N.F.W.O.
*** Research associate of the N.F.W.O.
**** Research associate of the I.I.K.W.

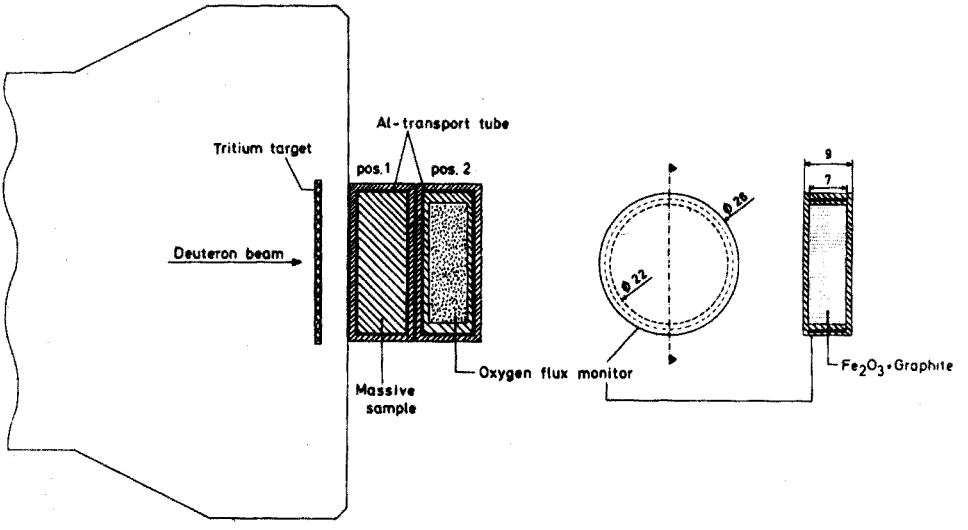

Fig. 1. Geometry for irradiation.

determination of K) have different neutron and γ-ray attenuations; and (c) since the sample is irradiated without a container and the oxygen standard in a cylindrical box, there is an additional difference in irradiation and counting geometry, which is not reflected in K.

It can be shown[1] that the weight of oxygen in the sample can be calculated from:

$$w_x = \frac{w_s}{K} \frac{A_x(1)}{A_s(2)} \cdot \frac{[\bar{\phi}_1]}{\bar{\phi}_1} \cdot \frac{S_x}{S_s} \cdot \frac{C_s}{C_x} \cdot \frac{D_s}{D_x} \tag{1}$$

where w_x = weight of oxygen in the sample;
w_s = weight of oxygen in the standard;
K = measured ^{16}N activity ratio for two identical oxygen standards;
$A_x(1)$ = measured ^{16}N activity of the sample, irradiated in position 1;
$A_s(2)$ = measured ^{16}N activity of the oxygen standard irradiated simultaneously in position 2;
$\bar{\phi}_1$ = the average 14-MeV neutron flux in the (void) space, occupied by a cylinder of 9 mm thickness and 26 mm diameter when irradiated in position 1;
$[\bar{\phi}_1]$ = the average 14-MeV neutron flux in the (void) space, occupied by the contents of the capsule (*i.e.* inner thickness 7 mm, inner diameter 22 mm), again in position 1;
S_x = "screening factor" which corrects for the screening of the standard in position 2 by the sample in position 1, during the irradiation;
S_s = "screening factor", with an oxygen standard in position 1;
C_x = "transmission factor" which takes into account the attenuation of the neutrons in the sample during activation and of the γ-rays during the counting (with respect to a 7.5 cm × 7.5 cm NaI(Tl) crystal, coupled to a single-channel analyser selecting the 4.5–6.5 MeV energy range);
C_s = "transmission factor" for the standard.

If no β-rays are detected because of appropriate shielding (*e.g.* 2 mm of copper), C_s/C_x can be considered as being the product of $(C_s/C_x)_n$ and $(C_s/C_x)_\gamma$, where $(C_s/C_x)_n$ and $(C_s/C_x)_\gamma$ take into account, respectively, the different neutron and γ-ray attenuations in sample and standard:

$$C_s/C_x = (C_s/C_x)_n \cdot (C_s/C_x)_\gamma \tag{2}$$

D_s/D_x = ratio of detection efficiency for ^{16}N γ-rays from standard and sample, when counted in position 1. This ratio, which was not taken into account in refs. 1–3, will be slightly different from unity, since the ^{16}N activity has a different spatial distribution in standard and sample, and was not taken into account in ref. 1.

Instead of the sample *versus* standard comparator method, many authors have hitherto preferred to use a boron trifluoride long counter for flux monitoring purposes. In this case eqn. (1) must be transformed into:

$$w_x = \frac{w_s}{K_{BF_3}} \cdot \frac{A_x(1)}{A_{BF_3}} \cdot \frac{[\bar{\phi}_1]}{\bar{\phi}_1} \cdot \frac{I_x}{I_s} \cdot \frac{C_s}{C_x} \cdot \frac{D_s}{D_x} \tag{3}$$

where K_{BF_3} = ratio of recorded ^{16}N activity in the oxygen standard (position 1) to the number of BF_3 counts recorded during the irradiation of this standard;

A_{BF_3} = number of counts recorded with the BF_3-counter during the irradiation of the sample;

I_x/I_s = ratio of the number of BF_3 counts with the sample in position 1 to that with the standard in position 1.

In this work the BF_3-counter was placed in a low geometry, about 4 m from the target.

$[\bar{\phi}_1]/\bar{\phi}_1$—GEOMETRY EFFECT AT THE IRRADIATION SITE

Experimental determination

$[\bar{\phi}_1]/\bar{\phi}_1$ has already been determined by Gijbels *et al.*[1–3] for an 18-mm target. However, in view of the more favorable irradiation conditions[8], a 30-mm diameter target is preferable. Therefore, this factor has been redetermined and the influence of the target diameter studied.

The flux factor $[\bar{\phi}_1]/\bar{\phi}_1$ takes two different effects into account:

(*a*) decrease in diameter: as a consequence of the important lateral flux gradients near the target axis, a decrease in the diameter from 26 to 22 mm results in an increased average neutron density and thus higher specific activity in the standard;

(*b*) decrease in thickness: as the axial flux gradients are convex, a decrease in thickness of 9 mm to 7 mm together with an increase in sample to target distance of 1 mm will result in a lower average neutron density.

The average flux density in samples of 26 or 22 mm diameter and 9 or 7 mm thickness can be calculated from the experimental flux distributions determined by Van Grieken *et al.*[9]. The neutron density in the considered volumes is obtained by integrating the flux distributions[9] for the planes close to the accelerator cap over a width of 26 or 22 mm. For a 30-mm target the results of this integration are given in Fig. 2.

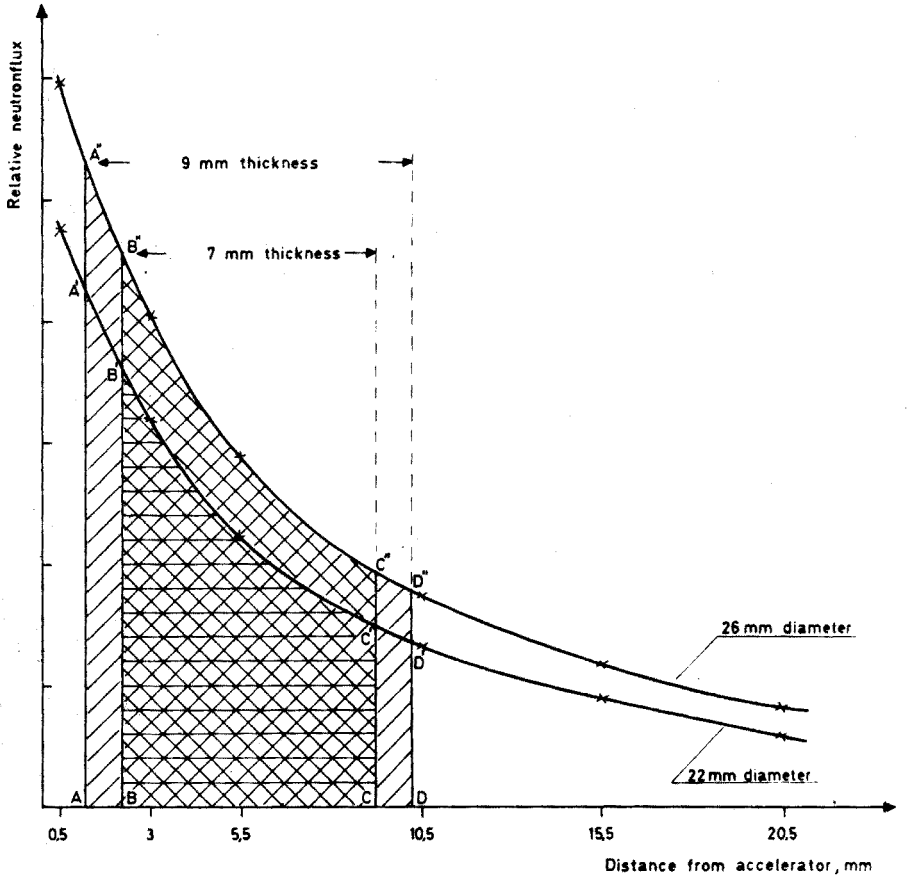

Fig. 2. Integrated axial flux course (30-mm tritium target).

TABLE I

RATIO OF AVERAGE FLUX IN SAMPLE AND STANDARD IN IRRADIATION POSITION 1

Target diameter (mm)	*Decrease in thickness (thickness 9→7 mm; diameter = 26 mm)*	*Decrease in diameter (diameter 26→22 mm; thickness = 7 mm)*	$[\bar{\Phi}_1]/\bar{\Phi}_1$
30	0.971	1.065	1.034
20	0.971	1.083	1.052
10	0.970	1.127	1.093
18 (ref. 1)	0.974	1.070	1.042 ± 0.006

The average flux ratio for samples with a diameter of 26 mm and a thickness of 7 or 9 mm is found by dividing the ratio of the surfaces BB″C″C and AA″D″D by the ratio of the corresponding volumes (3.72 and 4.78 cm^3). For targets of 10, 20 and 30 mm in diameter, the results are listed in Table I, column 2. In a similar way one obtains the average flux ratio for samples 7 mm in thickness but

22 or 26 mm in diameter; it is found from the ratio of the surfaces BB′C′C and BB″C″C divided by the corresponding volumes (2.66 and 3.72 cm^3). The results are given in Table I, column 3. The total "box-effect" is listed in column 4 and is given by the product of the values in columns 2 and 3.

Obviously, $[\bar{\phi}_1]/\bar{\phi}_1$ increases by several percent when the target diameter decreases from 30 to 10 mm. This is mainly due to the radial effect.

The agreement with the earlier value[1-3] is not entirely satisfactory. This is probably due to the experimental approach of Gijbels *et al.*[1-3] who also took neutron attenuation into account and studied radial contraction for a sample 9 mm in thickness.

Theoretical calculation

If the target is larger than the sample, the average flux density in sample and standard capsule can be calculated as follows (see Fig. 3)

$$\bar{\phi} = \frac{2\pi\omega}{\pi R_2^2 t}\int_0^t \mathrm{d}z \int_0^{R_2} r\,\mathrm{d}r \int_0^{2\pi} \mathrm{d}\phi \int_0^{\rho_{max}} \frac{\rho\,\mathrm{d}\rho}{\rho^2+(b+z)^2}$$

$$= \frac{2\omega}{R_2^2 t}\int_0^t \mathrm{d}z \int_0^{R_2} r\,\mathrm{d}r \int_0^{2\pi} \mathrm{d}\phi \{\tfrac{1}{2}\log[\rho_{max}^2+(b+z)^2] - \log(b+z)\}$$

$$\rho_{max} = r\cos\phi + (R_1^2 - r^2\sin^2\phi)^{\frac{1}{2}} \qquad (4)$$

where ω = the flux (n cm^{-2} s^{-1}) at the surface of the target: it is assumed that the target is radiating homogeneously;

R_1 = radius of the target (15 mm);

R_2 = radius of sample or standard capsule (13 or 11 mm);

t = thickness of sample or standard (9 or 7 mm);

b = distance from target to sample or standard (7.4 or 8.4 mm).

When the numerical integrations were calculated with a FORTRAN programmed PDP-9 computer, a correction factor $[\bar{\phi}_1]/\bar{\phi}_1 = 1.024$ was obtained. The difference between the calculated and experimental value (1.034) can probably be attributed[9] to neutron removal by the copper tritium support, the cooling

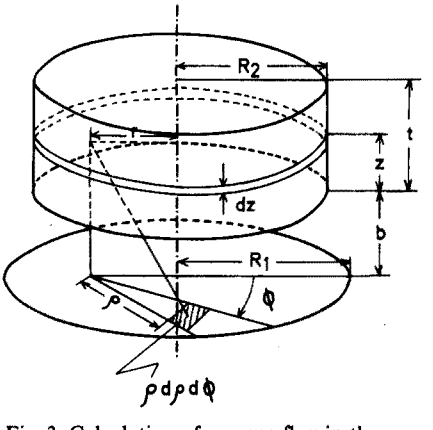

Fig. 3. Calculation of average flux in the sample.

water jacket and the aluminium accelerator cap. As pointed out by Van Grieken *et al.*[9], neutrons that activate the outside monitors on average leave the tritium target more obliquely, and hence the outer side of the flux curves will be relatively lower than theoretically expected, giving rise to sharper lateral flux gradients. This effect results in a greater experimental correction factor for decrease in diameter and hence in a greater total correction factor.

S_x/S_s—SCREENING OF THE FLUX MONITOR BY THE SAMPLE

An oxygen standard was irradiated in position 2, with different samples in position 1. Before and after each series of 4 different samples in position 1, the oxygen standard in position 2 was irradiated without a sample in position 1, by way of reference. This procedure allows the determination of the screening factors S_x for various materials. The results are given in Table II. The agreement with the value for iron given by Gijbels *et al.*[1–3] is very good and still improves when one considers the influence of the sample in position 1 on the BF_3-monitor used previously[1].

TABLE II

SCREENING FACTORS (S_x) AND CORRECTION FACTORS FOR SCREENING (S_x/S_s) FOR DIFFERENT SAMPLES

Sample	S_x	S_x/S_s
Al	0.944 ± 0.004^a	1.008 ± 0.006
Fe	0.894 ± 0.004^a	0.955 ± 0.006
Ni	0.869 ± 0.004^a	0.929 ± 0.006
Cu	0.877 ± 0.004^a	0.937 ± 0.006
Zr	0.932 ± 0.005^a	0.995 ± 0.007
Mo	0.908 ± 0.005^a	0.970 ± 0.007
Ag	0.904 ± 0.007^b	0.966 ± 0.009
Cd	0.932 ± 0.007^b	0.996 ± 0.009
Sn	0.942 ± 0.006^b	1.006 ± 0.008
Sb	0.937 ± 0.006^b	1.001 ± 0.008
Ta	0.880 ± 0.004^a	0.940 ± 0.006
W	0.869 ± 0.004^a	0.929 ± 0.006
Bi	0.927 ± 0.007^b	0.990 ± 0.009
Fe (ref. 1)		0.949 ± 0.006
Oxygen standard	$S_s = 0.936 \pm 0.004^a$	—

[a] Standard error of the mean of 25 determinations.
[b] Standard error of the mean of 10 determinations.

A detailed interpretation of neutron attenuation effects has been given in Part I.

I_x/I_s—INFLUENCE OF THE SAMPLE ON BF_3-MONITOR

Just as for the determination of S_x/S_s, different samples are irradiated in

TABLE III

I_x AND I_x/I_s FOR DIFFERENT SAMPLES

Sample	I_x	I_x/I_s
Al	1.004 ± 0.003^a	1.000 ± 0.004
Fe	1.013 ± 0.003^a	1.009 ± 0.004
Ni	1.006 ± 0.003^a	1.002 ± 0.004
Cu	1.018 ± 0.004^a	1.014 ± 0.005
Zr	1.013 ± 0.003^a	1.009 ± 0.004
Mo	1.026 ± 0.003^a	1.022 ± 0.004
Ag	1.036 ± 0.006^b	1.032 ± 0.007
Cd	1.020 ± 0.006^b	1.016 ± 0.007
Sn	1.017 ± 0.005^b	1.013 ± 0.006
Sb	1.018 ± 0.006^b	1.014 ± 0.007
Ta	1.032 ± 0.003^a	1.028 ± 0.004
W	1.039 ± 0.003^a	1.035 ± 0.004
Bi	1.015 ± 0.006^b	1.011 ± 0.007
Oxygen standard	$I_s = 1.004 \pm 0.003^a$	

[a] Standard error of the mean of 25 determinations.
[b] Standard error of the mean of 10 determinations.

position 1, while the flux during the irradiation is measured with a BF_3-counter. Before and after each series of 4 samples the flux is determined with no sample in position 1. Table III lists the ratio I_x of the measured flux with a sample in position 1 to that with no sample in this position. Obviously the presence of the sample increases the apparent neutron output measured with the BF_3-counter. This can be explained by inelastic scattering of the neutrons in the sample, whereby the latter acts as a nearly isotropic secondary neutron source. These secondary neutrons have energies much below 14 MeV, but are obviously detected by the BF_3 long counter. For high Z–high density materials, the macroscopic cross-section for inelastic scattering is such that this contribution is no longer negligible in a 9-mm thick sample, as appears from Table III. To the authors' knowledge, this effect has not been taken into account in previous work on 14-MeV neutron activation analysis.

$(C_s/C_x)_n$—NEUTRON ATTENUATION IN THE SAMPLE

If one considers a homogeneous, monodirectional neutron flux, the average flux $\bar{\phi}$ in a sample of thickness d does not equal the incident flux ϕ_0, as a consequence of neutron attenuation in the sample, but it is given by:

$$\bar{\phi} = \frac{\int_0^d \phi_0 \exp(-\Sigma x)\mathrm{d}x}{d} = \frac{\phi_0}{\Sigma d}[1 - \exp(-\Sigma d)] \tag{5}$$

where Σ = macroscopic cross-section for 14-MeV neutrons.

A thickness d_n, the "effective thickness for neutron attenuation" can be defined

where the local flux equals the average flux:

$$\bar{\phi} = \phi_0 \exp(-\Sigma d_n) = \frac{\phi_0}{\Sigma d}[1-\exp(-\Sigma d)] \tag{6}$$

or

$$d_n = \frac{1}{\Sigma} \log \frac{\Sigma d}{1-\exp(-\Sigma d)} \tag{7}$$

If $\Sigma d \ll 1$, eqn. (7) becomes

$$d_n = d/2 \tag{8}$$

Thus, for a homogeneous monodirectional neutron flux, the average flux in the sample equals the flux in the middle of the sample.

In 14-MeV neutron activation, homogeneous monodirectional fluxes do not occur, hence the average flux does not only include attenuation, but also—and especially—flux gradients. However, one can always define d_n by:

$$\exp(-\Sigma d_n) = \bar{\phi}/\bar{\phi}_0 \tag{9}$$

where $\bar{\phi}$ = average flux within the sample, including neutron attenuation;
$\bar{\phi}_0$ = average flux within the void volume to be occupied by the sample, thus without attenuation.

To approximate the definition of d_n in an experimental way one can consider a sample as being composed of 9 thin layers, each 1 mm thick, and change eqn. (9) into:

$$\exp(-\Sigma d_n) = \frac{\sum_{i=1}^{9} A_i}{\sum_{i=1}^{9} A_{0i}} \tag{10}$$

where A_i = induced activity in the ith layer of the sample;
A_{0_i} = induced activity in the same layer without neutron attenuation.

Experimental determination

A special aluminium sample holder was placed on the accelerator cap. In its center, behind 1.2 mm aluminium (representing the transfer tube), 9 discs (diameter = 26 mm, thickness = 1 mm) could be placed in a circular tube (diameter = 26 mm). When these discs were pressed together with a spring, the geometry was the same as in actual analyses. It was checked that the midpoint of the discs was on the axis of the neutron source by irradiating an iron disc, cutting it into 4 quadrants and counting the induced ^{56}Mn activity of each quadrant. Observed differences were less than 5%, implying that the deuteron beam was well centered.

If one irradiates the 9 discs that simulate a sample and counts them separately in the same geometry, the sum of the measured activities, after correction for decay and weight gives $\Sigma_{i=1}^{9} A_i$. If one now irradiates each disc separately in its normal position, with iron rings (int. diameter 24 mm, ext. diameter 26 mm, 1, 2, ... 7, 8 mm thick) as spacers, and one monitors the neutron output with a BF_3-counter, summation of the normalized activities corrected for decay and weight, yields

$\Sigma_{i=1}^{9} A_{0_i}$ after normalization to the same extrapolated activity at zero thickness as for the curve with attenuation. In order to investigate the independence of d_n on Σ, which can only be considered as an approximation, the value of d_n was determined for 3 different metals: Al, Fe and Cu by means of ^{27}Mg ($T_{\frac{1}{2}}$= 9.46 min; E_γ=0.84; 1.01 MeV), ^{56}Mn ($T_{\frac{1}{2}}$=2.58 h; E_γ=0.85; 1.81; 2.11 MeV) and ^{62}Cu($T_{\frac{1}{2}}$ = 9.72 min, β^+) activities, respectively. In the case of aluminium and copper, corrections were made for contributions from long-lived ^{24}Na ($T_{\frac{1}{2}}$ = 14.96 h; E_γ=1.37; 2.75 MeV) and ^{64}Cu ($T_{\frac{1}{2}}$=12.80 h; β^+). For the counting of the iron discs a cooling time of *ca.* 1 h was allowed, to ensure the decay of ^{53}Fe. Figure 4 gives the axial flux course as determined with copper discs with and without attenuation.

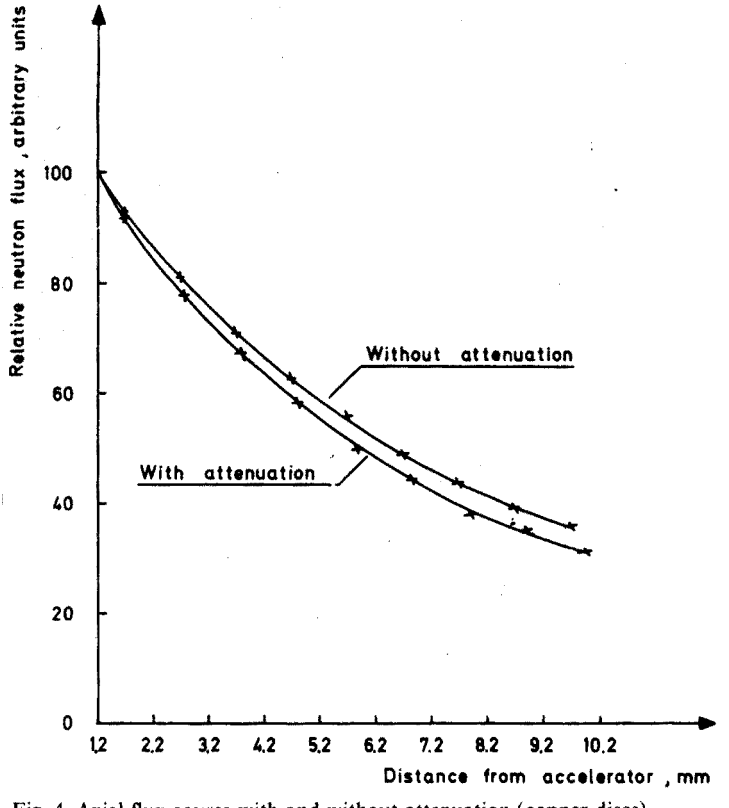

Fig. 4. Axial flux course with and without attenuation (copper discs).

For a 30-mm target, results are given in Table IV. Obviously the assumption that d_n is independent of Σ is valid within the precision of the actual determinations. The weighted average of d_n values is 0.41 ± 0.02.

The influence of different target diameters on d_n was studied. Results are given in Table V. Apparently the target or beam size does not critically influence the value of d_n.

TABLE IV

d_n (THE "EFFECTIVE THICKNESS FOR NEUTRON ATTENUATION") FOR DIFFERENT METALS WITH A 30-mm TARGET

Sample	$\Sigma(cm^{-1})$	$d_n(cm)$
Al	0.056	0.41 ± 0.03[a]
Fe	0.111	0.43 ± 0.03
Cu	0.129	0.40 ± 0.02

[a] Standard deviation from counting statistics.

TABLE V

d_n FOR IRON WITH DIFFERENT TARGET DIAMETERS

Target diameter (mm)	30	20	10
d_n (cm)	0.43	0.44	0.41

For any metal, $(C_x)_n$ can now be calculated directly from

$$(C)_n = \exp(-\Sigma d_n) \tag{11}$$

by means of the Σ-values given in Part I.

d_{n_s} was also determined for iron in a standard capsule. Seven iron discs (diameter = 22 mm, thickness = 1 mm) were irradiated in a similar box as that containing the standard mixture, and counted separately. This gave $\Sigma_{i=1}^{7} A_i$ after correction for decay and weight. $\Sigma_{i=1}^{7} A_{0_i}$ was obtained from integrated flux curves as given in Fig. 2. d_{n_s} was found to be 0.29 ± 0.02.

TABLE VI

CORRECTION FACTORS FOR NEUTRON AND γ-RAY ATTENUATION IN THE SAMPLE

Metal	$\Sigma\ (cm^{-1})$	$\mu\ (cm^{-1})$	$(C_s/C_x)_n$	$(C_s/C_x)_\gamma$	C_s/C_x	*Total correction factor (30 mm target)*
Al	0.056	0.071	0.993	0.985	0.978	1.013
Fe	0.111	0.239	1.016	1.042	1.059	1.039
Ni	0.138	0.285	1.027	1.058	1.086	1.037
Cu	0.129	0.276	1.023	1.055	1.079	1.039
Zr	0.069	0.220	0.997	1.036	1.033	1.056
Mo	0.095	0.351	1.009	1.081	1.091	1.088
Ag	0.099	0.371	1.011	1.088	1.099	1.091
Cd	0.069	0.309	0.998	1.065	1.062	1.087
Sn	0.058	0.234	0.994	1.040	1.034	1.069
Sb	0.064	0.241	0.996	1.043	1.039	1.069
Ta	0.125	0.691	1.021	1.209	1.234	1.192
W	0.138	0.809	1.027	1.258	1.292	1.234
Bi	0.075	0.429	1.001	1.109	1.110	1.129
Fe (ref. 1)					1.065 ± 0.005	

For the standard, one must also consider neutron attenuation by the front of the container (1 mm iron) (Fig. 1).

For the oxygen standard, $(C_s)_{n_s}$ can thus be calculated from:

$$(C_s)_n = \exp(-\Sigma_{Fe} \cdot 0.1) \cdot \exp(-\Sigma_s d_{n_s}) = 0.970 \tag{12}$$

where Σ_s = the macroscopic removal cross-section for the standard mixture, which can be calculated from

$$\Sigma_s = \frac{1}{V} \sum_{i=1}^{n} \frac{\sigma_i w_i N_A}{A_i} = 0.065 \tag{13}$$

where σ_i = microscopic cross-section for 14-MeV neutrons (cm^2) for the ith component; these values are tabulated by Nargolwalla *et al.*[6];

V = volume of the sample (cm^3);

w_i = weight of element i (g);

A_i = atomic mass of element i.

Correction factors $(C_s/C_x)_n$, calculated from the Σ-values given in Part I and from the experimental d_n and d_{n_s} values are given in Table VI, column 4.

Theoretical calculation

The number of nuclear reactions per second in the sample can be calculated from the following equation[10] (see Fig. 3):

$$N = 2\pi n\sigma\omega \int_0^t dz \int_0^{R_2} r\,dr \int_0^{2\pi} d\phi \int_0^{\rho_{max}} \frac{\rho \exp\left[\dfrac{-\Sigma z\{\rho^2+(b+z)^2\}^{\frac{1}{2}}}{b+z}\right] d\rho}{\rho^2+(b+z)^2} \tag{14}$$

If there were no attenuation, this would be:

$$N_0 = 2\pi n\sigma\omega \int_0^t dz \int_0^{R_2} r\,dr \int_0^{2\pi} d\phi \int_0^{\rho_{max}} \frac{\rho\,d\rho}{\rho^2+(b+z)^2} \tag{15}$$

where n = number of oxygen atoms per cm^3;

σ = cross-section for $^{16}O(n, p)^{16}N$ (cm^2).

N and N_0 values were obtained by numerical integration, after series expansion of the last integral, for Σ values ranging from 0.05 to 0.20 cm^{-1}. It was found that

$$N/N_0 = \exp(-\Sigma d_n) \tag{16}$$

with $d_n = 0.50$, independent of Σ.

The difference between calculated and experimental d_n values can be explained as follows:

(*a*) since the target diameter exceeds the sample diameter, some neutrons leaving the target edge do not enter through the front of the sample and hence travel a shorter path in the sample than is assumed in the calculations;

(*b*) the calculation procedure omits the radial variation of the detection efficiency at the counting.

$(C_s/C_x)_\gamma$—γ-RAY ATTENUATION IN THE SAMPLE

For γ-ray attenuation in the sample a similar reasoning holds as for neutron

attenuation. In the case of a homogeneous monodirectional γ-ray flux, a thickness d_γ exists in the sample so that, if all the activity were concentrated in that layer, as many γ-rays would leave the sample as with the real homogeneous activity distribution.

The average activity leaving the sample is then:

$$\bar{I} = I_0 \exp(-\mu d_\gamma) = \frac{\int_0^d I_0 \exp(-\mu x)\mathrm{d}x}{d} = \frac{I_0}{\mu d}[1-\exp(-\mu \mathrm{d})] \tag{17}$$

where I_0 = γ-intensity without attenuation;

μ = linear γ-ray attenuation coefficient (cm^{-1}).

If $\mu d \ll 1$, it follows from eqn. (17) that $d_\gamma \approx d/2$.

Again, monodirectional γ-ray fluxes and homogeneously distributed activities do not occur. The sample radiates γ-rays in a 4π-geometry and the activity is not homogeneously distributed as a consequence of flux gradients and neutron attenuation. Further, each layer of the sample has a different contribution to the recorded activity because of the difference in detection efficiency. However, one can always define d_γ by:

$$\exp(-\mu d_\gamma) = \bar{I}/I_0 \tag{18}$$

where $\bar{I}$ = activity counted by the detection system for a real sample, including γ-ray attenuation;

I_0 = activity counted by the detector for a hypothetical sample with the same activity distribution as an actual sample, but with no γ-ray attenuation.

It is possible to determine a d_γ value useful for different elements with the aid of other than ^{16}N γ-rays, on condition that the linear absorption coefficients are small. Indeed, if one considers a sample as being composed of 9 successive layers, each 1 mm thick, one can write eqn. (18) as

$$\bar{I}/I_0 = \exp(-\mu_N d_\gamma) = \frac{\sum_{i=1}^{9} A_i Ti_N \exp(-\mu_N x_i f_i)}{\sum_{i=1}^{9} A_i Ti_N} \tag{19}$$

where μ_N = linear γ-ray attenuation coefficient for ^{16}N γ-rays, counted between 4.5 and 6.5 MeV;

Ti_N = detection efficiency for ^{16}N γ-rays counted between 4.5 and 6.5 MeV, for the ith layer;

A_i = ^{16}N activity in the ith layer;

x_i = total thickness of the $(i-1)$ layers preceding the ith layer;

f_i = factor considering the fact that the γ-rays are not only emitted perpendicular to the detector surface, which results in an average increase of the distance travelled in the sample.

If the ratio of the detection efficiency for γ-rays of different energies is independent of the distance to the crystal, eqn. (19) can be written as:

$$\exp(-\mu_N d_\gamma) = \frac{\sum_{i=1}^{9} A_i Ti_x \exp(-\mu_N x_i f_i)}{\sum_{i=1}^{9} A_i Ti_x} \tag{20}$$

where Ti_x = detection efficiency for γ-rays of energy E_x for the ith layer. If $\mu_N \ll 1$, eqn. (20) can be reduced to:

$$d_\gamma = \frac{\sum_{i=1}^{9} A_i Ti_x x_i f_i}{\sum_{i=1}^{9} A_i Ti_x} \tag{21}$$

If $\mu_x \ll 1$, eqn. (21) can be transformed to:

$$\exp(-\mu_x d_\gamma) = \frac{\sum_{i=1}^{9} A_i Ti_x \exp(-\mu_x x_i f_i)}{\sum_{i=1}^{9} A_i Ti_x} = \frac{\bar{I}_x}{I_{0_x}} \tag{22}$$

where μ_x = linear γ-ray attenuation coefficient for γ-rays of energy E_x (photopeak counting).

Experimental determination

d_γ was determined via the ^{56}Mn and ^{24}Na activity induced in iron and aluminium samples. Nine discs (diameter 26 mm, 1 mm thick) were simultaneously irradiated in the same geometry as a sample. For the aluminium discs, the ^{24}Na activity ($E_\gamma = 2.76$ MeV) was counted in the 2.5–3.0 MeV energy region. The 9 discs were separately counted, the first directly on the copper β-ray shield, and the others placed on iron rings (internal diameter = 24 mm, external diameter = 26 mm) which were, respectively, 1, 2, ... 7, 8 mm thick, and thus in the same geometry as in a sample. The sum of the measured activities, after correction for decay and γ-ray attenuation in the 1-mm discs, gave I_{0_x}. The 9 discs were then simultaneously counted, placed on top of each other, yielding $\bar{I}_x$.

The same procedure was repeated for iron discs. The induced ^{56}Mn activity ($E_\gamma = 1.8$ and 2.11 MeV) was counted between 1.65 and 2.20 MeV. Figure 5 shows the detected γ-ray activities ($A_i Ti_x$) in the individually counted discs. d_γ values are listed in Table VII, column 2. The weighted average of the determined d_γ values is 0.33 ± 0.02.

d_γ can also be approximated by means of eqn. (21), for $f_i = 1$, and from experimental $A_i Ti_x$ values as represented in Fig. 5 for iron. Results are given in Table VII, column 3. For any metal, $(C_x)_\gamma$ can be calculated from:

$$(C_x)_\gamma = \exp(-\mu_N d_\gamma) \tag{23}$$

For the oxygen standard one can reasonably accept that $d_{\gamma_s} \approx d_{n_s} \approx 0.29$. Considering also the γ-ray attenuation by the front of the container (1 mm Fe), $(C_s)_\gamma$ can be calculated from:

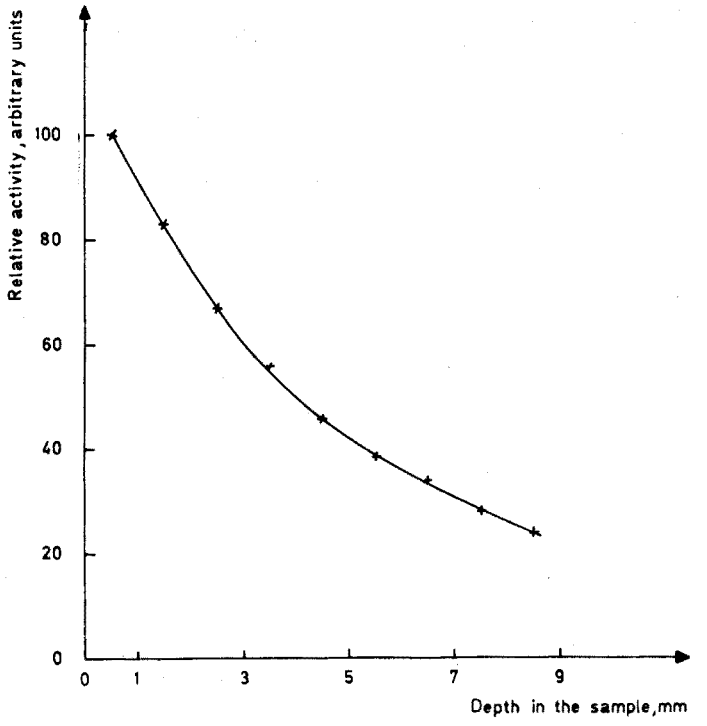

Fig. 5. Contribution to the measured activity from successive layers within the sample (without γ-attenuation) (iron discs).

TABLE VII

EXPERIMENTAL d_γ-VALUES

Metal	*d_γ from eqn. (22) (cm)*	*d_γ from eqn. (21) (cm)*
Al	0.39 ± 0.06[a]	0.35
Fe	0.32 ± 0.02	0.33

[a] Standard deviation from counting statistics.

$$(C_s)_\gamma = \exp(-\mu_{Fe} \cdot 0.1) \cdot \exp(-\mu_s d_{\gamma_s}) = 0.963 \tag{24}$$

μ_s can be calculated from:

$$\mu_s = \frac{1}{V} \sum_{i=1}^{n} \left(\frac{\mu}{\rho}\right)_i w_i = 0.047 \tag{25}$$

where $(\mu/\rho)_i$ = mass attenuation coefficient for the ith element in the standard mixture ($cm^2\ g^{-1}$);
w_i = weight of the ith element of the mixture;
V = internal volume of the container.
$(C_s/C_x)_\gamma$ values for the metals studied in this work, calculated from the

linear attenuation coefficients given by Storm and Israel[11], and from the experimental d_γ and d_{γ_s} values, are listed in Table VI, column 5. C_s/C_x values are given in column 6.

D_s/D_x – GEOMETRY EFFECT AT THE COUNTING SITE

This correction factor for difference in detection efficiency between standard and sample takes, just like $[\bar{\phi}_1]/\bar{\phi}_1$, two factors into account: decrease in thickness and decrease in radius. D_s/D_x can be calculated from the detection efficiencies for a 7.5 cm × 7.5 cm NaI(Tl) crystal[12] and the relative activities of 9 iron discs (diameter = 26 mm, thickness = 1 mm) irradiated in the position of a sample, and of 7 iron discs (diameter = 22 mm, thickness = 1 mm) irradiated in a standard box. The value $D_s/D_x = 0.994$ was found.

TOTAL CORRECTION FACTOR

For every solid sample, the total correction factor can be calculated from eqn. (1) or (3). Total correction factors are listed in Table VI. With the oxygen flux monitor, the total correction yields (for a 30-mm target) an apparent oxygen content of the standard (containing 412 mg of oxygen with a blank value of 4 mg) of 421, 432, 431, 432, 439, 452, 454, 452, 444, 444, 495, 512 and 469 mg for Al, Fe, Ni, Cu, Zr, Mo, Ag, Cd, Sn, Sb, Ta, W and Bi, respectively. These data were checked independently. Eight discs of Al, Cu and Fe (diameter = 26 mm, thickness = 1 mm) and 7 mylar foils were alternately piled to a height of 9 mm. This "sandwich" sample was kept together by three tiny screws in 3 holes drilled in the discs. Each time the same mylar foils were used on the same places between the discs to avoid differences caused by possible inhomogeneities in the mylar. The samples were irradiated in position 1, while the neutron flux was monitored simultaneously with an oxygen monitor and with the BF_3-counter. After correction for the blank value of the metal discs, and corrections for attenuation and screening, one should find the same value for the oxygen content of the foils, independent of the metal used and of the monitoring system. The results are summarized in Table VIII. The agreement between the mean values found with the BF_3-counter and oxygen flux monitoring confirms the proposed correction factors I_x/I_s and S_x/S_s. The differences between the mean values for different metals are within 1%, confirming the C_s/C_x values.

TABLE VIII

OXYGEN CONTENT (mg) FOUND IN MYLAR FOILS PILED BETWEEN DIFFERENT METAL DISCS

Metal	*BF_3-monitoring*	*O-monitoring*	*Mean value*
Al	209.8	211.8	210.8
Fe	212.1	212.9	212.5
Cu	212.5	212.6	212.6
Mean value	211.5	212.4	212.

In view of this, the overall accuracy is believed to be about 1%, except for metals with very high linear γ-ray attenuation coefficients (*e.g.* tantalum or tungsten) where the error might be somewhat larger.

Grateful acknowledgement is made to Prof. Dr. J. Hoste for his interest in this work. Thanks are due to Mr. C. Tombu (Métallurgie Hoboken) and J. Pauwels (Eurisotop) for providing part of the samples and to the "Nationaal Fonds voor Wetenschappelijk Onderzoek" and the "Interuniversitair Instituut voor Kernwetenschappen" for partial financial support.

SUMMARY

A general standardization method is described for the determination of oxygen in solid samples via the $^{16}O(n, p)^{16}N$ reaction. Two systems of flux monitoring are considered: the sample *versus* standard comparator method and BF_3 monitoring. The average flux in sample and standard, fast neutron shielding, fast neutron scattering, absorption of fast neutrons, absorption of ^{16}N γ-rays and counting efficiency of sample and standard are considered. The influence of the target diameter on the obtained correction factors has also been studied. Total achievable accuracy is believed to be about 1%.

RÉSUMÉ

Une méthode générale d'étalonnage est décrite pour le dosage de l'oxygène dans des échantillons solides, par la réaction $^{16}O(n, p)\ ^{16}N$. Deux systèmes sont pris en considération. D'autre part, divers paramètres sont examinés. L'exactitude totale que l'on peut atteindre peut être évaluée à environ 1%.

ZUSAMMENFASSUNG

Es wird eine allgemeine Standardisierungsmethode für die Bestimmung von Sauerstoff in festen Proben über die Reaktion $^{16}O(n, p)^{16}N$ beschrieben. Für die Flussüberwachung werden zwei Systeme betrachtet: die Vergleichsmethode Probe gegen Standard und die Verwendung eines BF_3-Monitors. Der mittlere Fluss in der Probe und im Standard, die Abschirmung und Streuung von schnellen Neutronen, die Absorption von schnellen Neutronen, die Absorption von ^{16}N-γ-Strahlen und der Zählwirkungsgrad von Probe und Standard werden behandelt. Der Einfluss des Target-Durchmessers auf die erhaltenen Korrektionsfaktoren wurde ebenfalls untersucht. Es wird angenommen, dass eine Gesamtgenauigkeit von etwa 1% erreichbar ist.

REFERENCES

1 R. Gijbels, A. Speecke and J. Hoste, *Anal. Chim. Acta*, 43 (1968) 183.
2 R. Gijbels, A. Speecke and J. Hoste, *Modern Trends in Activation Analysis*, NBS Spec. Publ. 312, Vol. II, 1968, p. 1298.
3 R. Gijbels, J. Hoste and A. Speecke, *The Industrialisation of 14 MeV Neutron Activation Analysis for Oxygen in Steel*, EUR-4297, Luxemburg, Sept. 1969.

4 D. Brune and K. Jirlow, *J. Radioanal. Chem.*, 2 (1969) 49.
5 S. S. Nargolwalla, M. R. Crambes and J. R. De Voe, *Anal. Chem.*, 40 (1968) 667.
6 S. S. Nargolwalla, M. R. Crambes and J. E. Suddueth, *Anal. Chim. Acta*, 49 (1970) 425.
7 J. Hoste, D. De Soete and A. Speecke, *The Determination of Oxygen in Metals by 14-MeV Neutron Activation Analysis*, EUR-3565e, Brussels, Sept. 1967.
8 R. Van Grieken, A. Speecke and J. Hoste, *J. Radioanal. Chem.*, in press.
9 R. Van Grieken, A. Speecke and J. Hoste, *J. Radioanal. Chem.*, 10 (1972) 95.
10 O. K. Nikolaenko and A. S. Shtan, *Radiation Technology*, Ed. 4, Atomizdat, 1969, p. 175.
11 E. Storm and H. I. Israel, *Photon Cross-sections from 1 keV to 100 MeV for Elements 1 through 100*, Academic Press, New York, 1970, pp. 565–681.
12 C. C. Grosjean and W. Bossaert, *Table of Absolute Detection Efficiencies of Cylindrical Scintillation Gamma-ray Detectors*, Ghent University, 1965.

Analytica Chimica Acta, 65 (1973) 19–34

SAMPLE PREPARATION FOR AND NITROGEN ISOTOPE ANALYSIS BY THE NOI-4 EMISSION SPECTROSCOPE

DENNIS R. KEENEY and MARINO J. TEDESCO

Department of Soil Science, University of Wisconsin, Madison, Wisc. 53706 (U.S.A.)

(Received 30th October 1972)

The recognized need for a suitable alternative to the mass spectrometer for routine analysis of ^{15}N has resulted in a recent renewal of interest in the application of emission spectroscopy to this purpose[1–8]. Emission spectrometry offers the primary advantages of lower initial investment, and less supervision and maintenance than mass spectrometry, and has the additional advantage, often of critical importance, that this method requires a much smaller sample for analysis[8].

The objective of the work in this paper was to develop a sample preparation method for use with emission spectrometry and evaluate problems in sample preparation and analysis of ^{15}N by a commercially available emission spectroscope (Statron, type NOI-4).

EXPERIMENTAL

Apparatus

A NOI-4 Optical ^{15}N Analyzer (Statron, Leipzig, D.D.R., equivalent to the Packard 1015 Nitrogen-15 Analyzer marketed by Packard Instruments, Zurich,

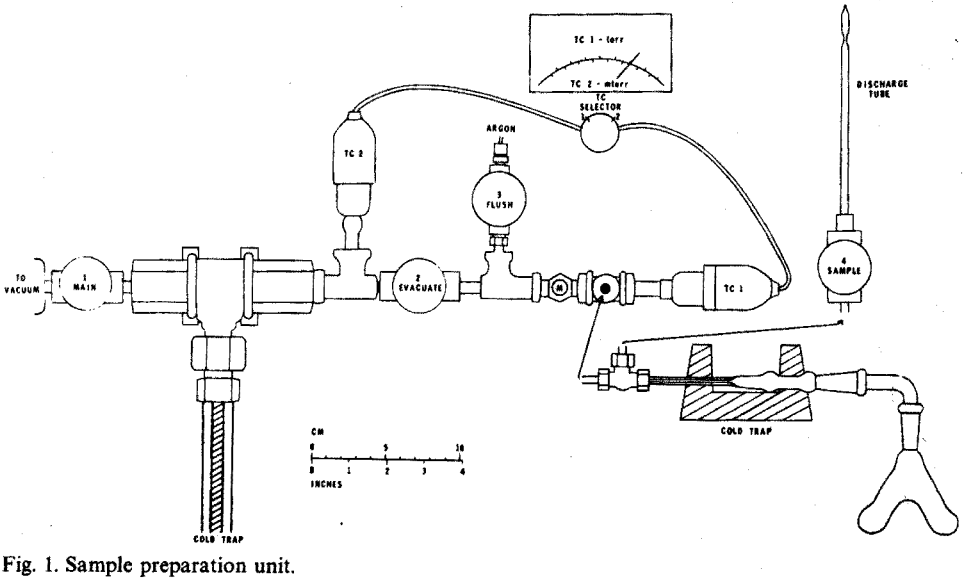

Fig. 1. Sample preparation unit.

Switzerland and Downers Grove, Ill., U.S.A.) coupled to a Honeywell Electronic 19 strip chart recorder was used. Mass spectrometric analysis of ^{15}N was conducted with a CEC 21-201 or a DuPont 21-621 instrument by methods described by Bremner[9].

The sample preparation unit (Fig. 1) consists of metal–Teflon bellows valves and metal–Teflon–metal or metal–Teflon–glass fittings and is equipped with a 2-stage roughing pump and an oil diffusion pump. The discharge tube assembly consists of a bellows valve and interchangeable glass discharge tubes. The unit is equipped with vacuum transducer probes and can be flushed with an inert gas (argon was used here). A detailed parts list can be obtained from the senior author on request.

The electrodeless discharge tubes are made from 6-mm o.d. standard wall Pyrex or Vycor tubing. The total length is 140 mm, with a constriction about 20 mm from the closed end of the tube. The micro-Rittenberg sample conversion assembly consists of a small "y" tube, an 0-ring ground-glass inner point connector, and a small styrofoam cold trap. The volumes of the various assemblies are as follows: Rittenberg tube, 9.5 ml; discharge tube, 1.5 ml; connectors, 1.2 ml; cold trap, 2.3 ml; sample vacuum gauge (TCl), 6.3 ml; for a total volume from valve 4 of about 21 ml.

Adopted method

Hypobromite solution. Dissolve 200 g of sodium hydroxide in 300 ml of water in a 1-l Erlenmeyer flask. Cool the mixture to *ca.* 10° with crushed ice and stir vigorously with a Teflon-coated stirring bar and a magnetic stirrer. Add 30 ml of liquid bromine at a rate of about 1.5 ml min^{-1}. Stopper the flask, refrigerate for 4–6 days and then filter the solution through glass fiber filter paper. Add 0.35 g of potassium iodide, dissolved in 10 ml of water, to the filtrate, mix, and store in a refrigerator. If the solution becomes turbid during storage, it can be refiltered through glass fiber filter paper.

Preparation of distillates. Collect and titrate distillates[9] in a 100-ml beaker. After titration, add 1 ml of 0.1 *M* hydrochloric acid and 0.1 g of chromatographic-grade neutral aluminum oxide. Bring the sample to dryness on a hot plate (80–95°). The dried material should be removed from the beaker with a spatula, and stored in glass or plastic vials for analysis.

Gas sample preparation. Insert a sample valve (4, Fig. 1) on the vertical "T" outlet, plug the other end of the outlet with a solid glass rod, and evacuate to less than 0.02 torr. Flush the discharge tube with argon while heating the tube with a small torch to *ca.* 400°. Repeat this sequence, except that argon should be left in the tube. Close the sample valve (4), remove the glass rod plug, and replace with a cold trap. Insert an L-shaped glass tubing fitted with T/S 10/30 0-ring inner joints into the cold trap (the 0-rings should be greased lightly with a high-vacuum grease).

During the discharge tube pump-down, prepare a Rittenberg tube by placing a subsample of the Al_2O_3–NH_4–boric acid indicator mixture, containing over 20 μg of nitrogen, in one side of the tube and moisten with a few drops of water. Add 1.5 ml of sodium hypobromite solution in the other side. Insert one end of the L-shaped tubing into the Rittenberg tube, fill the sample cold trap with liquid nitrogen, and evacuate to 0.01–0.02 torr. Flush the system with argon, and evacuate to 0 torr. Close valves M and 2, mix the contents of the Rittenberg tube, and briefly warm the mixture with a small burner to dispel the remaining gas. If more than 3 torr of

nitrogen is produced, evacuate the system, using M, to 3 torr. If less than 3 torr of gas is produced, add argon to bring the total pressure to 3 torr.

Isotope-ratio analysis. Insert the discharge tube in the r.f. oscillator terminal (sample holder) on the NOI-4 with the sample valve assembly protruding outside the instrument. Light the tube and then turn on the modulation switch. Focus the light beam on the entrance slit by using the fine horizontal focusing knob on the condenser lens. By manipulating the drive unit back and forth by hand, choose a suitable combination for the gain settings of the two bandheads. Holding the drive unit at the crest of the higher peak, bring this to about 80 chart division by using the same focusing knob. Turn on the drive unit and record 5 complete tracings. Obtain the average height for each peak in mm, and calculate the ratio, R, by the equation.

$$R = \frac{^{14}N\,^{14}N}{^{14}N\,^{15}N} \text{ or } R = \frac{(a)(II)}{(b)(I)} \tag{1}$$

for abundance less than 40 atom% ^{15}N,

a = average height of $^{14}N\,^{14}N$ peak,

b = average height of $^{15}N\,^{14}N$ peak,

I = corrected gain setting of the $^{14}N\,^{14}N$ peak,

II = corrected gain setting of the $^{14}N\,^{15}N$ peak.

For 40–80 atom% ^{15}N,

$$R' = \frac{^{14}N\,^{15}N}{^{15}N\,^{15}N} \tag{2}$$

Atom % ^{15}N can then be calculated by the formula[9]:

$$< 40 \text{ atom \%, atom \% } ^{15}N = \frac{100}{2R+1} \tag{3}$$

$$> 40 \text{ atom \%, atom \% } ^{15}N = \frac{100}{(R'/2)+1} \tag{4}$$

The calculated atom% ^{15}N value is then corrected by using a standard curve plot or a linear equation of optical *versus* mass spectrometer values in the same range of values as the unknown.

Comments

The liquid nitrogen trap should be cleaned with acetone and dried before reuse. It is convenient to have several traps on hand. Up to 0.5 ml of liquid sample can be used in the Rittenberg tubes. If more than 0.5 ml is used, the bumping occurring during pump-down causes mixing with the hypobromite. If greater than 200 μg of nitrogen is to be analyzed, larger Rittenberg tubes (*ca.* 15 ml capacity) should be used. The hypobromite solution recommended is a concentrated version of the preparation described by Bremner[9]. Use of this solution decreased the bumping problems found with the more dilute preparation. The use of alumina as a solid support is recommended to aid in transfer of the dried boric acid–indicator–NH_4Cl mixture. It was adopted after studies showed that identical ^{15}N values were obtained with an aqueous solution of 4.73 atom% ^{15}N standard or the same standard dried

either in the presence of boric acid–indicator–HCl or Al_2O_3–boric acid–indicator–HCl mixtures.

It is essential that the parameters used in calibrating the analyzer be preserved while measuring unknowns. These include partial pressures of nitrogen and argon in the discharge tube, photomultiplier voltage, entrance and exit slit width and gain settings. If the tracings for the unknown are not reproducible within the run, or the bandhead intensity decreases rapidly with time, results of that sample should be rejected. It is recommended that standards be prepared in sealed discharge tubes so that they can be reanalyzed periodically to check instrument calibration.

RESULTS

Effort has been concentrated on methodology to provide maximum sensitivity and accuracy in the normal to 10 atom% ^{15}N range, because these values will encompass most biological ^{15}N studies. Unless otherwise stated, the emission results presented were obtained by stadardizing against mass spectrometric values.

Nitrogen-15 analyzer

Base line. Typical tracings for an enriched and a normal abundance sample are given in Fig. 2. The baselines used are the same as recommended by Leickman *et al.*[4].

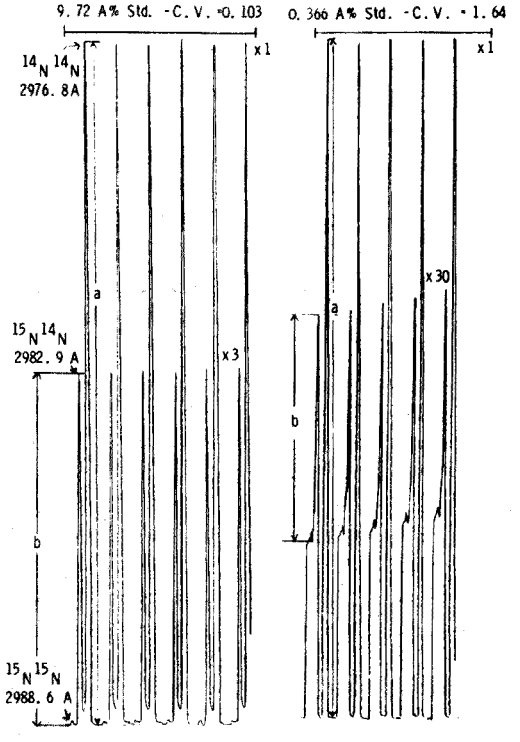

Fig. 2. Typical tracings indicating peaks and baseline.

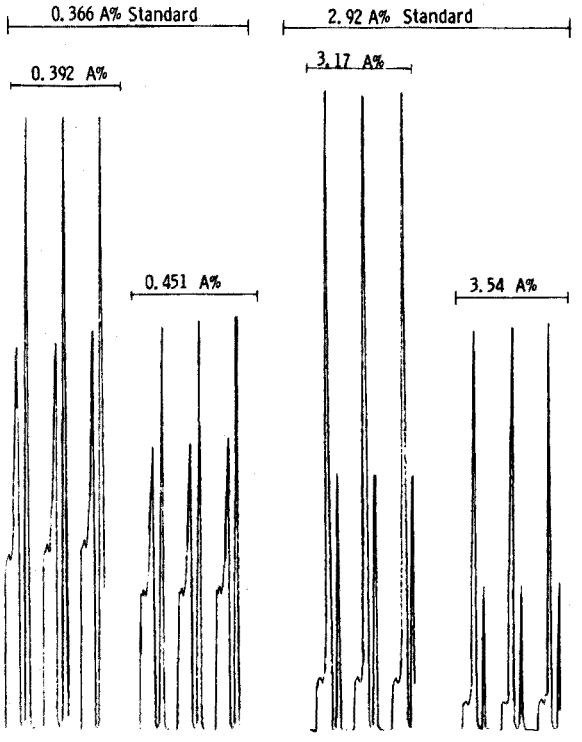

Fig. 3. Effect of peak height variation on ^{15}N atom% values.

Effect of peak height. In the initial evaluation of the NOI-4, it was observed that varying the peak height affected the atom% ^{15}N values obtained. This is illustrated in Fig. 3, which shows tracings obtained on the same sample, the only difference being that the peak height was varied by changing slightly the focus of the condensing lens. An increase of as much as 10% in the results was obtained by decreasing peak height by 30%. The reasons for this effect are uncertain. It may be due to electronic and/or mechanical lag times in the instrument and recorder. This finding indicates that peak height of primary standards and samples must be standardized by use of the appropriate condenser lens focus and amplifier settings.

Gain settings. During evaluation of the peak height effect, it was also noted that the amplifier settings are not necessarily those given on the instrument, all other factors being equal. For example, 10× gives a peak height less than 33% of the height at 30× (Fig. 4). Thus the worker should calibrate the most commonly used gain settings for each instrument.

Corrected gain is calculated by using the average peak height values for $^{14}N^{14}N$ and $^{14}N^{15}N$ of a number of runs on a natural abundance standard (0.366 atom% ^{15}N, $R = 136.11$). Attenuation of the $^{14}N^{14}N$ peak is 1, and of $^{14}N^{15}N$ is the unknown. An example calculation is given below (see also Fig. 5).

Average peak heights: $^{14}N^{14}N$, 221.4 mm
$^{14}N^{15}N$, 74.4 mm

Then,

$$R = 136.11 = \frac{221.4 \times \text{gain of } {}^{14}N\,{}^{15}N \text{ peak}}{74.4 \times \text{gain of } {}^{14}N\,{}^{14}N \text{ peak}} \tag{5}$$

or

$$\text{Gain for } {}^{14}N\,{}^{15}N \text{ peak} = \frac{136.11 \times 74.4 \times 1}{221.4} = 45.74$$

$$\text{Gain for } 10\times = \frac{45.74}{3.65} = 12.54$$

$$\text{Gain for } 3\times = \frac{12.54}{4.62} = 2.72$$

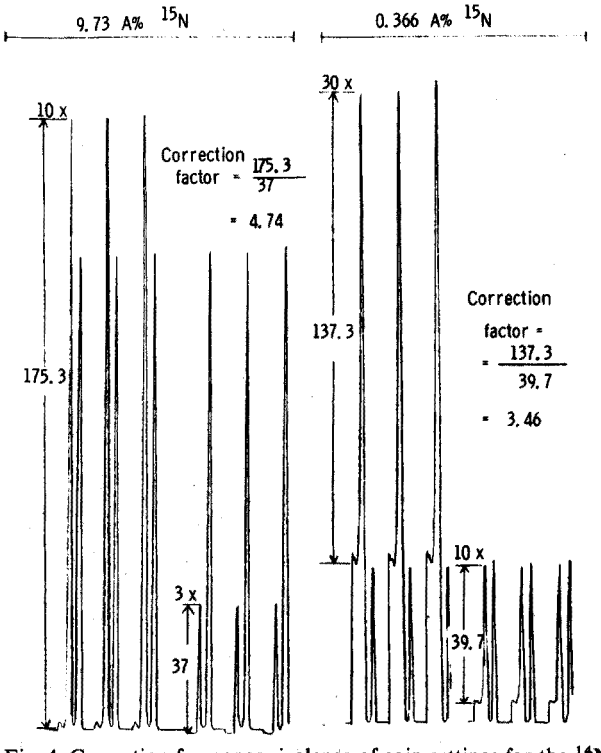

Fig. 4. Correction for nonequivalence of gain settings for the $^{14}N\,^{15}N$ bandhead.

This correction forces the standard curve of emission *versus* mass spectrometric values through a 1:1 point at 0.366 atom% ^{15}N. The results in Table I illustrate that the correction does remove the disparity in results at different gain settings. It is not absolutely necessary to use corrected values as long as proper standard curves are established. However, in practice there are some advantages in this approach. For example, attenuation change from 30× to 10× for the $^{14}N\,^{15}N$ peak occurs in the range 2–3 atom% ^{15}N. Use of the corrected values makes additional standard curves unnecessary.

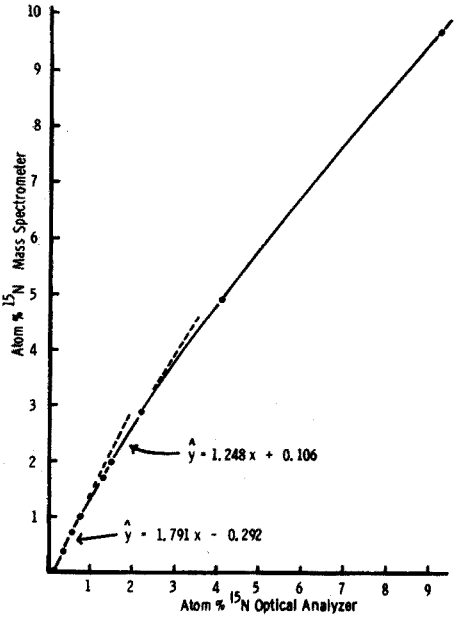

Fig. 5. Calibration curve. Entrance slit height, 3 mm. Entrance slit width, 40 μm. Exit slit width, 40 μm. Photomultiplier, 1180 V.

TABLE I

EFFECT OF CORRECTION ON THE PREDICTED ATOM% VALUES[a]

Mass spec value	*Gain 30-1*		*Gain 10-1*	
	Uncorrected	*Corrected*	*Uncorrected*	*Corrected*
1.70	2.03	1.34	1.74	1.35
1.99	2.25	1.49	1.81	1.45
2.92	3.58	2.37	2.81	2.37

[a] All values are averages of 3 replicates.

Use of a linear regression equation for a standard curve of the form, $y = mx + b$ simplifies prediction of y (Table II). With these equations and using either corrected or the uncorrected values, the standards were predicted to within $\pm 5\%$ in most cases, with the natural abundance sample being predicted to within 0.6%.

Standardization. The standard curve over the 0.366–10 atom% ^{15}N range was not linear (Fig. 5). The curve obtained consisted of at least two approximately linear portions, namely between 0.366 and 1 atom% ^{15}N and between 1 and 3 atom% ^{15}N. Even more deviation from linearity might have been detected, had more standards in the 4–8 atom% ^{15}N range been available. It is obvious that standardization must consist of several points on the curve in the range in which one is working.

The reasons for lack of linearity, even when using the values corrected for

TABLE II

OBSERVED AND PREDICTED ATOM% ^{15}N VALUES WITH THE EQUATIONS IN FIG. 5

Mass spec. values	*Observed emiss on values*	*Predicted values*		*Error (%)*	
		Uncorrected	*Corrected*	*Uncorrected*	*Corrected*
0.366[a]	0.366	0.374	0.364	+2.2	−0.6
0.719[a]	0.586	0.757	0.758	+5.3	+5.4
1.07[a]	0.746	1.034	1.044	−5.5	−2.8
1.07[b]	0.746	1.07	1.04	0	−3.0
1.70[b]	1.34	1.75	1.78	+3.5	+4.7
1.99[b]	1.48	1.92	1.97	−3.4	−1.0
2.92[b]	2.24	2.93	2.90	+0.3	−0.7

[a] 30× amplification of $^{14}N^{15}N$ bandhead.
[b] 10× amplification of $^{14}N^{15}N$ bandhead.

TABLE III

PRECISION OF ^{15}N ANALYSIS WITHIN A RUN AND BETWEEN RUNS ON THE SAME SAMPLE

(All values are in atom% ^{15}N)

Mass spec. values	*Within a run*[a]			*Between runs*[b]		
	Av.	*s.d.*[c]	*c.v.*[d]	*Av.*	*s.d.*	*c.v.*
0.366	0.362	0.006	1.64	0.362	0.025	6.81
2.92	2.66	0.001	0.04	2.70	0.008	0.30
9.73	9.35	0.009	0.10	9.45	0.008	0.09

[a] Values obtained by using 5 tracings.
[b] Values obtained by averaging results obtained on 5 different days of 5 tracings of sealed standards.
[c] s.d. = standard deviation.
[d] c.v. = coefficient of variation in %.

gain settings, is not clear. Possible explanations could include a combination of non-constant errors in the instrument and/or sample preparation.

Precision. Table III (see also Fig. 1) illustrates the precision obtainable on the NOI-4 with Vycor tubes. These values were obtained on individual sealed tubes and thus do not include errors in sampling and sample preparation. The precision data are similar to that obtained by other workers[1–4,8].

Sample preparation

Conversion to nitrogen. Two approaches[9] have been used to obtain pure nitrogen gas for mass spectrometric analysis. These are: (1) oxidation of ammonium salts by alkaline hypobromite; and (2) combustion of the dry sample in a sealed tube at about 500° in the presence of copper oxide (Dumas method). These procedures have also been adapted for emission spectrometry by Faust[1,2]. Both approaches have certain advantages. The combustion approach, for example, can theoretically be

applied to virtually any dry nitrogenous compound (*e.g.*, soil or plant material, proteins), and is probably simpler and faster than the hypobromite approach. It has several disadvantages, however. For one, the Dumas method consistently gives less precise results than the hypobromite method[2], presumably because of interfering gaseous compounds not removed during combustion. Also, the total pressure in the discharge tube must be about 2–5 torr for maximum emission[4]; this requires that the amount of sample in the tube be accurately known in microgram amounts. This latter requirement also obviates the direct combustion of biological samples because of subsampling problems[8]. Further, the tube must be sealed, and cannot be reused.

When conducted properly, the hypobromite method is quantitative and free of interferences. It has been used almost exlusively for preparation of nitrogen samples for mass spectrometry[9] and in most of the early work with optical spectroscopy[4,5,10–12]. It does require that all nitrogen compounds to be analyzed are converted to ammonium. This is no problem, as besides the standard Kjeldahl procedure and modification thereof for total nitrogen, specific and sensitive steam distillation procedures are available to determine various organic and inorganic forms of combined nitrogen[9]. The hypobromite procedure has one major drawback. Because of problems of bumping and resultant mixing of hypobromite with the sample during evacuation, and the vigor of the reaction, rather large "y" tubes must be used. This system thus has considerable dead volume and relatively large amounts of nitrogen, compared to the combustion method, are required to produce sufficient gas pressure. This drawback can be countered to some extent by use of an inert gas to sustain discharge in tubes with a low partial pressure of nitrogen gas[3].

The features that a successful gas preparation unit should include were: (*a*) ability to monitor gas pressure in the discharge tube; (*b*) ability to flush the system with an inert gas and to provide for use of a partial pressure of inert gas in the discharge tube; (*c*) ability to reuse the discharge tubes; and (*d*) provision of maximum accuracy and sensitivity in conjunction with simple and rapid manipulation and preparation of the sample.

The unit sketched in Fig. 1 incorporates most of these requirements, although, as will be discussed later, further improvement is needed with regard to requirement (*d*). It is essentially all metal and utilizes Teflon bellows valves and Teflon ferrule seals on the interchangeable parts. Constrictions have been avoided to reduce the time required for evacuation. The design of the hypobromite oxidation glassware (Fig. 1) is similar in most respects to the system described by Faust[1]. The major modification involves the use of an interchangeable flow through cold trap rather than a freeze out of the "y" tube after gas production.

Discharge tubes. Because the optical range of interest is in the near ultraviolet region, the discharge tubes should be of quartz or high-silica glass. However, because of the memory problems encountered and resultant need for a new tube when analyzing samples low in ^{15}N, Pyrex glass (which is less expensive and easily handled) was also evaluated with respect to its use in discharge tubes. The tube materials and shape were evaluated with respect to reproducibility of values obtained with a 0.366 atom% ^{15}N $(NH_4)_2SO_4$ standard.

The design includes a capillary restriction. The discharge intensity at this restriction is much greater than in the remainder of the tube. Light from this restriction

is focused on the entrance slit of the analyzer. The tube also must have sufficient volume so that enough nitrogen is present to sustain the discharge for several minutes.

When Pyrex was used for the discharge tube, considerable deviation ($\pm 10\%$) was found in repeated analyses. Also peak intensity was diminished, discharge tube life shortened, starting more difficult, and the memory effect greater than with Vycor or quartz tubes. The lack of reproducibility was traced to variations in the thickness of the capillary portion of the tube and to differences among batches of Pyrex. Therefore, the use of Pyrex cannot be recommended except for semi-quantitative work. Unfortunately, it was impossible to obtain Uviol, a Pyrex glass transparent to ultraviolet, which has been used in much of the European work.

A similar evaluation was made of Vycor and quartz discharge tubes. Both materials gave highly reproducible values unaffected by capillary dimensions, and in all respects Vycor was comparable to quartz. Because of its lower cost, Vycor discharge tubes are recommended. Unless otherwise stated, the tubes used in this work were made by drawing a capillary and sealing the end of a length of 13 cm × 6

TABLE IV

EFFECT OF AGEING DISCHARGE TUBES AFTER BAKING ON THE ATOM% OF NATURAL ABUNDANCE SAMPLES

Run	*Storage period (days)*			
	0	*1*	*2*	*3*
1	0.392	0.361	0.349	0.352
2	0.367	0.314	0.383	0.363
3	0.354	0.363	0.369	0.352
4	0.370	0.349	0.343	0.370
5	0.376	0.356	0.336	0.367
Av.	0.372	0.349	0.356	0.361

TABLE V

EFFECT OF PARTIAL PRESSURE OF NITROGEN ON ISOTOPE RATIOS[a]

Sample ^{15}N atom %	*Size (μg N)*	*Partial pressure (torr)*		*Observed ^{15}N atom %*
		N_2	*Ar*	
0.366	20	1.0	2.0	0.368
	100	2.0	1.0	0.371
	500	3.0	0	0.371
2.92	10	0.5	2.5	2.93
	20	1.0	2.0	2.92
	100	2.0	1.0	2.94
	500	3.0	0	2.93

[a] All samples were run on new (*i.e.*, not previously used) tubes.

mm o.d. standard wall Vycor tubing. The tube is cured at 650° for 12 h in a muffle, and stored in a dessicator over P_2O_5 for at least two days before use. The heating and storage treatment was adopted because this led to more reproducible results than tubes used immediately after being made (Table IV). It is likely that changes in the crystalline structure of quartz are involved.

Partial pressure of nitrogen. No investigations of the effect of the partial pressure of nitrogen on the isotope ratios obtained by emission spectrometry have been conducted. However, Broida and Chapman[11] found that changing the nitrogen pressure by ± 1 mm Hg produced a maximum change of 13% in intensity and 4% in the isotopic ratio. In their studies, no inert gas was added. The effect of partial pressure is important, because it also is related directly to sample size at a given volume. In the sample preparation procedure used here, argon is routinely added when needed to provide a total pressure of 3 torr.

This procedure was adopted after investigations (Table V) showed that there was little effect on the ratio values at different partial pressures of nitrogen. However, below 0.5 torr partial pressure of nitrogen, tube life tended to be shorter, and often the discharge could not be sustained for more than 2–3 min. The results in Table V also show that the minimum amount of nitrogen that can be analyzed with the hypobromite preparation procedure was 10 μg. In practice, 20–200 μg of nitrogen is recommended.

The results with the 2.92 atom% ^{15}N sample also show that no leaks occurred and that nitrogen adhering to the walls of the tube[2] is removed by the flaming procedure recommended. Any leaks or extraneous nitrogen would have lowered the observed value as sample size was decreased. This was further evaluated by use of a ^{15}N depleted sample of ammonium sulfate (0.008 atom% ^{15}N). Any atmospheric contamination of this sample would have markedly increased the ^{15}N content. This was not found, however, and the results obtained with the depleted sample fit on the standard curve (see Fig. 2). The use of ^{15}N depleted samples is recommended as the most sensitive way to check for leaks in a preparation system.

Effect of organic contaminants. Previous research[4] has indicated that water and oxygen interfere at low levels. These gases are eliminated in the present procedure by the liquid nitrogen freeze trap. However, in some of the preliminary research, valves and discharge tubes were inadvertently contaminated with vacuum stopcock grease. The contaminated tubes would light for only a few seconds before extinguishing, and the same effect was observed when contaminated valves were combined with new tubes. This is probably due to reaction of the free radical nitrogen with organics[13]. It was also noted that rubber O-rings evolved sufficient organic contaminants to interfere with the analysis. Therefore, the unit described has all metal-to-Teflon or glass–Teflon greaseless seals after the sample cold trap.

Memory. The memory or cross-contamination problem is one that is familiar to researchers experienced in ^{15}N analysis. It can occur via sorption of ammonia onto surfaces of glass used in sample distillation[9]. If a low enrichment sample is distilled following a high enrichment one, significant contamination of the low enrichment sample with ^{15}N can occur. The reverse can also happen. This problem has been effectively overcome by washing the distillation apparatus with hot ethanol between distillations[9]. Apparently nitrogen is not particularly reactive with glass surfaces, for no problems have been reported with mass spectrometric procedures,

provided that suitable precautions, such as allowing sufficient pumping time before the next gas sample is introduced, are followed.

While little information is available on the subject, apparently the situation with nitrogen in a glowing discharge tube is quite different. Mannella[13] reviewed the extensive literature to 1961 on "active nitrogen" or the afterglow that exists when the discharge is discontinued. By assuming that the afterglow phenomenon is chemically similar to the actual discharge, one can infer the processes occurring during discharge. However, active nitrogen contains only bands from the first positive system ($B^3IIg-A^3\Sigma_u^+$) while the discharge also contains the second positive system.

In essence, active nitrogen is a very reactive free radical, capable of reacting with many compounds including nitrous oxide, oxygen, carbon monoxide, and various surface films such as glass. No information is available on the type of sorption or reactions of active nitrogen on glass. Goleb and Middelboe[3] found that nitrogen was adsorbed by quartz when it was excited in a discharge, and that this nitrogen was not removed by flaming the tube. Faust[2] found that flaming the emission tube reduced the dilution of ^{15}N by ^{14}N, which he attributed to air adhering to the tube. However, the results of Goleb and Middelboe[3] would indicate that during discharge nitrogen reacts chemically or physically with the glass in a combination which cannot be removed rapidly by heat. While it has not been reported, it is very likely that this nitrogen would reequilibrate with the nitrogen in the discharge tube atmosphere on relighting. Thus a memory would result if a discharge tube is reused. Sommer and Kick[12] found considerable memory when analysis of a normal abundance sample was conducted after a 20.0 atom% ^{15}N sample in the same discharge tube. Goleb and Middelboe[3] found that xenon would "plug" the quartz surface of the discharge tube and decrease nitrogen sorption. Unfortunately, the high expense of xenon probably makes its use impractical. However, Leickman *et al.*[4] did not observe any memory when a natural abundance sample was analyzed after a 10 atom% ^{15}N sample with the same discharge tube. They attributed Sommer and Kick's findings to failure to flame the tube between analyses.

The memory effect of successive analyses in the same tube was evaluated in this work by the decrease in atom% ^{15}N of an enriched sample after analysis of a natural abundance sample, or the increase in natural abundance after an enriched sample. In addition, the change in relative intensity with time of the $^{14}N^{14}N$ and $^{14}N^{15}N$ peaks during discharge was evaluated. This approach allowed an estimate of the degree of sample contamination with time owing to exchange of sample nitrogen with the nitrogen sorbed onto the glass.

Unless otherwise stated, all work reported also involved heating the discharge tube under vacuum and under argon as described in the Experimental section. This step has been recommended by others[2] as being required for removing atmospheric nitrogen adhering to the tube walls, and thus was not evaluated further.

The effect of consecutive runs with the same Vycor tube is given in Table VI. Almost identical results were obtained with a quartz tube. The first 2 runs of the 2.92 atom% ^{15}N sample were below theoretical when following the normal abundance sample. Likewise, normal abundance values were greater than theoretical until about the fifth run. Further, with the contaminated samples, the second tracing of each run reflected the type of contamination, *i.e.*, the observed ratio decreased with time when the 2.92 atom% ^{15}N sample followed the normal abundance sample,

TABLE VI

MEMORY EFFECT WITH A VYCOR TUBE SUBJECTED TO CONSECUTIVE DETERMINATIONS

Sample atom% ^{15}N	*Run*[a]	*Tracing (atom% ^{15}N*	
		First 5	*Second 5*
0.366	1	0.364	0.367
	2	0.365	0.366
2.92	1	2.71	2.67
	2	2.90	2.86
	3	2.79	2.79
	4	2.88	2.77
0.366	1	0.475	0.485
	2	0.399	0.414
	3	0.382	0.396
	4	0.399	0.405
	5	0.372	0.372
	6	0.364	0.362
	7	0.365	0.376
	8	0.366	0.364
2.92	1	2.69	2.66
	2	2.87	2.80
	3	2.95	2.92
	4	2.93	2.91

[a] Each run denotes a separate sample on the same tube.

but increased with time when the normal abundance sample followed the enriched sample. This was due in most cases to changes in the $^{14}N^{15}N$ peak height. An error of about 30% was introduced by the memory effect for normal following a 2.92 atom% ^{15}N sample. The evaluation used was conservative, because often more highly enriched samples will be analyzed, leading to even greater memory effects.

The data in Table VI indicate that glass-sorbed nitrogen is exchanging with nitrogen in the tube, and that this exchange occurs over a prolonged time span. There is no preferential sorption of ^{14}N or ^{15}N. It is difficult to hypothesize the type of bonding involved, but a relatively strong bond is indicated because heating to 400–500° in vacuum does not remove the sorbed nitrogen.

Several approaches were used in an attempt to find a pretreatment method for contaminated tubes which would remove the memory effect. These included: (*a*) discharge in an atmosphere of argon; (*b*) heating in a muffle furnace at 700° for 12 h; (*c*) heating in an argon atmosphere; and (*d*) chemical pretreatments. Of these treatments, only (*b*) showed promise (Table VII). The results in Table VII are quite encouraging, and indicate that the memory effect may be eliminated if prolonged heating is used. It is likely that, over time, the enriched nitrogen is displaced by atmospheric nitrogen. Further work is required, however, before a final conclusion can be reached. For example, higher enrichments should be evaluated, and the memory from normal abundance samples elucidated.

TABLE VII

EFFECT OF HEATING CONTAMINATED VYCOR TUBES AT 700° FOR 12 h ON THE ATOM% ^{15}N OF A NORMAL ABUNDANCE (0.366%) SAMPLE

Enrichment of previous sample	*First contamination of tube*	*Second contamination of tube*[a]
2.92	0.366±0.02	0.364±0.01
1.07	0.365±0.03	0.363±0.04

[a] The same tube used in the first column was again contaminated with the indicated enriched sample and subsequently removed from the sample holder and heated at 700° for 12 h.

TABLE VIII

MASS SPECTROMETRIC AND EMISSION SPECTROMETRIC ATOM% ^{15}N VALUES ON BIOLOGICAL SAMPLES[a]

Sample	*Mass spectrometer*	*NOI-4*
Lake sediment		
NH_4-N	4.572	4.46
NH_4-N	5.902	5 94
NH_4-N	0.364	0.371
Total N	0.576	0.564
Total N	0.549	0 549
Rye-grass tissue		
Total N	0.598	0.610
Total N	0.613	0.609
Soil		
NO_3-N	0.493	0.489
NH_4-N	2.316	2.294
Total N	0.506	0.499

[a] Averages of duplicate analyses.

Comparison with mass spectrometric results. Several workers[2,4,8] have reported excellent agreement between mass spectrometric and emission spectrographic results using standard samples. The results in Table VIII illustrate the good agreement found for biological samples in the present work.

Overall evaluation of the method

Overall precision data for the method (sample preparation and analysis) with normal to 5 atom% ^{15}N range are given in Table IX. Standard deviations were essentially unaffected by enrichment and were about 0.015 atom% ^{15}N. Thus, the 95% confidence interval is ±0.02 atom% ^{15}N while the 99% confidence interval is ±0.03 atom% ^{15}N. This precision is within acceptable limits for most enrichment studies with biological systems. It does indicate, however, that experiments must be designed to give enrichments of at least 0.03 atom% ^{15}N excess (*i.e.*, enrichments to at least 0.40 atom% ^{15}N).

TABLE IX

PRECISION OF EMISSION SPECTROMETRY ATOM% ^{15}N RESULTS WITH $(NH_4)_2SO_4$ STANDARDS[a]

Sample	*Range*	*Av.*	*Standard deviation*	*Coefficient of variation (%)*
0.366	0.352–0.370	0.362	0.0175	4.85
1.70	1.70–1.86	1.81	0.0100	0.552
2.92	2.92–3.13	3.04	0.0185	0.608
4.73	4.71–5.84	4.79	0.0150	0.369

[a] Five subsamples, each run on a different day.

DISCUSSION

The NOI-4 instrument is suitable for analysis of ^{15}N in most experiments with enriched ^{15}N materials. The method in its present state of development offers simplicity and lower maintenance than mass spectrometers but at a sacrifice in sensitivity and precision. Further developments in instrumentation could improve this situation.

The sample preparation unit reported here proved in general quite satisfactory. Further development is needed, particularly in reducing the memory problem and decreasing the sample preparation time required. At the present, new Vycor tubes are used for low enrichment, and baked tubes for the higher enrichment samples. Further research on this critical problem is planned. In practice, 20–25 samples can be run by one operator in a normal working day. This is comparable to the output of most mass spectrometric methods, especially if one considers the maintenance time required with the mass spectrometer.

This research was supported by the College of Agricultural and Life Sciences, University of Wisconsin, Madison. M.J.T. gratefully acknowledges the support provided by USAID. Appreciation is expressed to Dr. A. P. Edwards, Soil and Fertilizer Research Branch, Tennessee Valley Authority, for his helpful suggestions and for supplying the ^{15}N standards, and to the Tennessee Valley Authority for partial support.

SUMMARY

A sample preparation unit was developed for use in emission spectrometric analysis of ^{15}N, and the unit and the NOI-4 spectroscope were evaluated. The sample preparation unit was designed to permit use of reusable discharge tubes, monitoring of pressure in the tube, and flushing with and addition of an inert gas to the tube. It utilizes the hypobromite oxidation approach for production of nitrogen gas. Instrument problems and sources of error included nonlinear gain settings, baseline determination, overlapping bandheads and nonlinearity of the standard curve. Problems in the sample preparation method adopted were limited to memory in the discharge tube; this was reduced by prolonged baking of the tubes at 700°.

Minimum sample size is about 10 μg N. In the normal to 5 atom% ^{15}N range, the overall method (sample preparation and analysis) gave 0.01 confidence intervals of $\pm$0.03 atom% ^{15}N.

RÉSUMÉ

Une méthode est décrite pour la préparation d'échantillons destinés à l'analyse isotopique de l'azote. Ce procédé permet la réutilisation des tubes à décharge, le contrôle de la pression dans le tube et le remplissage par un gaz inerte. On utilise l'oxydation à l'hypobromite pour la production d'azote. Les quantités limites et la précision de la méthode sont indiquées.

ZUSAMMENFASSUNG

Eine Probenvorbereitungseinheit wurde für die emissionsspektrometrische Analyse von ^{15}N entwickelt; die Einheit wurde zusammen mit dem Spektrometer NOI-4 erprobt. Mit der entwickelten Probenvorbereitungseinheit können wiederverwendbare Entladungsröhren benutzt werden; eine Kontrolle des Druckes in der Röhre sowie Spülung mit einem Inertgas und dessen Zuführung zur Röhre sind vorgesehen. Das Stickstoff-Gas wird durch Hypobromit-Oxidation erzeugt. Die instrumentellen Probleme und Fehlerquellen schlossen nichtlineare Gewinnung, Basislinienbestimmung, überlappende Banden und Nichtlinearität der Eichkurve ein. Probleme bei der angewendeten Probenvorbereitungsmethode waren auf einen Memory-Effekt in der Entladungsröhre beschränkt; dieser wurde durch längeres Erhitzen der Röhren bei 700° vermindert. Die minimale Probenmenge beträgt etwa 10 μg N. Im normalen ^{15}N-Bereich bis zu 5 Atom-% ergab die Gesamtmethode (Probenvorbereitung und Analyse) 0.01 Vertrauensintervalle von $\pm$0.03 Atom-% ^{15}N.

REFERENCES

1 H. Faust, *Isotopenpraxis*, 1 (1965) 62.
2 H. Faust, *Isotopenpraxis*, 3 (1967) 100.
3 J. A. Goleb and V. Middelboe, *Anal. Chim. Acta*, 43 (1968) 229.
4 J. P. Leickman, V. Middelboe and G. Proksch, *Anal. Chim. Acta*, 40 (1968) 487.
5 J. J. Oertli, *Plant Soil*, 25 (1966) 49.
6 H. Perschke and G. Proksch, in *Nitrogen-15 in Soil-Plant Studies*, Int. At. Energy Agency, Vienna, 1971, p. 223–225.
7 J. A. Goleb, *Argonne Rev.*, 6 (1970) 11.
8 R. Fiedler and G. Proksch, *Plant Soil*, 36 (1972) 371.
9 J. M. Bremner, in C. A. Black, *Methods of Soil Analysis*, Part 2, Amer. Soc. Agron. Inc., Madison, Wisc., 1965, p. 1256–1286.
10 H. Faust, *Z. Anal. Chem.*, 175 (1960) 9.
11 H. P. Broida and M. W. Chapman, *Anal. Chem.*, 30 (1958) 2049.
12 K. Sommer and H. Kick, *Z. Anal. Chem.*, 2 (1966) 21.
13 G. G. Mannella, *Chem. Rev.*, 63 (1963) 1

Analytica Chimica Acta, 65 (1973) 35–40

DETERMINATION OF TRACES OF GOLD BY HOLLOW-CATHODE EMISSION

W. W. HARRISON and E. H. DAUGHTREY

Department of Chemistry, University of Virginia, Charlottesville, Va. 22901 (U.S.A.)

(Received 10th November 1972)

The hollow-cathode discharge tube is best known today as a line source for atomic absorption spectrometry. However, long before this application, it was recognized[1] that the high energy available in the discharge offered potential utility as an analytical emission technique for trace analysis. That hollow-cathode emission has not become more widely used can be at least partially attributed to the considerable outlay of effort required to initially design and build a demountable hollow-cathode tube and associated vacuum system. Previous work in this laboratory[2,3] has described two different tube designs and their application. While these tubes worked well and were convenient to use, it was clear that wider acceptance and utilization of the hollow-cathode emission technique would result if a commercially available hollow-cathode tube-vacuum system package were available.

Such a unit has recently become available[4], marketed principally as a source for atomic absorption spectrometry. The demountable tube met the desired criteria of stabilized discharge, high emission intensity, and short turnaround time which should be characteristic of a hollow-cathode emission system. The commercial tube provided greater ruggedness and ease of demountability, as well as faster clean-up over the previously used designs. The maximum current capabilities were less than might be desired for an emission source, but good sensitivities were obtained.

Applicability of the tube to the analysis of gold-containing solutions was demonstrated as a part of a joint study with the University of Virginia Medical School involving treatment of rheumatoid arthritis patients with myochrysine, an organo-gold salt. The hollow-cathode emission response of both standard gold solutions and myochrysine solutions was studied.

EXPERIMENTAL

Hollow-cathode tube

The Glomax demountable hollow-cathode lamp (Barnes Engineering Co.) was used for this investigation with one modification. The polyethylene gas lines and fittings were replaced with brass machine fittings to which a short length of 0.25-in copper tubing had been soldered. This allowed the attachment of the hollow-cathode tube to an existing vacuum system[2] by means of a 0.25-in Cajon Ultra Torr fitting. The system was operated under static pressure conditions by plugging one gas port.

The tube was mounted on an Ealing vertical and transverse motion carrier

which provided translation along two axes for optical alignment with the spectrometer slit.

Cathodes were machined from copper, aluminum, and stainless steel to the required dimensions. Graphite cathodes supplied by the manufacturer were also used.

Vacuum system

The vacuum system (10^{-5} mm) consisted of a two-stage mercury diffusion pump backed by an oil rotary pump, along with the associated traps, vacuum monitors, and a gas inlet manifold. The hollow-cathode tube was connected to the vacuum system by 0.25-in copper tubing and a stainless-steel flexible bellows coupled by Cajon Ultra Torr fittings. The filler gas pressure was read on a differential oil manometer filled with Apiezon oil. Static operation, rather than a flow system, was chosen because the analysis of solutions required only short-term operation.

Measurement system

The radiation from the hollow-cathode source was directed to a Jarrell-Ash 0.5-m spectrometer, the resultant output signal from the photomultiplier being fed into a P.A.R. Model 122 Lock-In amplifier, producing an output signal which was fed into a Sargent Model SRG recorder. The hollow-cathode tube was powered by a Kepco Model BHK 2000 power supply which can provide regulated current up to 200 mA with a maximum operating potential of 1000 V.

Reagents

Reagent-grade chemicals were used throughout the investigation. Gold standards were prepared by dilution of a 100-p.p.m. stock which was made by dissolving gold sponge in aqua regia, followed by proper dilution. The myochrysine standard (Merck, Sharp, and Dohne, Westpoint, Pa.) was prepared by dilution of a 1-ml, 50-mg ampoule of the drug. Distilled, deionized water was used for making up all standard solutions and for rinsing.

Procedure

Standard gold solutions of different concentrations were prepared and 0.1 ml of the test solution was transferred to the cathode cavity by a 100-μl syringe. After evaporation to dryness under an infrared lamp, the cathode was placed in the cathode block, and the system was evacuated, flushed with the desired filler gas, re-evacuated, and filled to the proper pressure of rare gas. The constant current power supply was pre-set to the desired operating value and the discharge was initiated. The spectrometer and associated read-out produced a display of emission intensity as a function of time. Owing to the very small amount of test element present, the recording trace showed a rapid rise in emission intensity followed by a decrease to a background level. This peak intensity was taken in each case. Approximately 5–10% r.s.d. was observed. Blanks were run to determine the contribution to the emission intensity from the cathode material itself.

Cathodes were re-used by cleaning with aqua regia followed by rinsing copiously with distilled, deionized water.

RESULTS AND DISCUSSION

The strongest analytical emission lines for gold are listed[5] as 242.8 nm and 267.6 nm, the former being the more intense. However, because of high background in the 242.8-nm region from all of the cathode materials except copper, the 267.6-nm line was chosen.

Copper, aluminum, graphite, and stainless steel were investigated as possible cathode materials. Copper and aluminum were sputtered too easily for stable discharge at the conditions necessary to yield reasonable sensitivity for gold. Graphite proved unsuitable, owing to lack of sensitivity and reproducibility arising from the porosity of the graphite. Stainless steel has been the most satisfactory cathode material despite its complex emission spectrum, which included interference with the strongest gold resonance line. The steel cathodes held up well under repeated tube firings, produced the best overall signal, and cleaned up readily.

Surface preparation of the electrode cavity appears to be a critical factor in both signal intensity and reproducibility. The aqua regia cleaning between runs showed best results. Sputter release of the gold from a previously used cathode without such acid treatment yielded a greatly reduced sensitivity. In general, every effort must be made to maintain a reproducible cavity surface.

Helium, neon, and argon were investigated as filler gases. Neon has an overlapping emission line with the 267.6-nm gold line, unresolved by the spectrometer, and was therefore rejected as a filler gas. Optimization of tube current and filler gas pressure for helium and argon was performed. Helium was not satisfactory because it gave a much lower signal-to-background ratio than argon and was in a region of rapidly changing background intensity with wavelength. For argon as a filler gas, the response of emission intensity as a function of filler gas pressure is given in Fig. 1.

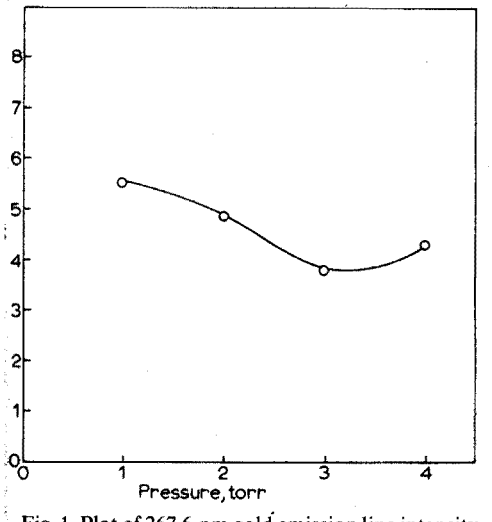

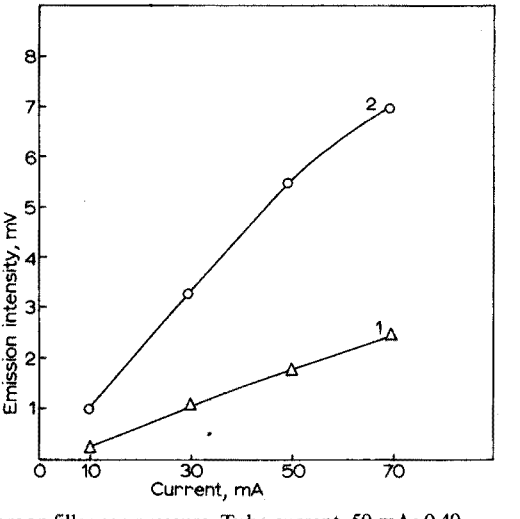

Fig. 1. Plot of 267.6-nm gold emission line intensity *vs.* argon filler gas pressure. Tube current, 50 mA; 0.40 μg gold.

Fig. 2. Plot of 267.6-nm gold emission line intensity *vs.* tube current for (1) background from cathode and (2) signal plus background for 0.40 μg Au. Filler gas, argon at 1 torr; other conditions as in Fig. 1.

The best sensitivity and stability were found at 1 torr pressure of argon. Below one torr, the discharge became difficult or impossible to initiate. Beyond the 4-torr value shown in Fig. 1, an unstable discharge resulted. Figure 2 shows the effect of tube current on both gold intensity and cathode background. Optimal current was taken to be 50 mA, which with the 1-torr pressure offered the best compromise between stability and emission intensity. Argon was thus used for all measurements in this study.

The type of signal obtained from the discharge is shown in Fig. 3. Within the first few seconds after initiation, the gold emission had peaked out and dropped rapidly to the rackground emission level. The background response was slower, allowing a favorable signal-to-background level early in the discharge period.

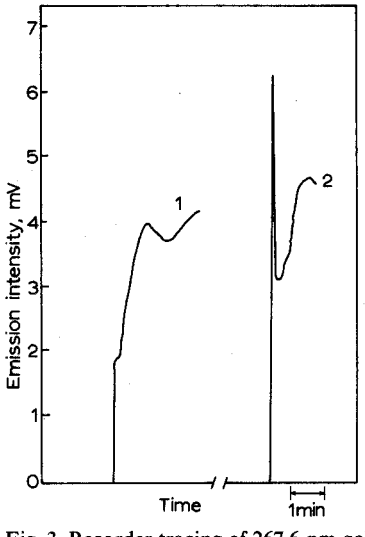

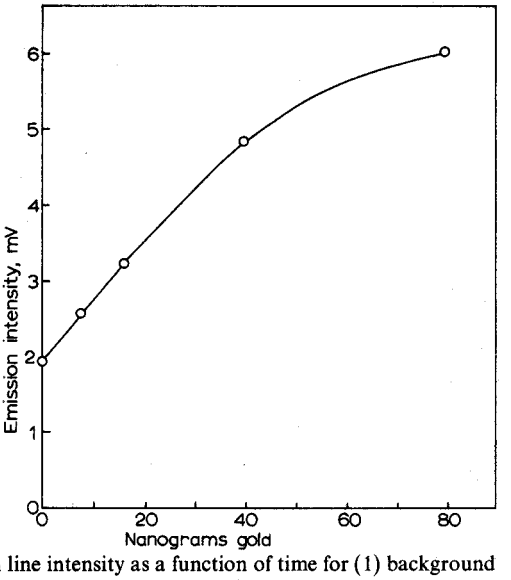

Fig. 3. Recorder tracing of 267.6-nm gold emission line intensity as a function of time for (1) background from cathode and (2) signal plus background of 80 ng Au as myochrysine. Filler gas, argon at 1 torr; tube current, 50 mA.

Fig. 4. Working curve for gold as myochrysine at 267.6 nm. Conditions as in Fig. 3.

Working curves for gold were constructed with standard solutions prepared from (*a*) gold as the metal dissolved in aqua regia and (*b*) gold as myochrysine. Figure 4 shows the lower limits of effective working range for the hollow-cathode technique. Multiple sample applications could further improve this. At a higher working range, the emission response of gold solutions as dissolved metal and myochrysine in the hollow-cathode discharge is shown in Fig. 5. The negative deviation from linearity of emission intensity at the higher concentrations might be partially at tributed to the recorder pen response (1 s f.s.d.) as the maximum gold response occurred extremly rapidly. The slight difference in the response of myochrysine and dissolved metal would seem to be related to their relative ease of decomposition in the discharge. At higher concentrations (>1 p.p.m.), myochrysine produces a

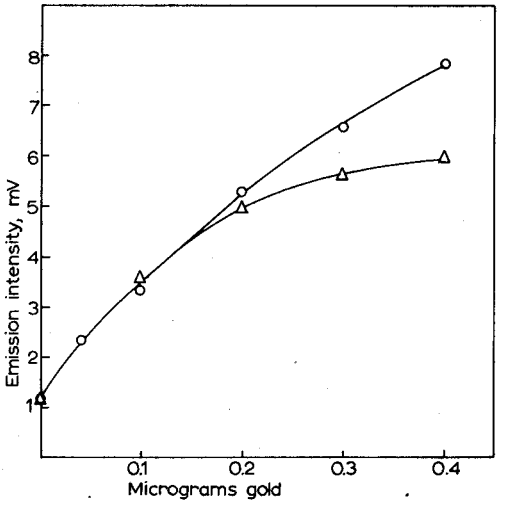

Fig. 5. Working curves for gold at 267.6 nm as (1) myochrysine (○) and (2) metal dissolved in aqua regia (△). Filler gas, argon at 1 torr; tube current, 50 mA.

somewhat greater signal intensity and a more rapid signal rise to the peak value. The

$$\mathrm{Au{-}S{-}\overset{\displaystyle CH_2COONa}{\overset{|}{C}}HCOONa}$$

myochrysine molecular structure, may allow gold release more easily by breaking of the gold–sulfur linkage in the hallow-cathode discharge. The small difference in response is not particularly critical as any biological sample analyzed by hollow-cathode emission would be ashed to the inorganic salt before analysis.

Conclusion

The results reported in the above work demonstrate the utility of a commercially available hollow-cathode tube as an excitation source for emission spectrometric trace analysis of solutions. Further optimization of equipment and parameters should improve both sensitivity and reproducibility. Currently under investigation in this laboratory are cathode geometry, surface effects, and solvent extraction techniques. The simple design and ready availability of the commercial tube should encourage the use of hollow-cathode emission as a complementary technique to other trace analysis procedures.

This work was supported by Grant No. GM-14569, USPHS.

SUMMARY

The utility of a commercially available demountable hollow-cathode tube for emission spectrometric trace element analysis of solutions is demonstrated. The effects of cathode material, clean-up procedure, filler gas, and tube current were investigated to determine the conditions resulting in a satisfactory compromise between sensitivity and stability. Solutions of gold as myochrysine and as the metal dissolved in aqua regia were analyzed to show application of the commercial tube.

RÉSUMÉ

L'utilité d'un tube à cathode creuse démontable pour l'analyse de traces par spectrométrie d'émission est démontrée. Divers paramètres sont examinés, matériel cathodique, gaz de remplissage, courant de la lampe, afin de trouver un compromis satisfaisant entre sensibilité et stabilité. Des solutions d'or, comme myochrysine et comme métal dissous dans l'eau régale ont été analysées pour montrer l'utilité d'une telle lampe dans le commerce.

ZUSAMMENFASSUNG

Die Anwendbarkeit einer handelsüblichen demontierbaren Hohlkathodenröhre für die emissionsspektrometrische Analyse von Spurenelementen in Lösungen wird gezeigt. Die Einflüsse von Kathodenmaterial, Aufbereitungsverfahren, Füllgas und Röhrenstrom wurden zur Festlegung der Bedingungen untersucht, bei denen sich ein zufriedenstellender Kompromiss zwischen Empfindlichkeit und Stabilität ergibt. Gold in Form von gelöstem Myocrisin und als Königswasserlösung wurde analysiert, um die Anwendung der kommerziellen Röhre zu demonstrieren.

REFERENCES

1 J. R. McNally, G. R. Harrison and E. Rowe, *J. Opt. Soc. Amer.*, 37 (1947) 93.
2 W. W. Harrison and N. J. Prakash, *Anal. Chim. Acta*, 49 (1970) 151.
3 N. J. Prakash and W. W. Harrison, *Anal. Chim. Acta*, 53 (1971) 421.
4 *Glomax Demountable Hollow Cathode Lamp Operating and Service Manual*, Barnes Engineering Company, Stamford, Conn.
5 *Experimental Transition Probabilities for Spectral Lines of Seventy Elements*, NBS Monograph 53, U.S. Government Printing Office, Washington, D.C., 1962.

Analytica Chimica Acta, 65 (1973) 41–47

DETERMINATION OF LEAD IN ATMOSPHERIC PARTICULATES BY FLAMELESS ATOMIC ABSORPTION SPECTROMETRY WITH A GRAPHITE TUBE

M. JANSSENS and R. DAMS

Institute for Nuclear Sciences, Ghent University, Ghent (Belgium)

(Received 27th November 1972)

Flameless atomic absorption spectrometry is a sensitive, rapid, selective and precise technique which is very attractive for the routine analysis of small liquid and solid samples. Little pretreatment of the samples is necessary, so that the risk of contamination is small. Recently, this technique has been applied by Omang[1] and by Woodriff and Lech[2] to the determination of lead in atmospheric particulates.

In the present study the optimal conditions for rapid atmospheric analysis were determined. Aerosols were collected by passing air through a cellulose filter. A fraction of this filter was subjected to ultrasonic vibration in a suitable solvent to remove the particulate matter. The lead content of this solution was determined directly by atomic absorption with a Massmann oven. This method has a routine sensitivity for lead of 0.01 μg m^{-3} of air for one-eighth of a 24-h filter.

EXPERIMENTAL

Apparatus and instrument settings

All measurements were done with a Perkin-Elmer Model 303 double-beam atomic-absorption spectrophotometer, equipped with a Perkin-Elmer HGA-70 graphite cell, a deuterium background corrector, a Hitachi-Perkin-Elmer recorder Model 159 and an Intensitron lead hollow-cathode lamp.

Optimal operating conditions were found to be as follows: lamp current 40 mA, slit 4, monochromator U.V., wavelength 283.3 nm, program 2 (drying at 100°) or program 5 (drying at 100° and charring at 490°) and an atomization voltage of 9 V (2400°). Samples of 10–50 μl were injected into the graphite tube with Eppendorf micropipettes.

Ultrasonic removal of the lead from the filter was carried out with a Branson ultrasonic cleaner, consisting of an ultrasonic generator Model LG-150 and an ultrasonic tank-type transducer LTH-60.

The low-temperature asher was from International Plasma Corporation. The working conditions were as follows: temperature below 150°, oxygen flow 60–70 cm^3 min^{-1}, pressure 1 mm Hg, ashing period 1 h. The ash was dissolved in 100 ml of 0.1 *M* nitric acid.

Reagents and solutions

Merck Suprapure nitric acid (14 *M*) was diluted to 0.1 *M*. The lead stock

solution was made from 1.599 g of reagent-grade lead nitrate dried at 110°, dissolved in 0.1 *M* nitric acid and diluted with 0.1 *M* nitric acid to 1 l. The solution was standardized by electrolysis and contained 1.000 mg Pb ml^{-1}. The stock solution was diluted with 0.1 *M* nitric acid to concentrations varying from 20 to 250 μg Pb l^{-1}. These dilutions were prepared weekly.

Sampling

Air particulates were collected by passing air through Whatman No. 41 cellulose filter paper. Two types of pump were employed[3]. The samples used to determine the working conditions were collected with a low-vacuum high-volume Unico 550-Turbine Jet Sampler (initial flow 70 m^3 h^{-1}), equipped with 20 cm × 25 cm filter holders. Routine samples were collected with high-vacuum Becker pumps (20 m^3 h^{-1}) and filter holders of 10 cm diameter. For the two sets of samplers a 24-h collection period was equivalent to, respectively, about 1200 m^3 and 400 m^3 of air, or 3 m^3 and 6 m^3 of air per cm^2 of exposed filter. A 10-cm^2 piece was cut from the 20 cm × 25 cm filters, and a one-eighth segment from the 10-cm diameter filters, for the lead determination. The major part of the filter was then available for the determination of other components.

Analytical procedure

Transfer the filter sector into *ca.* 50 ml of 0.1 *M* nitric acid and expose it to ultrasonic vibration for 10 min. Decant the solution and repeat the ultrasonic treatment in 30 ml of 0.1 *M* nitric acid for 5 min. Wash the beaker several times with 0.1 *M* nitric acid, combine all extracts and washings, and dilute to 100 ml in a volumetric flask. Treat a blank filter in the same way. Use only glassware which has been pretreated with nitric acid for 24 h.

Determine lead by injecting 10–50 μl of the extract into the graphite cell. Record the % absorption at the 283.3-nm resonance line. Measure each extract at least twice in different series of readings of standard and sample solutions. Convert the average peak height to absorbance. Subtract the absorbance value obtained after injecting the same volume of an extract of a blank filter, and determine the concentration from a calibration curve.

Construct the calibration curve by injecting standard solutions, in aliquots with the same fixed volume as that of the samples. This method is preferable to injecting variable volumes of one standard solution. Measure each standard solution at least three times and plot the averages against the total amount of lead present in the furnace. The calibration curve was linear up to 5 ng and 1% absorption was obtained for 0.1 ng of lead. The coefficient of variation of the readings was about 4% and 2% in the 20% and 40% absorption range, respectively.

Establishment of the working conditions

Extraction procedure. To dissolve the lead-containing particles from the cellulose filter, ultrasonic vibration was applied to the filters in nitric acid solutions. To select the most suitable acid concentration, a 20 cm × 25 cm filter was cut into twenty-four 10-cm^2 sections. After ultrasonic treatment, the % absorption was recorded as a function of acid concentration. Figure 1, curve a, shows that the peak height was strongly dependent on the acidity of the extracting solvent. How-

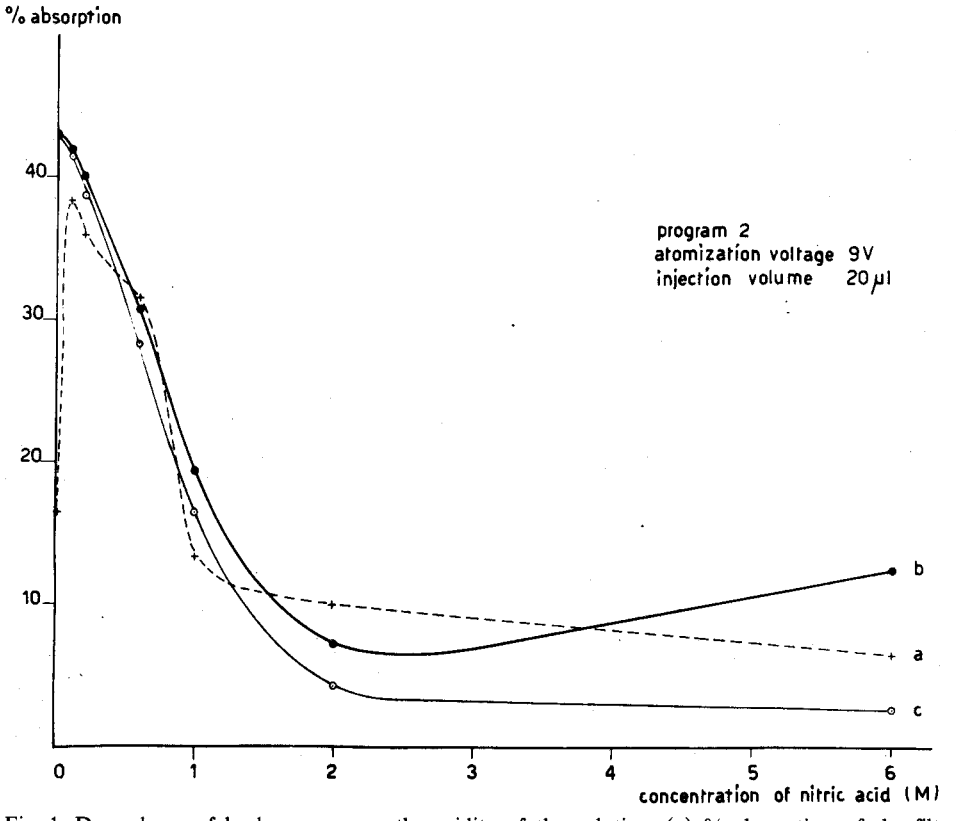

Fig. 1. Dependence of lead recovery on the acidity of the solution. (a) % absorption of the filter solutions after ultrasonic treatment in different acid concentrations as a function of the acidity; (b+c) % absorption of a standard solution of 200 μg Pb l^{-1} as a function of acidity: blank filter value not subtracted (b), blank filter value subtracted (c).

ever, measurement of a standard lead solution indicated that the % absorption was also strongly dependent on the acid concentration, as shown in curve b. Moreover, high acidity caused high blank values as shown in curve c. The results indicate the importance of running standards, blanks and samples at the same acidity. It was concluded further that the acidity should be as low as possible in order to avoid low and irreproducible signals. On the other hand, distilled water was not effective in completely removing the lead from the filter. Consequently, 0.1 *M* nitric acid was selected as the best compromise for quantitative extraction and high sensitivity.

To investigate the time dependence of the ultrasonic treatment, three successive extractions with fresh acid were carried out during 15 min, 5 min and 5 min, or during 5 min, 5 min and 5 min. Each fraction was separately analysed after dilution to 100 ml. The results (Table I) indicated that a 5-min treatment was generally sufficient but that high lead concentrations required a second treatment. Jernigan *et al.*[4] found that 5-, 10-, 15-, 20- or 25-min ultrasonic extractions resulted in the same peak heights. In the present work, 30-ml extracts of three successive 5-min extractions were combined, and the absorbances were compared

TABLE I

SUCCESSIVE ULTRASONIC TREATMENTS FOR THE RECOVERY OF LEAD

(Results are expressed as μg per 100 ml)

Filters	*5 min*	*5 min*	*5 min*		
Filter A 1	49.2	1.0	0.4		
2	48.2	1.0	0.2		
Filter B	54.0	1.0	0.7		
Filter C	67.6	23.0	0.9		
		15 min		*5 min*	*5 min*
Filter A 1		49.4		1.6	0.5
2		51.2		2.1	0.1

to those obtained from other 10-cm^2 segments of the same filter after a single 15-min extraction with 30 ml of acid. No significant difference could be found. The volume of the first ultrasonic cleaning could also be varied from 30 to 60 ml without any influence on the results. These experiments suggest that the lead was nearly quantitatively removed from the filter by the adopted procedure. This conclusion was confirmed by ashing 10-cm^2 filter segments in a low-temperature asher. The same results were obtained by ultrasonic extraction and by low-temperature ashing, namely, 13.59 ± 0.20 μg m^{-3} (13 determinations) and 13.60 ± 0.14 μg m^{-3} (4 determinations), respectively. Vigorous shaking for 15 min also appeared to be as efficient as ultrasonic cleaning, but resulted in a total destruction of the filter so that program 5 (ashing at 490°) had to be used for the atomic absorption in order to obtain reproducible absorption peaks.

Analytical-grade nitric acid was found to contain easily detectable amounts of lead, in agreement with Omang's findings[1], whereas suprapure acid did not show a significant absorption peak after injecting 20 μl of a 0.1 *M* solution. Owing to the very low signal recorded from blank filters, the lead concentration of the filters could not be calculated with a reasonable precision. The absorbance value, recorded in the same experimental conditions as for the samples, was, however, subtracted from the sample absorbance value.

No loss and no increase of lead caused by absorption on, or exchange with, the glassware was observed after 0.1 *M* nitric acid solutions had been aged for one week.

Atomic absorption spectrophotometry. Amounts of solution ranging from 10 to 100 μl could be injected, but for routine analysis 20 μl was used. Since a comparison of program 5 with program 2 gave the same results, the latter was routinely applied. Only when small air samples were to be analysed, which required the use of a larger filter sector (a quarter of a 10-cm diameter filter) in 50 ml of acid solution and injection of 50 μl of solution, did ashing at 490° in program 5 appear to give more reproducible results. A variation of the atomization voltage from 3 to 10 V indicated a maximal peak height in the range from 7.5 to 9.5 V. As a result 9 V was chosen as an optimal working condition. Recordings with and without a deuterium background corrector showed no effects from non-specific

background absorption. No absorption peak appeared when standard solutions of other metals, *e.g.* Na, K, Ca, Mg and Cu, were injected in concentrations 5 times higher than can be expected in aerosols.

RESULTS AND DISCUSSION

The standard deviation of the atomic absorption technique was found to lie between 2 and 4% for absorbance values larger than 0.1. The standard deviation of the complete procedure *i.e.* fractionation of the filter, ultrasonic cleaning and atomic absorption, was 5.5% when 10 cm^2 (± 30 m^3 air) of a 20 cm × 25 cm filter (13 measurements, absorbance = 0.171) was used, and 3.0% when one-eighth segment (± 50 m^3 air) of a circular filter (8 measurements, absorbance = 0.186) was used. No systematic inhomogeneities were found over the filter. These results indicate that a small fraction of the filter is representative of the complete filter. This finding is in agreement with that of Pierce and Meyer[5] who concluded from a statistical analysis that the lead estimate based on one 50% segment was no more precise or more accurate than that based on one 10% segment of a filter. The sensitivity for 1% absorption was 0.1 ng. With an injection volume of 20 μl, the lead content of 100 ml of solution can thus be as low as 0.5 μg. When a one-eighth segment of a 24-h circular filter was used, *i.e.* the particulates from about 50 m^3 of air, the lowest detectable concentration in the air was 0.01 $\mu g\ m^{-3}$. As typical concentrations in urban air are 0.5 $\mu g\ m^{-3}$, the sampling time can be reduced to 30 min. If sensitivity were a problem, as with very low concentrations of lead in the air or very short sampling periods, the detection limit can be lowered by another order of magnitude by the use of a more sensitive resonance line (217.0 nm) or by extracting a larger segment of the filter and diluting to only 50 ml instead of 100 ml.

APPLICATION

An automatic sample changer, equipped with twenty-four 10-cm filters, and a Becker KVT 40 pump[6] were used to take a series of 93 consecutive 15- or 20-min

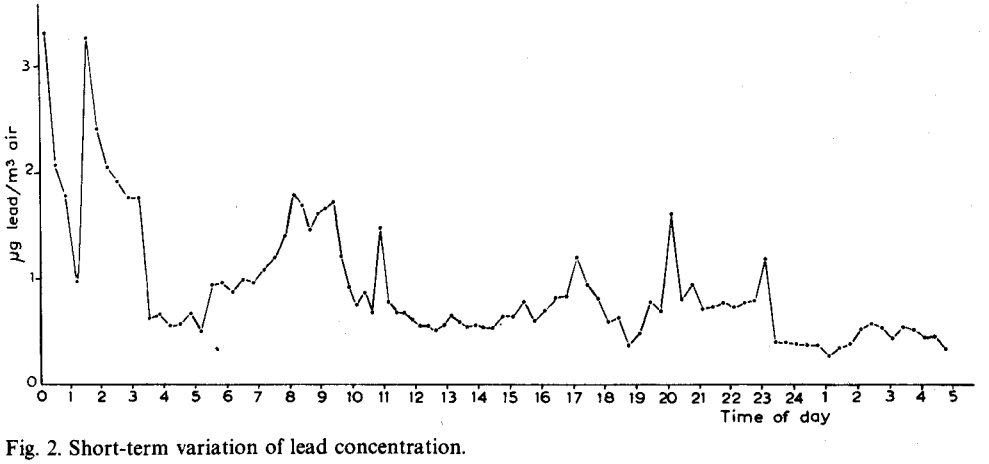

Fig. 2. Short-term variation of lead concentration.

samples in downtown Liège, Belgium. The sampler was located on a roof, about 10 m above ground level and 50 m from the nearest street. The flow rate of the sampler was about 0.5 m^3 min^{-1}. About 7–10 m^3 of air passed through each filter and one quarter of each filter was used for the analysis. After extraction, the solution was diluted to 50 ml, 20 μl or 50 μl of which was injected. Figure 2 is a plot of the concentrations *versus* time. The concentrations varied from 0.3 to 3.3 $\mu g\ m^{-3}$. Because the % absorptions were always higher than 10%, the relative standard deviation was estimated to be less than 5%. Therefore, the irregular shape of the concentration curve is believed to be due to real atmospheric variations. Although not all the variations can be explained, some trends are obvious. The broad peaks in the morning and in the late afternoon and evening are probably related to traffic maxima. A strong industrial source of lead to the east of Liège, may have caused the high nocturnal concentrations in the first few samples because there was a light breeze from the eastern sector during that time. During the second midnight the wind was from the south, and only low lead concentrations were found.

The authors are highly indebted to Prof. Dr. J. Hoste for his continuous interest and helpful suggestions. They thank Prof. Dr. F. Verbeek and Prof. Ir. F. Bosch, respectively, for the use of the atomic absorption and ashing equipment. They acknowledge valuable discussions with Mr. G. Demolder.

SUMMARY

A procedure for the determination of atmospheric particulate lead by flameless atomic absorption spectrometry is described. Aerosols are collected on 10-cm Whatman 41 filters with high-volume pumps. The lead is removed from a one-eighth sector of the filter by two ultrasonic treatments in 0.1 *M* nitric acid for 10 and 5 min, respectively. Investigations, including comparison with samples pre-ashed at low temperature, indicated that the lead was completely recovered. Routinely 20-μl amounts of the solution are injected into a graphite tube and the % absorption at 283.3 nm is measured. The elements normally encountered in atmospheric aerosols do not interfere. The sensitivity for 24-h samples is 0.01 $\mu g\ m^{-3}$ of air. Sampling time can be reduced to a few minutes in urban air when a larger segment of the filter is used and a larger volume is injected. The reproducibility of the complete procedure is 3% for a typical lead concentration of 0.35 $\mu g\ m^{-3}$. The method was applied to short-period variations of the lead concentration in urban air.

RÉSUMÉ

On décrit une méthode pour le dosage spectrophotométrique par absorption atomique sans flamme du plomb atmosphérique. Les aérosols sont recueillis sur filtres Whatman 41. Un fragment du papier est traité aux ultrasons, dans l'acide nitrique 0.1 *M* pour dissoudre le plomb. Des volumes de 20 μl de solution sont injectés dans un tube de graphite. Le % d'absorption est mesuré à 283.3 nm. Les éléments normalement présents dans des aérosols atmosphériques ne gênent pas. La sensibilité pour des échantillons de 24 h est de 0.01 $\mu g\ m^{-3}$ d'air. La durée du

prélèvement peut être réduite à quelques minutes. La reproductibilité est de 3% pour une concentration typique de plomb de 0.35 μg m^{-3}.

ZUSAMMENFASSUNG

Ein Verfahren für die Bestimmung von Blei in atmosphärischen Aerosolen mittels flammenloser Atomabsorptionsspektrometrie wird beschrieben. Die Aerosole werden auf Whatman 41Filtern von 10 cm Durchmesser mit Hochleistungspumpen gesammelt. Das auf einem Achtelsektor des Filters befindliche Blei wird durch zwei Ultraschallbehandlungen von 10 bzw. 5 min Dauer in 0.1 *M* Salpetersäure entfernt. Die Untersuchungen sowie der Vergleich mit Proben, die vorher bei niedriger Temperatur verascht worden waren, ergaben, dass das Blei vollständig erfasst wurde. Bei Routineanalysen wird eine 20 μl-Probe der Lösung in ein Graphit-Heizrohr injiziert und die Absorption bei 283.3 nm gemessen. Die normalerweise in atmosphärischen Aerosolen vorliegenden Elemente stören nicht. Die Empfindlichkeit für 24 h-Proben ist 0.01 μg m^{-3} Luft. Die Zeitdauer der Probenahme in Stadtluft kann auf wenige Minuten herabgesetzt werden, wenn ein grösseres Filtersegment und ein grösseres Volumen für die Bestimmung verwendet werden. Die Reproduzierbarkeit des gesamten Verfahrens beträgt 3% für eine typische Bleikonzentration von 0.35 μg m^{-3}. Die Methode wurde auf Stadtluft angewendet, deren Bleikonzentration in kurzen Zeitabständen variiert.

REFERENCES

1 S. H. Omang, *Anal. Chim. Acta*, 55 (1971) 439.
2 R. Woodriff and J. F. Lech, *Anal. Chem.*, 44 (1972) 1323.
3 R. Dams and R. Heindryckx, *Atmos. Environ.*, in press.
4 E. L. Jernigan, B. L. Ray and R. A. Duce, *Atmos. Environ.*, 5 (1971) 881.
5 J. O. Pierce and J. H. Meyer, *Atmos. Environ.*, 5 (1971) 811.
6 K. A. Rahn and G. Windels, to be published.

Analytica Chimica Acta, 65 (1973) 49–58

DUAL-WAVELENGTH SPECTROPHOTOMETRY

PART IV. QUALITATIVE AND QUANTITATIVE ANALYSIS BY MEANS OF FIRST-DERIVATIVE SPECTRA

SHOZO SHIBATA, MASAMICHI FURUKAWA and KAZUO GOTO
Government Industrial Research Institute, Nagoya Kita-ku, Nagoya (Japan)
(Received 25th November 1972)

The merit of directly recording a curve of the first-order differential coefficient of absorbance A or transmission T with respect to wavelength λ, *i.e.* $dA/d\lambda$ *versus* wavelength, has been pointed out by Giese and French[1] and Saidel[2]. The first-derivative spectrum can be recorded by using a conventional double-beam instrument with an attachment, or a specially designed derivative spectrophotometer[3,4], but these techniques are rather complicated. However, such spectra can be recorded easily by dual-wavelength measurements, if the two wavelengths λ_1 and λ_2 are set very close to each other (usually 1–2 nm) and scanned simultaneously. In previous papers of this series, the general technique of dual-wavelength measurement[5], simultaneous determinations of mixtures[6,7] and high-sensitivity spectrophotometry[8] have been reported. Recently, Porro[9] reviewed the analytical possibilities of dual-wavelength spectrophotometry.

The principle of the dual-wavelength measurement is quite simple. Instead of one monochromator, two identical monochromators are used. The radiation entering the system is divided equally between the two monochromators, which are time-shared through a single cell by means of a chopper, and the transmitted radiation is then detected by means of photomultipliers. The signals from the photomultipliers enter the difference circuit, and the output ΔA is recorded.

The merits of directly recording a curve of the first-order differential coefficient of absorbance or transmission are as follows.

1. Even when two or more absorption bands overlap entirely or very closely, each of the bands can be detected.

2. Very small absorption bands which lie on a steep portion of an absorption curve, and any shoulders in the absorption curves are clearly resolved.

3. Very broad absorption bands can be located precisely.

4. Generally, the differential coefficients at specific wavelengths are linearly related to the concentration of the corresponding components, thus permitting their determination.

5. Variations in turbidity or background do not affect measurements because λ_1 and λ_2 are set close to each other.

Therefore, it seems probable that derivative spectrophotometry will facilitate the detection and determination of, for example, impurities in drugs and chemicals, and food additives as well as industrial wastes.

In this paper, practical examples are given which typify the applications of derivative spectra.

EXPERIMENTAL

Reagents

Rare-earth metal solutions. These were prepared by dissolving 99.99% Johnson Matthey oxide with perchloric acid; the final solutions were 1 *M* in perchloric acid solution.

2,4-Dichlorophenol and *2,4,6-trichlorophenol* were purified by conventional methods.

All other reagents used were prepared from high-purity materials or purified reagents, and all solutions were prepared with redistilled water.

Apparatus

A Hitachi 356 two-wavelength spectrophotometer was used with 1-cm quartz cells. This apparatus can be used both as a dual-wavelength and a classical double-beam recording spectrophotometer. The baseline was recorded by using the solvent alone.

QUALITATIVE ANALYSIS

An accurate analysis of a complex absorption is difficult to obtain by classical

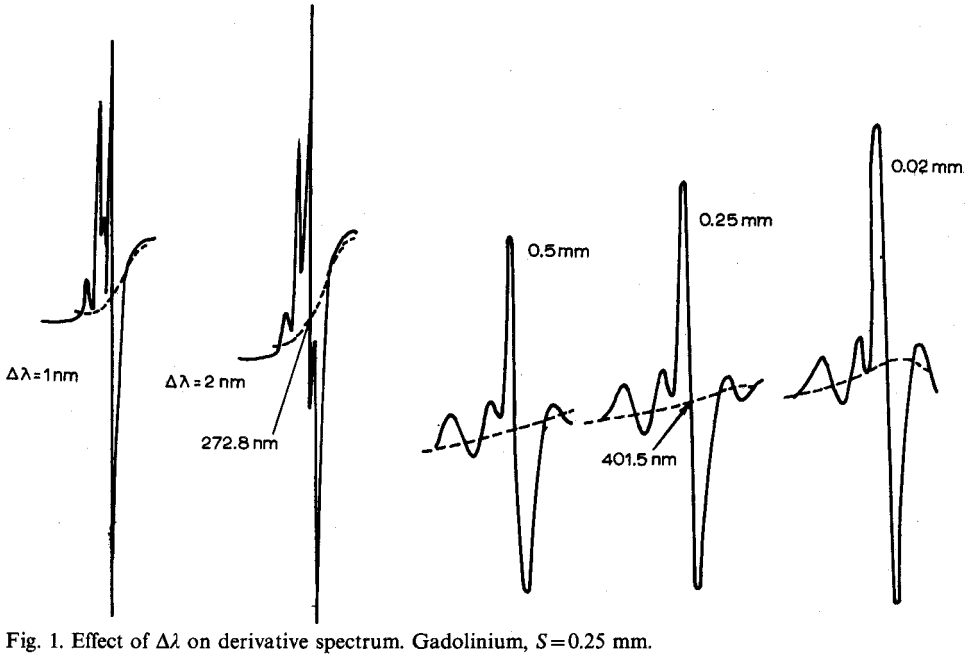

Fig. 1. Effect of $\Delta\lambda$ on derivative spectrum. Gadolinium, $S=0.25$ mm.

Fig. 2. Effect of slit width (S) on the absorption spectrum. Samarium, $\Delta\lambda=2$ nm.

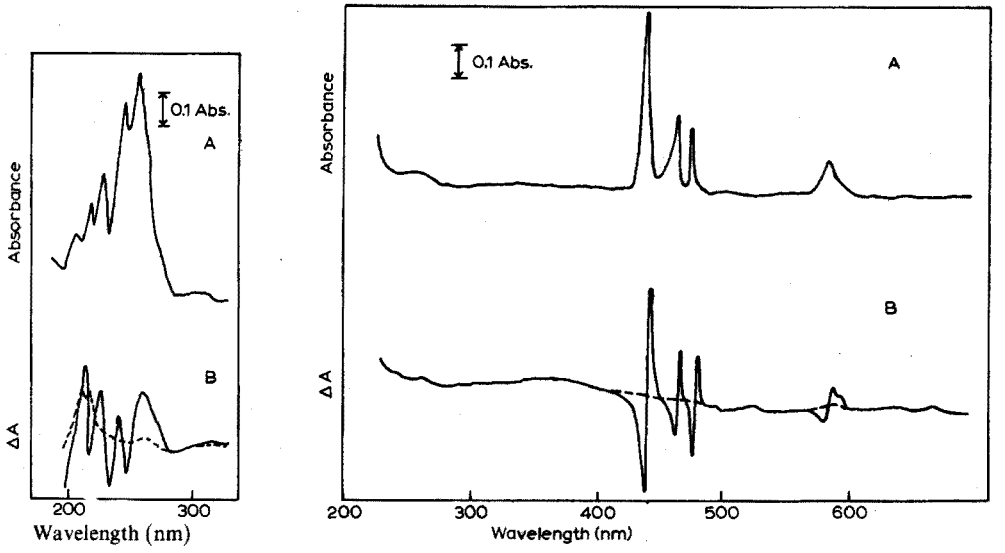

Fig. 3. Absorption (A, $\lambda_1 = \lambda_2$) and derivative (B, $\Delta\lambda = 2$ nm, $S = 0.25$ mm) spectra of cerium. 0.0075 g CeO_2 dissolved in and diluted to 25 ml with 1 *M* perchloric acid, 0.5-cm cell.

Fig. 4. Absorption (A, $\lambda_1 = \lambda_2$) and derivative (B, $\Delta\lambda = 2$ nm, $S = 0.25$ mm) spectra of praseodymium. 0.537 g Pr_6O_{11} dissolved in and diluted to 25 ml with 1 *M* perchloric acid, 0.5-cm cell.

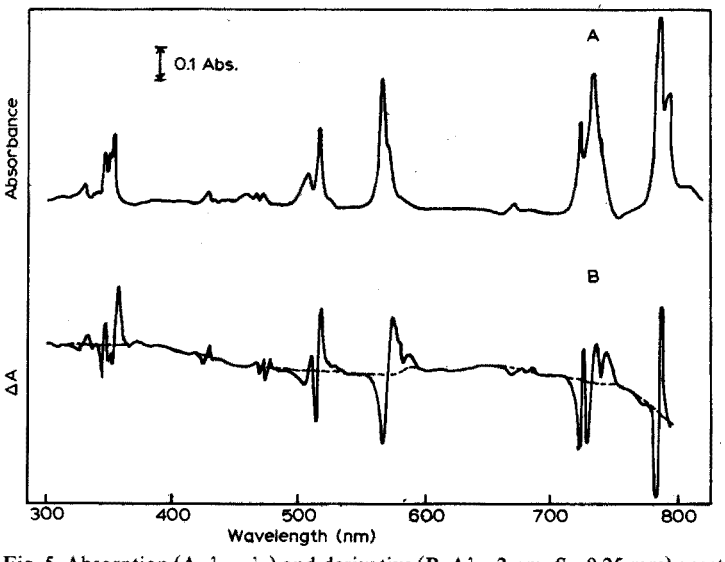

Fig. 5. Absorption (A, $\lambda_1 = \lambda_2$) and derivative (B, $\Delta\lambda = 2$ nm, $S = 0.25$ mm) spectra of neodymium. 0.546 g Nd_2O_3 dissolved in and diluted to 25 ml with 1 *M* perchloric acid, 0.5-cm cell.

double-beam spectrophotometry. Moreover, the analysis is further complicated when the individual components in a complex spectrum absorb in nearly the same wavelength region. In such cases, when absorption spectra represent overlapping bands, it is desirable to resolve these bands.

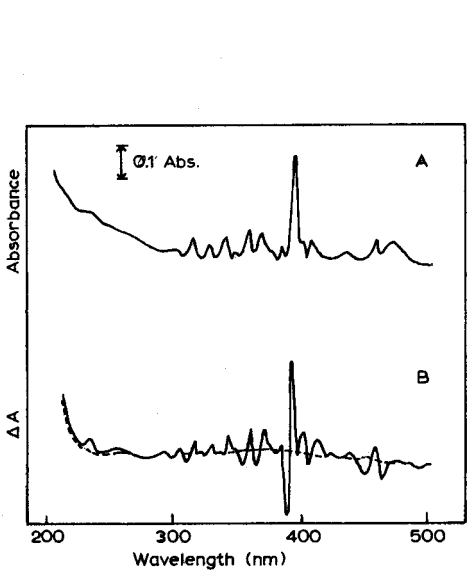

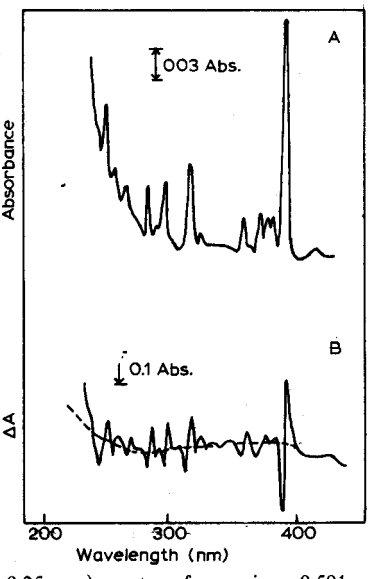

Fig. 6. Absorption (A, $\lambda_1 = \lambda_2$) and derivative (B, $\Delta\lambda = 2$ nm, $S = 0.25$ mm) spectra of samarium. 0.501 g Sm_2O_3 dissolved in and diluted to 25 ml with 1 *M* perchloric acid, 1-cm cell.

Fig. 7. Absorption (A, $\lambda_1 = \lambda_2$) and derivative (B, $\Delta\lambda = 2$ nm, $S = 0.25$ mm) spectra of europium. 0.550 g Eu_2O_3 dissolved in and diluted to 25 ml with 1 *M* perchloric acid, 1-cm cell.

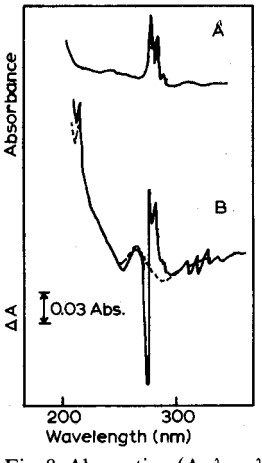

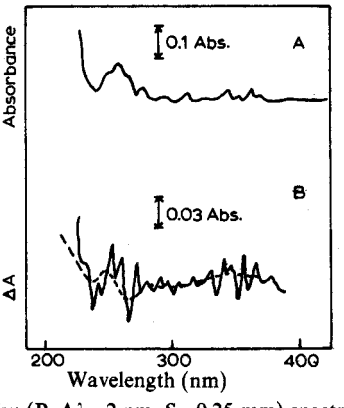

Fig. 8. Absorption (A, $\lambda_1 = \lambda_2$) and derivative (B, $\Delta\lambda = 2$ nm, $S = 0.25$ mm) spectra of gadolinium. 0.538 g Gd_2O_3 dissolved in and diluted to 25 ml with 1 *M* perchloric acid, 1-cm cell.

Fig. 9. Absorption (A, $\lambda_1 = \lambda_2$) and derivative (B, $\Delta\lambda = 2$ nm, $S = 0.25$ mm) spectra of terbium. 0.551 g Tb_2O_3 dissolved in and diluted to 25 ml with 1 *M* perchloric acid, 1-cm cell.

The most important factors for measurement of derivative spectrum are the differential wavelength ($\Delta\lambda$) and the slit width (S). The difference between the maximal ΔA value and the derivative zero line gives the maximal rate of change of absorbance per $\Delta\lambda$ between sample (λ_2) and reference (λ_1) beams when the first-

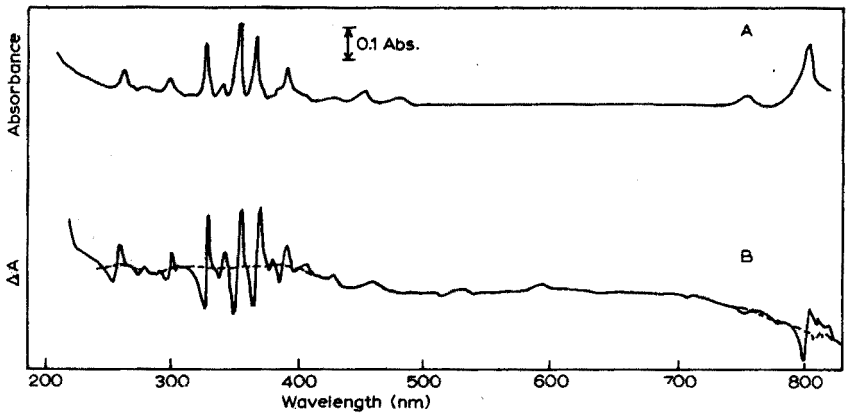

Fig. 10. Absorption (A, $\lambda_1 = \lambda_2$) and derivative (B, $\Delta\lambda = 2$ nm, $S = 0.25$ mm) spectra of dysprosium. 0.551 g Dy_2O_3 dissolved in and diluted to 25 ml with 1 *M* perchloric acid, 1-cm cell.

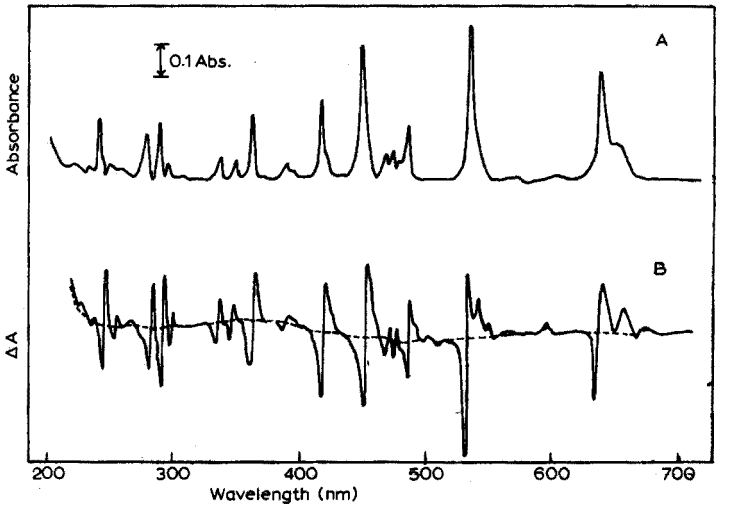

Fig. 11. Absorption (A, $\lambda_1 = \lambda_2$) and derivative (B, $\Delta\lambda = 2$ nm, $S = 0.25$ mm) spectra of holmium. 0.546 g Ho_2O_3 dissolved in and diluted to 25 ml with 1 *M* perchloric acid, 1-cm cell.

derivative spectrum is plotted. It is apparent that the size of ΔA can be increased by increasing $\Delta\lambda$ (see Fig. 1). However, if $\Delta\lambda$ is made too large, compared to the half-band width of the absorption band and to the selected spectral bandpass, the resolution of the derivative curve will be decreased. For best resolution of an absorption spectrum, the slit width should be kept narrow. The size of ΔA can be increased by decreasing S (see Fig. 2). In any particular case, these values should be decided from the shape of the absorption spectrum.

Although the spectra of the rare-earth metals have many characteristic absorption peaks, some shoulders or overlapped absorption peaks are not determined precisely by normal absorption spectrophotometry. These absorption peaks can be determined by measurement of the first-derivative spectra. As typical examples,

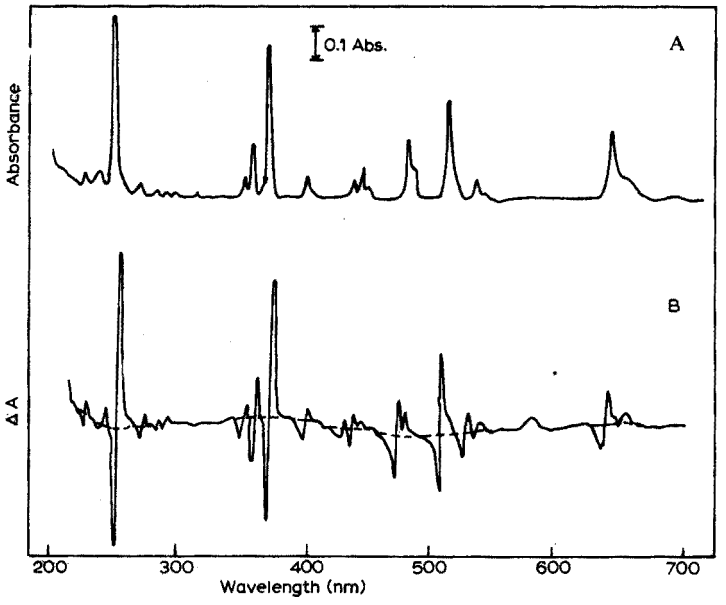

Fig. 12. Absorption (A, $\lambda_1 = \lambda_2$) and derivative (B, $\Delta\lambda = 2$ nm, $S = 0.25$ mm) spectra of erbium. 0.556 g Er_2O_3 dissolved in and diluted to 25 ml with 1 *M* perchloric acid, 1-cm cell.

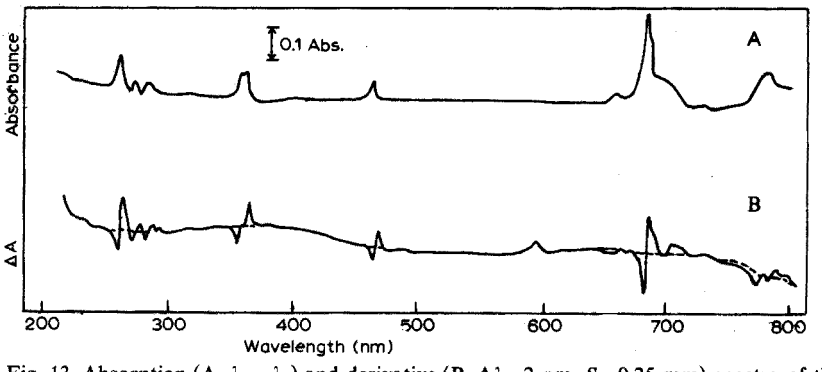

Fig. 13. Absorption (A, $\lambda_1 = \lambda_2$) and derivative (B, $\Delta\lambda = 2$ nm, $S = 0.25$ mm) spectra of thulium. 0.557 g Tm_2O_3 dissolved in and diluted to 25 ml with 1 *M* perchloric acid, 1-cm cell.

the derivative spectra of rare-earth perchlorates were measured. The results obtained are shown in Figs. 3–13 with normal absorption spectra. The results for holmium and neodymium by means of the derivative spectrum are shown in Table I.

Qualitative detection of a mixture of phenols is shown in Fig. 14. Although with normal absorption spectra, the components are not distinguished, the derivative spectra show clearly two components, *i.e.* 2,4-dichlorophenol and 2,4,6-trichlorophenol.

QUANTITATIVE ANALYSIS

Theoretical background for derivative spectrophotometry

When one of the monochromators is set to start at a slightly different wave-

TABLE I

ABSORPTION PEAKS OR SHOULDERS OF NEODYMIUM AND HOLMIUM PERCHLORATE FROM THE FIRST-DERIVATIVE SPECTRA

Holmium (nm)		*Neodymium (nm)*	
219.0	422.0	249.5	509.8
233.0	451.4	258.5	512.0
241.0	468.0	288.7	521.5
249.4	473.2	297.5	531.0
259.5	480.0	327.9	575.5
278.0	485.2	339.9	578.0
287.1	537.0	347.2	679.3
293.0	543.0	351.2	681.5
333.5	550.6	354.5	732.0
345.5	641.0	427.5	740.7
361.5	753.0	433.0	746.0
385.8		461.0	794.5
390.0		469.3	801.0
416.7		475.5	

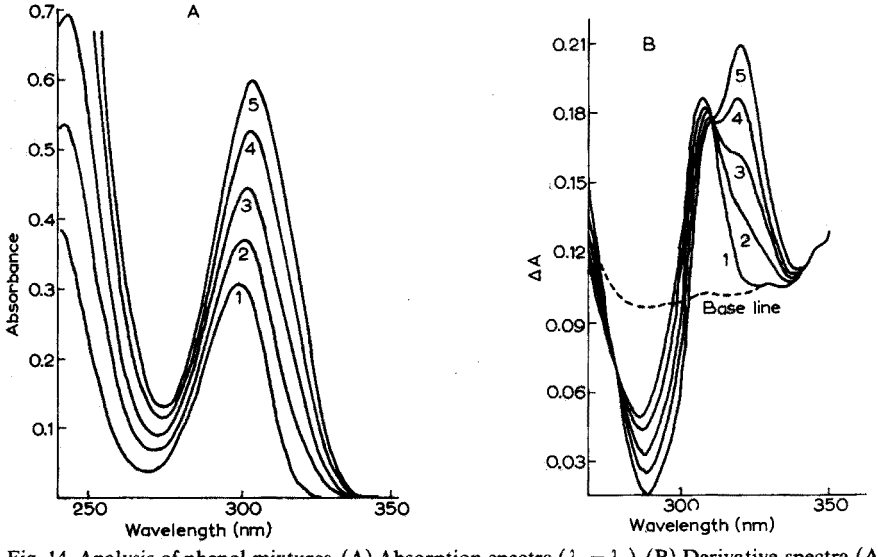

Fig. 14. Analysis of phenol mixtures. (A) Absorption spectra ($\lambda_1 = \lambda_2$). (B) Derivative spectra ($\Delta\lambda = 2$ nm, $S = 0.25$ mm). (1) 2,4-Dichlorophenol, 10 p.p.m., (2) 1 plus 5 p.p.m. 2,4,6-trichlorophenol (TCP), (3) 1 plus 10 p.p.m. TCP, (4) 1 plus 15 p.p.m. TCP, (5) 1 plus 20 p.p.m. TCP.

length (λ and $\lambda + \Delta\lambda$) from the other, a derivative output is obtained. The signals measured S_λ and $S_{\lambda+\Delta\lambda}$ are

$$S_\lambda = I_\lambda D_\lambda \exp[-\varepsilon_\lambda cl] \quad (1)$$

and

$$S_{\lambda+\Delta\lambda} = I_{\lambda+\Delta\lambda} D_{\lambda+\Delta\lambda} \exp[-\varepsilon_{\lambda+\Delta\lambda} cl] \quad (2)$$

where S_λ and $S_{\lambda+\Delta\lambda}$ are the output signals at wavelengths λ and $\lambda + \Delta\lambda$; I_λ and $I_{\lambda+\Delta\lambda}$

are the light intensities of input at wavelengths λ and $\lambda+\Delta\lambda$; D_λ and $D_{\lambda+\Delta}$ are the instrumental functions at wavelengths λ and $\lambda+\Delta\lambda$; c is the concentration of sample; and l is the length of the cell.

The value of $S_{\lambda+\Delta\lambda}$ against S_λ may be written as:

$$\frac{S_{\lambda+\Delta\lambda}}{S_\lambda} = \frac{I_{\lambda+\Delta\lambda}D_{\lambda+\Delta\lambda}\exp[-\varepsilon_{\lambda+\Delta\lambda}cl]}{I_\lambda D_\lambda \exp[-\varepsilon_\lambda cl]} \tag{3}$$

Equation (3) may be written as:

$$-\log\frac{S_{\lambda+\Delta\lambda}}{S_\lambda} = -\log\frac{I_{\lambda+\Delta\lambda}D_{\lambda+\Delta\lambda}}{I_\lambda D_\lambda} - \varepsilon_{\lambda+\Delta\lambda}cl+\varepsilon_\lambda cl \tag{4}$$

The base line without sample may be written as:

$$-\log\frac{S'_{\lambda+\Delta\lambda}}{S'_\lambda} = \log\frac{I_{\lambda+\Delta\lambda}D_{\lambda+\Delta\lambda}}{I_\lambda D_\lambda} \tag{5}$$

where S'_λ and $S'_{\lambda+\Delta\lambda}$ are the output signals of the blank at wavelengths λ and $\lambda+\Delta\lambda$.

Thus, the expression for the derivative value can be shown from eqns. (4) and (5) to be:

$$\log\frac{S_\lambda}{S_{\lambda+\Delta\lambda}} - \log\frac{S'_\lambda}{S'_{\lambda+\Delta\lambda}} = cl(\varepsilon_\lambda-\varepsilon_{\lambda+\Delta\lambda}) \tag{6}$$

Accordingly, the components can be determined quantitatively by using the derivative value.

The possibility of using the characteristic absorption spectra of the rare-earth elements for quantitative analysis has been recognized for many years. Many workers have studied the rare-earth nitrates, chlorides, perchlorates, and acetates. However, nearly all the rare-earth bands are extremely narrow, and few instruments are capable of completely resolving them. Moreover, some rare earths have their

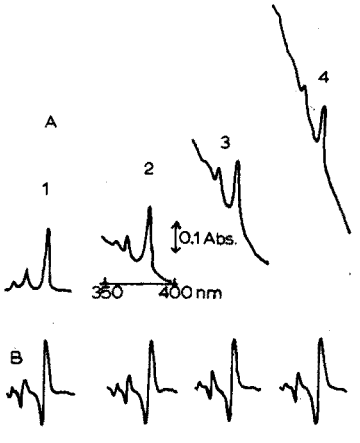

Fig. 15. Determination of erbium in the presence of cerium. (A) Absorption spectra. (B) Derivative spectra ($\Delta\lambda=2$ nm). (1) Erbium, 6000 p.p.m., (2) 1 plus 800 p.p.m. cerium, (3) 1 plus 2000 p.p.m. cerium, (4) 1 plus 3000 p.p.m. cerium.

absorption peaks at almost same wavelength region, hence some corrections are necessary for quantitative analysis. In these cases, if the derivative spectra are measured, such problems can be completely avoided.

Normal absorption spectra and derivative spectra of erbium in the presence of increasing concentrations of cerium are shown in Fig. 15. The derivative spectra for calibration of europium in the presence of samarium are shown in Fig. 16,

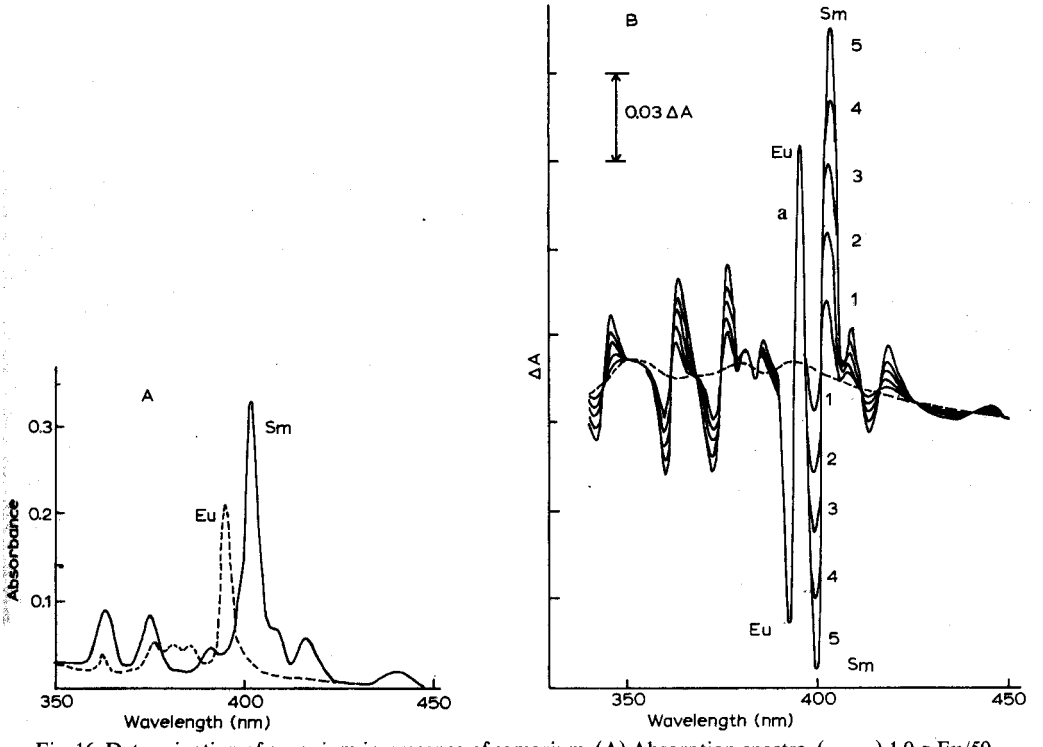

Fig. 16. Determination of europium in presence of samarium. (A) Absorption spectra. (----) 1.0 g Eu/50 ml; (——) 1.0 g Sm/50 ml; $\lambda_1 = \lambda_2$. (B) Derivative spectra. $\Delta\lambda = 2$ nm. (----) base line. (a) 0.1 g Eu/10 ml, (1), (a) plus 0.02 g Sm/10 ml, (2), (a) plus 0.04 g Sm/10 ml, (3), (a) plus 0.06 g Sm/10 ml, (4), (a) plus 0.08 g Sm/10 ml, (5), (a) plus 0.10 g Sm/10 ml.

where the normal absorption spectra are given for comparison. Even when the concentration of a coexisting substance changes considerably, as shown in Fig. 15, the distance between the maximum and minimum of the differential coefficient on the absorption band of interest undergoes no substantial change; this means that the background underlying the absorption band of interest is cancelled. Furthermore, even when the absorption band of interest overlaps other normally interfering bands, the background absorption is eliminated in the first-derivative spectra, so that a working curve can be easily prepared.

In the case of first-order or nearly first-order background, *i.e.* background which does not change sharply in intensity with wavelength, the above statements are valid. But, in the case of the second-order background, involving rapid changes, some corrections may be necessary. This problem will be discussed in a later paper.

SUMMARY

Derivative spectrophotometry has many important applications, *e.g.* detecting trace chemicals in mixture and analyzing isomers or turbid samples, but such measurements have been difficult instrumentally. The first-derivative spectrum can be recorded easily by using dual-wavelength measurements, if the two wavelengths λ_3 and λ_2 are set very close to each other (usually 1–2 nm apart) and scanned simultaneously. Practical applications of derivative spectra in the analysis of rare earths and phenol mixtures are described.

RÉSUMÉ

Une étude est effectuée sur la spectrophotométrie dérivée permettant de déceler des traces, d'analyser des isomères ou des échantillons troubles. Le premier spectra dérivé peut être enregistré facilement, par mesure à double longueur d'onde, si les deux longueurs d'onde λ_1 et λ_2 sont très proches l'une de l'autre (1–2 nm) et fixées simultanément. On propose quelques applications pratiques pour l'analyse des terres rares et de mélanges de phénols.

ZUSAMMENFASSUNG

Derivativ-Spektrophotometrie ist von besonderer Bedeutung z.B. für den Nachweis von Spurenverbindungen in einem Gemisch und für die Analyse von Isomeren oder trüben Proben. Solche Messungen sind jedoch bislang in instrumenteller Hinsicht schwierig gewesen. Das Derivativ-Spektrum (erste Ableitung) kann leicht durch Messung bei zwei Wellenlängen aufgezeichnet werden, wenn diese sehr dicht (normalerweise 1–2 nm) nebeneinander liegen und gleichzeitig abgetastet werden. Praktische Anwendungen der Derivativ-Spektren bei der Analyse von Seltenen Erden und Phenol-Gemischen werden beschrieben.

REFERENCES

1 A. T. Giese and C. S. French, *Appl. Spectrosc.*, 9 (1955) 78.
2 L. J. Saidel, *Arch. Biochem. Biophys.*, 54 (1955) 185.
3 D. T. Williams and R. N. Hager, Jr., *Appl. Opt.*, 9 (1970) 1957.
4 F. Grum, D. Paine and L. Zoeller, *Appl. Opt.*, 11 (1972) 93.
5 S. Shibata, M. Furukawa and K. Goto, *Anal. Chim. Acta*, 46 (1969) 271.
6 S. Shibata, M. Furukawa and K. Goto, *Anal. Chim. Acta*, 53 (1971) 369.
7 S. Shibata, K. Goto and Y. Ishiguro, *Anal. Chim. Acta*, 62 (1972) 305.
8 S. Shibata, M. Furukawa and K. Goto, *XVI Colloq. Spectrosc. Int., Heidelberg, 1971*, Adam Hilger, London, Preprint Vol. 1, 1971, p. 114.
9 T. J. Porro, *Anal. Chem.*, 44 (1972) 93A (April).
10 T. Moeller and J. C. Brantley, *Anal. Chem.*, 22 (1950) 433.
11 C. V. Banks and D. W. Klingman, *Anal. Chim. Acta*, 15 (1956) 356.

Analytica Chimica Acta, 65 (1973) 59–67

PHOTOLUMINESCENCE OF 6- AND 7-AMINOQUINOLINES

S. G. SCHULMAN, K. ABATE, P. J. KOVI, A. C. CAPOMACCHIA and D. JACKMAN
College of Pharmacy, University of Florida, Gainesville, Fla. 32601 (U.S.A.)
(Received 24th March 1972)

Recently, the fluorescences of several isomeric aminoquinolines, in various states of protonation, have been investigated[1–3]. The 2-, 3- and 4-isomers have been found to fluoresce intensely from the neutral, singly protonated and doubly protonated species in a variety of solvents, polar and apolar. The singly protonated 3-isomer is a well behaved arylamine[2] while the singly protonated 2- and 4- isomers appear to undergo valence tautomerism and to exist predominantly as cyclic amidines[3]. In contrast, the singly protonated isomers substituted in the homocyclic ring which have been studied (the 5- and 8-isomers), fluoresce weakly or not at all in hydroxylic solvents[1]. This has been attributed to quenching by hydrogen-bonding interactions in the excited state. Moreover, while the excited doubly protonated 2-, 3- and 4-isomers all fluoresce in concentrated sulfuric acid, no emission has been observed from the excited doubly protonated 5- and 8-isomers in fluid concentrated sulfuric acid solutions. This has been attributed to the great decrease in basicity of the exocylic amino groups in the 5- and 8-isomers, upon excitation, so that even in the most concentrated sulfuric acid solutions available, the excited doubly protonated species of the 5- and 8-isomers are not thermodynamically obtainable[1,4]. Because of our interest in correlations of electronic spectra with molecular electronic structure, the present extension of the previous studies to 6-aminoquinoline and 7-aminoquinoline was undertaken.

EXPERIMENTAL

Reagents

6-Aminoquinolinium hydrochloride (Pfaltz and Bauer, Inc., Flushing, N.Y.) was recrystallized several times from ethanol. The free base 6-aminoquinoline was prepared by precipitation from aqueous solutions of the hydrochloride with sodium hydroxide solution. The precipitate was filtered, washed several times with water and vacuum-sublimed. The purities of these materials were established by agreement of the electronic absorption spectra with those previously published[5]. The pure hydrochloride was stable indefinitely but the free base oxidized on standing in air with the formation of a brown material. Consequently, studies were performed with the free base immediately after preparation and purification. 6-N,N-dimethylaminoquinaldine (Eastman Organic Chemicals, Rochester, N.Y.) was purified by vacuum sublimation. The hydrochloride was prepared by precipitation from ether solution with hydrochloric acid. This compound was employed to evaluate the possibility of dissociation of the amino group and to evaluate the nature of hydrogen-bonding

interactions of the amino protons with hydrogen-bond acceptor solvents. The methyl group in the 2-position of the quinoline ring appears to result in slightly longer absorption and fluorescence wavelengths compared with the unsubstituted quinoline derivative; however, this is not critical to the nature of these studies.

7-Nitroquinoline was prepared by the method of Bradford *et al.*[6] and then reduced to 7-aminoquinoline by allowing it to stand, for 2 days, in an excess of aqueous ammonium sulfide. The light yellow product was extracted with ether and dried. The absorption spectra of this material were in good agreement with the published spectra of 7-aminoquinoline[5]. The free base darkened on standing in air. Consequently, it was converted to and stored as the hydrochloride. For spectral studies the free base was generated by neutralization of the hydrochloride and measurements were made as quickly as possible.

Spectroquality *n*-hexane, 1,4-dioxane, acetonitrile and ethanol and analytical-grade sulfuric acid were employed as solvents. Phosphate and citrate buffers in distilled deionized water were employed to study the pH region. The corrected Hammett acidity scale of Jorgenson and Hartter[7] was employed to calibrate the sulfuric acid solutions. For absorptiometric and fluorimetric titrations, 100 μl of stock solution of the appropriate quinoline derivative, in aqueous solution, was delivered to each buffer or sulfuric acid solution in a 10-ml volumetric flask. Each flask was injected with the sample immediately before taking spectra, to minimize decomposition errors.

Apparatus

Absorption spectra were taken on a Beckman DB-GT spectrophotometer. Fluorescence spectra were taken on a Perkin-Elmer MPF-2A fluorescence spectrophotometer, the monochromators of which were calibrated against the xenon line emission spectrum; the output was corrected for instrumental response by means of a rhodamine-B quantum counter. Phosphorescence spectra were taken at 77°K in a rotating shutter phosphoroscope. Phosphorescence spectra were uncorrected for instrumental response.

RESULTS

The long wavelength absorption and fluorescence maxima of 6-aminoquinoline, 6-dimethylaminoquinaldine and 7-aminoquinoline and of their hydrochlorides, in media of different acidities, polarities and hydrogen-bonding capabilities, are presented in Table I. The hydrochloride derivatives of these compounds were found to be too insoluble to obtain spectra in hexane. In addition to the spectra of the neutral species and singly protonated cations in half a dozen different solvents and of the doubly protonated cation in concentrated sulfuric acid at room temperature, the fluorescence maxima of all three prototropic forms of each compound at 195°K (dry ice–acetone bath) in aqueous media and at 77°K (liquid nitrogen) in ethanolic media are also presented in Table I.

With the phosphoroscope in place, only 6-aminoquinoline showed phosphorescence. However, phosphorescence was observed from all three prototropic species derived from 6-aminoquinoline. The neutral and singly protonated species showed phosphorescence bands in which the vibrational structure was badly blurred.

TABLE I

LONG WAVELENGTH ABSORPTION AND EMISSION MAXIMA OF 6-AMINOQUINOLINE, 6-DIMETHYLAMINOQUINALDINE AND 7-AMINOQUINOLINE AND THEIR HYDROCHLORIDES

(Excitation was effected at $\bar{\nu}_{abs}$ in each case)

Solvent	*6-Aminoquinoline*			*6-Dimethylaminoquinaldine*		*7-Aminoquinoline*	
	$\bar{\nu}_{abs}^{(\mu m^{-1})}$	$\bar{\nu}_{f}^{(\mu m^{-1})}$	$\bar{\nu}_{p}^{(\mu m^{-1})}$	$\bar{\nu}_{abs}^{(\mu m^{-1})}$	$\bar{\nu}_{f}^{(\mu m^{-1})}$	$\bar{\nu}_{abs}^{(\mu m^{-1})}$	$\bar{\nu}_{f}^{(\mu m^{-1})}$
298°K 18 *M* H_2SO_4	3.20	2.63 + 1.84		3.17	2.63 + 1.73	3.24	2.62 + 2.01
Water, pH 3.8[a]	2.61	1.84		2.32	1.73	2.55	2.01
Ethanol[a]	2.42	1.84		2.28	1.75	2.42	2.00
Acetonitrile[a]	2.51	1.84		2.31	1.72	2.47	2.02
Dioxane[a]	2.55	1.90		2.36	1.82	2.48	1.96
Chloroform[a]	2.57	2.04		2.31	1.91	2.52	2.04
Water, pH 13.2[b]	2.94	2.18		2.90	2.02	2.90	2.20
Ethanol[b]	2.83	2.26		2.67	2.19	2.80	2.26
Acetonitrile[b]	2.84	2.38		2.70	2.22	2.84	2.37
Dioxane[b]	2.82	2.40		2.70	2.22	2.80	2.37
Chloroform[b]	2.89	2.49		2.69	2.27	2.86	2.38
n-Hexane[b]	2.94	2.61		2.75	2.42	2.88	2.52
195°K 18 *M* H_2SO_4		2.69 + 1.90			2.70 + 1.74		2.63 + 2.08
9 *M* H_2SO_4		1.85			1.74		2.04
Water, pH 3.8[a]		1.84			1.78		2.04
Water, pH 13.2[b]		2.26			2.19		2.26
77°K 18 *M* H_2SO_4		2.82	2.04		2.84		2.80
Ethanol[a]		2.06	2.04		1.96		2.16
Ethanol[b]		2.40	2.14		2.34		2.38

[a] Hydrochloride. [b] Free base.

The doubly protonated species demonstrated extraordinarily clear vibrational structure with 0–0 band at 2.17 μm^{-1}. The phosphorescence maxima of the neutral and singly protonated 6-aminoquinoline and the approximate band center of the doubly protonated species, are also listed in Table I.

The variations of fluorescence intensity with pH and Hammett acidity of 6- and 7-aminoquinoline are presented in Figs. 1 and 2. In both 6- and 7-aminoquinoline, intense emissions from the singly protonated species are present throughout the Hammett acidity range, while the singly protonated species derived from 6-dimethylaminoquinaldine fluoresces extremely weakly in fluid concentrated acid media at room temperature.

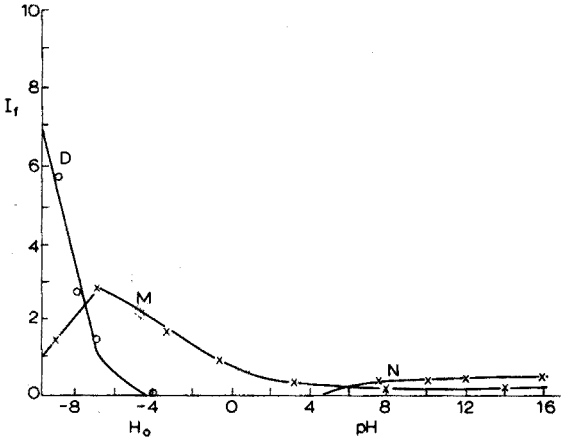

Fig. 1. Variations with pH and Hammett acidity (H_0) of the relative fluorescence intensities (I_f) of the dication (D), monocation (M) and neutral species (N), derived from 6-aminoquinoline.

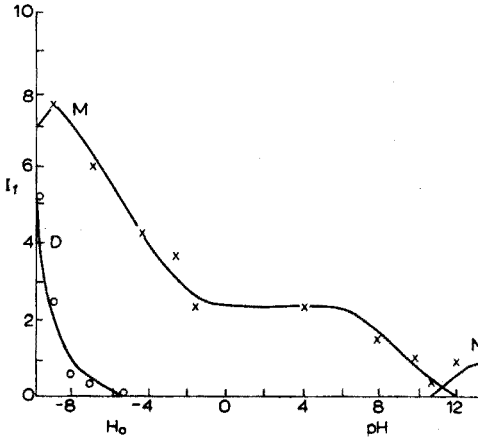

Fig. 2. Variations with pH and Hammett acidity (H_0) of the relative fluorescence intensities (I_f) of the dication (D), monocation (M) and neutral species (N), derived from 7-aminoquinoline.

While all of the media studied at liquid nitrogen temperature (77°K) were rigid glasses, concentrated sulfuric acid (18 *M*) did not rigidify at dry ice–acetone temperature (195°K), but rather, became a very viscous fluid. This problem was not encountered with the aqueous solutions which did form glasses at 195°K. In order to observe the dications in rigid as well as viscous media at 195°K, the sulfuric acid was diluted to 9 *M* with water; it then solidified in the dry ice–acetone bath.

DISCUSSION

Solvent dependence of the electronic spectra

The solvent dependences of the electronic spectra of the neutral species derived from the aminoquinolines studied here are similar. The fluorescence maxima show a continuous decrease in frequency with increasing solvent polarity and especially with hydrogen-bond donor strength of the solvent. However, the long wavelength absorption maxima, while showing a general red shift with increasing polarity also

indicate a blue shifting tendency with increasing hydrogen-bond donor strength of the solvent. The theoretical basis of these types of shifts has been previously discussed[2]. Thus it is apparent that the lowest excited singlet states of the free bases are π–π^* states in which the electronic dipole moment is greater than in the ground state. The shift to higher frequencies of the absorption spectra with increasing hydrogen-bond donor strength must be due to hydrogen bonding in the ground and Franck–Condon excited states, involving the lone pairs on the exocyclic nitrogen atoms. This effect must be very strong in order to overwhelm the red shifting effect of hydrogen bonding at the lone pair at the ring nitrogen and of the dielectric stabilization of the excited state. That water produces the largest red shift of all solvents, of the fluorescences of the free bases, indicates that, in the excited-state equilibrium solvent cage, the hydrogen bonds to the lone pairs on the exocyclic nitrogen atoms do not exist, having been broken by the transfer of the lone pair into the aromatic system upon excitation. Also, the deposition of charge on the heterocyclic nitrogen atoms in the excited state strengthens hydrogen bonding of the lone pairs on the latter nitrogen atoms and reinforces the red shift of fluorescence with increasing hydrogen-bond donor strength of the solvent.

It is noteworthy that dioxane which is nonpolar but is a hydrogen-bond acceptor produces a substantial red shift of both absorption and fluorescence compared to the spectra obtained in hexane. This is indicative of hydrogen bonding with the hydrogen atoms on the exocyclic amino groups of 6- and 7-aminoquinoline. That the red shift also occurs (although to a lesser extent) with the 6-dimethylamino derivative, in which there are no hydrogen atoms available for hydrogen bonding, suggests that 1,4-dioxane may somewhat affect the energies of solvated ground state and excited molecules by virtue of its bond moments, even though the net molecular dipole moment is zero.

The absorption and fluorescence spectra of the singly protonated cations follow the same general solvent dependences as the neutral species, but the shifts are much smaller, especially in the fluorescence. These results confirm the importance of hydrogen bonding in the ground state (but not in the excited state) involving the lone pairs belonging to the exocyclic nitrogen atoms and of stronger hydrogen bonding of the lone pairs belonging to the heterocyclic nitrogen atoms in the neutral molecules in the excited state than in the ground state. Presumably, it is

LE II

UND (pK_a) AND LOWEST EXCITED SINGLET (pK_a^*) STATE DISSOCIATION CONSTANTS

prototropic equilibria are those represented in Scheme 1, and the constants are estimated from the shifts in ption spectra, shifts in fluorescence spectra and variations of fluorescence quantum yields with acidity)

	pK_{a_1}	$pK_{a_1}^*$		pK_{a_2}	$pK_{a_2}^*$		
		Absorption shift	*Fluorescence shift*		*Absorption shift*	*Fluorescence shift*	*Fluorimetric titration*
inoquinoline	1.2	−11.2	−15.4	5.6	12.5	12.7	—
inoquinoline	0.0	−14.5	−12.8	6.7	14.1	10.7	11.9
ethylaminoquinaldine	1.9	−16.0	−17.0	6.8	19.0	12.9	15.2

the loss of the lone pairs on the heterocyclic nitrogens in the singly protonated cations that accounts for the much lower solvent sensitivity of the spectra of the latter species relative to those of the neutral species.

Acidity dependences of the electronic spectra

The ground-state prototropic equilibria of 6- and 7-aminoquinoline are depicted in Scheme 1. The dissociation constants for these equilibria have been determined by Brown and Plasz[5] and are listed in Table II. The corresponding pK_{a_1} and pK_{a_2} values for 6-dimethylaminoquinaldine were determined spectrophotometrically in this work, and found to be 1.9 and 6.8, respectively.

Scheme 1

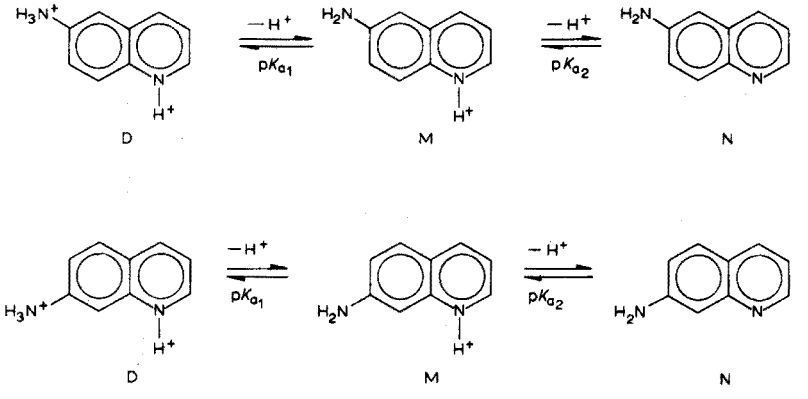

The shifts of the long wavelength absorption and fluorescence maxima of the aminoquinolines studied here, are qualitatively similar to those observed for other aminoquinolines substituted in the homocyclic ring[1,4] and indicate that in the lowest excited singlet state, the dications (D) are stronger acids and the monocations (M) are weaker acids than in their ground states. With the data of Table I, it was possible to calculate the $pK_{a_1}^*$ and $pK_{a_2}^*$ values of the excited dications and monocations with the aid of the Förster cycle[8]. The pK_a^* values calculated from absorption and from fluorescence shifts are presented in Table II. Also presented are the $pK_{a_2}^*$ values of 7-aminoquinoline and 6-dimethylaminoquinoline determined by fluorimetric titration in concentrated sodium hydroxide solutions. The conversion of the fluorescence of the monocation of 6-aminoquinoline to that of the neutral species occurred at *ca.* pH 5.6 (the ground state pK_{a_2}).

It was thought that the extremely low frequency emission of 6-aminoquinoline in dilute acid might actually originate from a zwitterion of the type

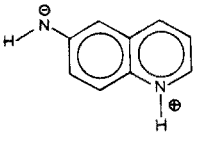

However, the appearance of a similar low-frequency fluorescence from 6-dimethylaminoquinaldine in dilute acid, in which such a zwitterionic species is impossible,

precludes this possibility and the low-frequency emissions in dilute acid are thus assigned to the monocations protonated at the ring nitrogen atoms.

The fluorimetric titrations of the dications were incomplete even when the most concentrated sulfuric acid solutions ($H_0 - 10.0$) were employed, and some dication fluorescence was observed throughout most of the Hammett acidity range. Consequently, it is assumed that prototropic equilibrium was in no case attained during the lifetime of the lowest excited singlet state. As a result, no $pK_{a_1}^*$ values determined by fluorimetric titration are reported.

The fluorimetric titration behaviors of the singly protonated cations are considerably more complex than those of the dications and neutral species. In both the 6- and 7-aminoquinolines, the emissions of the monocations increase with increasing acidity in sulfuric acid and then decrease in the most concentrated acid solutions. In the acidity region where the long-wavelength emissions are increasing there is a gradual blue shift of the emission maximum which suggests the involvement of hydrogen bonding of the lone pairs on the amino groups of the excited monocations, and indicates that the variation of the monocation fluorescence quantum yields with sulfuric acid conentration is probably a solvent composition effect rather than an acidity effect.

The reasons for discrepancies between pK_a^* values calculated from absorption spectral shifts, fluorescence spectral shifts or fluorescence quantum yield variations with acidity, have been discussed previously[2]. The $pK_{a_1}^*$ values of Table II all indicate that the doubly protonated aminoquinolines studied here are too strong acids, in their respective excited states, to be generated appreciably even in the most concentrated sulfuric acid solutions, and are thus in agreement with the failure to observe equilibrium between the excited doubly protonated and singly protonated cations. The observation of emission from the doubly protonated cations in fluid sulfuric acid solutions is probably due to kinetic factors. The doubly protonated species being the only ground-state species excited in concentrated sulfuric acid, may not have time to dissociate completely to the monocations, after excitation, in the viscous acid media. It is extremely interesting that the exocyclic nitrogen atom of 6-dimethylaminoquinolinium ion is less basic than that of the 6-aminoquinolinium ion itself in the excited state, a situation opposite to that in the ground state. This can be attributed to the relative inductive effects of the two methyl groups on the 6-amino nitrogen, in the chemical process (protonation) and in the spectroscopic processes (absorption or emission). In the excitation process, the electron-repelling effect of the methyl groups results in greater charge transfer away from the dimethylamino group than from the unsubstituted amino group. Thus, in the excited state the lone pair on the dimethylamino group is less available for protonation.

The data of Table I show that in extremely viscous 18 *M* sulfuric acid at 195°K, fluorescence is observed from both the doubly and singly protonated cations of all three aminoquinolines. Moreover, in 9 *M* sulfuric acid at 195°K, a rigid matrix, fluorescence in all cases occurs exclusively from the singly protonated species, although in both viscous and rigid media the dications are the sole species excited. These results indicate that excited-state proton transfer from the doubly protonated aminoquinolines to the solvent occurs even in very viscous and rigid media, owing to the great acidities of the dications in the excited state. It should be noted that in the viscous and rigid media, rotational and translational reorientation of the solvent

cage after excitation is impossible, so that excited-state dissociation occurs within the Frank–Condon solvent cage, probably by vibrational readjustment of a hydrogen bond between a proton of the arylammonium group with an oxygen atom belonging to a solvent molecule. In this regard, it is noteworthy that the fluorescence spectra taken at 77°K do not demonstrate excited-state dissociation. Probably, the great lowering in temperature reduces the vibrational energy of the thermally equilibrated (at 77°K) dications sufficiently that dissociation via the vibrational relaxation process in the Franck–Condon solvent cage is not possible.

The phosphorescences of the prototropic forms of 6-aminoquinoline (Table I) can be used in conjunction with the Förster cycle to calculate the triplet-state dissociation constants pK_{T_1} and pK_{T_2}. The dissociation constant pK_{T_1} for the equilibrium between the dication and monocation derived from 6-aminoquinoline is 1.2, while the dissociation constant pK_{T_2} for the equilibrium between the monocation and neutral species is 7.7. These values are typical of triplet-state dissociation constants of arylammonium ions and nitrogen heterocyclics[9] relative to the ground-state constants, and indicate that the dramatic intramolecular charge-transfer processes accompanying excitation to the lowest excited singlet state in the prototropic forms of 6-aminoquinoline do not occur on excitation to the lowest triplet state. While the phosphorescences of the neutral species and doubly protonated cation of 6-aminoquinoline occur at considerably lower frequencies than the fluorescences from these species at 77°K, the phosphorescence and fluorescence of the singly protonated cation are similar in frequency, indicating that the lowest excited singlet and triplet states of the monocation are nearly degenerate. That the triplet state normally lies lower in energy than the singlet state of the same electronic configuration is a result of electron correlation. However, the intramolecular charge transfer and solvent interaction accompanying excitation to the lowest π, π^* singlet lowers the energy of the singlet to the point where it is almost the same as that of the corresponding triplet which does not have a substantial charge-transfer component and is not very sensitive to the solvent.

SUMMARY

The fluorescences of 6- and 7-aminoquinoline and 6-dimethylaminoquinaldine were studied in media of different acidities, polarities, hydrogen-bonding capabilities and temperatures. The excited state acidities and solvent dependences of the fluorescences of these compounds are typical of aminoquinolines substituted in the homocyclic ring. The acidities of the doubly protonated cations are so great in the lowest excited singlet state, however, that prototropic dissociation in the excited state occurs even in rigid media at 195°K. The lowest triplet state of the singly charged cation of 6-aminoquinoline is found to be nearly degenerate with the lowest excited singlet state of the same molecule. This is attributed to the great charge-transfer component of the $S_1 \leftarrow S_0$ transition which is not present in the $T_1 \leftarrow S_0$ transition, and the interaction of the S_1 state with the polar solvent.

RÉSUMÉ

Une étude est effectuée sur les fluorescences des amino-6 et -7-quinoléines

et diméthylamino-6-quinaldine en fonction de divers paramètres (acidité, polarité, affinité et température). Les acidités à l'état excité et le rôle du solvant sur les fluorescences de ces composés sont caractéristiques des aminoquinoléines substituées dans leur chaine homocyclique. Une discussion est donnée expliquant ces mécanismes.

ZUSAMMENFASSUNG

Die Fluoreszenz von 6- und 7-Aminochinolin und 6-Dimethylaminochinaldin wurde in Medien unterschiedlicher Aciditäten, Polaritäten, Neigungen zur Wasserstoffbrückenbildung und Temperaturen untersucht. Die Aciditäten der angeregten Zustände und Lösungsmittelabhängigkeiten der Fluoreszenz dieser Verbindungen sind typisch für Aminochinoline, die im homocyclischen Ring substituiert sind. Die Aciditäten der zweifach protonierten Kationen sind jedoch im niedrigsten angeregten Singulettzustand so gross, dass die prototrope Dissoziation im angeregten Zustand sogar in unterkühlten Medien bei 195°K auftritt. Der niedrigste Triplettzustand des einfach geladenen Kations von 6-Aminochinolin ist nahezu mit dem niedrigsten angeregten Singulettzustand desselben Moleküls entartet. Dies wird dem grossen Charge-transfer-Anteil des $S_1 \leftarrow S_0$-Überganges zugeschrieben, der bei dem $T_1 \leftarrow S_0$-Übergang nicht vorhanden ist.

REFERENCES

1 S. G. Schulman and L. B. Sanders, *Anal. Chim. Acta*, 56 (1971) 83.
2 S. G. Schulman and A. C. Capomacchia, *Anal. Chim. Acta*, 58 (1972) 91.
3 P. J. Kovi, A. C. Capomacchia and S. G. Schulman, *Anal. Chem.*, 44 (1972) 1611.
4 S. G. Schulman and K. Abate, *J. Pharm. Sci.*, 61 (1972) 1576.
5 E. V. Brown and A. Plasz, *J. Heterocycl. Chem.*, 7 (1970) 335.
6 L. Bradford, T. J. Elliott and F. M. Rowe, *J. Chem. Soc.*, (1947) 442.
7 M. Jorgenson and D. R. Hartter, *J. Amer. Chem. Soc.*, 83 (1963) 878.
8 T. Förster, *Z. Elektrochem.*, 54 (1950) 42.
9 G. Jackson and G. Porter, *Proc. Roy. Soc.*, A260 (1961) 13.

Analytica Chimica Acta, 65 (1973) 69–75

THE CHEMISTRY AND QUANTITATIVE UTILITY OF SODIUM COBALTINITRITE IN THE DETERMINATION OF PHENOLS

ROBERT V. SMITH and MARY J. GARST

Division of Medicinal Chemistry, College of Pharmacy, The University of Iowa, Iowa City, Iowa 52240 (U.S.A.)

(Received 28th February 1972)

Numerous qualitative and quantitative methods for the determination of phenols are described in the literature. However, many of these procedures are not readily applicable to the analysis of *para*-substituted phenols[1,2]. Feigl[3,4], using some earlier work by Illinsky and Knorre[5], described a reaction with potential for determining *para*-substituted phenols. This reaction involves heating the phenol with sodium cobaltinitrite in an aqueous acetic acid solution. The resulting *o*-nitrosophenol (I) in its tautomric oxime form (II) yields a colored chelate (III) with cobalt(III) as depicted below.

$$Co(NO_2)_6^{3-} + 6\,H^+ \rightarrow Co^{3+} + 6\,HNO_2$$

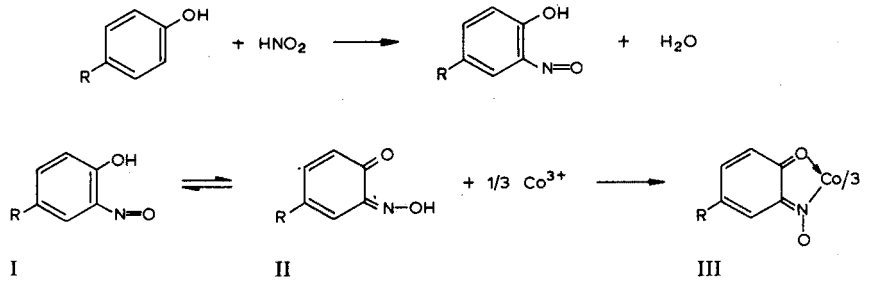

I
Ia, R = CH_3

II
IIa, R = CH_3

III
IIIa, R = CH_3

The chelate formed *in situ* readily partitions into solvents such as chloroform or ether, as long as the parent phenol does not contain other hydrophilic sulfonic acid or hydroxyl groups[3,4]. The described method has been employed in the qualitative analysis of a variety of phenols[3,4] and has recently been applied to detection of the phenolic constituents of *Cannabis*[6].

It was proposed that Feigl's method could provide a sensitive quantitative procedure for *para*-substituted phenols. Determination of the resulting chelate might be effected directly by colorimetry or indirectly by atomic absorption analysis for cobalt content. A study was undertaken to evaluate the qualitative and quantitative aspects of the reaction of cobaltinitrite with the model compound, *p*-cresol (Ia). The results of this study are described in this report.

EXPERIMENTAL

Reagents

p-Cresol solution. Dissolve 4.0–12.0 mg of *p*-cresol (Aldrich; distilled under vacuum) in 10 ml of 30% methanol in water.

Sodium cobaltinitrite solution. Dissolve 500 mg of sodium cobaltinitrite (Matheson, Coleman and Bell) in 10 ml of water. This solution must be prepared daily.

Reference compounds. *m*-Cresol, 4-nitro-*m*-cresol, 6-nitro-*m*-cresol, *p*-cresol, 2-nitro-*p*-cresol, 3-nitro-*p*-cresol, 2-nitrophenol, 4-nitrophenol (Aldrich) and phenol (Mallinckrodt) were distilled (under vacuum) or recrystallized from ethanol before use.

All other compounds or reagents were of analytical-reagent grade.

Apparatus

Ultraviolet and visible determinations were performed with Gilford-240 and Beckman DK-2 spectrophotometers. Atomic absorption analyses were conducted with a Jarrell-Ash Atomsorb spectrophotometer. Infrared spectra were obtained in nujol or KBr with a Beckman IR-20 spectrophotometer. N.m.r. spectra were determined with a Varian T-60 spectrometer; solutions were prepared with deutero-chloroform containing tetramethylsilane as internal standard.

Thin-layer chromatography

T.l.c. was performed with silica gel GF plates (250 μm; Analtech) developed with chloroform.

Characterization of reaction products

Analytical-scale reaction. A chloroform extract obtained as indicated under Method A (below) was subjected to t.l.c. (see Fig. 1).

Preparative-scale reaction. *p*-Cresol (2 g) in 100 ml of aqueous 30% methanol, 100 ml of anhydrous acetic acid, and 100 ml of 5% sodium cobaltinitrite solution were

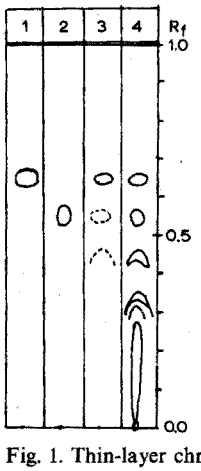

Fig. 1. Thin-layer chromatogram. (1) 2-Nitro-*p*-cresol (IV); (2) 2,2′-dihydroxy-3,3′-dinitro-5,5′-dimethylbiphenyl (V); (3) analytical-scale reaction mixture; (4) preparative-scale reaction mixture.

combined. The reaction mixture was heated in a waterbath at 60° with stirring for 2 h. The solution was adjusted to pH 10 with 6 *M* sodium hydroxide and extracted with chloroform. The alkaline portion was re-acidified to pH 2 with concentrated hydrochloric acid and extracted with chloroform. The latter chloroform extract was treated with anhydrous magnesium sulfate, and reduced to dryness *in vacuo*. The residue was chromatographed on a silica gel column (60–80 mesh; 38 g; 35 cm × 2 cm i. d.) with chloroform which yielded a quickly eluting yellow band. The latter showed two spots on t.l.c.: compound IV, $R_F = 0.65$ and compound V, $R_F = 0.55$. Fractional crystallization from ethanol effected separation of IV from V. Table I lists physical constants and spectral data of compounds IV and V.

TABLE I

PHYSICAL AND SPECTRAL DATA OF COMPOUNDS IV AND V

	2-Nitro-p-cresol	*IV*	*V*
Structure		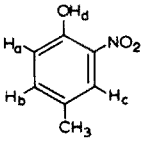	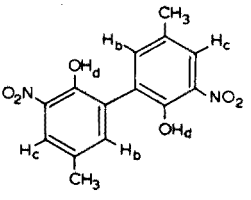
Melting point (°)	32	31.5–32	214
R_F^a	0.65	0.65	0.55
I.r.[b]	Superimposable		Similar except for intense absorption at 1050 cm^{-1}
U.v.			
Chloroform		280(6640)[c]	280(9160)
	366(3450)	366(3290)	380(6510)
Alkali[d]	433(4680)	433(4230)	—
N.m.r.			
CH_3	2.35(s, 3)[e]		2.42(s, 6)
H_a	7.05(d, 1)	Identical	Absent
H_b	7.42(dd, 1)		7.45(d, 2)
H_c	7.88(s, 1)		8.05(d, 2)
H_d	10.40(s, 1)		10.80(s, 2)
Molecular weight	—	—	304[f]
CHN	—	—	*Calc.* *Found*
		%C	55.27 55.04
		H	3.98 4.07
		N	9.21 9.14

[a] Obtained on silica gel GF plates developed with chloroform.
[b] In nujol.
[c] Wavelength, nm (molar absorptivity).
[d] 1 *M* sodium hydroxide.
[e] Chemical shift, p.p.m. (multiplicity, s = singlet, d = doublet, dd = doublet or doublets; number of protons).
[f] Determined by mass spectrometry.

Quantitative analyses

Method A. Combine a 2-ml aliquot of sample or standard *p*-cresol solution, 2 ml of anhydrous acetic acid, and 2 ml of sodium cobaltinitrite solution. Prepare a blank using 2 ml of aqueous 30% methanol instead of the *p*-cresol solution. Heat the solutions in a waterbath for 10 min at 60° (or until the blank turns a bright pink color), then extract three times with 20-ml portions of chloroform. Combine the chloroform portions and bring to 100 ml with chloroform. Measure the absorbance at 366 nm and compare to the *p*-cresol standard.

Method B. Prepare sample and blank solutions as described in Method A. After heating, dilute the solutions with 60 ml of 1 *M* sodium hydroxide; a precipitate forms. Filter and dilute the filtrates to 100 ml with 1 *M* sodium hydroxide. Measure the absorbance at 433 nm and compare to the *p*-cresol standard.

RESULTS AND DISCUSSION

Reaction of *p*-cresol with cobaltinitrite in aqueous acetic acid gave a yellow-colored product which readily partitioned into chloroform. The material recovered was presumed to be IIIa; however, atomic absorption analyses failed to reveal the presence of cobalt. T.l.c. of the product showed essentially one major and one minor spot, as shown in Fig. 1. The compounds representing these spots were labelled IV and V, respectively. A preparative-scale reaction yielded a more complex mixture (Fig. 1) which may have resulted from the different ratio of reagents that was employed relative to the analytical-scale reaction[7]. However, compounds IV and V were formed in sufficient proportion to permit their isolation.

Structure determinations

Spectral analyses and determination of other physical constants showed that compound IV is identical to 2-nitro-*p*-cresol (Table I). Identification of compound V was principally aided by n.m.r. and mass spectral analyses. The loss of absorption attributable to proton(s) *ortho* to the phenolic hydroxyl group(s) in the n.m.r. spectrum of compound V and a mass spectrally determined molecular weight of 304 suggested that compound V was 2,2′-dihydroxy-3,3′-dinitro-5,5′-dimethylbiphenyl, the dimeric product of IV. The remaining spectral data and mass spectrum are consistent with this structure[8,9].

Cobaltinitrite as a nitrating agent

The discovery that acidified cobaltinitrite acts as a nitrating rather than a nitrosating reagent contradicts the reports of Feigl[3,4]. However, since this reagent is a source of nitrous acid, the result is not too surprising. It has been shown that while nitrous acid can react with phenols to form nitroso derivatives, the latter can be rapidly converted to nitro compounds[10] in the presence of catalytic amounts of nitric acid[11]. Since nitric acid is formed in aqueous media from the disproportionation of nitrous acid[12], nitration can predominate as depicted in the following reactions.

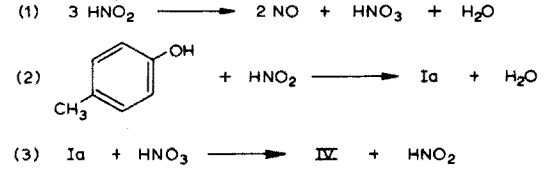

It is important to note that a number of reports have appeared which indicate that nitrous acid nitrates phenols under conditions analogous to those employed in this investigation[10,13–15].

Feigl states[3,4] that during reaction of phenols with acidified cobaltinitrite, cobalt(III) directs nitrosation *ortho* to hydroxyl groups. While nitrosation cannot be shown under the conditions utilized, it has been found that some directive influence may be exerted by the reagent on the course of nitration. The reaction of cobaltinitrite with phenol and *m*-cresol was examined qualitatively and semi-quantitatively by t.l.c. While the reaction mixtures in both instances appeared more complex than that of *p*-cresol, known nitro compounds were detected and the reaction is estimated to favor formation of the appropriate *ortho*-substituted derivatives by at least a factor of ten. Nitration and nitrosation of phenols by nitrous acid is reported markedly to favor *para*-substitution[16–18]. Thus, the apparent directive effect of cobalt ion on nitration is worth noting. Since a number of products are formed when cobaltinitrite is reacted with phenols having free *para*-positions, the potential analytical usefulness of this reagent is probably limited to *para*-substituted phenols.

Quantitative analyses

Two methods were devised for the determination of *p*-cresol with acidified cobaltinitrite. Method A involves measurement at 366 nm of the 2-nitro-*p*-cresol formed, after extraction into chloroform. Method B employs treatment with 1 *M* sodium hydroxide which causes conversion of compound IV to its anion which is determined at 433 nm. A Beer's law plot derived with method A was linear over a concentration range of $5 \cdot 10^{-5}$–$5 \cdot 10^{-4}$ *M*, while method B showed linear results

TABLE II

COMPARISON OF ANALYSES OF *p*-CRESOL BY METHODS A AND B

Method	*Wavelength (nm)*	*% Recovery*[a]	*Mean*	*Relative standard deviation*
A	366	100.6	100.0	0.59
		100.8		
		100.0		
		100.2		
		99.4		
		100.6		
		100.4		
		98.8		
		99.6		
		100.0		
B	433	101.7	99.7	1.82
		100.0		
		100.4		
		100.0		
		100.0		
		95.8		

[a] Final concentration of sample solutions = $2 \cdot 10^{-4}$ *M*.

for concentrations of $2 \cdot 10^{-5}$–$2 \cdot 10^{-4}$ *M*. Results of multiple analyses are indicated in Table II. Method A is superior in precision and is more rapidly performed. Method B provides greater sensitivity and potential selectivity.

The authors are grateful to Dr. G. Subba Rao of the Laboratory of Chemistry, National Heart and Lung Institute, National Institutes of Health, for mass spectral analyses.

SUMMARY

The reaction of *p*-cresol with acidified cobaltinitrite has been qualitatively and quantitatively studied. On an analytical scale, the reaction predominantly leads to 2-nitro-*p*-cresol. The dimer of this compound has also been identified as a minor product. Two methods have been devised for quantitative analysis. These procedures represent rapid, accurate and precise techniques for analyzing *p*-cresol and may be applicable to other *p*-substituted phenols.

RÉSUMÉ

Une étude qualitative et quantitative est effectuée sur la réaction du *p*-crésol avec le cobaltinitrite de sodium. Il se forme principalement le 2-nitro-*p*-crésol et en quantité moindre le dimère de ce composé. Deux méthodes d'analyse quantitative sont proposées; elles permettent un dosage rapide, exact et précis du *p*-crésol. Ces techniques sont applicables à d'autres phénols *p*-substitués.

ZUSAMMENFASSUNG

Die Reaktion von *p*-Kresol mit angesäuerter Kobalt(III)nitrit-Lösung wurde qualitativ und quantitativ untersucht. Im analytischen Massstab führt die Reaktion im wesentlichen zu 2-Nitro-*p*-kresol. Als Nebenprodukt wurde das Dimere dieser Verbindung identifiziert. Für die quantitative Analyse wurden zwei Methoden ausgearbeitet. Diese stellen schnelle, genaue und reproduzierbare Verfahren für die Bestimmung von *p*-Kresol dar und können möglicherweise auf andere *p*-substituierte Phenole angewendet werden.

REFERENCES

1 N. D. Cheronis and T. S. Ma, *Organic Functional Group Analysis by Micro and Semimicro Methods*, Interscience, New York, 1964, pp. 445–456.
2 I. M. Kolthoff and P. J. Elving (Editors), *Treatise on Analytical Chemistry*, Part III, Vol. 2, Interscience, New York, 1971, pp. 490–493.
3 F. Feigl, *Anal. Chem.*, 27 (1955) 1315.
4 F. Feigl, *Spot Tests in Organic Analysis*, Elsevier, Amsterdam, 7th Ed., 1966, pp. 183–184 and 393–394.
5 M. Illinsky and G. Knorre, *Chem. Ber.*, 18 (1885) 699.
6 A. Caldas, *Anal. Chim. Acta*, 49 (1970) 194.
7 J. St L. Philpot and P. A. Small, *Biochem. J.*, 32 (1938) 534.
8 R. V. Smith, M. J. Garst and G. S. Rao, *Appl. Spectrosc.*, in preparation.
9 H. Budzikiewicz, C. Djerassi and D. H. Williams, *Mass Spectrometry of Organic Compounds*, Holden-Day, San Francisco, 1967, pp. 515–519 and 115–118.

10 C. A. Bunton, E. D. Hughes, G. J. Minkoff and R. I. Reed, *Nature*, 158 (1946) 514.
11 C. K. Ingold, *Structure and Mechanism in Organic Chemistry*, Cornell University Press, Ithaca, 2nd Ed., 1969, pp. 337–340.
12 C. Hanegraaff and N. Chastagner, *Ann. Pharm. Fr.*, 27 (1969) 663.
13 C. A. Bunton, E. D. Hughes, C. K. Ingold, D. I. H. Jacobs, M. H. Jones, G. J. Minkoff and R. I. Reed, *J. Chem. Soc.*, (1950) 2628.
14 F. LePerdriel, C. Hanegraaff, N. Chastagner and E. de Montety, *Ann. Pharm. Fr.*, 26 (1968) 227.
15 L. Chafetz, R. E. Daly, H. Schriftman and J. L. Lommer, *J. Pharm. Sci.*, 60 (1971) 463.
16 G. Cronheim, *J. Org. Chem.*, 12 (1947) 1.
17 B. C. Challis and A. J. Lawson, *J. Chem. Soc., B*, (1971) 770.
18 J. L. G. Nilsson and I. Skanberg, *Acta Pol. Pharm.*, 28 (1971) 241.

Analytica Chimica Acta, 65 (1973) 77–85

THE EXTRACTION OF EDTA BY SOLUTIONS OF ALIQUAT-336 IN 1,2-DICHLOROETHANE

H. M. N. H. IRVING and R. H. AL-JARRAH

Department of Inorganic and Structural Chemistry, University of Leeds, Leeds LS2 9JT (England)

(Received 28th November 1972)

In 1971 the extraction of chromium(III) in the form of its anionic complex, $CrY(H_2O)^-$, with ethylenediaminetetraacetic acid (EDTA; H_4Y) by solutions of the long-chain quaternary ammonium salt, tetra-*n*-hexylammonium chloride, in 1,2-dichloroethane was described[1]. These studies have since been extended to the liquid–liquid extraction of V(IV), V(V), Cr(III), Mn(II), Mn(III), Fe(III), Co(II), Co(III), Ni(II), Cu(II), Zn(II), Cd(II), Pd(II), Hg(II), Ca(II), Mg(II), Pb(II) and Bi(III), by the commercially available liquid anion-exchanger Aliquat-336 (tricaprylmethylammonium chloride)[2]. Standardised conditions were employed in these measurements in order to facilitate intercomparisons, and a 10% excess of the complexone was used with every metal ion studied. Since aqueous solutions of EDTA can contain the anionic species H_3Y^-, H_2Y^{2-}, HY^{3-} and Y^{4-} in proportions dependent upon the pH, in addition to the neutral species H_4Y (and the cations H_5Y^+ and H_6Y^{2+} present in strongly acidic solutions), it was clearly desirable to see to what extent the anionic species could compete with chloride ions (or other inorganic anions) and metal complexonate anions MY^{n-} in forming extractable ion-pairs with the quaternary ammonium cation, Q^+, of the liquid exchanger.

The pH of various solutions of 0.0100 *M* EDTA was adjusted to values in the range 4–11 by adding dilute potassium hydroxide. After equilibration with an equal volume of 0.109 *M* Aliquat-336 in dichloroethane (3 min) at room temperature (22°), the mixture was centrifuged and the two phases were carefully separated. The concentration of EDTA in each phase was determined by direct titration with a standard solution of bismuth(III) in the presence of pyrocatechol violet and dithizone as the indicator for the aqueous and organic phase, respectively. The distribution coefficient, q, defined by

$$q = \frac{\text{total concentration of EDTA in the organic phase}}{\text{total concentration of EDTA in the aqueous phase}} \quad (1)$$

was then calculated. Detailed procedures are given in the experimental section. The concentration of chloride ions in the aqueous phase left after equilibration was determined with a silver/silver chloride electrode in conjunction with Hg_2SO_4–K_2SO_4 as a reference electrode. It was first shown that chloride ion concentrations determined in this way were not affected by changes of pH or EDTA concentration over the range of values to be used. The experimental results are summarized in Table I.

From the plot of percentage extraction against pH (Fig. 1), it is clear that there is relatively little extraction below pH 4.0, whereafter there is an increase to a

TABLE I

LIQUID–LIQUID EXTRACTION OF 0.010 *M* EDTA BY A 0.1090 *M* SOLUTION OF ALIQUAT-336-CHLORIDE IN 1,2-DICHLOROETHANE

pH	*q*	$-\Delta E(V)$	$[Cl^-]_{aq}$ $(x \cdot 10^{-2}\ M)$	% *extracted, E*	
				Found	*Calcd.*[a]
4.03	0.238	0.2205	0.711	19.2	20.0
4.63	0.316	0.2245	0.835	24.0	23.6
6.13	0.521	0.2352	1.294	34.3	32.2
6.48	0.581	0.2365	1.355	36.8	35.2
9.32	0.664	0.2432	1.794	39.9	38.2
10.25	0.688	0.2469	2.070	40.8	40.6
11.80	0.492	0.2507	2.426	33.0	34.2

[a] Values of E (calcd.) were obtained from eqn. (6) with $\bar{K}_1^{ex}=0.0003$, $\bar{K}_2^{ex}=0.0014$, $\bar{K}_3^{ex}=0.0022$ and $\bar{K}_4^{ex}=0.00365$

TABLE II

PROPORTION OF DIFFERENT ANIONIC SPECIES OF EDTA AS A FUNCTION OF pH.

pH	*Percentage*[a] *of total EDTA in the form*				
	H_4Y	H_3Y^-	H_2Y^{2-}	HY^{3-}	Y^{4-}
3.50	0.40	12.8	86.6	0.20	
4.00	0.05	4.5	94.7[5]	0.70	
4.50		1.4	96.5	2.1	
5.00		0.4	93.2	6.4	
5.50		0.1	82.0	17.9	
6.00		0.03	59.1	40.9	
6.50			31.4	68.6	0.01
7.00			12.6	87.4	0.05
7.10			10.3	89.7	0.06
7.14			9.5	90.5	0.07
7.18			8.7	91.3	0.08
7.20			8.4	91.6	0.08
7.28			7.1	92.9	0.10
7.30			6.8	93.2	0.10
7.32			6.5	93.5	0.11
8.00			1.4	98.1	0.5
9.00			6.1	94.7	5.2
10.00			0.01	64.5	35.5
10.5				36.5	63.5
11.0				15.4	84.6
12.0				1.8	98.2

[a] Calculated from the proton formation β_n ($n=1$, 2, 3 and 4) given in the text.

maximum at pH 9.5 and then a decrease as the pH is increased still further. From the information in Table II, which shows the percentage of EDTA anions present in aqueous solutions at various pH values, it is clear that at pH *ca.* 4 the

negatively charged species, H_2Y^{2-}, predominates in aqueous solution, while at pH 9–10 EDTA exists mostly as the negative ion, HY^{3-}.

If it is postulated that each of the anions H_3Y^-, H_2Y^{2-}, HY^{3-} and Y^{4-} is potentially extractable as an ion pair $Q_{4-j}^{+}(H_jY)^{j-4}$ ($j=0, 1, 2, 3$), the extraction process can be generalised by the equation

$$(4-j)[QCl]_{org}+\sum_0^3[H_jY]^{-(4-j)} \overset{\bar{K}_n^{ex}}{\rightleftharpoons} \sum_0^3[Q_{(4-j)}H_jY]_{org}+(4-j)Cl^- \quad (2)$$

with an extraction constant $\bar{K}_n^{ex}$ for the species H_jY^{j-4} defined by

$$\bar{K}_n^{ex}=\frac{[Q_{(4-j)}H_jY]_{org}[Cl^-]^{(4-j)}}{[QCl]_{org}^{4-j}[(H_jY)^{-(4-j)}]} \quad (3)$$

where $n=4-j$, and the subscript org distinguishes species present in the organic phase.

If all the ion-pairs are extracted simultaneously, a combination of eqns. (1), (2) and (3) yields

$$q=\sum_0^3[Q_{(4-j)}^{+}(H_jY)^{(j-4)}]_{org}/\sum_0^4[H_jY^{(j-4)}]$$

$$=\frac{\dfrac{\bar{K}_1^{ex}[Q^+Cl^-]_{org}[H_3Y^-]}{[Cl^-]}+\dfrac{\bar{K}_2^{ex}[Q^+Cl^-]_{org}^2[H_2Y^{2-}]}{[Cl^-]^2}+\dfrac{\bar{K}_3^{ex}[Q^+Cl^-]_{org}^3[HY^{3-}]}{[Cl^-]^3}+\dfrac{\bar{K}_4^{ex}[Q^+Cl^-]_{org}^4[Y^{4-}]}{[Cl^-]^4}}{[H_4Y]+[H_3Y^-]+[H_2Y^{2-}]+[HY^{3-}]+[Y^{4-}]} \quad (4)$$

By introducing the overall proton formation constants[3]: $\beta_1=[HY^{3-}]/[H^+][Y^{4-}]=1.82\cdot10^{10}$, $\beta_2=[H_2Y^{2-}]/[H^+]^2[Y^{4-}]=2.63\cdot10^{16}$, $\beta_3=[H_3Y^-]/[H^+]^3[Y^{4-}]=1.51\cdot10^{19}$, and $\beta_4=[H_4Y]/H^+]^4[Y^{4-}]=1.51\cdot10^{21}$ we obtain

$$q=\frac{\dfrac{\bar{K}_1^{ex}\beta_3[H^+]^3[QCl]_{org}}{[Cl^-]}+\dfrac{\bar{K}_2^{ex}\beta_2[H^+]^2[QCl]_{org}^2}{[Cl^-]^2}+\dfrac{\bar{K}_3^{ex}\beta_1[H^+][QCl]_{org}^3}{[Cl^-]^3}+\dfrac{\bar{K}_4^{ex}[QCl]_{org}^4}{[Cl^-]^4}}{\beta_4[H^+]^4+\beta_3[H^+]^3+\beta_2[H^+]^2+\beta_1[H^+]+1} \quad (5)$$

where for simplicity (and subsequently) [QCl] is written in place of $[Q^+Cl^-]$.

This equation is of the form

$$A\bar{K}_1^{ex}+B\bar{K}_2^{ex}+C\bar{K}_3^{ex}+D\bar{K}_4^{ex}=q\cdot f_H \quad (6)$$

where $A=[QCl]_{org}\beta_3[H^+]^3/[Cl^-]$, $B=[QCl]_{org}^2\beta_2[H^+]^2/[Cl^-]^2$, $C=[QCl]_{org}^3\beta_1[H^+]/[Cl^-]^3$, $D=[QCl]_{org}^4/[Cl^-]^4$ and $f_H=\beta_4[H^+]^4+\beta_3[H^+]^3+\beta_2[H^+]^2+\beta_1[H^+]+1$.

By inserting the experimental values of A, B, C, D and f_H in eqn. (6), seven simultaneous equations result, from which the four extraction constants may be calculated. In practice the solution proved troublesome, for at pH *ca.* 4 the percentage of the species H_3Y^- (which is the most significant term for the calculation of $\bar{K}_1^{ex}$) is very low (*cf.* Table II), thus leading to ill-conditioned equations. However, the values $\bar{K}_1^{ex}\approx0.0003$, $\bar{K}_2^{ex}=0.0014$, $\bar{K}_3^{ex}=0.0022$ and $\bar{K}_4^{ex}=0.00365$ gave the best fit over the whole pH range with a minimal value for $(E_{calc.}-E_{exp.})^2$. This is demonstrated in Fig. 1 where the continuous line calculated from these constants is shown together with the experimental results (open circles).

An attempt was made to prepare a solution of EDTA below pH 4, where the species H_3Y^- would exist in considerable concentration, by dissolving an

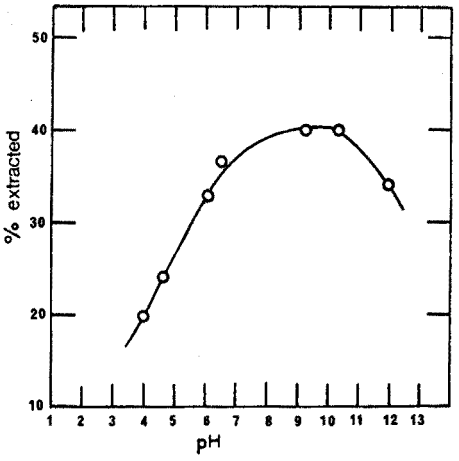

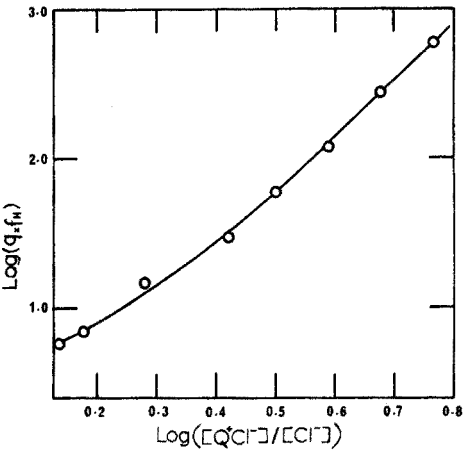

Fig. 1. Extraction of EDTA anions by a solution of Aliquat-336-Cl in 1,2-dichloroethane. Experimental results shown as open circles. The continuous curve is calculated from eqn. (6) with $\bar{K}_1^{ex} = 0.0003$, $\bar{K}_2^{ex} = 0.0014$, $\bar{K}_3^{ex} = 0.0022$ and $\bar{K}_4^{ex} = 0.00365$.

Fig. 2. The plot of log $(q \cdot f_H)$ against log $([Q^+Cl^-]_{org}/[Cl^-])_{calc.}$.

equimolar mixture of Na_2H_2Y, $2H_2O$ and H_4Y in boiled-out distilled water, but solid separated at the temperature of measurement and interfered with the subsequent equilibration with Aliquat-336. A suitable solution could not be prepared simply by adding a mineral acid to lower the pH, for this would introduce anions that could compete in the liquid–liquid extraction equilibrium.

It is obvious from eqn. (5) that the distribution coefficient, q, varies with $[Cl^-]$ as well as $[H^+]$ and [Aliquat-336]. This was examined by extracting aqueous solutions of 0.0100 M EDTA containing different chloride ion concentrations in the range $8 \cdot 10^{-3}$ to $8 \cdot 10^{-2}$ M but all adjusted to the same pH (7.22). The values of q obtained after extraction by an equal volume of 0.1090 M Aliquat-336-Cl in dichloroethane at 22° are shown in the fourth column of Table III.

TABLE III

VARIATION IN THE EXTRACTION OF 0.010 M EDTA BY A 0.1090 M SOLUTION OF ALIQUAT-336-CHLORIDE IN DICHLOROETHANE WITH THE CONCENTRATION OF ADDED CHLORIDE IONS AT pH 7.22 ± 0.09

$[Cl^-]$ added	Calculated values of		Distribution coefficient q	
	$[Cl^-]_{aq}$	$[Q^+Cl^-]_{org}$	Found	Calcd.
0.008	0.0170	0.1000	0.371	0.411
0.016	0.0216	0.1034	0.195	0.223
0.024	0.0273	0.1057	0.093	0.119
0.032	0.0339	0.1071	0.050	0.065
0.040	0.0411	0.1079	0.029	0.038
0.056	0.0564	0.1086	0.015	0.015
0.072	0.0722	0.1088	0.008	0.007
0.080	0.0802	0.1089	0.005	0.005

Provided that $[H^+]$ and $[Q^+Cl^-]$ are constant, eqn. (5) could be presented in the form

$$q \cdot f_H = \frac{a}{[Cl^-]} + \frac{b}{[Cl^-]^2} + \frac{c}{[Cl^-]^3} + \frac{d}{[Cl^-]^4} \quad (7)$$

where a, b, c and d are constants. The plot of $\log(q \cdot f_H)$ against $-\log[Cl^-]$ should therefore be a curve with a slope ranging between 1 and 4, depending on which species of EDTA are best extracted under the experimental conditions. The actual plot (not reproduced) shows a slope ranging between 1 and 3.4, implying that *each* of the four anions H_3Y^-, H_2Y^{2-}, HY^{3-} and Y^{4-} is extractable. However at pH 7.22 the aqueous solution should contain *ca.* 91% HY^{3-}, *ca.* 8.9% H_2Y^{2-} and 0.07% Y^{4-} with virtually no H_3Y^-, and the experimental results could only be explained if the extraction coefficients $\bar{K}_1^{ex}$ and $\bar{K}_4^{ex}$ are much larger than $\bar{K}_2^{ex}$ and $\bar{K}_3^{ex}$; this conflicts with earlier results.

The discrepancy originates in the incorrect assumptions that a, b, c and d are constants. Explicitly

$$a = \bar{K}_1^{ex}[QCl]_{org}\beta_3[H^+]^3, \quad b = \bar{K}_2^{ex}[QCl]_{org}^2\beta_2[H^+]^2,$$
$$c = \bar{K}_3^{ex}[QCl]_{org}^3\beta_1[H^+] \quad \text{and} \quad d = \bar{K}_4^{ex}[QCl]_{org}^4$$

and the equilibrium concentration $[QCl]_{org}$ will increase as the total chloride ion concentration increases, and eqn. (2) will be displaced to the left, even though $[QCl]_{total}$ is constant.

Now

$$[QCl]_{tot} = [QCl]_{org} + \bar{K}_1^{ex}[H_3Y^-]([QCl]_{org}/[Cl]) + 2\bar{K}_2^{ex}[H_2Y^{2-}]([QCl]_{org}/[Cl])^2 + 3\bar{K}_3^{ex}[HY^{3-}]([QCl]_{org}/[Cl])^3 + 4\bar{K}_4^{ex}[Y^{4-}]([QCl]_{org}/[Cl])^4 \quad (8)$$

and

$$[Cl^-]_{tot} = [QCl]_{org} + [Cl^-]_{aq} \quad (9)$$

The total chloride ion concentration in the system being known, a trial value of $[Cl^-]_{aq}$ gave the corresponding value of $[QCl]_{org}$ by eqn. (9), and the insertion of these two values into eqn. (8) together with the previously known value of $\bar{K}_n^{ex}$ ($n = 1, 2, 3, 4$) and the concentration of the various anionic species of EDTA appropriate to pH 7.22 gave a calculated value for $[QCl]_{tot}$. The difference $Z = [QCl]_{tot}$ (calc.) $- [QCl]_{tot}$ (exp.) was then computed for different assumed values of $[Cl^-]_{aq}$ until a zero value was obtained. Because $[H_3Y^-]$ is very small at pH 7.22, the second term in eqn. (8) could be omitted.

The accuracy of the calculated values of $[Q^+Cl^-]_{org}$ and $[Cl^-]_{aq}$ given in columns 2 and 3 of Table III was checked by inserting them in eqn. (5) and calculating values of the distribution coefficient, q. Table III (last column) shows that the agreement is satisfactory. Furthermore the plot of $\log(q \cdot f_H)$ against the logarithm of the ratio $([QCl]_{org}/[Cl^-])_{calc.}$ shown in Fig. 2 has a slope lying between 2 and 3.7, which implies that the extractable species are H_2Y^{2-}, HY^{3-} and Y^{4-} as inferred previously.

Since chloride ions can displace the anions of EDTA from an organic extract by Aliquat-336 as expressed by eqn. (2) and the experimental values of $\bar{K}_n^{ex}$ ($n = 1, 2, 3$ and 4) derived above, it was of interest to see whether other common

TABLE IV

VARIATION IN THE DISTRIBUTION COEFFICIENT FOR THE EXTRACTION OF 0.010 *M* EDTA AT pH 7.56 BY AN EQUAL VOLUME OF 0.1090 *M* ALIQUAT-336-Cl IN DICHLOROETHANE PRODUCED BY ADDING SULPHATE OR PHOSPHATE IONS

Concentration of added SO_4^{2-} *or* PO_4^{3-}	*Distribution coefficient q*	
	Sulphate present	*Phosphate present*
0.008	0.460	0.666
0.016	0.295	0.574
0.024	0.207	0.519
0.040	0.124	0.415
0.080	0.052	0.272
0.120	0.036	0.194

anions would have a greater or lesser effect. Equilibria expressed generally by eqns. (10) and (11)

$$2[Q^+Cl^-]_{org} + SO_4^{2-} \rightleftharpoons [Q_2^+SO_4^{2-}]_{org} + 2Cl^- \quad (10)$$

$$3[Q^+Cl^-]_{org} + PO_4^{3-} \rightleftharpoons [Q_3^+PO_4^{3-}]_{org} + 3Cl^- \quad (11)$$

would imply that the presence of sulphate (or phosphate ions) could be expected to reduce the extraction of EDTA both by reducing the concentration of free quaternary ammonium ions and by increasing that of chloride ions in the aqueous phase.

Experiments similar to those previously reported (*cf.* Table IV) showed that the extraction by a solution of 0.1090 *M* Aliquat-336 in dichloroethane of solutions of 0.010 *M* EDTA at pH 7.56 containing various amounts of sulphate or phosphate ions decreased as the concentration of inorganic anion increased. By comparison with the results obtained in the presence of chloride ions, it is clear that the effectiveness in decreasing the extraction of EDTA increases in the order $PO_4^{3-} < SO_4^{2-} < Cl^-$.

While this work was in progress, Zaman *et al.*[4] published a detailed study of the extraction at pH 4, 7 and 11 of hydroxyethylethylenediaminetriacetic acid (HEDTA; H_3Z) by solutions of Aliquat-336-chloride in benzene. Evidence was presented for the extraction of the species Z^{3-} and HZ^{2-} at pH 11 and 7, but the formation of emulsions at pH 4 made it impossible to establish with certainty how well the uninegative anion H_2Z^- extracted. The extraction constants for HZ^{2-} and Z^{3-} were given as 0.0316 and 0.200, respectively; a 2.75-fold polymerization of the quaternary salt was postulated, and each aggregate $(Q^+Cl^-)_{2.75}$ was assumed to exchange only a single chloride ion in forming extractable species such as $\{(Q^+Cl^-)_{1.75}...Q^+\}_m H_{3-m}Y^{m-}$. Although there is no evidence for aggregation of Aliquat-336 salts under the conditions of the present experiments, the general results of Zaman *et al.* agree with our own in showing that—contrary to the commonly held view that extraction should decrease with increasing negative charge on an anion—it is in fact species such as Z^{3-} and HZ^{2-} with HEDTA, and Y^{4-}, HY^{3-} and H_2Y^{2-} with EDTA, that extract well.

EXPERIMENTAL

A stock solution of Aliquat-336-Cl (General Mills Ltd.) prepared by weight in chloroform was washed with dilute sodium hydroxide until free from traces of acid, then with sodium chloride solution and finally with distilled water. A suitable aliquot portion was then placed in a 100-ml beaker and the solvent was removed as completely as possible in an evacuated desiccator over calcium chloride. The residue was taken up in 50 ml of redistilled 1,2-dichloroethane, b.p. 82–84°, to give a *ca.* 0.11 *M* solution, the precise concentration of which was determined as described by Irving and Nabilsi[5].

Measurements of chloride ion concentration

Four silver–silver chloride electrodes were prepared as described by Brown[6], plated and aged in the same solution of 0.002 *M* silver nitrate, when no pair showed a potential difference exceeding 0.5 mV and each electrode was shown to give a linear response by measurements in a series of solutions of potassium chloride of known concentration.

The independence of the response from changes in pH was tested by measuring the potential between a silver–silver chloride electrode and a Hg_2SO_4/K_2SO_4 reference electrode when immersed at $21.7 \pm 0.3°$ in 0.0200 *M* potassium chloride in various acetic acid–acetate buffers of total ionic strength 1.0 *M* (KNO_3). Over the pH range 2.52–7.55 (9 different buffers), the potentials of three different electrodes were -0.3097 ± 0.0005, -0.3097 ± 0.0004 and -0.3097 ± 0.0005, which confirmed that changes in pH had no effect.

Since silver ions do form (weak) complexes with EDTA[3], it would be expected that the potential of a silver–silver chloride electrode might vary with [EDTA] and pH. Mixtures of 10 ml of 0.200 *M* Na_2H_2Y with *x* ml of 0.1 *M* KCl ($x = 0.1$, 0.2, 0.5, 1.0, 1.5, 5.0, 10.0, 15.0 and 25 ml) were adjusted to pH 4.35 with sodium acetate–acetic acid buffer and ionic strength 1.0 *M* (KNO_3) while being made up to 50.0 ml. The chloride ion concentration was then measured in terms of the potential difference of the silver–silver chloride $-Hg_2SO_4/K_2SO_4$ reference electrode. The plot of ΔE (V) against log $[Cl^-]$ was a straight line of slope -0.0591 and from similar measurements made in the absence of EDTA (Table V) it is clear that chloride ion determinations can be made at least up to [EDTA] = 0.04 *M* and pH 4.3 without the need for separate calibration curves for different sets of conditions.

Equilibration procedure

Aliquot portions of 0.050 *M* Na_2H_2Y were adjusted to a suitable pH with dilute potassium hydroxide and diluted to a final volume of 25 ml and final $[EDTA]_{tot} = 0.0100$ *M*. Portions (10 ml) were equilibrated at 22° in stoppered centrifuge tubes with an equal volume of 0.1090 *M* Aliquat-336-Cl in dichloroethane. The mixture was centrifuged, the phases were separated and the pH of the aqueous phase was measured. The total concentration of EDTA in each phase was then determined.

Aliquot portions (4.0 ml) of the aqueous phase were made up to 50 ml and pH *ca.* 2 with 0.01 *M* nitric acid; after the addition of 4 drops of pyrocatechol violet (0.1% in water) titration was carried out into a standard solution of 0.0100 *M*

TABLE V

MEASUREMENTS OF THE POTENTIAL OF A SILVER–SILVER CHLORIDE ELECTRODE IN THE PRESENCE AND ABSENCE OF 0.0400 *M* EDTA AT 22.0° AND pH 4.3 WITH $I = 1.0$ *M* (KNO_3)

$[Cl^-]$ *added*	ΔE *(V)*	
	EDTA present	*EDTA absent*
$2 \cdot 10^{-4}$	−0.1948	−0.1948
$4 \cdot 10^{-4}$	−0.2113	−0.2118
$1 \cdot 10^{-3}$	−0.2333	−0.2337
$2 \cdot 10^{-3}$	−0.2511	−0.2508
$4 \cdot 10^{-3}$	—	−0.2683
$1 \cdot 10^{-2}$	−0.2900	−0.2900
$2 \cdot 10^{-2}$	−0.3080	−0.3080
$3 \cdot 10^{-2}$	−0.3180	−0.3182
$4 \cdot 10^{-2}$	—	−0.3253

bismuth(III) until the colour changed from clear yellow to bluish violet. Aliquot portions of the organic phase (4.0 ml) were diluted to 60 ml with 0.100 *M* nitric acid and after the addition of 5.0 ml of a $5 \cdot 10^{-5}$ *M* solution of dithizone in carbon tetrachloride, titration was carried out with 0.0100 *M* bismuth(III), the solution being shaken well after each addition. The end-point was marked by the appearance of the orange $Bi(HDz)_3$ in the organic phase in place of the green colour of the reagent H_2Dz.

The chloride ion concentration in the aqueous phase was determined by transferring 4.0 ml to a 50-ml standard flask, adjusting the pH to about 4.6 by adding 5.0 ml of acetate buffer and making up to a final volume of 50 ml and ionic strength 1.0 *M* by suitable additions of potassium nitrate and deionized water. The silver–silver chloride electrode and the Hg_2SO_4–K_2SO_4 reference electrode were inserted, and the potential difference was measured after thermostatting at 22°. The chloride ion concentration was read off from a calibration curve.

Similar measurements were carried out with solutions of constant pH but varying added chloride ion concentrations. Results obtained in the presence of sulphate and phosphate ions are given in Table IV.

One of us R. H. Al-J. wishes to thank the Ministry of Oil (Iraq) for financial support. We are grateful to General Mills Ltd. for the gift of chemicals.

SUMMARY

The extraction of ethylenediaminetetraacetic acid (EDTA; H_4Y) from aqueous solutions of different pH and total chloride ion concentration by a solution of Aliquat-336-chloride in 1,2-dichloroethane has been studied. The species H_3Y^-, H_2Y^{2-}, HY^{3-} and Y^{4-} all partition with extraction constants, $\bar{K}_n^{ex}$, of *ca.* 0.0003, 0.0014, 0.0022 and 0.00365 respectively. Addition of chloride, sulphate and phosphate ions decreases the percentage of EDTA extracted, the effect decreasing in the order $Cl^- > SO_4^{2-} > PO_4^{3-}$.

RÉSUMÉ

On examine les possibilités d'extraction de l'EDTA en solution aqueuse, à divers pH et en fonction de la concentration totale en chlorure, en utilisant un échangeur anionique liquide, le chlorure d'Aliquat-336 dans le dichloro-1,2-ethane. Une addition de chlorure, de sulfate et de phosphate diminue le pourcentage d'EDTA extrait, dans l'ordre décroissant suivant: $Cl^- > SO_4^{2-} > PO_4^{3-}$.

ZUSAMMENFASSUNG

Die Extraktion von Äthylendiamintetraessigsäure (EDTA; H_4Y) aus wässrigen Lösungen bei verschiedenen pH-Werten und Gesamtchloridionen-Konzentrationen durch eine Lösung von Aliquat-336-Chlorid in 1,2-Dichloräthan wurde untersucht. Die Spezies H_3Y^-, H_2Y^{2-}, HY^{3-} und Y^{4-} verteilen sich mit Extraktionskonstanten $\bar{K}_n^{ex}$ von *ca.* 0.0003, 0.0014, 0.0022 und 0.00365. Durch Zugabe von Chlorid-, Sulfat- und Phosphationen wird der prozentuale Anteil des extrahierten EDTA herabgesetzt, wobei der Effekt in der Reihenfolge $Cl^- > SO_4^{2-} > PO_4^{3-}$ abnimmt.

REFERENCES

1 H. M. N. H. Irving and R. H. Al-Jarrah, *Anal. Chim. Acta*, 55 (1971) 135.
2 H. M. N. H. Irving and R. H. Al-Jarrah, to be published shortly.
3 G. Schwarzenbach and H. Flaschka, *Complexometric Titrations*, translated by H. M. N. H. Irving, Methuen, London, 1969.
4 N. Zaman, E. Merciny and G. Duyckaerts, *Anal. Chim. Acta*, 56 (1971) 261.
5 H. M. N. H. Irving and A. H. Nabilsi, *Anal. Chim. Acta*, 41 (1968) 505.
6 A. S. Brown, *J. Amer. Chem. Soc.*, 56 (1934) 646.

Analytica Chimica Acta, 65 (1973) 87–98
Elsevier Scientific Publishing Company, Amsterdam – Printed in The Netherlands

COMPLEXES DE L'EUROPIUM(II) AVEC LES ACIDES IMINO-DIACÉTIQUE ET NITRILOTRIACÉTIQUE EN SOLUTION AQUEUSE

E. COLLANGE et G. THOMAS

Laboratoire de Chimie Analytique II, Université Claude Bernard–Lyon I, 43 Boulevard du 11 Novembre 1918, 69621-Villeurbanne (France)

(Reçu le 29 septembre 1972)

Si la formation de complexes avec les ions tripositifs de terres rares a suscité de nombreux travaux, notamment avec les acides polyaminopolycarboxyliques[1,2], peu de publications sont consacrées à l'étude des complexes avec les cations de degré d'oxydation inférieur. Parmi ceux-ci, l'europium(II), le moins oxydable en raison de sa configuration électronique à sept électrons externes semble particulièrement intéressant. Nous citerons les travaux concernant les complexes formés avec l'EDTA, les acides citrique, tartrique et lactique[3], le DCTA[4] et l'acide pyridine-2-carboxylique[5].

Ce mémoire présente une étude potentiométrique des systèmes europium(II)–acide iminodiacétique (IMDA) et europium(II)–acide nitrilotriacétique (NTA) en solution aqueuse, de force ionique $\mu = 0.5$, en milieu perchlorate de sodium, ainsi que les résultats concernant la réduction polarographique de l'europium(III) en présence des mêmes aminoacides.

TECHNIQUES EXPÉRIMENTALES

L'ion Eu^{2+} étant oxydé à l'air[6], toutes les manipulations sont effectuées en atmosphère inerte; l'obtention par voie électrochimique des solutions d'europium(II), le dosage de la concentration en Eu^{2+}, de l'acidité libre et les courbes de neutralisation en présence d'agent complexant, sont effectuées sous courant d'azote purifié par passage sur de la tournure de cuivre chauffée à 350°. Les solutions sont préparées avec de l'eau désaérée, en caisse étanche Setaram purgée par trois gonflages successifs à l'azote d'un ballon sonde, et maintenue ensuite sous balayage d'azote.

Obtention des solutions d'europium(II)

Les solutions d'europium(II) sont préparées par électrolyse de solutions d'europium(III) obtenues par dissolution d'oxyde (Péchiney à 99.9%) dans un excès d'acide perchlorique. La cellule d'électrolyse inspirée de l'appareillage décrit par Mercier[5] est constituée d'un vase cylindrique en pyrex (hauteur 100 mm, diamètre 100 mm) sur lequel est adapté un anneau de polystyrène expansé par lequel passent une électrode de référence au calomel saturé remplie d'une solution de chlorure de sodium saturé, une arrivée et une sortie d'azote qui serviront ensuite au soutirage de la solution; le compartiment anodique central est un vase poreux (diamètre 55 mm, épaisseur 5 mm) muni d'un dispositif d'aspiration permettant

de renouveler en continu la solution anodique. La cathode est un panier de toile de platine (hauteur 55 mm, diamètre 68 mm), recouvert de mercure suivant le procédé préconisé par Ramaley *et al.*[7], fixé sur l'anneau de polystyrène. Le courant d'électrolyse est fourni par un potentiostat ASA 4 BT Tacussel, le potentiel de réduction est déterminé par tracé d'un polarogramme d'une solution de composition identique à la solution à électrolyser. Nous avons travaillé avec une valeur du potentiel cathodique de -1 V *vs.* E.C.S. La solution cathodique est constituée par une solution 10^{-1} *M* en Eu^{3+}, environ 0.5 *M* en acide perchlorique, en milieu perchlorate de sodium 1 *M*. La solution anodique ne contient pas d'europium. L'évolution de la réaction est suivie par dosage des cations et enregistrement du courant d'électrolyse en fonction du temps. Les solutions d'europium(II) sont soutirées sous azote, en ampoules scellées immédiatement après l'opération.

Dosage des solutions

Europium(II). La prise d'essais effectuée en atmosphère inerte est additionnée à une solution contenant un excès de fer(III). Nous titrons le fer(II) formé par dosage classique au bichromate de potassium.

Europium(III). Nous avons le plus souvent dosé les solutions d'europium(III) par l'EDTA dans l'hexaméthylènetétramine; l'indicateur est le noir ériochrome T[8]. Cependant, en milieu acétique, l'électrode indicatrice à goutte de mercure[9] donne une détermination précise du point d'équivalence. La solution d'europium(III) peut être encore réduite par passage sur une colonne de Jones; l'europium(II) est dosé comme précédemment.

Acidité libre. En présence d'europium(II) ou -(III), nous ne pouvons atteindre le pH de neutralisation sans avoir précipitation d'hydroxyde. Nous avons appliqué la méthode d'exploitation de Gran[10] en utilisant les premiers points de la courbe de neutralisation.

Etude potentiométrique

Les neutralisations sont effectuées dans des cellules Tacussel RM 06 thermostatées à $25 \pm 0.1°$, munies d'ouvertures rodées pour le passage des électrodes et d'un robinet permettant de régler le débit d'azote. Pour les solutions contenant de l'europium(II), la cellule est introduite dans la caisse étanche par l'intermédiaire du sas à vide et bouchée hermétiquement après introduction des réactifs. Dès sa sortie de la caisse étanche, elle est mise sous circulation d'azote.

Le pH est mesuré à l'aide d'un potentiomètre Metrohm E 388 avec une électrode en verre U.X. Metrohm et une électrode au calomel munie d'une allonge au chlorure de sodium, l'étalonnage étant effectué au moyen de solutions étalons de Bates[11]. La correspondance entre la valeur lue du pH (pH_0) et le cologarithme de la concentration en ions H^+ dans la solution $\{-\log(H^+)\}$ est établie au moyen de solutions de titre connu en acide ou en soude, en milieu perchlorate de sodium 0.5 *M*. La différence ΔpH entre $-\log(H^+)$ et pH_0 reste sensiblement constante entre pH 2 et 10; pour les deux électrodes que nous avons utilisées $\Delta pH = 0.16$ pour l'une, 0.19 pour l'autre. Les solutions de soude sont étalonnées au biphtalate de potassium, l'acide perchlorique, les solutions d'acide IMDA et NTA sont préparées à partir des produits commerciaux (R.P. Prolabo, Fluka, Merck).

Etude polarographique

Nous avons utilisé un polarographe enregistreur à 3 électrodes, PRT 20-2 Tacussel équipé d'une cellule Meci thermostatée à $25 \pm 0.1°$ comportant un robinet à trois voies qui permet d'assurer une circulation d'azote purifié au sein de la solution ou en surface lors des mesures. Les caractéristiques de l'électrode à goutte sont les suivantes: $t = 2.6$ s, $m = 6$; tous les potentiels sont exprimés par rapport à l'électrode au calomel saturée.

CONSTANTES DE DISSOCIATION DES AGENTS CHÉLATANTS

En solution aqueuse les acides IMDA (I) et NTA (II) existent sous forme de "zwitterions":

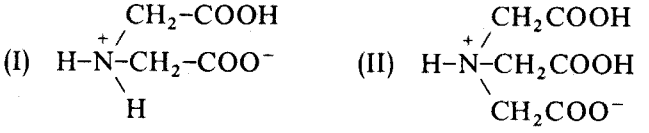

Nous avons neutralisé par de la soude 0.5 M, des solutions $5 \cdot 10^{-3}$ M en acide complexant en présence d'acide perchlorique 10^{-2} M. Le nombre moyen de protons fixés par la molécule d'agent complexant H_jA est calculé d'après la relation:

$$\bar{n}_H = \frac{T_E + J\,T_A + [OH] - [H] - [B]}{T_A}$$

où T_A est la concentration totale en agent chélatant, T_E la concentration en $HClO_4$, et [B] la concentration de base ajoutée. Les courbes de formation obtenues tendent effectivement vers $\bar{n}_H = 2$ pour l'IMDA, $\bar{n}_H = 3$ pour le NTA.

Pour l'acide iminodiacétique, les valeurs du pH pour $\bar{n}_H = 1.5$ et $\bar{n}_H = 0.5$ conduisent après affinement par la méthode des moindres carrés à:

$$pK_1^a = 2.63 \quad \text{et} \quad pK_2^a = 9.39$$

en bon accord avec les résultats publiés dans la littérature pour diverses valeurs de la force ionique[2,12–15].

Pour l'acide nitrilotriacétique, les valeurs approchées des constantes sont déterminées par $pK_3^a = [pH]_{\bar{n}_H = 0.5}$ et par les valeurs de la pente au point milieu pour $\bar{n}_H = 2$, et de la constante moyenne. Après affinement:

$$pK_1^a = 1.97 \quad pK_2^a = 2.43 \quad pK_3^a = 9.33$$

Nous avons remarqué que la valeur de pK_3^a ($\mu = 0.5$) diffère notablement des valeurs antérieurement publiées[16–19]. L'écart observé est imputable à la différence de force ionique: nous avons vérifié que, en milieu $NaClO_4$ 0.1 M nous obtenions des valeurs en excellent accord avec celles déterminées en milieu KCl 0.1 M[19]:

$$pK_1^a = 1.97 \quad pK_2^a = 2.43 \quad pK_3^a = 9.75 \ (NaClO_4\ 0.1\ M).$$

ÉTUDE POTENTIOMÉTRIQUE DES SYSTÈMES EUROPIUM(II)–ACIDE IMINODIACÉTIQUE ET EUROPIUM(II)–ACIDE NITRILOTRIACÉTIQUE

Elle est effectuée par la méthode de Calvin et Wilson[20]. On neutralise une

solution contenant le cation (10^{-3} M) et l'agent complexant en présence d'un excès d'acide libre, par une solution de soude, en mesurant le pH. Plusieurs courbes sont tracées pour des rapports T_A/T_M variant de 1 à 5. Le nombre de formation est calculé d'après la relation:

$$\bar{n} = \frac{1}{T_M}\left[T_A-(J\,T_A+T_E)-[H]+[OH]-[B]\,\frac{\sum_0^J \beta_j^H[H]^j}{\sum_1^J j\beta_j^H[H]^j}\right]$$

La concentration en coordinat libre est calculée d'après la relation:

$$[A] = \frac{J\,T_A+T_E-[H]+[OH]-[B]}{\sum_1^J j\beta_j^H[H]^j}$$

β_j^H est la constante de stabilité d'ordre j de H_jA, T_M est la concentration totale en cation métallique, les autres symboles sont définis dans le paragraphe précédent.

Système europium(II)–acide iminodiacétique

L'acide iminodiacétique forme avec les ions Eu(II) les complexes EuA et EuA_2^{2-}; l'hydroxyde précipite vers pH 10. La Fig. 1 présente les courbes de formation obtenues pour les rapports $T_A/T_M=3$ et 5; les constantes sont déterminées d'après les valeurs de pA pour $\bar{n}=0.5$ et $\bar{n}=1.5$ et conduisent après affinement à:

$\log K_1=4.93$ $\log K_2=2.58$ soit $\log \beta_2=7.51$

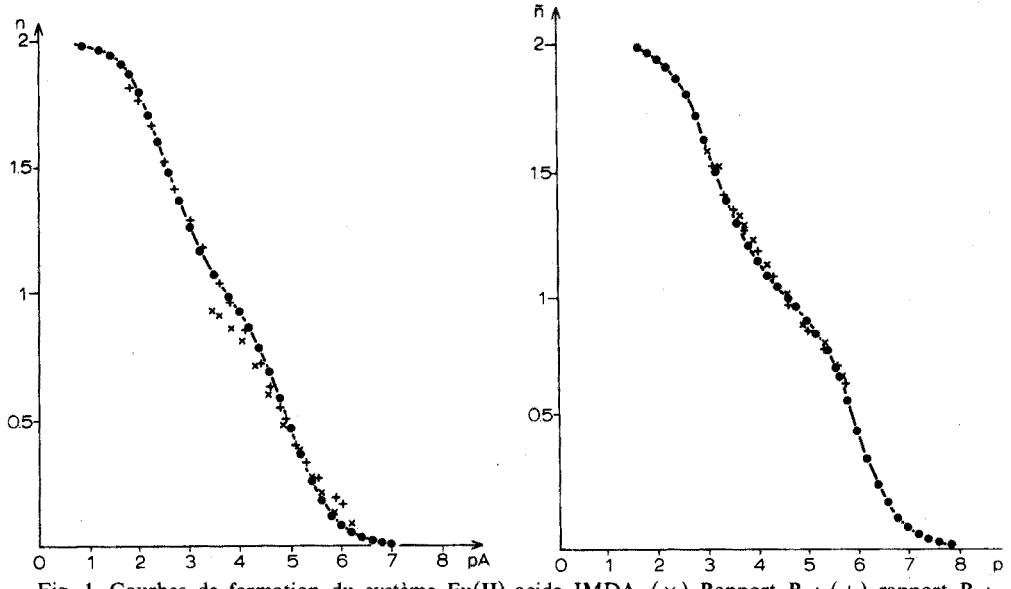

Fig. 1. Courbes de formation du système Eu(II)–acide IMDA. (×) Rapport R_3; (+) rapport R_5; (●) points recalculés.

Fig. 2. Courbes de formation du système Eu(II)–acide NTA. (×) Rapport R_2; (+) rapport R_3; (●) points recalculés.

Système europium(II)–acide nitrilotriacétique

L'acide nitrilotriacétique forme avec les ions Eu(II) les complexes EuA^- et EuA_2^{4-} ainsi qu'un complexe acide EuHA donnant EuA^- entre pH 7 et 8. La Fig. 2 présente les courbes de formation calculées à partir des neutralisations effectuées avec des rapports acide/métal égals à 2 et 3 et pour des valeurs du pH > 6. Nous en avons déduit la valeur de $\log K_2 = (pA)_{\bar{n}=1.5}$ et estimé $\log K_1$ d'après la constante moyenne $\log K = (pA)_{\bar{n}=1}$. Après affinement:

$$\log K_1 = 5.80 \qquad \log K_2 = 3.07$$

La courbe recalculée, sans tenir compte de la formation du complexe MHA, correspond assez bien avec la courbe expérimentale pour $\bar{n} > 0.7$.

Afin d'obtenir une meilleure valeur de K_1 ainsi que la constante de stabilité acide du complexe MHA, définie par $K^H_{MHA} = [MHA]/[MA][H]$, nous avons suivi une méthode graphique inspirée des travaux de Giron-Forest et Thomas[21]. Pour un rapport acide/métal égal à 1:

$$T_M = T_A = [MA] + [MHA] + [M] = [MHA] + [MA] + \Sigma(H_jA)$$
$$[M] = \Sigma(H_jA)$$

La concentration en protons liés, h, s'exprime par:

$$h = [MHA] + \sum_0^J j(H_jA) = T_E + 3T_A - [B] - [H] - [OH]$$

Compte tenu des équilibres de dissociation, ces équations conduisent à:

$$[A] = \frac{\left(1 + \frac{1}{K^H_{MHA}[H]}\right)h - T_A}{\sum_1^J j\,\beta_j^H [H]^j \left(1 + \frac{1}{K^H_{MHA}[H]}\right) - \sum_0^J \beta_j^H [H]^j}$$

$$[MA] = T_A - h - \sum_0^J (H_jA) + \sum_1^J j(H_jA)$$

Nous choisissons différents couples de valeurs expérimentales (ml, pH) correspondant à la zone de neutralisation du complexe MHA. En attribuant des valeurs arbitraires à $\log K^H_{MHA}$, nous pouvons calculer pour chaque couple ($\log K^H_{MHA}$ varient de 6.00 à 7.80), [A], [M], [MA] donc des valeurs de K_1. La représentation graphique de $\log K_1 = f(\log K^H_{MHA})$ donne (Fig. 3) un réseau de courbes se coupant en un seul point (K_1, K^H_{MHA}), solution unique pour toute la courbe de neutralisation. On en déduit:

$$\log K_1 = 5.55 \qquad \log K^H_{MHA} = 7.40 \qquad \log \beta_2 = 8.62$$

La valeur approchée de $\log K_1$ déterminée précédemment est de 5.8. Nous pouvons calculer la constante de formation du complexe MHA, $K_{MHA} = [MHA]/[M][H][A]$:

$$\log K_{MHA} = \log K^H_{MHA} + \log K_1 = 12.95.$$

La Fig. 4 présente le diagramme de répartition des différentes espèces en fonction du pH. Le complexe MHA est pratiquement le seul complexe présent jusqu'à pH 5, et atteint sa concentration maximale à pH 6.5.

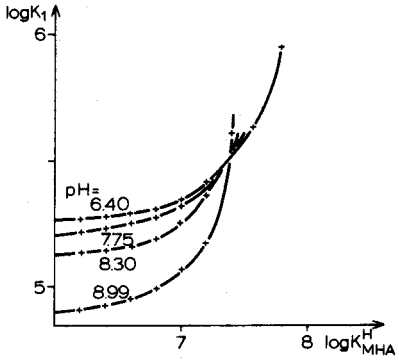

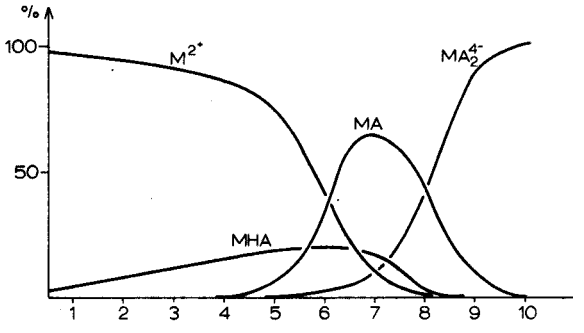

Fig. 3. Faisceau de courbes log $K_1 = f(\log K^H_{MHA})$, pour la détermination de K_1, K^H_{MHA}; système Eu(II)–acide NTA.

Fig. 4. Diagrammes de répartition du système Eu(II)–acide NTA en fonction du pH. $T_M = 10^{-3}$; $T_A = 2 \cdot 10^{-3}$.

Discussion

Bien que les valeurs des constantes de stabilité soient assez élevées:

$\log \beta_1 = 4.93$, $\log \beta_2 = 7.51$ avec l'acide IMDA;

$\log \beta_1 = 5.85$, $\log \beta_2 = 8.62$ avec l'acide NTA.

La formation de complexes de l'europium(II), ne protège pas de l'oxydation le cation Eu^{2+}; des solutions renfermant les complexes 1–2 sont rapidement oxydées en présence d'air.

Ces valeurs peuvent être comparées aux constantes des complexes de l'europium(III) que nous avons déterminées par potentiométrie, aucun résultat n'ayant été publié en milieu $NaClO_4$ $\mu = 0.5$[2,14,15,19,22,23].

Eu(III)–acide IMDA: formation successive de trois complexes

EuA^+: $\log \beta_1 = 6.62$; EuA_2^-: $\log \beta_2 = 11.13$; EuA^{3-}: $\log \beta_3 = 15.47$

Eu(III)–acide NTA: formation de deux complexes

EuA: $\log \beta_1 = 10.51$; EuA_2^{3-}: $\log \beta_2 = 19.51$

Les complexes de l'europium(II) sont moins stables; cette diminution de la stabilité se retrouve en présence d'EDTA[3], d'acide pyridine 2-carboxylique[5]. Elle peut être attribuée à la diminution de la charge ionique et à l'augmentation du rayon ionique du cation (1.09 Å au lieu de 0.96 Å) qui tendent à réduire la force de liaison terre rare coordinat, de nature principalement électrostatique.

RÉDUCTION POLAROGRAPHIQUE DE L'EUROPIUM(III) EN PRÉSENCE DES ACIDES IMINODIACÉTIQUE ET NITRILOTRIACÉTIQUE

La réaction de réduction Eu(III)–Eu(II) est généralement irréversible, le degré d'irréversibilité dépendant de la composition de la solution[3,24–31]. Après avoir repris quelques travaux concernant la réduction de Eu(III) à l'électrode à gouttes en

milieu perchlorate, et retrouvé les résultats d'études antérieures[24,25], nous nous sommes attachés à l'étude des vagues polarographiques obtenues en présence des acides concernés.

Résultats expérimentaux

Réduction de Eu(III) en milieu perchlorate de sodium. Les solutions sont 10^{-3} *M* en Eu(III), $1.6 \cdot 10^{-2}$ *N* en $HClO_4$, avec des concentrations croissantes en $NaClO_4$ de 10^{-2} *M* à 2 *M* (pH = 1.80). La Fig. 5 présente les variations du potentiel de demi-vague et de la pente réciproque (pente de la droite $E = f \log i/(i_d - i)$) en fonction de la concentration en perchlorate. La réaction n'est réversible qu'en milieu dilué; la valeur 60 mV/unité log de la pente en milieu 10^{-2} *M* augmente rapidement pour atteindre une limite voisine de 97 mV/unité log pour environ 1 *M*. Le potentiel de demi-vague suit une loi de variation semblable. Pour une concentration en perchlorate égale à 0.5 *M* (milieu utilisé pour notre étude) la pente réciproque est de 94 mV/unité log et $E_{\frac{1}{2}} = -0.695$ V. Nous avons vérifié, sur plusieurs solutions de force ionique 0.5 *M* et de pH variable compris entre 2 et 4.5, que la valeur de $E_{\frac{1}{2}}$ reste très voisine de -0.695 V.

Réduction de Eu(III) en présence d'acide IMDA. Influence du pH. Les solutions à polarographier sont $5 \cdot 10^{-4}$ *M* en Eu^{3+}, le rapport $T_A/T_M = 30$; $\mu = 0.5$; le pH varie de 1.6 à 10. La Fig. 6 présente le réseau de courbes obtenues. En milieu acide, les vagues de réduction sont évidemment très peu différentes de celles de l'europium seul. Quand le pH augmente, la vague de réduction se déplace vers des potentiels plus négatifs et est bien définie pour des pH voisins de 9 où le complexe d'europium(III) en solution est EuA_3^{3-}. A pH 9.75 $E_{\frac{1}{2}} = -1.32$ V et cette valeur ne varie pas pour des pH > 10. La mesure de la valeur du courant limite de diffusion en fonction de la hauteur de mercure montre que le processus est contrôlé par la diffusion.

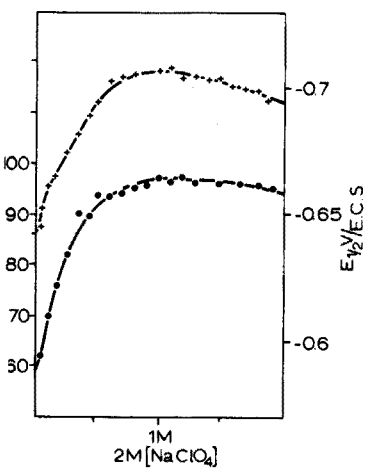

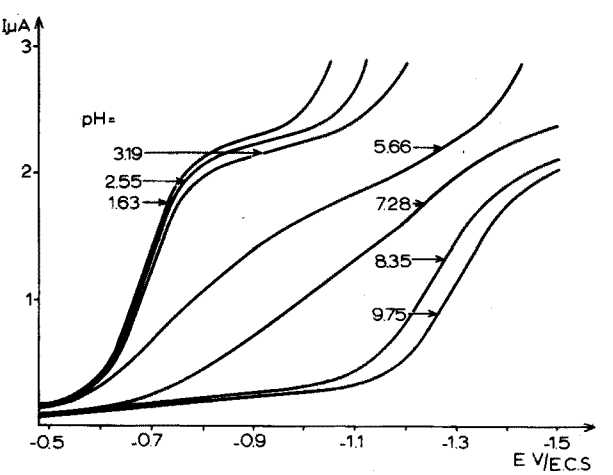

Fig. 5. Réduction polarographique Eu(III)–Eu(II) en milieu $NaClO_4$. Variation de la pente réciproque (+) et de $E_{\frac{1}{2}}$ (●) en fonction de la concentration en perchlorate de sodium.

Fig. 6. Système Eu(III)–acide IMDA. Influence du pH sur les vagues de réduction. $T_M = 5 \cdot 10^{-4}$ *M*; $T_A = 1.5 \cdot 10^{-2}$ *M*.

TABLEAU I

SYSTÈME EUROPIUM(III)–ACIDE IMDA. VARIATION DE $E_{\frac{1}{2}}$ ET DE LA PENTE RÉCIPROQUE AVEC LA CONCENTRATION EN AGENT CHÉLATANT

$R = T_A/T_M$	*pH*	*log [IMDA]*	$E_{\frac{1}{2}}$ *(V vs. E.C.S.)*	*Pente réciproque (mV/unité log*
0	2.10		−0.695	95
20	9.23	−2.30	−1.28	155
30	9.26	−2.04	−1.30	159
40	9.30	−1.87	−1.32	157
50	9.24	−1.74	−1.33	160
80	9.28	−1.64	−1.36	159

Déplacement de $E_{\frac{1}{2}}$ en fonction de la concentration en acide IMDA à pH constant 9.3. Les solutions sont $5 \cdot 10^{-4}$ *M* en Eu^{3+}, $\mu = 0.5$, avec des rapports $R = T_A/T_M = 20$, 30, 40, 50, 80. Quelle que soit la concentration en agent complexant, le système est irréversible, la valeur de la pente réciproque voisine de 160 mV/unité log. Le Tableau I rassemble les résultats obtenus.

La variation de $E_{\frac{1}{2}} = f(\log [IMDA])$ est linéaire; la pente de la droite est de −0.133 V par unité log.

Réduction de Eu(III) en présence d'acide NTA. Influence du pH. Les solutions polarographiées sont 10^{-3} *M* en Eu(III) et $3 \cdot 10^{-2}$ *M* en acide NTA; $\mu = 0.5$; le pH varie de 1 à 11.30. Comme le montre la Fig. 7 la vague de réduction ($E_{\frac{1}{2}} = -0.695$ V à pH 1) est déplacée vers les potentiels négatifs quand le pH augmente. Dès pH 7, où la totalité du complexe EuA_2^{3-} est présente, la vague de réduction est très nette, $E_{\frac{1}{2}} = -1.69$ V ne varie pas avec le pH; le processus est contrôlé par la diffusion.

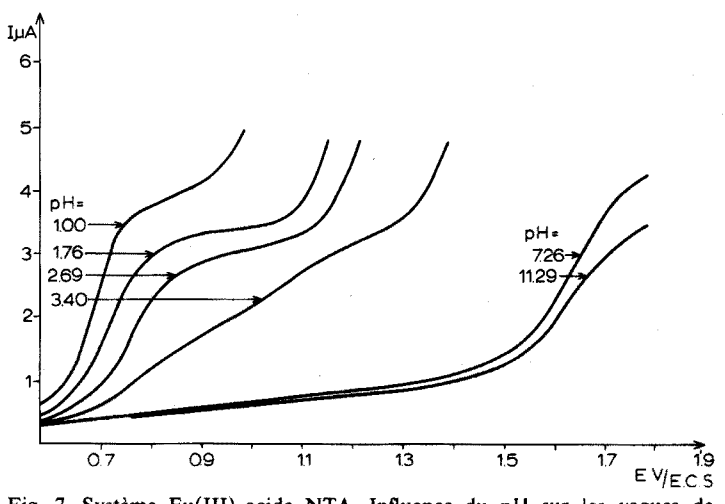

Fig. 7. Système Eu(III)–acide NTA. Influence du pH sur les vagues de réduction. $T_M = 10^{-3}$ *M*; $T_A = 3 \cdot 10^{-2}$ *M*.

TABLEAU II

SYSTÈME EUROPIUM(III)–ACIDE NTA. VARIATION DE $E_{\frac{1}{2}}$ AVEC LA CONCENTRATION EN AGENT CHÉLAT NT

$R = T_A/T_M$	*pH*	$E_{\frac{1}{2}}$ *(V vs. E.C.S.)*	*Pente (mV/unité log)*
0	2.10	−0.695	95
10	9.06	−1.685	96
20	9.22	−1.69	95
30	9.27	−1.69	94
40	9.30	−1.68	95
50	9.32	−1.69	95

Influence de la concentration en agent complexant à pH constant pH = 9.3. Le Tableau II présente les résultats relatifs à cinq solutions $5 \cdot 10^{-4}$ *M* en Eu(III) pour des rapports $T_A/T_M = 10, 20, 30, 40, 50$; $\mu = 0.5$.

Le processus est irréversible, mais ici la valeur de la pente réciproque pour chaque cas est pratiquement celle trouvée pour la réduction du cation en absence d'agent complexant. La valeur du potentiel de demi-vague est très négative −1.69 V au lieu de 0.695 V et est indépendante de la concentration en acide NTA.

Discussion des résultats

Malgré l'irréversibilité d'un système, l'analyse des courbes polarographiques peut apporter des renseignements en particulier sur les espèces électroréductibles. D'après Koryta[32] on peut décomposer le processus de réduction d'un ion complexe au plusieurs étapes: transfert du voisinage de l'électrode de la particule dépolarisante MA_p existant en solution, entrée de cette particule dans la double couche, suivie éventuellement d'une dissociation conduisant à une autre espèce MA_k qui est réduite par transfert électrochimique. Il est encore possible que le produit de la réaction quittant la double couche subisse une transformation chimique pour donner le complexe MA_q qui est transporté en solution, mais généralement k = q. Vlcek[24] signale qu'un tel processus est toujours irréversible.

Dans cette hypothèse, le courant de réduction est proportionnel à la concentration en complexe MA_k dans la double couche et pour une valeur constante du potentiel, si $\beta_{MA_p} \gg \beta_{MA_k}$

$$\frac{i}{i_d - i} = 0.0886 t^{\frac{1}{6}} D^{-\frac{1}{2}} k_e \frac{\beta_{MA_k}}{\beta_{MA_p}} \frac{[A]^k}{[A]^p} \qquad (1)$$

où t est le temps de chute des gouttes, D le coefficient de diffusion du complexe MA_p, et k_e la constante de vitesse de la réaction.

C'est à dire que le graphe de la fonction $\log i/(i_D - i) = f(\log [A])$ doit être une droite dont la pente donne $-p+k$.

Pour le système Eu(III)–acide IMDA nous avons calculé cette fonction d'après les vagues de réduction présentées, correspondant au Tableau I, pour quatre valeurs du potentiel −1.25, −1.35, −1.40, −1.50 V. [A] est déterminée en négligeant la formation de complexes car nous sommes en présence d'un grand excès d'agent complexant. La Fig. 8 présente le réseau de droites obtenues, droites parallèles avec

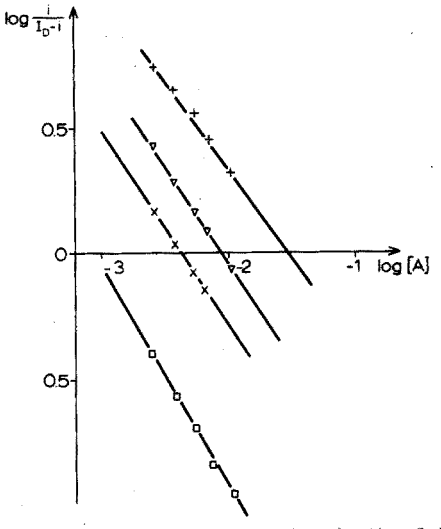

Fig. 8. Réseau de droites $\log i/(i_d - i) = f(\log [A])$ pour le système (Eu(III)–IMDA. (□) $E = -1.25$ V *vs.* E.C.S.; (×) $E = -1.35$ V *vs.* E.C.S.; (▽) $E = -1.40$ V *vs.* E.C.S.; (+) $E = -1.50$ V *vs.* E.C.S.

une valeur moyenne de la pente égale à -0.85. Donc $-p+k=-1$ et puisque $p=3$, $k=2$ c'est donc le complexe EuA_2^- résultant de la dissociation de EuA_3^{3-} qui est réduit à l'électrode en EuA_2^{2-} selon:

$$EuA_3^{3-} \rightarrow EuA_2^- + A^{2-}$$

$$EuA_2^- + e \rightarrow EuA_2^{2-}$$

D'autre part la relation (1) peut nous conduire à la constante de vitesse k_e de la réaction à l'électrode:

$$\log k_e = \log \frac{i}{i_d - i} - \log 0.886 t^{\frac{1}{2}} D^{-\frac{1}{2}} - \log \frac{\beta_{MA_k}}{\beta_{MA_p}} - (k-p) \log [A] \qquad (2)$$

k_e est liée à la constante de dissociation standard k_0 et au potentiel par:

$$k_e = k_0 \exp \left\{ - \frac{\alpha n F}{RT} (E - E_0') \right\}$$

ou encore:

$$\log k_e = \log k_0 + \frac{\alpha E_0'}{0.058} - \frac{\alpha E}{0.058}$$

E_0' est le potentiel normal d'oxydo-réduction de la réaction considérée; α le coefficient de transfert est alors donné par la pente de la droite représentant la fonction $\log k_e = f(E)$.

Les valeurs de k_e sont déterminées d'après les coordonnees de l'intersection des droites $\log i/(i_d - i) = f(\log [A])$ (Fig. 8) avec l'axe des abscisses; nous avons calculé une valeur approchée du coefficient de diffusion moyen du complexe EuA_3^{3-} par application de l'équation d'Ilkovic: $D = 1.58 \cdot 10^{-6}$ cm^2 s^{-1}; $t = 2.6$ s.

$$\log \beta_{MA_p} = \log \beta_{EA_3^{3-}} = 15.47; \quad \log \beta_{MA_k} = \log \beta_{EuA_2^-} = 11.13.$$

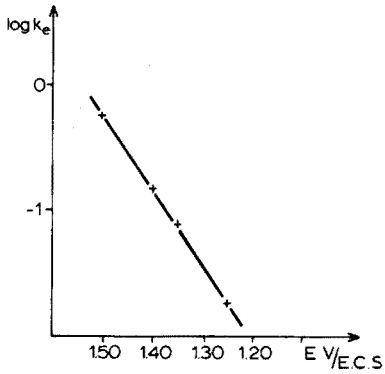

Fig. 9. Système Eu(III)–acide IMDA. Fonction log $k_e = f(E)$.

La Fig. 9 représente la variation linéaire log $k_e = f(E)$. k_e est d'autant plus grand que le potentiel est plus négatif; la valeur de la pente est de -6.06 unité log par volt, ce qui correspond à un coefficient de transfert $\alpha = 0.35$ en accord avec la valeur (160 mV) de la pente des droites $E = f\{\log i/(i_d - i)\}$.

Avec le système Eu(III)–acide NTA. Pour une valeur déterminée du potentiel log $i/(i_d - i)$ reste constant quand la concentration en agent complexant varie. Les complexes MA_p et MA_k ont le même nombre de coordinats, la réaction de réduction s'écrit:

$$EuA_2^{3-} + e^- \rightarrow EuA_2^{4-}$$

La valeur de la pente réciproque 95 mV/unité log étant pratiquement celle correspondant au cation seul en milieu 0.5 *M*, nous pouvons avoir une valeur approchée de la constante globale de stabilité du complexe 1–2 de l'Eu(II)) en remplaçant dans l'expression établie par Lingane[33] la valeur théorique 0.058 par 0.095 ($\alpha = 0.61$).

$$\Delta E_{\frac{1}{2}} = -0.095 \log (\beta_{EuA_2^{3-}}/\beta_{EuA_2^{4-}}) \quad \text{avec} \quad \Delta E_{\frac{1}{2}} = -(1.69 - 0.695) = -0.995 \text{ V}$$

soit log $(\beta_{EuA_2^{3-}}/\beta_{EuA_2^{4-}}) = 10.47$; log $\beta_{EuA_2^{4-}} = 9.0$; valeur proche de celle déterminée par potentiométrie.

RÉSUMÉ

Les constantes de dissociation des acides iminodiacétique et nitrilotriacétique ont été déterminées en milieu perchlorate de sodium $\mu = 0.5$ à 25°. L'étude potentiométrique des complexes de l'europium(II) avec les acides iminodiacétique et nitrilotriacétique a mis en évidence la formation des espèces 1:1 et 1:2 dont on détermine les constantes. Un complexe MHA se forme en milieu acide en présence d'acide nitrilotriacétique. La réduction polarographique de l'europium(III) en présence des acides complexants est un processus irréversible; en présence d'acide iminodiacétique la réaction à l'électrode est précédée d'une dissociation du complexe EuA_3^{3-}.

SUMMARY

The dissociation constants of iminodiacetic acid and nitrilotriacetic acid have

been determined in sodium perchlorate medium ($\mu=0.5$) at 25°. A potentiometric study of the europium(II) complexes of these acids has indicated the formation of 1:1 and 1:2 species; the formation constants have been determined. A MHA complex is formed in acidic medium in the presence of nitrilotriacetic acid. The polarographic reduction of europium(III) in the presence of these complexing acids is irreversible; in the presence of iminodiacetic acid, the reaction at the electrode is preceded by dissociation of the EuA_3^{3-} complex.

ZUSAMMENFASSUNG

Die Dissoziationskonstanten von Iminodiessigsäure und Nitrilotriessigsäure wurden in Natriumperchlorat-Medium ($\mu=0.5$) bei 25° bestimmt. Eine potentiometrische Untersuchung der Europium(II)-Komplexe dieser Säuren ergab, dass 1:1- und 1:2-Spezies gebildet werden; die Bildungskonstanten wurden ermittelt. Ein MHA-Komplex wird in saurem Medium in Gegenwart von Nitrilotriessigsäure gebildet. Die polarographische Reduktion von Europium(III) in Gegenwart dieser komplexierenden Säuren ist irreversibel; in Gegenwart von Iminodiessigsäure geht der Reaktion an der Elektrode die Dissoziation des EuA_3^{3-}-Komplexes voraus.

BIBLIOGRAPHIE

1 T. Moeller, D. F. Martin, L. C. Thompson, R. Ferrus, G. R. Feistel and W. J. Randall, *Chem. Rev.*, 65 (1965) 1.
2 I. Grenthe, *Acta Chem. Scand.*, 25 (1971) 1401.
3 L. Holleck, *Z. Elektrochem.*, 59 (1955) 202.
4 E. P. Horwitz, *Doctoral Dissertation*, University of Illinois, 1957.
5 R. C. Mercier, *Thèse*, Lyon, 1967.
6 H. Maccoy, *J. Amer. Chem. Soc.*, 58 (1936) 1577.
7 L. Ramaley, R. L. Brubaker et C. G. Enke, *Anal. Chem.*, 35 (1964) 1808.
8 R. Wehber, *Z. Anal. Chem.*, 35 (1965) 149.
9 C. N. Reilley, R. W. Schmid et D. W. Lawson, *Anal. Chem.*, 30 (1958) 953.
10 G. Gran, *Analyst*, 77 (1952) 661.
11 R. G. Bates, *J. Res. Natl. Bur. Stand.*, 66A (1962) 179.
12 G. Schwarzenbach et E. Kampistch, *Helv. Chim. Acta*, 28 (1945) 1183.
13 G. Schwarzenbach et H. Senn, dans L. G. Sillen et A. Martell, *Stability Constants*, 1964, p. 427.
14 S. Chabereck et A. E. Martell, *J. Amer. Chem. Soc.*, 74 (1952) 5022.
15 L. C. Thompson, *Inorg. Chem.*, 1 (1962) 490.
16 A. E. Martell et V. L. Hughes, *J. Amer. Chem. Soc.*, 74 (1952) 5022.
17 G. Schwarzenbach, E. Kampistch et R. Steiner, *Helv. Chim. Acta*, 28 (1945) 828.
18 G. Schwarzenbach et R. Gut, *Helv. Chim. Acta*, 34 (1956) 1589.
19 T. Moeller et R. Ferrus, *Inorg. Chem.*, 1 (1962) 55.
20 M. Calvin et K. W. Wilson, *J. Amer. Chem. Soc.*, 67 (1945) 2003.
21 D. Giron-Forest et G. Thomas, *Bull. Soc. Chim. Fr.*, 1 (1972) 390.
22 S. Misumi, *Rev. Polarogr. (Kyoto)*, 11 (1963) 146.
23 S. C. Lewy et J. E. Powell, *U.S. At. Energy Comm.*, Février 1961.
24 A. A. Vlcek, *Chem. Listy*, 52 (1958) 214.
25 L. Gierst et P. Cornelissen, *Collect. Czech. Chem. Commun.*, 25 (1960) 3004.
26 J. E. B. Randles, *Trans. Faraday Soc.*, 48 (1952) 937.
27 S. Misumi, *Bull. Soc. Chem. Jap.*, 39 (1966) 10.
28 N. F. Kinard, *J. Electroanal. Chem.*, 25 (1970) 373.
29 D. J. Macero, H. B. Herman et A. J. Dukat, *Anal. Chem.*, 37 (1965) 675.
30 C. W. De Kreuk, *J. Electroanal. Chem.*, 28 (1970) 391.
31 E. I. Onstott, *J. Amer. Chem. Soc.*, 74 (1962) 3773.
32 J. Koryta, *Chem. Listy*, 51 (1941) 1544.
33 J. J. Lingane, *Chem. Rev.*, 29 (1941) 1.

Analytica Chimica Acta, 65 (1973) 99–104

THE EXTRACTION OF MERCURY FROM AQUEOUS SOLUTION WITH SULFIDE-TREATED POLYURETHANE FOAM

M. A. J. MAZURSKI, A. CHOW and H. D. GESSER

Department of Chemistry, University of Manitoba, Winnipeg, Manitoba R3T 2N2 (Canada)

(Received 13th November 1972)

Present separation methods for inorganic pollutants, such as co-precipitation[1], ion exchange[2], freeze concentration[1], adsorptive bubble separations[3], membrane techniques[3] and gas-chromatographic methods[4], have been applied to their extraction from aqueous solutions with limited success. Generally, these methods require extensive pretreatment of the solution, are non-specific, or could be susceptible to fouling.

High-molecular-weight amines[5] have been used in solvent extractions for the removal of mercury from solutions of brine and other chlorides, but the method is not specific for mercury. Agricultural products[6] and by-products have been shown to be capable of adsorbing methylmercury(II) chloride and mercury(II) chloride from aqueous solutions, but recovery of mercury from these products was not quantitative.

In 1970, a report[7] appeared which examined distribution ratios and adsorption capacities of polyurethane foams for a few selected elements. The extraction of gold[8] from aqueous solutions by means of polyurethane foam has also been studied. Specially treated polyurethane foam has been used as the stationary phase for the chromatographic separation of nickel and palladium[9]. Materials similar to polyurethane foams have also been used to adsorb mercury. Carbohydrates and polyamine polymers[10] have been shown to be capable of adsorbing mercury(II) chloride from aqueous solutions and treated polyamine foams[11] have been produced which act as ion exchangers. Polyamine–polyurea resins extract such ions as Cu(II), Ni(II), Au(II) and Co(II) from aqueous solutions[12]. Polyurethane foam has been used as an extraction material in such processes as cigarette filters[13], oil spill cleanups[14,15], phenol adsorption[16], and more recently for the removal of pesticides from aqueous solutions[17,18].

This present paper reports a study of the adsorption of mercury(II) chloride and methylmercury(II) chloride by polyurethane foams which had been treated with hydrogen sulfide. The extraction of mercury in concentrations of 4.0–0.0004 p.p.m., and the recovery of the adsorbed mercury from the foams are discussed.

EXPERIMENTAL

Apparatus and reagents

A Perkin-Elmer Model 306 atomic absorption spectrophotometer was used with a Graphicorder (Dynatronic Instr. Corp., Model 8020) and a mercury hollow-

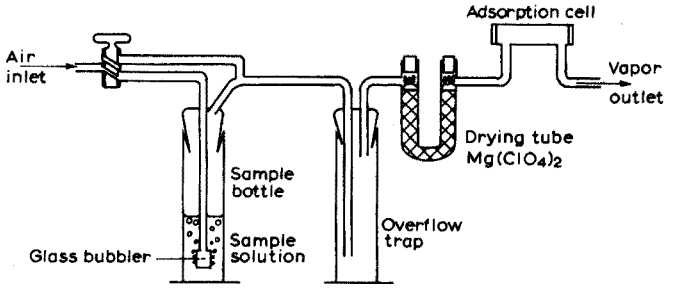

Fig. 1. Aeration system for low concentration mercury analysis (not to scale).

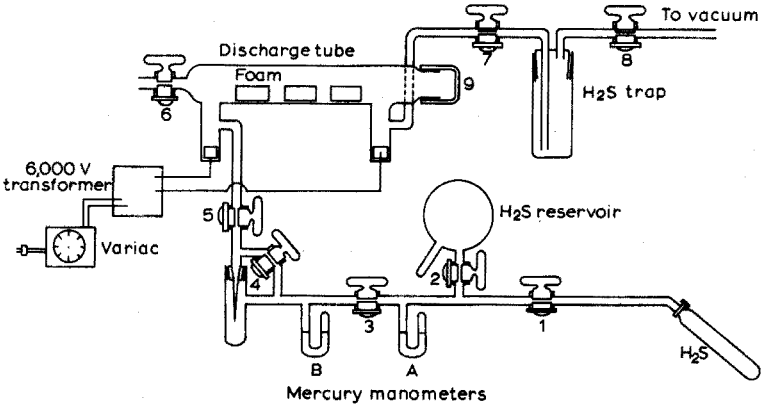

Fig. 2. Gas rack used to produce sulfide-treated polyurethane foam (not to scale).

cathode lamp (Varian Techtron). The aeration system for mercury analysis is shown in Fig. 1, and the vacuum gas rack with a high-voltage discharge tube in Fig. 2. The other equipment used included a Soxhlet extraction apparatus, and an Ott planimeter type 16 (American Industrial and Scientific Co., Los Angeles, Calif.). Polyurethane foams were of 22 mm diameter by 40 mm length (Canlab, Winnipeg).

All the chemicals used were of reagent grade. The water used was doubly distilled and then deionized.

Preparation of standard solutions

The methylmercury(II) chloride was obtained from Environment Canada, Freshwater Institute, Winnipeg 19, Canada, at a concentration of 500 p.p.m. methylmercury in an ethyl acetate solution. This solution was diluted to several concentrations between 2.0 and 0.0004 p.p.m. methylmercury for use. A stock solution of 1000 p.p.m. mercury as mercury(II) chloride in 2 *M* hydrochloric acid was also diluted to several concentrations between 4.0 and 0.0004 p.p.m. mercury for study.

Preparation of foams

The vacuum gas rack (Fig. 2) with a high-voltage discharge tube, was specifically designed for the production of sulfide-treated polyurethane foams. Three

polyurethane foams were placed 1 cm apart in the discharge tube through cap 9. The entire gas rack was pumped down with a vacuum pump and the hydrogen sulfide reservoir was then filled. A potential of 2,000 V was applied across the discharge tube containing hydrogen sulfide for 150 s. The discharge was controlled by the Variac to produce an even blue discharge. The treated polyurethane foams were removed from the discharge tube, Soxhleted with water from 8 h and then air-dried. These foams were stored in sealed polyethylene bottles until use. Successive production of the treated foams required that the hydrogen sulfide trap be replaced by a clean one to prevent the gas from leaking into the vacuum pump when the discharge chamber was being pumped down again.

Procedure

The treated polyurethane foams were fitted into glass columns that had a slightly smaller diameter than the foams. The foams were placed in the column with as little space as possible between them in such a way as not to compress their normal 40-mm length. Standard mercury solutions were passed through the foams in 100-ml aliquots and collected in glass sample bottles. Each successive sample that was collected from a fresh 100-ml aliquot passed through the same foams was numbered 1, 2, 3, etc. A constant flow rate of 40 ml min^{-1} was obtained by regulating the teflon stopcocks at the bottom of the columns. A slight air pressure was used to remove most of the solution left in the foams after each 100-ml aliquot of standard had been passed through them. Simultaneously, blanks that were matrix-matched to the standards, along with the standards themselves, and the standard solutions that had passed through the foams, were analyzed.

The procedure for analysis was similar to a standard flameless atomic absorption spectrophotometric method[19,20]. A quartz-windowed, 10-cm spectrophotometric cell was used and the sample bottle housing the sintered glass bubbler had a capacity of 300 ml. The methylmercury samples consisted of 100-ml solutions to which 1 ml of (1+4) sulfuric acid and 1 ml of 4% potassium permanganate solution had been added. After heating to boiling and cooling to room temperature, 8 drops of hydroxylamine hydrochloride and 4 ml of 20% tin(II) chloride solution were added to the samples before analysis. For the mercury(II) chloride samples, only the addition of 4 ml of the tin(II) solution was required. The air flow in the system was maintained at such a rate as to give complete aeration of a standard mercury sample in about 5 min. Generally, fresh magnesium perchlorate was placed in the drying tube after 25 samples had been aerated. The areas under the peaks recorded for the standards, the standards that had been passed through the foams, and the blanks were all measured by a planimeter, the average of three evaluations being used. A standard deviation was obtained from the determination of several identical standards. This standard deviation is recorded in the Tables, expressed as the deviation in the percentage mercury removed.

RESULTS

The results for the absorption of mercury(II) chloride by the sulfide-treated polyurethane foams are given in Table I. Repeated analyses of various test concentrations showed the reproducibility of the method. The treated foam showed a

TABLE I

ABSORPTION OF MERCURY(II) CHLORIDE BY SULFIDE-TREATED POLYURETHANE FOAM

(Unless otherwise mentioned, three foams were used per column)

Number of pass through foam[a]	*Hg concentration taken (p.p.m.)*	*Hg removed (%)*	*Number of pass through foam*[a]	*Hg concentration taken (p.p.m.)*	*Hg removed (%)*
1	4.0	69±2	1	0.04[c]	99±1
2		46±2	2		99±1
3		23±2	3		99±1
1	4.0	74±2	1	0.004	96±1
2		46±2	2		98±1
3		20±2	3		98±1
1	0.4	99±1	1	0.0004	99±1
2		99±1	2		99±1
3		98±1	3		99±1
1	0.04[b]	99±1	4		99±1
2		99±1	5		99±1
3		99±1	6		99±1

[a] Each series of numbers represents the first, second, ... pass of a fresh 100-ml aliquot of the mercury standard through the same foam with each resultant sample then being analyzed.
[b] This result was entirely reproducible with a different foam column.
[c] In this case, six foams were used in the column.

TABLE II

ABSORPTION OF METHYLMERCURY(II) CHLORIDE BY SULFIDE-TREATED POLYURETHANE FOAM

(Three foams were used per column in all cases)

Number of pass through foam	*Hg concentration taken (p.p.m.)*	*Hg removed (%)*	*Number of pass through foam*	*Hg concentration taken (p.p.m.)*	*Hg removed (%)*
1	2.0	50±2	1	0.004	94±2
2		34±2	2		91±2
3		29±2	3		83±2
1	0.4	75±2	1	0.0004	80±2
2		47±2	2		80±2
3		33±2	3		72±2
1	0.04	80±2			
2		75±2			
3		66±2			

saturation pattern during two successive passes through the foam of fresh 100-ml aliquots of the 4.0-p.p.m. mercury(II) chloride standard. This saturation effect was also shown at 0.4 p.p.m. with the third 100-ml aliquot of standard. At lower concentrations, the results indicate nearly complete absorption of all the mercury. The effectiveness of the sulfide foam for absorbing mercury does not appear to be

dependent on storage time, as freshly prepared and one-month old foams gave similar absorption of 0.04-p.p.m. solutions.

The sulfide-treated foams were also tested for methylmercury(II) chloride; the results are summarized in Table II. There is a distinct saturation pattern shown over the entire concentration range, but it is most pronounced at the higher concentrations. The effective capacity of the foams for mercury seems to be much higher for mercury(II) chloride than methylmercury(II) chloride, which may reflect some effect of steric hindrance by the methyl group on the mercury compared to the chlorine.

The percentage of mercury absorbed generally increased when the concentration of mercury used was decreased. Increasing the number of foams per column, as in Table I at the 0.04-p.p.m. mercuric chloride concentration, showed no change in the percentage of mercury removed, although the capacity for mercury absorption should increase. Increasing the amount of time that the solution is in contact with the foam, should increase the amount of mercury absorbed.

DISCUSSION

Polyurethane foam treated with hydrogen sulfide was shown to be very efficient for separating and concentrating mercury(II) chloride from aqueous solutions over the concentration range 4.0–0.0004 p.p.m. mercury. The foam was shown to remove methylmercury(II) chloride from aqueous solutions over the concentration range 2.0–0.0004 p.p.m. methylmercury, but somewhat less effectively. The results obtained were shown to be reproducible and the overall method appears very simple and inexpensive.

This method would be very useful for concentrating very low concentrations of mercury from large volumes of water, for aqueous solutions pass easily through the foams at relatively high flow rates. These foams should make useful monitoring devices for mercury levels in industry, in environmental analysis and in the laboratory if quantitative removal of the mercury from the foams can be achieved. Results from Soxhleting the foams with 2 *M* hydrochloric acid indicate that quantitative extraction and recovery of the mercury from the foams is possible. The effect of other ions competing against mercury for absorption does not appear to be important when these ions are at the levels generally found in tap water. Over 1500 l of domestic tap water were run through three sulfide-treated polyurethane foams before these foams were tested with a 0.04-p.p.m. mercury(II) chloride solution. The percentage of mercury removed was equivalent to that removed by three sulfide-treated polyurethane foams after the normal procedure of a preliminary Soxhleting with water.

This procedure is presently being extended to the selective extraction of other metals by the use of various complexing agents on various foams.

This work has been supported by the Faculty of Graduate Studies, University of Manitoba and by the Environmental Research Committee (Manitoba Scientists to Combat Pollution) by a LIP and Province of Manitoba Grant.

SUMMARY

Polyurethane foams treated in an electrical discharge with hydrogen sulfide to

incorporate sulfhydryl groups in the foam were examined for their ability to adsorb mercury(II) chloride and methylmercury(II) chloride from aqueous solutions. The concentration ranges studied were 4.0–0.0004 p.p.m. for mercury(II) and 2.0–0.0004 p.p.m. for methylmercury. Analysis showed that the adsorption of the mercury approached 100% in many cases.

RÉSUMÉ

Des mousses de polyuréthane, traitées par décharge électrique avec sulfure d'hydrogène pour leur incorporer des groupes sulfhydryles, sont examinées en vue de déterminer leur pouvoir d'adsorption en chlorure de mercure(II) et chlorure de méthylmercure(II), en solution aqueuse. Les quantités traitées vont de 4.0 à 0.0004 p.p.m. de mercure(II) et de 2.0 à 0.0004 p.p.m. pour le méthylmercure(II). L'analyse montre que l'adsorption du mercure est voisine de 100% dans la plupart des cas.

ZUSAMMENFASSUNG

Polyurethan-Schäume, die zwecks Einführung von Sulfhydryl-Gruppen in einer elektrischen Entladung mit Schwefelwasserstoff behandelt worden waren, wurden auf ihre Fähigkeit zur Adsorption von Quecksilber(II)-chlorid und Methylquecksilber(II)-chlorid aus wässrigen Lösungen untersucht. Die untersuchten Konzentrationsbereiche waren 4.0–0.0004 p.p.m. bei Quecksilber(II) und 2.0–0.0004 p.p.m. bei Methylquecksilber. Die Analyse ergab, dass in vielen Fällen eine 100%ige Adsorption des Quecksilbers erreicht wurde.

REFERENCES

1 E. W. Berg, *Physical and Chemical Methods of Separations*, McGraw Hill, New York, 1963.
2 W. Rieman, *Ion Exchange in Analytical Chemistry*, Pergamon Press, New York, 1970.
3 L. L. Ciacco (Editor), *Water and Water Pollution Handbook*, Marcel Dekker, New York, 1971, Ch. 11, 2, and p. 558.
4 R. W. Moshier and R. E. Sievers, *Gas Chromatography of Metal Chelates*, Pergamon Press, New York, 1965.
5 F. L. Moore, *Environ. Sci. Tech.*, 6 (1972) 525.
6 M. Freidman and A. C. Waiss, *Environ. Sci. Tech.*, 6 (1972) 457.
7 H. J. M. Bowen, *J. Chem. Soc.*, (1970) 1082.
8 P. Schiller and G. B. Cook, *Anal. Chim. Acta*, 54 (1971) 364.
9 T. Braun and A. B. Farag, *Anal. Chim. Acta*, 61 (1972) 265.
10 M. S. Masri and M. Friedman, *Environ. Sci. Tech.*, 6 (1972) 745.
11 S. Nonagaki, S. Makishima and Y. Yoneda, *J. Phys. Chem.*, 62 (1958) 601.
12 J. Dingman, S. Siggia, C. Barton and K. B. Hiscock, *Anal. Chem.*, 44 (1972) 1351.
13 R. L. Strickman, *U.S. Pat. 3,618,618; Chem. Abstr.*, 76, 97051 (1971).
14 R. G. Will and J. F. Grutsch, *U.S. Pat. 3,617,552; Chem. Abstr.*, 76, 27828 (1971).
15 E. C. A. Cadron and L. Jourquin, *Belg. Pat. 764,805; Chem. Abstr.*, 76 158074 (1971).
16 R. C. Schljcht and F. C. McCoy, *U.S. Pat. 3,617,531.*
17 H. D. Gesser, A. Chow, F. C. Davis, J. F. Uthe and J. Reinke, *Anal. Lett.*, 4 (1971) 883.
18 H. D. Gesser, J. F. Uthe and J. Reinke, *Environ. Lett.*, 3 (1972) 117.
19 The Dow Chemical Co., *Determination of Mercury by Atomic Absorption Spectrophotometric Method*, Method CAS-AM-70.13.
20 W. R. Hatch and W. L. Ott, *Anal. Chem.*, 40 (1968) 2085.

Analytica Chimica Acta, 65 (1973) 105–113

THERMAL PROPERTIES OF SOME COMPLEXES OF QUINOLINIC ACID WITH DIVALENT METAL IONS

G. D'ASCENZO, U. BIADER CEIPIDOR, A. MARINO and A. MAGRÌ
Istituto di Chimica Analitica, Università degli Studi di Roma, 00100 Roma (Italy)
(Received 1st August 1972)

In continuation of the studies of the compounds obtained by reaction between metal ions and the pyridine-2,*m*-dicarboxylic acids, as a function of the position of the carboxyl group farther from the aza group[1–3], thermoanalytical data for the solid compounds obtained by reactions of Mn(II), Fe(II), Co(II), Ni(II), Cu(II) and Zn(II) with quinolinic acid ($m=3$) have been obtained, and the results are reported in this paper.

Some hypotheses about the influence of the *m* position ($3 \geqslant m \leqslant 5$) are reported for similar compounds obtained by reaction between the above-mentioned metal ions and isocinchomeronic acid ($m=5$) or lutidinic acid ($m=4$).

EXPERIMENTAL

Instrumentation

The instruments used were the same as previously described[4]. The highest temperatures attained were 500° for differential thermal analysis (DTA) and 1000° for thermogravimetry (TG). A heating rate of 10° min^{-1} was employed.

Preparation of compounds

Quinolinic acid (Aldrich Chemical Co, Inc., Milwaukee, Wisc.) was used. The other chemicals employed were of reagent grade. The compounds were prepared in the same way as the complexes of lutidinic acid[3]; the only difference was the use

TABLE I

COMPLEXIMETRIC TITRATION OF THE METAL CONTENT OF THE ANHYDROUS COMPOUNDS

Compound	*Metal (%)*	
	Found	*Theoretical*
Mn(2,3PC)	24.8	24.85
Fe(2,3PC)	25.4	25.16
Co(2,3PC)	26.5	26.18
Ni(2,3PC)	25.8	26.11
Cu(2,3PC)	27.3	27.66
Zn(2,3PC)	28.3	28.24

of ethanol–ether mixtures to modify the solution conditions to obtain precipitation, when this was not achieved from aqueous or aqueous ethanol solutions.

All the precipitates were dried *in vacuo* for 48 h at room temperature. Thermogravimetry was used to determine the water content and the residual metal oxide; the metal content was also established by complexiметric titration of the anhydrous compound (Table I).

RESULTS

The temperatures referred to are the procedural decomposition temperatures at the heating rate indicated. The data obtained by thermogravimetry in nitrogen or in air and by DTA in nitrogen are summarized in Table II.

Manganese(II) pyridine-2,3-dicarboxylate

A cream-coloured hydrated compound $Mn(2,3\text{-}PC)\cdot 3H_2O$ precipitated

TABLE II

PROCEDURAL DECOMPOSITION TEMPERATURES FROM TG AND DTA CURVES OF ME PYRIDINE-2,3-DICARBOXYLATES IN NITROGEN OR AIR ATMOSPHERE

Metal	*Atm*	*TG*					*DTA*			
		I° H_2O	II° H_2O	I	II	III	I° H_2O	II° H_2O	I	II
Mn(II)	N_2	125[a]		415			130[b]		420	
		75–160		300–500	500→		80–165		300–500	
	Air	140		322	362					
		110–175[c]		300–325	325–380					
Fe(II)	N_2	80		400			85		405	
		30–150		300–500	500→		30–150		300–510	
	Air	90		310	410	575				
		35–150		255–320	320–500	500–680				
Co(II)	N_2	60	120	355	495		60	120	350	490
		30–75	75–145	240–400	400–610	610→	35–80	80–140	245–400	400–
	Air	70	120	280	400	500				
		35–90	90–145	250–290	290–445	445–575				
Ni(II)	N_2	100		320	440		110		320	400–
		50–170		270–390	390–475	550→	50–170		270–400	
	Air	105		265	455					
		50–175		175–330	330–550					
Cu(II)	N_2	75		260	450		75		260	450
		35–175		225–275	275–525	525→	40–175		225–275	275–
	Air	75		215	350	650				
		45–175		205–220	230–500	550–720				
Zn(II)	N_2	45	65	325			45	70	350	
		30–60	50–125	275–500	500→		30–55	55–125	275–500	
	Air	45	65	200	335					
		30–50	50–125	140–255	255–400					

[a] Maximal rate.
[b] Peak minimum.
[c] Temperatures at beginning and end of reaction.

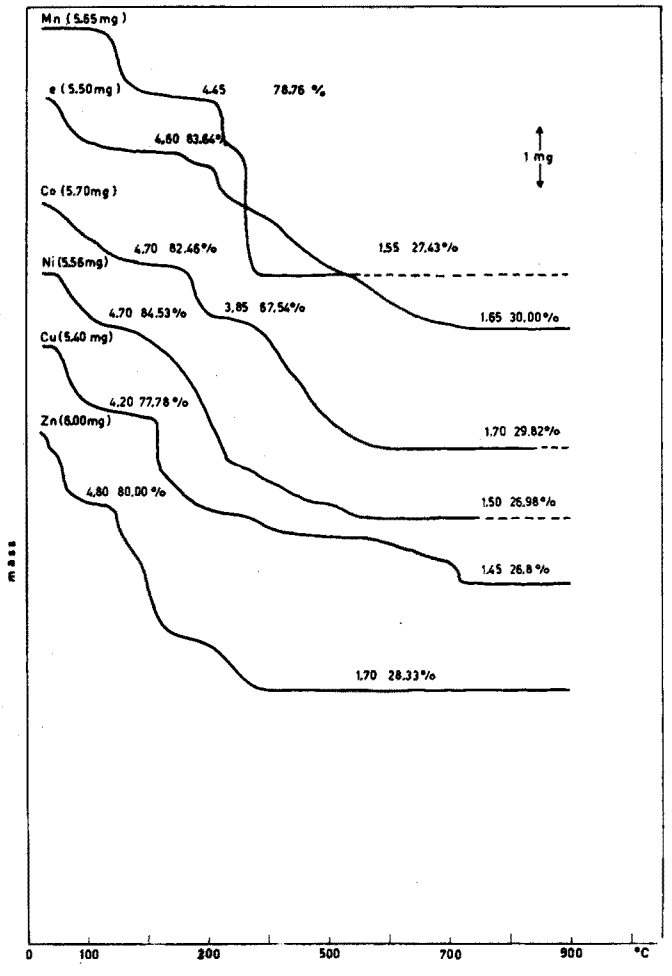

Fig. 1. Mass loss curves of metal pyridine-2,3-dicarboxylates. Air atmosphere; 10° min^{-1}.

from water–ethanol solutions; the given formula was indicated by the metal determination (Table I) and the thermogravimetric data. Thermogravimetry in nitrogen and in air showed that the water loss occurred in only one step (theor. 19.70%; found 19.4% in air (Fig. 1) and 19.6% in nitrogen (Fig. 2)). DTA in nitrogen (Fig. 3) showed an endothermic type of reaction but gave no other information about the steps of the water loss, there being only one peak. The same results were obtained by differential scanning calorimetry. The anhydrous compound was stable up to 300°. Beyond this temperature in a nitrogen atmosphere, an endothermic decomposition occurred (Fig. 3). Thermogravimetry in air (Fig. 2) showed two steps, the second of which reached the constant weight of the oxide, Mn_3O_4, at 380° (theor. 27.85%; found 27.4%).

Iron(II) pyridine-2,3-dicarboxylate

A red-brown compound precipitated from water–ethanol–ether solution. The

simplest formula which was in accordance with the thermogravimetric data and with the metal determination (Table I), was $Fe(2,3\text{-PC})\cdot 2.5H_2O$. This compound lost its water molecules in air (Fig. 1) and in nitrogen (Fig. 2) in a single stage which started at room temperature (theor. 16.82%; found 16.5% in air, and 16.6% in nitrogen). DTA in nitrogen indicated for the water loss a single endothermic process (Fig. 3), the resolution of which was impossible even by differential scanning calorimetry.

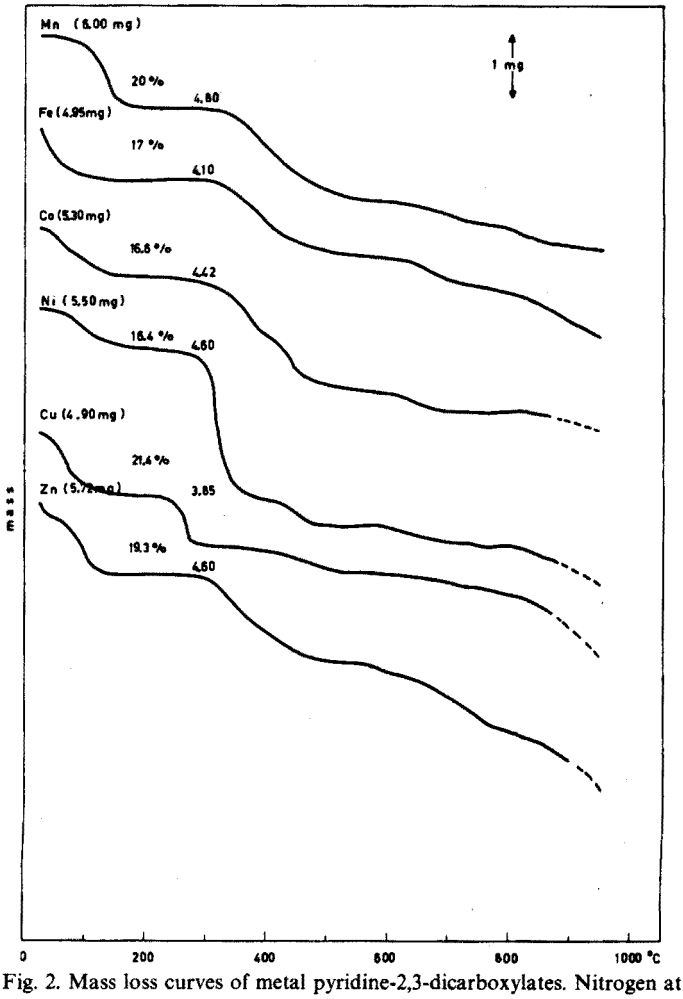

Fig. 2. Mass loss curves of metal pyridine-2,3-dicarboxylates. Nitrogen atmosphere; 10° min^{-1}.

The decomposition of the anhydrous compound in air started at 250° (Fig. 1) and occurred in three steps until the oxide Fe_2O_3 was obtained (theor. 29.91%; found 30.0%). In a nitrogen atmosphere, thermogravimetry still showed three steps (Fig. 2), but constant weight was not attained; DTA in nitrogen showed an endothermic peak for the first step of the decomposition process.

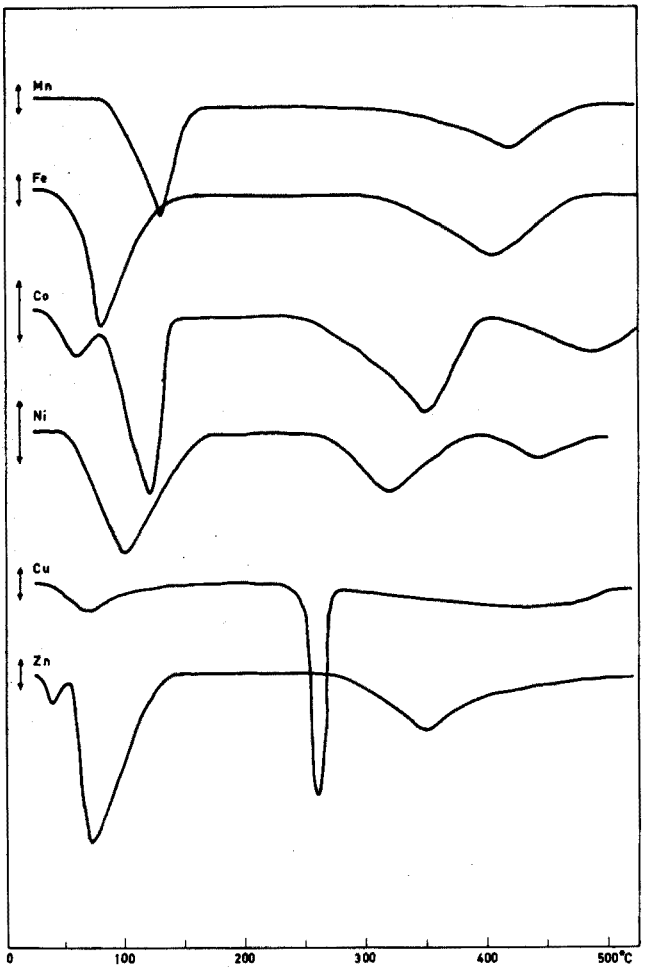

Fig. 3. DTA curves of metal pyridine-2,3-dicarboxylates. Nitrogen atmosphere; 10° min^{-1}.

Cobalt(II) pyridine-2,3-dicarboxylate

A pink compound was precipitated from a water–ethanol–ether solution. The simplest formula in accordance with the results of thermogravimetric analysis and with the metal determination of the metal (Table I) was $Co(2,3\text{-}PC)\cdot 2.5H_2O$. The water was evolved in two steps in air and in nitrogen (Figs. 1 and 2) (theor. 16.72%, found 16.6% in air, and 16.6% in nitrogen). DTA in nitrogen showed two endothermic peaks for water evolution. The anhydrous compound was stable up to 240° in nitrogen, and then decomposed in three steps without reaching constant weight (Fig. 2). In air the decomposition gave the oxide Co_3O_4 (Fig. 1) (theor. 29.82%; found 29.8%). DTA in nitrogen showed only endothermic peaks for the decomposition of the anhydrous compound.

Nickel(II) pyridine-2,3-dicarboxylate

A blue compound with the simplest formula $Ni(2,3\text{-}PC)\cdot 2.5H_2O$, derived

from the thermogravimetric data and the metal content (Table I), precipitated from a water–ethanol solution. Thermogravimetry showed that water molecules were evolved in a single step in air (Fig. 1) and in nitrogen (Fig. 2) (theor. 16.71%; found 16.3% in air, and 16.4% in nitrogen). DTA in nitrogen showed only an endothermic peak for the water loss. In air, the anhydrous compound started to decompose just after the water loss (Fig. 1); after two steps, the final product was the oxide NiO (theor. 27.09%; found 27.5%). In nitrogen decomposition occurred in three steps, the last of which did not reach constant weight. DTA showed that this decomposition in nitrogen was an endothermic process.

Copper(II) pyridine-2,3-dicarboxylate

From an aqueous solution precipitated a violet solid which, according to the thermogravimetric data and the metal determination, had the simplest formula Cu-(2,3-PC)·3.5H_2O. In air or nitrogen atmosphere (Figs. 1 and 2) there were water losses corresponding, respectively, to 21.3% and 21.4% (theor. 21.52%). DTA in a nitrogen atmosphere showed for this process only one endothermic peak. Decomposition in air occurred in three steps (Fig. 1), the last of which gave a constant weight corresponding to CuO (theor. 26.8%; found 27.18%). In nitrogen, the anhydrous complex decomposed in three steps but did not reach constant weight. DTA in nitrogen showed two endothermic peaks, the first of which was very sharp (Fig. 3).

Zinc(II) pyridine-2,3-dicarboxylate

A white compound precipitated from a water–ethanol solution. Its simplest formula according to the thermogravimetric data and the metal determination was Zn(2,3-PC)·3 H_2O. The compound lost its water molecules in two separate steps in air or nitrogen atmosphere. The weight losses in air were, respectively, 5.8% and 13.3% for the first and second steps, for a total weight loss of 19.1% (theor. 18.93%). In nitrogen atmosphere there was a total weight loss of 19.3%. Both the reactions were endothermic (Fig. 3). The decomposition of the anhydrous compound occurred in two steps in air or in nitrogen (Figs. 1 and 2). In air the second step gave a constant weight corresponding to the oxide ZnO (theor. 28.60%; found 28.3%). The decomposition reaction was endothermic in a nitrogen atmosphere (Fig. 3).

DISCUSSION

The order of thermal stability resulting from the peak temperatures by DTA in nitrogen, with regard to the first decomposition process, is:

$$Mn(II) > Fe(II) > Zn(II) \simeq Co(II) > Ni(II) > Cu(II)$$

The peak temperatures were chosen as the significant temperatures, because in DTA equilibrium conditions are not realized. This fact is more important when the reactions give rise to gaseous products. The diffusion of the gaseous products through the solid mass is the factor decreasing the reaction rate. This rate is highest when the partial pressure of the decomposition products equals that of the ambient atmosphere. Therefore, the peak temperature is closest to the highest reaction rate at the applied pressure.

The temperature sequence thus determined is in agreement with what was previously found for isocinchomeronic[1] and lutidinic[3] acids, and with the scale

proposed by Wendlandt *et al.*[5,6] for the thermal stability of other complexes of the examined metals. An hypothesis to justify this sequence, which is in inverse order to the sequence reported by Irving and Williams[7] for the stability constants of the complexes in solution, has been reported previously[3]. In the above sequence, the procedural decomposition temperatures of the anhydrous quinolinic acid complexes are lower than those of the lutidinic acid complexes. The differences are of the order of 40–50° for Mn(II), Fe(II), and Cu(II), and of 80–100° for Co(II), Ni(II), and Zn(II). The pK_{a^1} values for lutidinic and quinolinic acids, determined under the same conditions, are slightly different. The pK_{a^1} value of the lutidinic acid is higher than that of the quinolinic acid by *ca.* 0.1 units. Within the limits of an electrostatic model and the coordinate ion being equal, the strength of the metal–ligand bond increases as an inverse function of the ligand acidity. Support for these suggestions can be found in work by Carunchio and Bondoli[8].

The higher thermal stability of the lutidinic acid complexes with respect to the quinolinic acid complexes can therefore be explained by the fact that the central atom–ligand bond strength for quinolinates is bigger than that for lutidinates. In fact, as previously explained[3], an increase in the internal bond strength of the molecule causes a decrease in the bond strength between the solid lattice molecules.

It is indicative that such an increase is larger with ions like copper(II), nickel(II), and zinc(II), which better resemble the electrostatic model, than with manganese(II) and iron(II), where the d orbital population is smaller and the orbital overlapping in complex formation plays a main role. An intermediate case is represented by copper(II), where the energy separation between the 3d level and the subsequent 4s level is very small.

A comparison with the isocinchomeronic acid complexes has not been possible, because of the different M/L ratio.

The investigated complexes, with M/L ratio either 1:1 or 2:1, must be neutral to be able to precipitate and, therefore, must be of the type M-2,*m*-PC(I) or M-(2,*m*-HPC)$_2$ (II) (where *m* indicates the second carboxyl group position). If both species I and II are in equilibrium in solution with the species *M*-2,*m*-HPC$^+$ (III), the acidity of the latter favours the formation of I, by the reaction:

$$H_2O + \text{M-2,}m\text{-HPC}^+ \rightarrow H_3O^+ + \text{M-2,}m\text{-PC} \qquad 2$$

rather than the formation of II, by the reaction

$$\text{M-2,}m\text{-HPC}^+ + 2,m\text{-HPC}^- \rightarrow \text{M-(2,}m\text{-HPC)}_2$$

In species III, however, when the metal is bound to the aza- and to the 2-carboxyl groups, a resonance effect through the heterocyclic ring causes a positive polarization in position 4 rather than in 3 or 5.

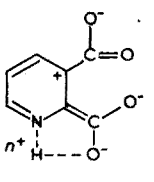

M-2,3-PC

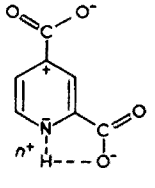

M-2,4-PC

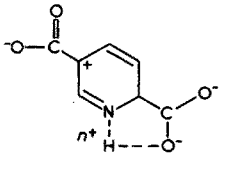

M-2,5-PC

Therefore, for forms III of the considered acids, an acidity order M-2,4-HPC$^+$ < M-2,5-HPC$^+$ < M-2,3-HPC$^+$ would be expected. Consequently, the formation of a precipitate with a ligand–metal ratio of 2 : 1 should be favoured with the same acidity order. This does in fact happen for isocinchomeronic acid, while solids with molar ligand–metal ratio of 1 : 1 were obtained with quinolinic acid. On the other hand, the pK_a values show the same predictable sequence[9–11]: 2.23(2,4-HPC) < 2.31(2,5-HPC) < 2.36(2,3-HPC). Apparently, in the case of the investigated quinolinates, an inductive effect of the 2-carboxyl group, bound to a positive metal ion, contributes to the increase in the acidity of species III.

With regard to dehydration phenomena, it should be noted that two DTA peaks are slightly marked only with cobalt and zinc complexes, while for the other cases a single overlapped peak was obtained. Probably the dehydration reaction takes place in two consecutive steps:

1. hydrated compound $\rightarrow H_2O_{liq}$ + anhydrous compound
2. $HO_{liq} \rightarrow HO_{vap}$

Owing to the high enthalpy of reaction (2), reaction (1) is experimentally detectable only when it occurs at temperatures considerably lower than 100° at atmosphere pressure. Under different conditions, an overlapped peak is found at *ca.* 100° corresponding to both reactions. Moreover, the enthalpy of the dehydration reaction has a direct influence on the water evaporation, thus allowing the observation of the phenomena even by thermogravimetry.

SUMMARY

Studies of the complexes of pyridinecarboxylic acids with divalent metal ions as a function of the position of the carboxyl groups were extended. The thermal properties of the complexes of quinoline acid (pyridine-2,3-dicarboxylic acid) with several divalent metal ions were determined by thermogravimetry (TG) and differential thermal analysis (DTA). A correlation between these compounds and others obtained by reaction between the studied metal ions with similar acids (lutidinic acid (pyridine-2,4-dicarboxylic acid) and isocinchomeronic acid (pyridine-2,5-dicarboxylic acid) is discussed in terms of the position of the carboxyl group far from the aza group. The thermal stability of the metal complexes is in the order

$$Mn(II) > Fe(II) > Zn(II) \simeq Co(II) > Ni(II) > Cu(II).$$

RÉSUMÉ

Une étude est effectuée sur les complexes des acides pyridinecarboxyliques avec ions métalliques divalents, en fonction de la position des groupes carboxyliques. Les propriétés thermiques des complexes de l'acide quinolinique (acide pyridinedicarboxylique-2,3) avec divers ions métalliques divalents ont été déterminées par thermogravimétrie et analyse thermique différentielle. Une comparaison est faite avec des acides similaires (acides pyridinedicarboxyliques-2,4 et -2,5). La stabilité thermique des complexes est dans l'ordre suivant:

$$Mn(II) > Fe(II) > Zn(II) \simeq Co(II) > Ni(II) > Cu(II).$$

ZUSAMMENFASSUNG

Die Untersuchungen der Komplexe von Pyridincarbonsäuren mit zweiwertigen Metallionen als Funktion der Stellung der Carboxylgruppen wurden weitergeführt. Die thermischen Eigenschaften der Komplexe von Chinolinsäure (Pyridin-2,3-dicarbonsäure) mit verschiedenen zweiwertigen Metallionen wurden durch Thermogravimetrie (TG) und Differenzthermoanalyse (DTA) bestimmt. Eine Beziehung zwischen diesen Verbindungen und anderen, die durch Reaktion zwischen den untersuchten Metallionen mit ähnlichen Säuren (Lutidinsäure (Pyridin-2,4-dicarbonsäure) und Isocinchomeronsäure (Pyridin-2,5-dicarbonsäure)) erhalten werden, wird bezüglich der Stellung der weiter von der Azagruppe entfernten Carboxylgruppe diskutiert. Die Reihenfolge der thermischen Stabilität der Komplexe ist

$$Mn(II) > Fe(II) > Zn(II) \simeq Co(II) > Ni(II) > Cu(II) .$$

REFERENCES

1 G. De Angelis, E. Chiacchierini and G. D'Ascenzo, *Gazz. Chim. Ital.*, 96 (1966) 39.
2 G. D'Ascenzo and W. W. Wendlandt, *Gazz. Chim. Ital.*, 100 (1970) 371.
3 G. D'Ascenzo, U. Biader Ceipidor and G. De Angelis, *Anal. Chim. Acta*, 58 (1972) 175.
4 G. D'Ascenzo and W. W. Wendlandt, *Anal. Chim. Acta*, 50 (1970) 79.
5 W. W. Wendlandt, J. H. Van Tossel and G. R. Horton, *Anal. Chim. Acta*, 23 (1960) 332.
6 W. W. Wendlandt and G. R. Horton, *Anal. Chem.*, 34 (1962) 1098.
7 H. Irving and R. J. P. Williams, *J. Chem. Soc.*, (1953) 3192.
8 V. Carunchio and A. Bondoli, *J. Inorg. Nucl. Chem.*, 34 (1972) 3491.
9 V. D. Canic, *Glas. Khem. Brushtra Beogr.*, 20 (1955) 29 in *Chem. Zentralbl.*, 1 (1957) 381.
10 R. M. Tichane and W. E. Bennet, *J. Amer. Chem. Soc.*, 79 (1957) 1293.
11 M. Yasuda and K. Yamasaki, *Naturwiss.*, 45 (1958) 84.

Analytica Chimica Acta, 65 (1973) 115–126

REVERSED-PHASE FOAM CHROMATOGRAPHY

CHEMICAL ENRICHMENT AND SEPARATION OF GOLD IN THE TRIBUTYLPHOSPHATE–THIOUREA–PERCHLORIC ACID SYSTEM

T. BRAUN and A. B. FARAG

Institute of Inorganic and Analytical Chemistry, L. Eötvös University, 1443 Budapest P.O. Box 123 (Hungary)

(Received 7th December 1972)

The most widely used methods for the dissolution of gold from its ores are those involving cyanide or halide ions as complexing agents. Many papers[1–6] have been published describing liquid–liquid extraction procedures for these complexes of gold. Recently, Bowen reported[7] that gold(III) can be extracted by solid polyurethane foams from hydrochloric, hydrobromic and hydroiodic acid solutions, and recommended[8] the application of polyurethane foam for the recovery of gold(III) from liquid mineral wastes. Schiller and Cook[9] applied polyurethane foam for the preconcentration of gold(III) from natural sweet waters, but reported that a shaking time of 90 min was necessary to obtain acceptable results.

Independently, Lodeishchikov *et al.*[10] and Tataru[11] suggested the use of acidic solution of thiourea for the dissolution of gold in ground ore bodies. Lodeishchikov and Panchenko[12] also described a method for the recovery of the gold–thiourea complex from acidic thiourea solutions with active carbon.

In a recent publication, Groenewald and Jones[13] studied the behaviour of the gold–thiourea complex during liquid–liquid extraction with a wide variety of diluted organic extractants. They checked liquid anion exchangers, such as trialkylammonium chloride, solvating ligand extractants, such as tri-*n*-octylphosphine oxide and tributylphosphate, and liquid cation exchangers, such as sodium dioctylsulphosuccinate and di(2-ethylhexyl)phosphoric acid. Unfortunately, it was not possible to find a suitable extractant for the direct extraction of the gold–thiourea complex.

In the present paper, a new method is described for the chemical enrichment and separation of the gold–thiourea complex from acidic solutions on polyurethane foam loaded with tri-*n*-butylphosphate. A detailed study of the various factors influencing the quantitative separation of gold–thiourea complex was carried out. An attempt was made to clarify the probable constitution of the solvated complex formed. This work allows the application of the reversed-phase foam chromatographic method[14–16] to be extended to the chemical enrichment and separation of gold from acidic solutions. The use of this procedure to replace the active carbon method for gold recovery in ore processing and thiourea leach solutions will be described in a later paper.

EXPERIMENTAL

Reagents and materials

All reagents used were of analytical grade unless otherwise mentioned. Tri-*n*-butylphosphate (TBP) used in solvent extraction and as a stationary phase in column extraction was purified as described by Hamlin *et al.*[17]. Polyurethane foam, a polyether of open-cell type, was supplied by the North Hungarian Chemical Works, Sajóbábony, Hungary.

Gold, cobalt and nickel chloride solutions, and zinc and copper sulphate solutions, were prepared by dissolving the required salt in distilled water. Palladium and iron(III) chloride solutions were prepared by dissolving their chloride salts in 0.25 and 1 *M* hydrochloric acid solution, respectively. Antimony solution was prepared as described by Šulcek and Sixta[18], and the bismuthyl perchlorate solution as described earlier[14]. All the solutions were standardized by conventional methods[19,20]. The gold solution was spiked with ^{198}Au (Institute of Isotopes, Budapest, Hungary).

Instrumentation

For activity measurement an NaI(Tl) detector and an energy-selective counting device (type NK-107/B, Gamma, Budapest, Hungary) were employed.

Column preparation

Glass columns of 25 mm diameter and 12 cm length were used. The polyurethane foam was washed, dried and loaded with purified TBP as previously described[14]; 5 g of the dried loaded foam was packed in the column, to produce a 5-cm bed height.

Separation of gold from zinc, cobalt or nickel

The feed solution contained 1 ml of spiked gold chloride solution (10 μg Au^{3+} ml^{-1}), 20 ml of zinc, cobalt or nickel solution (50 mg Me^{2+} ml^{-1}) and 20 ml of 0.2 *M* perchloric acid solution containing 6% thiourea and 2% sodium perchlorate (solution I). This mixture was fed into the column at a flow-rate of 50–60 ml min^{-1}; 20 ml of 0.1 *M* perchloric acid solution containing 3% thiourea and 1% sodium perchlorate (solution II) was then used to wash the column. Finally, the column was washed with distilled water and the effluent was collected in a 100-ml volumetric flask.

Separation of gold from iron, copper or antimony

The feed solution contained 2 ml of spiked gold chloride solution (1 μg Au^{3+} ml^{-1}), 4 ml of iron(III) chloride solution (50 mg Fe^{3+} ml^{-1}) or 4 ml of copper sulphate solution (0.5, 5 or 50 mg Cu^{2+} ml^{-1}), and an equal volume of the above solution I. This mixture was placed on the column as described above; 20 ml of solution II was used to wash the column. The elution of the interfering element was then continued with distilled water, and the eluate was collected in a 100-ml volumetric flask.

For the separation of gold from antimony, the feed solution contained 2 ml of gold chloride solution (1 μg Au^{3+} ml^{-1}), 10 ml of potassium antimonyl tartrate

(20 mg Sb^{3+} ml^{-1}) and an equal volume of 0.2 *M* perchloric acid solution containing 2% thiourea[18] and 2% sodium perchlorate. The column was washed with 20 ml of perchloric acid solution containing 2% thiourea and 1% sodium perchlorate, and the elution was continued as described above.

Separation of gold from bismuth or palladium

The feed solution containing 2 ml of spiked gold chloride solution (1 μg Au^{3+} ml^{-1}), 10 ml of bismuthyl perchlorate or palladium chloride solution (1 mg Bi^{3+} or Pd^{2+} ml^{-1}) and 10 ml of solution I, was added to the column as described above; 20 ml of solution II was used to wash the column. The bismuth–thiourea complex was eluted with 0.5 *M* perchloric acid solution, and the palladium–thiourea complex with distilled water[14].

Chemical enrichment of gold

The spiked gold chloride solution (10 ml of a 10 μg Au^{3+} ml^{-1} solution) was diluted to 1 l with solution II. This solution was allowed to pass through the foam column at a flow-rate of 50–60 ml min^{-1}, and the effluent was collected in a stoppered flask.

Analytical methods

The unextracted gold complex was determined by measuring the radioactivity of 5 ml of the effluent solution, and the extracted gold was calculated by difference. In some experiments, the gold complex retained on the foam was determined directly by dissolving the foam material in 20 ml of hot concentrated nitric acid on a boiling water bath. After complete decomposition of the foam material, the activity of the nitric acid solution was measured.

In all cases, each of the interfering elements was determined in the effluent solution by conventional methods[19,20]. In some cases, *e.g.* copper, it was necessary to mineralize the eluate by evaporating to dryness in the presence of aqua regia on a boiling water bath before titration with EDTA.

RESULTS AND DISCUSSION

The main purpose of the present study was to develop a rapid and reliable column chromatographic method for the chemical enrichment and separation of the gold–thiourea complex from acid solutions. Reversed-phase foam chromatography has provided a convenient solution for various separation problems[14–16,21]. This method, which uses a support of new geometrical form (foam), combines the advantages of reversed-phase extraction chromatography with improved hydrodynamic properties and kinetics of partition[14]. Moreover, polyurethane foam retains a much higher amount of organic extractants than other available granular supports[14].

Before the column experiments were done, it was considered advisable to obtain some information about the chemical composition of the gold–thiourea complex in the organic phase and its behaviour during liquid–liquid extraction. Many investigations have already been made on the interaction of gold with thiourea in aqueous solutions, applying polarography[22], and amperometric[22,23]

and potentiometric titrations[22, 24, 25]. Several studies have been concerned with the precipitation and concentration of gold from acidic solutions of thiourea[26, 27]. The electrolytic separation of gold from thiourea solution has also been reported[28]. From these studies, it can be concluded that gold(III) is first reduced by thiourea[29] to the monovalent ion:

$$Au^{3+} + 2H_2N \cdot CS \cdot NH_2 \rightarrow \begin{matrix} HN & & NH_2 \\ \| & & / \\ C\text{–}S\text{–}S\text{–}C & & \\ / & & \| \\ H_2N & & NH \end{matrix} + Au^{+} + 2H^{+}$$

and the latter then reacts with the excess of thiourea to form a soluble gold–thiourea complex of the formula $Au(H_2NCSNH_2)_2^+$.

No study seems to have been done on the solvent extraction of the gold–thiourea complex, apart from the unsuccessful work of Groenewald and Jones[13].

Extraction of the gold–thiourea complex

The liquid–liquid extraction of the gold–thiourea complex with tri-*n*-butyl-phosphate (TBP) was investigated in this work with gold-198. Preliminary experiments showed that the extraction depended upon the shaking time, the thiourea concentration in the aqueous phase, and the TBP concentration in the organic phase; the failure reported by Groenewald and Jones[13] was probably due to the very low TBP concentration used. In order to study the effect of shaking time, fixed amounts of TBP (3.66 *M*), gold (10 μg), thiourea (3%), and sodium perchlorate (1%) were used. A shaking period of 5 min was selected, because this was found to be more than required for complete extraction of the gold–thiourea complex into the TBP layer.

The influence of the concentration of thiourea in the aqueous phase on the extraction of gold(III) in the presence of perchlorate ion was investigated for thiourea concentrations of 1.0 *M* to $1.0 \cdot 10^{-5}$ *M*, all the other parameters remaining constant. All the gold was extracted into the TBP layer at all thiourea concentrations tested. This may be attributed to the extraction of both gold–chloride and gold–thiourea complexes into TBP under these experimental conditions.

Yadav and Khopkar[5] reported that chloroaurate(III) can be extracted by TBP, but the extracted gold can be stripped from the organic phase by washing with ammonia solution. In the present work, it was found that the gold–thiourea complex was not stripped from TBP by 2 *M* ammonia solution. This was further proved by the extraction of a fixed amount (10 μg) of gold(III), under the same conditions, in the absence and presence of thiourea in the aqueous solution. In both cases, gold was quantitatively extracted into the TBP layer, but when the TBP layer was shaken with 10 ml of 2 *M* ammonia solution, gold was completely stripped from the organic layer in the first case, while in the latter case gold did not appear at all in the aqueous phase. This difference in behaviour made it possible to study the effect of thiourea concentration on the extraction of gold(III) by TBP. The results are presented in Fig. 1.

The distribution coefficient *D* was determined under equilibrium conditions as a function of the thiourea concentration in the aqueous phase. The metal–thiourea ratio of the extracted species was calculated by the slope method (Fig. 2). This indicates the presence of one molecule of thiourea for each gold atom in the

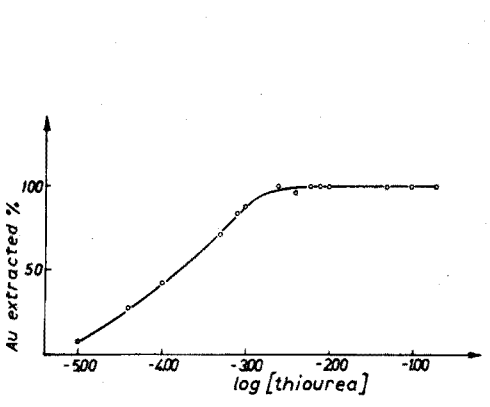

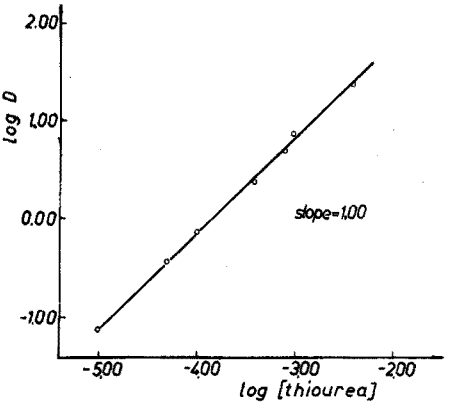

Fig. 1. Effect of thiourea concentration on the extraction of the gold–thiourea complex in TBP (equal volumes of aqueous and organic phases). Au^{3+}, $1.25 \cdot 10^{-5}$ *M*; $HClO_4$, 0.1 *M*; $NaClO_4$, 1%; NH_4OH, 2 *M*; TBP, 3.66 *M*.

Fig. 2. Effect of thiourea concentration on the distribution ratio of the gold complex. Au^{3+}, $1.25 \cdot 10^{-5}$ *M*; $HClO_4$, 0.1 *M*; $NaClO_4$, 1%; TBP, 3.66 *M*.

organic phase. This result disagrees with those reported in the literature[24, 28] which suggested the formation of an $Au(H_2NCSNH_2)_2^+$ complex in aqueous acidic solution containing an excess of thiourea. However, the results obtained in the present experiments may be explained by a rearrangement of $Au(H_2NCSNH_2)_2^+$ complex to $Au(H_2NCSNH_2)^+$ during extraction with TBP.

The distribution ratio of the gold–thiourea complex was also determined at different concentrations of TBP, with toluene as diluent, in an attempt to establish the probable composition of the solvated species. Figure 3 presents a plot of log *D* *vs.* log TBP concentration; the slope of the curve indicates the presence of

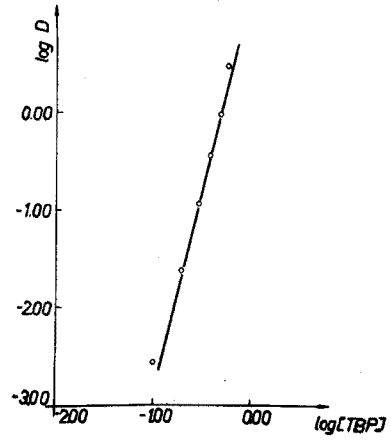

Fig. 3. Effect of TBP concentration on the distribution ratio of the gold–thiourea complex. Au^{3+}, $1.25 \cdot 10^{-5}$ *M*; thiourea, 3%; $NaClO_4$, 1%; $HClO_4$, 0.1 *M*. Shaking time, 5 min. Weight of loaded foam, 0.1 g.

four molecules of TBP in the extracted species. Accordingly, the formula of the extracted species is probably: $[Au(H_2N \cdot CS \cdot NH_2)]ClO_4 \cdot 4TBP$.

The effect of acid and perchlorate ion concentrations in the aqueous phase on the extraction of the gold–thiourea complex by TBP was also investigated. Although the acidity of the aqueous solution or the perchlorate ion concentrations had no effect on the extraction of the gold complex, yet rapid and clear separation was attained by adjusting the acidity to 0.1 *M* and using 1% sodium perchlorate (salting-out effect).

Adsorption on TBP-loaded foam

The rate of extraction of the gold–thiourea complex by TBP-loaded polyurethane foam was investigated by the batch technique[14,30]. A series of these kinetic experiments was performed to determine the effect of various interfering elements on the rate of adsorption of the gold–thiourea complex on to TBP-loaded foam.

The elements which can interfere with the analytical and industrial separation of gold are: Zn^{2+}, Co^{2+}, Ni^{2+}, Cu^{2+}, Fe^{3+}, Sb^{3+}, Bi^{3+}, Pd^{2+} and Ag^{+}. These elements are divided into three categories:

(*a*) elements which do not interact with thiourea under the experimental conditions used, *e.g.* Zn^{2+}, Co^{2+} and Ni^{2+};

(*b*) elements which form thiourea complexes, but are not extracted or only partially extracted with TBP-loaded foam, *e.g.* Cu^{2+}, Fe^{3+} and Sb^{3+};

(*c*) elements which form stable thiourea complexes which are strongly extracted by the loaded foam material, *e.g.* Pd^{2+}, Bi^{3+} and Ag^{+}.

In the present investigation, zinc(II), iron(III) and bismuth(III) were selected to represent all kinds of elements. It can be seen from Figs. 4–7 that the uptake of the gold complex by the loaded foam is fast and is not affected considerably by the presence of these interfering elements. The half-life times of equilibrium adsorption of gold alone and in presence of Zn^{2+}, Fe^{3+} or Bi^{3+} were calculated to be 0.4, 0.6, 1.0 and 0.9 min, respectively.

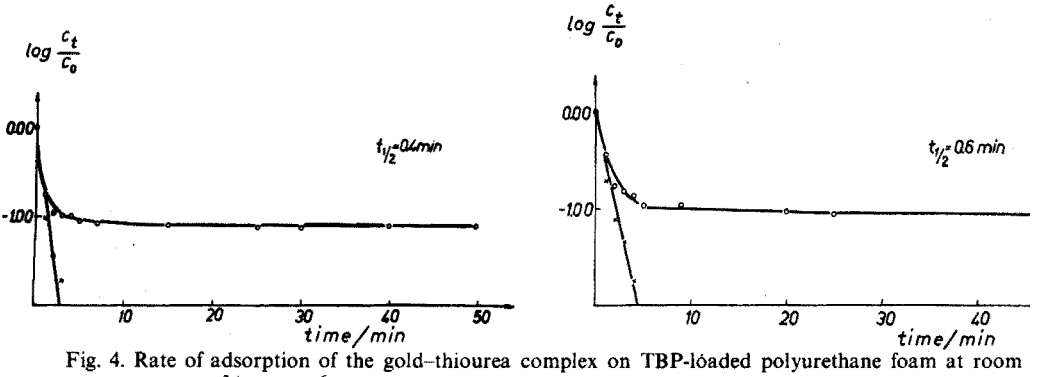

Fig. 4. Rate of adsorption of the gold–thiourea complex on TBP-loaded polyurethane foam at room temperature. Au^{3+}, $5 \cdot 10^{-6}$ *M*; thiourea, 3%; $NaClO_4$, 1%; $HClO_4$, 0.1 *M*. Loaded foam, 0.1 g. C_t = [Au] at time t, C_0 = [Au] at time 0.

Fig 5. Rate of adsorption of the gold–thiourea complex on TBP-loaded polyurethane foam in the presence of zinc(II). Au^{3+}, $5 \cdot 10^{-6}$ *M*; Zn^{2+}, $1.5 \cdot 10^{-1}$ *M*; other conditions as in Fig. 4.

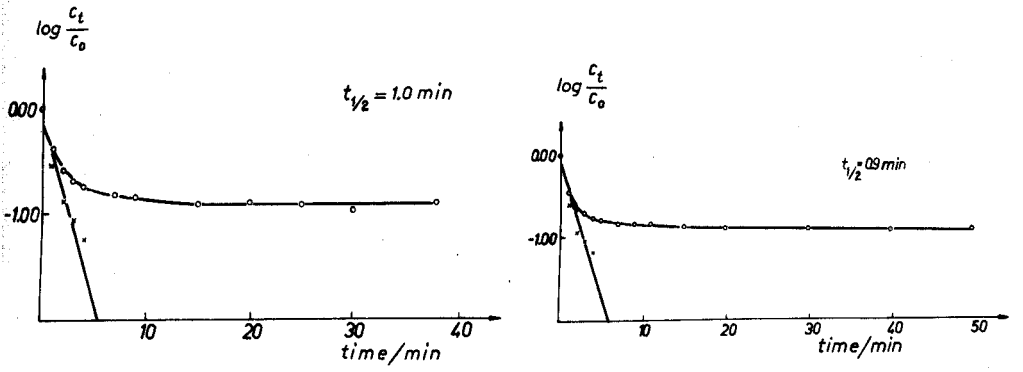

Fig. 6. Rate of adsorption of the gold–thiourea complex on TBP-loaded foam in the presence of iron(III). Au^{3+}, $5 \cdot 10^{-6}$ *M*; Fe^{3+}, $1 \cdot 10^{-2}$ *M*; other conditions as in Fig. 4.

Fig. 7. Rate of adsorption of the gold–thiourea complex on TBP-loaded foam in the presence of bismuth(III). Au^{3+}, $5 \cdot 10^{-6}$ *M*; Bi^{3+}, $5 \cdot 10^{-4}$ *M*; other conditions as in Fig. 4.

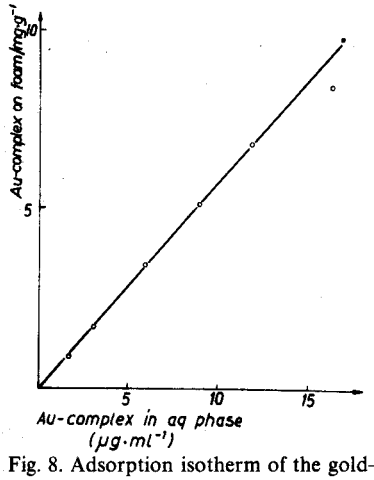

Fig. 8. Adsorption isotherm of the gold–thiourea complex on TBP-loaded polyurethane foam.

As in the case of the palladium–thiourea complex[14], the uptake of the gold–thiourea complex by TBP-loaded foam was found to depend on the concentration of the complex in the aqueous phase. Figure 8 shows a plot of the concentration of the gold–thiourea complex in the aqueous phase *versus* its concentration on the foam material. The isotherm shows a good linear relationship over a relatively wide range of gold concentrations.

Effect of flow-rate

An important property of the foam column is the possibility of high flow-rates; these can be attained simply by gravity flow, *i.e.* without applying any external pressure. A detailed study was therefore made of the effect of flow-rate on the efficiency of retention of the gold complex; various concentrations of TBP in toluene were used to load the dry polyurethane foam (2 g) in a short column (5 cm bed height). Flow-rates from 10 to 150 ml min^{-1} were applied at room

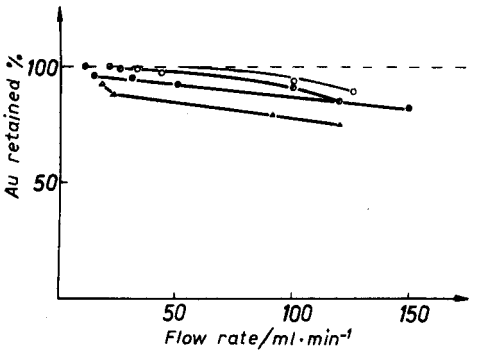

Fig. 9. Effect of flow-rate on the extraction efficiency of columns packed with TBP-loaded foam. TBP loading: ○ 3.66 *M*; ◐ 3.00 *M*; ● 2.00 *M*; △ 1.00 *M*.

temperature. The results are shown in Fig. 9. Generally, the efficiency of extraction of 10 μg of gold from 100 ml of 0.1 *M* perchloric acid solution containing 3% thiourea and 1% sodium perchlorate is decreased by increasing the flow-rate. However, when undiluted TBP solution is used to load the foam material, relatively high flow-rates (up to 100 ml min^{-1}) can be applied without appreciable loss in column performance. On the basis of these results, undiluted TBP was used as a stationary phase in the subsequent investigations.

In order to test the feasibility of using short foam columns for the separation of the gold–thiourea complex at relatively high flow-rates, the useful capacity of a column packed with 5 g of TBP-loaded foam was determined. A solution containing $5 \cdot 10^{-5}$ *M* gold(III) in 0.1 *M* perchloric acid, 3% thiourea and 1% sodium perchlorate, was allowed to pass through the column at a flow-rate of 50–60 ml min^{-1} at room temperature. The effluent solution was collected in 100-ml volumetric flasks. The activity of each fraction of the effluent was measured and the amount of gold retained by the column was calculated by difference. The percentage of gold retained decreased gradually from 100% in the first fractions to about 96% after 1 l of the solution had passed through the column. The useful capacity of the foam column is therefore quite high; 10 mg of gold(III) can be retained by the column satisfactorily from 1 l of aqueous solution.

Analytical applications

The practical utility of foam-filled columns was tested by studying their ability to separate gold quantitatively from interfering elements, *i.e.* Zn^{2+}, Co^{2+}, Ni^{2+}, Fe^{3+}, Sb^{3+}, Cu^{2+}, Bi^{3+}, Pd^{2+} and Ag^{+}.

Separate experiments with each element showed that zinc(II), cobalt(II) and nickel(II) are not extracted by the TBP-loaded foam. This may be due to the fact that these elements are not complexed by thiourea under the experimental conditions used[31]. When the short foam column was used with a flow-rate of 50–60 ml min^{-1}, it was possible to separate small amounts of Au^{3+} (10 μg) from high amounts of Zn^{2+}, Co^{2+} or Ni^{2+} (1 g), because these elements moved with the solvent front, while the gold–thiourea complex was completely retained. The results are summarized in Table I.

TABLE I

SEPARATION OF GOLD FROM VARIOUS ELEMENTS

Element	*Amount*		*Au^{3+}: interfering ion*	*No. of detns.*	*Average Au % in effluent*	*Average Au % on the foam ($\bar{X}$)*	*Variance*	*s*	*s_r*	*Relative standard error $t_{0.95}$*	*Bias*
	Au^{3+} (μg)	*Element (mg)*									
—	10	—	—	6	1.60	98.40	1.216	1.102	1.120	1.175	-1.60 ± 1.175
Zn^{2+}	10	1000	$1:10^5$	5	2.30	97.70	0.225	0.474	0.485	0.601	-2.30 ± 0.601
Co^{2+}	10	1000	$1:10^5$	5	2.86	97.14	0.263	0.512	0.527	0.653	-2.86 ± 0.653
Ni^{2+}	10	1000	$1:10^5$	5	2.30	97.70	0.070	0.264	0.270	0.334	-2.30 ± 0.334
Fe^{3+}	2	200	$1:10^5$	5	4.24	95.76	2.173	1.474	1.539	1.905	-4.24 ± 1.905
Sb^{3+}	2	200	$1:10^5$	5	6.02	93.98	2.587	1.600	1.702	2.109	-6.02 ± 2.109
Cu^{2+}	2	2	$1:10^3$	4	2.05	97.95	0.123	0.351	0.358	0.570	-2.05 ± 0.570
Cu^{2+}	2	20	$1:10^4$	4	3.07	96.93	2.660	1.630	1.680	2.673	-3.07 ± 2.673
Cu^{2+}	2	200	$1:10^5$	5	11.38	88.62	0.867	0.931	1.050	1.301	-11.38 ± 1.301
Bi^{3+}	2	10	$1:5 \cdot 10^3$	5	2.34	97.66	1.270	1.127	1.154	1.430	-2.34 ± 1.430
Pd^{2+}	2	10	$1:5 \cdot 10^3$	5	2.40	97.60	0.075	0.273	0.279	0.346	-2.40 ± 0.346

Gold in the effluent was determined by measuring its radioactivity and the amount of gold retained on the column was calculated by difference. In all cases, the amounts of the interfering elements were determined in the effluent by conventional methods[19,20].

On the other hand, iron(III), antimony(III) and copper(II) are known to interact with thiourea to form red, yellow and colourless complexes, respectively[18]. The thiourea complexes of these elements were found to be partially extracted by the foam column, but they were completely washed from the column with water leaving the gold complex on the foam. It was noticed that copper(II) when present in large amounts, interfered seriously with the determination of gold (Table I).

Palladium(II), bismuth(III) and silver(I) form thiourea complexes[14,32] under the experimental conditions applied, and their complexes are completely extracted by the foam column together with the gold–thiourea complex. With palladium(II) and bismuth(III), it was possible to elute their complexes from the column by water and 0.5 *M* perchloric acid, respectively, without affecting the retention of the gold complex (Table I).

However, the silver complex could not be completely removed from the column without affecting the gold complex. Detailed studies on the silver interference and the behaviour of the silver–thiourea complex on TBP-loaded foam will be the subject of another investigation.

Finally, the proposed foam method was found to be useful for the chemical enrichment of small amounts of gold from dilute solutions. Passing 1 l of a solution containing 100 μg of gold(III) in 0.1 *M* perchloric acid, 3% thiourea and 1% sodium perchlorate, through a column filled with 5 g of TBP-loaded foam at a flow-rate of 50–60 ml min^{-1}, 95–97% of gold was retained by the column.

A few experiments were performed to determine how the gold complex, once extracted by the foam column, could best be recovered from it. The complex showed such a high distribution constant in the TBP on the column that washing the column with 3 *M* inorganic acids (HCl, H_2SO_4, $HClO_4$ and HNO_3), organic solvents (acetone, methyl isobutyl ketone) or 2 *M* ammonia solution, did not yield complete elution of gold. Attention was then directed towards the recovery of gold by dissolution of the foam material itself. It was found that gold(III) which had been retained on 5 g of the polyurethane foam could be quantitatively recovered by dissolving the foam material in 20 ml of hot concentrated nitric acid on a water bath.

SUMMARY

Gold(III) is quantitatively extracted from acidic solution of thiourea into tri-*n*-butyl phosphate (TBP). The extracted species contains one molecule of thiourea and four molecules of TBP for each atom of gold. On short columns of TBP-loaded polyurethane foam, gold(III) can be separated from many other elements by retention from 0.1 *M* perchloric acid solution containing 3% thiourea and 1% sodium perchlorate. Flow-rates of 50–60 ml min^{-1} are possible. Trace amounts of gold can be separated quantitatively from high concentrations of Zn^{2+}, Co^{2+}, Ni^{2+}, Fe^{3+}, Sb^{3+}, Cu^{2+}, Bi^{3+} and Pd^{2+}, which have a negligible effect on the

rate of adsorption of the gold–thiourea complex. The chemical enrichment of gold from dilute aqueous solutions is also possible.

RÉSUMÉ

L'or(III) est extrait quantitativement en solution acide de thiourée, dans le tri-*n*-butylphosphate (TBP). A chaque atome d'or correspond une molécule de thiourée et quatre molécules de TBP. Il est possible de séparer quantitativement des traces d'or en présence de concentrations élevées de Zn^{2+}, Co^{2+}, Ni^{2+}, Fe^{3+}, Sb^{3+}, Cu^{2+}, Bi^{3+} et Pd^{2+}. Un enrichissement chimique de l'or de solutions aqueuses diluées est également possible.

ZUSAMMENFASSUNG

Gold(III) wird aus sauren Thioharnstofflösungen mit Tri-n-butylphosphat (TBP) quantitativ extrahiert. Die extrahierte Spezies enthält ein Molekül Thioharnstoff und vier Moleküle TBP pro Goldatom. An kurzen Säulen, die mit TBP beladenen Polyurethan-Schaum enthalten, kann Gold(III) von vielen anderen Elementen abgetrennt werden, indem es aus 0.1 *M* Perchlorsäure-Lösung mit einem Gehalt von 3% Thioharnstoff und 1% Natriumperchlorat zurückgehalten wird. Fliessgeschwindigkeiten von 50–60 ml min^{-1} sind möglich. Spurenmengen von Gold können quantitativ von hohen Konzentrationen von Zn^{2+}, Co^{2+}, Ni^{2+}, Fe^{3+}, Sb^{3+}, Cu^{2+}, Bi^{3+} und Pd^{2+} abgetrennt werden, die auf die Adsorptionsgeschwindigkeit des Gold–Thioharnstoff-Komplexes einen vernachlässigbaren Einfluss ausüben. Die chemische Anreicherung von Gold aus verdünnten wässrigen Lösungen ist ebenfalls möglich.

REFERENCES

1 T. Groenewald, *Anal. Chem.*, 40 (1968) 863.
2 M. C. Greaves, *Nature*, 199 (1963) 552.
3 T. Groenewald, *Anal. Chem.*, 41 (1969) 1012.
4 I. Akaza, T. Kiba and T. Kiba, *Bull. Chem. Soc. Jap.*, 43 (1970) 2063.
5 A. A. Yadav and S. M. Khopkar, *Sep. Sci.*, 5 (1970) 637.
6 J. S. Fritz and W. G. Millen, *Talanta*, 18 (1971) 323.
7 H. J. M. Bowen, *J. Chem. Soc. A*, (1970) 1082.
8 H. J. M. Bowen, *Radiochem. Radioanal. Lett.*, 7 (1971) 71.
9 P. Schiller and G. B. Cook, *Anal. Chim. Acta*, 54 (1971) 364.
10 V. V. Lodeishchikov, A. F. Panchenko and L. N. Briantseva, *Nauchn. Tr. Irkutsk, Gos. Nauk, Issled. Inst. Redk. Tsvetn. Met.*, 19 (1968) 72.
11 S. Tataru, *Rev. Roum. Chim.*, 13 (1968) 891.
12 V. V. Lodeishchikov and A. F. Panchenko, *Tsvetn. Met.*, 41 (1968) 25.
13 T. Groenewald and B. M. Jones, *Anal. Chem.*, 43 (1971) 1689.
14 T. Braun and A. B. Farag, *Anal. Chim. Acta*, 61 (1972) 265.
15 T. Braun, L. Bakos and É. Huszár, *Anal. Chim. Acta*, in press.
16 T. Braun, L. Bakos and Ss. Szabó, *Anal. Chim. Acta*, in press.
17 A. G. Hamlin, B. J. Roberts, W. Loughlin and S. G. Walker, *Anal. Chem.*, 33 (1961) 1547.
18 Z. Šulcek and V. Sixta, *Collect. Czech. Chem. Commun.*, 37 (1972) 1993.
19 A. I. Vogel, *Quantitative Inorganic Analysis*, Longmans, London, 3rd Ed., 1961.
20 G. Schwarzenbach and H. Flaschka, *Die komplexometrische Titration*, F. Enke, Stuttgart, 1965.
21 T. Braun, A. B. Farag and A. Klimes-Szmik, *Anal. Chim. Acta*, in press.

22 A. I. Pashchenko and B. T. Taskarin, *Sb. Statei Aspir. Soiskatelei Min. Vyssh. Sredn. Spets. Obrazov Kaz. SSR, Khim. Khim. Tekhnol.*, 5 (1966) 121.
23 A. I. Pashchenko, O. A. Songina and N. I. Korgina, *Zavodsk. Lab.*, 31 (1965) 1312.
24 E. N. Ovsepyan, V. M. Tarayan and G. N. Saposhnikova, *Armyansk. Khim. Zh.*, 19 (1966) 412.
25 V. P. Kazakov, A. I. Lapshin and B. I. Paschevitskii, *Zh. Neorg. Khim.*, 9 (1964) 1299.
26 S. Tataru, *Rev. Roum. Chim.*, 13 (1968) 185.
27 A. I. Maslii and A. V. Zadonskaya, *Izv. Sib. Otd. Akad. Nauk, SSSR, Ser. Khim. Nauk*, 5 (1970) 61.
28 S. Tataru, *Rev. Chim. (Bucharest)*, 20 (1969) 223.
29 K. Hayashi, Y. Sasaki, D. Araki and S. Ito, *Jap. Anal.*, 19 (1970) 1370.
30 K. H. Lieser and H. Bernhard, *Z. Anal. Chem.*, 219 (1966) 401.
31 K. Swaminathan and H. M. N. H. Irving, *J. Inorg. Nucl. Chem.*, 28 (1966) 171.
32 A. T. Pilipenko and T. S. Lisetskaya, *Ukr. Khim. Zh.*, 19 (1953) 81; W. S. Fyfe, *J. Chem. Soc.*, (1955) 1032.

Analytica Chimica Acta, 65 (1973) 127–138

GAS-CHROMATOGRAPHIC DETERMINATION OF SELENIUM

JAMES W. YOUNG*

Kentucky State Department of Health, Instrumentation Laboratory, Frankfort, Ky. 40601 (U.S.A.)

and GARY D. CHRISTIAN**

Department of Chemistry, University of Kentucky, Lexington, Ky, 40506 (U.S.A.), and Department of Chemistry, University of Washington, Seattle, Wash. 98195 (U.S.A.)

(Received 8th November 1972)

The toxic effects of selenium have been known for several years. Selenium was discovered to be the toxic substance in grains and forages of South Dakota and other parts of the American West that caused "alkali disease" and "blind staggers" in livestock[1]. The toxicity of selenium is apparently related in part to interference with sulfur absorption[2]. In spite of the toxic nature of this element, it is now well documented that traces of selenium are essential for the prevention of certain diseases in animals. Schwarz and Foltz[3] in 1957 identified selenium as an integral part of "Factor 3". It plays a synergic role with vitamin E which may be explained in terms of a seleno-lipoprotein carrier of vitamin E in blood and tissues[4]. Dickson and Tappel[5] describe the role of selenium as catalyzing reactions involving the sulfhydryl groups on proteins, especially the formation and breaking of the all-important disulfide bridges within and between peptide changes.

Selenium has not yet been defined to be an essential element for humans, although small amounts are present in the body. The biological function and distribution of selenium has been recently summarized by Christian and Feldman[6].

The biological properties of selenium have prompted the development of rapid, sensitive, and accurate methods for its determination, at both toxicological and nutritional levels. Simple colorimetric procedures involve reduction of selenium to the element to form a pink colloidal suspension which can be compared with the color intensity of standards[7–11]. These procedures are generally long and frequently require separation of the selenium by distillation. Smaller (microgram) amounts of selenium can be determined more simply and under less rigorous conditions by collecting the element on Millipore filters and comparing the coloration of the filter with that of standards[12].

Historically, small amounts of selenium are determined by reaction with an *o*-diamine to form the corresponding piaselenol. Hoste[13] studied the complexing properties of 3,3′-diaminobenzidine with selenium and found that an intense yellow compound was produced which could form the basis of a spectrophotometric measurement. Cheng[14], Parker and Harvey[15], Strenge[16], and others have refined

* Present address: The Department of the Treasury, Division of Alcohol, Tobacco and Firearms, Cincinnati, Ohio.

** Present address: Department of Chemistry, University of Washington, Seattle, Wash. 98195.

this spectrophotometric procedure. Lott *et al.*[17] investigated 2,3-diaminonaphthalene as a selenium reagent. Both the selenium–3,3′-diaminobenzidine[18–20] and the selenium–2,3-diaminonaphthalene[16] complexes fluoresce. Both fluorimetric measurements are very sensitive, but the latter procedure is more subject to interference, particularly from copper. Selenium has been determined in biological materials by utilizing the polarographic measurement of the 3,3′-diaminobenzidine complex[21,22]. Other *o*-diamines used for the determination of selenium include *o*-phenylenediamine[23] and 1,2-diaminonaphthalene[24].

The most sensitive and most widely used methods of determinating submicrogram quantities of selenium are the above-mentioned fluorimetric methods, and neutron activation analysis[25–27]. The former methods have been reported to be subject to extraneous fluorescence when applied to biological samples and it has been the authors' experience that extreme care must be taken to avoid large blank readings. Neutron activation analysis of biological materials frequently requires long periods of time for completion of the analysis; periods up to three weeks are needed to allow the high concentrations of radioactive sodium isotopes to decay away.

The present report describes a procedure for the rapid and selective determination of submicrogram amounts of selenium by gas chromatography. The selenium–2,3-diaminonaphthalene complex is formed and extracted into hexane, and an aliquot of the hexane layer is injected into the gas chromatograph. Electron capture is used for detection. The complex can be formed and extracted at pH 2, an advantage over the 3,3′-diaminobenzidine complex, which must be extracted from neutral or alkaline solution; no interferences were found. The method has been applied to the determination of physiological amounts of selenium in human blood and urine. Complete analysis time for a single sample is less than 3 h, including time for digestion of the sample and 2 h for formation of the complex.

EXPERIMENTAL

Reagents and equipment

Reagent-grade chemicals were used throughout, except that nanograde hexane was used for extractions. Nitric acid was purified by distillation from all-glass apparatus. 2,3-Diaminonaphthalene solutions were prepared in 0.10 *M* hydrochloric acid and stored at 4°, as were all other complexing agent solutions used in comparison studies. Unless otherwise noted, all the 2,3-diaminoaphthalene solutions were 0.1%. A stock selenium(IV) solution was standardized gravimetrically. Dilute standards were prepared by making appropriate dilutions of the stock solution.

The acid digestion mixture was prepared by dissolving 2.0 g of sodium molybdate ($Na_2MoO_4 \cdot 2H_2O$) in 40 ml of water; 50 ml of concentrated sulfuric acid was added to this. Upon cooling, 10 ml of 70% perchloric acid was added.

An Arthur H. Thomas Labconco Micro-Kjeldahl apparatus equipped with 30-ml Kjeldahl flasks was used for digestions.

Beckman G.C.-5 and Varian Aerograph 1800 gas chromatographs equipped with electron-capture detectors were used for all chromatographic measurements. The column was 6 ft × $\frac{1}{8}$ in stainless steel packed with 3% SE-30 on 60–80 mesh Chromosorb G. The column temperature was maintained at 165°. The carrier gas

was ultrapure helium maintained at a flow rate of 40 ml min^{-1}. The inlet temperature was maintained at 250° and the detector temperature at 300°.

A Leeds and Northrup Expanded Scale pH Meter was used for pH measurements.

All extractions were performed in 25-ml separatory funnels fitted with Teflon stopcocks.

Samples

Approximately 5 ml of blood was drawn through a stainless steel needle into a Vacutainer. The blood was immediately centrifuged, and the serum collected with a Pasteur disposable pipet. The serum sample was immediately placed in a cold box at 4°.

Urine samples (24 h) made 1 *M* in nitric acid were used for all urine analyses.

Recommended procedure for serum

To 30-ml Kjeldahl flasks add several glass boiling beads, 5 ml of concentrated nitric acid and 3 ml of the digestion mixture. Into separate flasks transfer 1 ml of serum, 1 ml of a standard selenium solution, and 1 ml of distilled water, to serve as sample, calibration standard, and reagent blank, respectively. Heat each mixture initially slowly and then at full heat, until the solution boils vigorously, red fumes appear and evolve, the digest turns clear, and white fumes evolve for 1–2 min. This takes 20–25 min. Cool the flasks to room temperature and transfer to a 50-ml beaker, using three 5-ml washes of distilled water. Add 2 ml of 0.1 *M* EDTA, and adjust the pH to 2.0–2.1 with concentrated ammonia. Add 5 ml of 0.1% 2,3-diaminonaphthalene solution, and allow the mixture to stand for 2 h; then, extract the complex into hexane by shaking with the organic solvent. Separate the small volume (0.1 ml) of organic phase from the aqueous phase by draining the bottom aqueous layer from a 25-ml separatory funnel, until the 0.1-ml organic phase is located in the constriction above the stopcock of the funnel. The organic phase is then readily accessible to a 10-μl syringe. Inject a 1–5 μl aliquot of the hexane layer into the gas chromatograph using a 10-μl syringe.

Recommended procedure for urine

Digest 10 ml of urine with 2 ml of nitric acid and 2 ml of the digestion mixture in the above manner, and extract into 0.1 ml of hexane. Inject a 1–5 μl aliquot as above.

Preparation of calibration curve

Prepare the calibration curve from aqueous standard selenium solutions. Adjust the pH to pH 2.0–2.1 with hydrochloric acid or ammonia and add 5 ml of 0.1% reagent solution. After 2 h, extract the complex into hexane, and inject an aliquot of the hexane layer into the gas chromatograph, as described above.

Experiments showed that recoveries from samples are quantitative by the recommended procedure, and so addition of molybdenum and EDTA to standards is not required for any compensating effect.

Comparison with neutron activation

Comparative studies were performed by neutron activation analysis. Serum samples (2 ml) were lyophilized by freezing the serum in a dry ice–acetone bath and using a vacuum desiccator as the freeze-drying apparatus[28]. The dried samples were then transferred to quartz vials and sealed. A standard (1 μg) was added to quartz powder contained in a quartz vial. After neutron activation, samples were allowed to decay for three weeks before the activity of the ^{75}Se isotope was counted. The possibility of losses of selenium resulting from lyophilization of the serum was examined by analyzing the serum by gas chromatography before and after the lyophilization step.

Recovery and limit of detection

To determine the percentage recovery of selenium in the digestion procedure, known amounts of selenium were added to commercially available (selenium-free) lyophilized serum and digested in the usual manner. Recovery was measured by comparison against undigested aqueous selenium standards.

Limits of detection of selenium for the gas-chromatographic procedure were determined for the 2,3-diaminonaphthalene complex and also for complexes formed with other aromatic *o*-diamines.

RESULTS AND DISCUSSION

Polynuclear aromatic hydrocarbons, including naphthalene and 3,4-benzo-(a)-pyrene, have been determined in submicrogram amounts by gas chromatography with an electron-capture detector in studies related to air pollution. It was thought that the selenium–2,3-diaminonaphthalene complex would be sufficiently stable and volatile that it could be determined by this technique.

The complex was formed by a modification of the method of Lott *et al.*[17]. These authors separated selenium on an ion-exchange column to prevent interferences from macro amounts of foreign ions present in the samples to be analyzed for selenium. The nature of the samples used throughout the present study precluded the presence of macro amounts of ions and this step was omitted from the procedure. Preliminary studies confirmed the work of Lott *et al.*[17] for the conditions necessary for the formation of the complex. The formation of the complex was observed by recording the absorption spectrum of the complex.

Chromatographic conditions

Chromatographic conditions were arbitrarily chosen to determine the feasibility of using the electron-capture detector for the selenium complex. The SE-30 liquid phase was chosen, because in previous work excellent resolution could be obtained for polynuclear aromatic hydrocarbons. The helium flow rate was maintained at 30 ml min^{-1}, and the column temperature maintained at 150°. Under these conditions, a retention time of 5.5 min was observed for the complex at several concentrations of selenium. By varying the carrier-gas flow rate and column temperature, adequate resolution could be obtained with a retention time of 2.1 min for the complex (Fig. 1). The final parameters were 40 ml min for the carrier-gas flow rate and 165° for the column temperature.

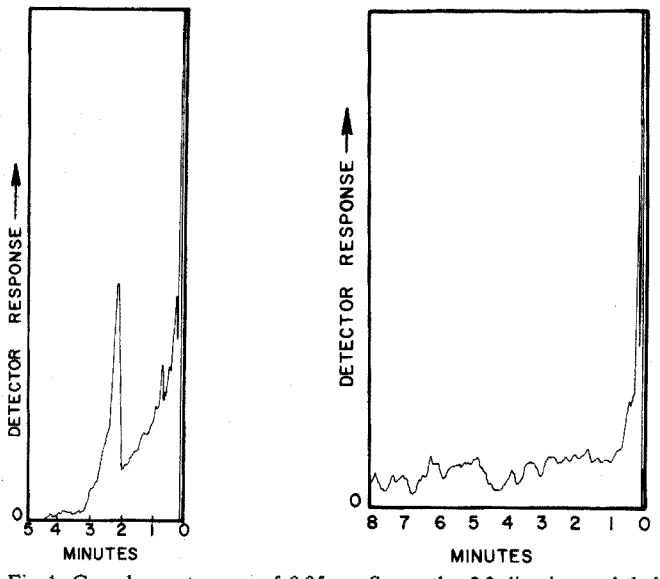

Fig 1. Gas chromatogram of 0.05 μg Se as the 2,3-diaminonaphthalene complex. The column temperature is 165°. The carrier gas (helium) flow rate is 40 ml min^{-1}. Retention time is 2.1 min. Selenium extracted into 0.1 ml of hexane and 5 μl injected.

Fig. 2. Gas chromatogram of a "blank": 1 ml of distilled water digested and extracted by the recommended procedure. Conditions as in Fig. 1.

Formation of the selenium complex

Allaway and Cary[29] recommended at least 1.5 h to insure the formation of the complex. Lott *et al.*[17] indicated that maximum complex formation occurs at pH 2 after 100 min of standing. The color is stable for 4 h. Although maximal color could be developed by keeping the mixture in a boiling water bath for 10 min, this is not recommended because of the instability of the reagent. In gravimetric studies, quantitative precipitation of selenium occurred in 2.5–3 h at room temperature. Watkinson[30] recommended placing the reacting mixture in a water bath, in the dark, for 20 min at 50°. In the present work, chromatograms obtained at 30 min and 2 h indicated that the complex formation occurs in as little as 30 min at room temperature; the same peak heights were obtained in each case.

Extraction of the complex

Lott *et al.*[17] have shown that the complex can be extracted from acid solution by toluene. Their work also indicated that some unreacted 2,3-diaminonaphthalene is extracted by toluene, which necessitates running a reagent blank with each analysis in their fluorimetric measurement. In the present procedure a single chromatographic peak was obtained, the height of which was linear over several ranges of selenium concentrations, indicating that unreacted 2,3-diaminonaphthalene does not interfere. Also, when a blank solution (1 ml of distilled water) was digested in the usual manner and reacted with 2,3-diaminonaphthalene, no peaks were evident in the chromatogram of the hexane extract (Fig. 2).

Parker and Harvey[31] showed that cyclohexane is a better extracting solvent for this selenium complex than is toluene. The present study indicates that hexane may be used with extraction efficiencies as good as cyclohexane. The same peak heights were obtained for the complex extracted in hexane and cyclohexane. In addition, hexane permitted resolution of the selenium complex peak at shorter retention times.

Interferences

According to Allaway and Cary[29] tungsten and vanadium, added as sodium salts at the level of 1 mg of vanadium or tungsten per 0.1 μg of selenium, do not interfere with the fluorimetric determination of selenium with 2,3-diaminonaphthalene. The interferences of a large number of other ions with the formation of the complex were investigated by Lott *et al.*[17]. The present work confirmed their report that interference from elements found in biological materials could be eliminated by incorporating 0.1 *M* EDTA as a masking agent. Molybdenum employed as a catalyst in the digestion mixture did interfere in the formation of the complex, but could be conveniently masked with EDTA. The molybdenum could easily be masked at a 250,000-fold excess of molybdenum over selenium.

In experiments designed to determine the optimal amount of 0.1 *M* EDTA necessary for masking the molybdenum present in the digestion mix, samples containing 0.1 μg of selenium were digested in the usual manner. Various amounts of 0.1 *M* EDTA were added and the selenium was allowed to react with 2,3-diaminonaphthalene. The complex was extracted and the amount present determined by gas chromatography. The results are summarized in Table I. These indicate that for 3.0 ml of the digestion mixture used in a routine digestion, greater than 1.5 ml of the 0.1 *M* EDTA satisfactorily eliminates the molybdenum interference. Below 1.5 ml the molybdenum interferes to the degree that no peak is observed for 0.1 μg of selenium added to the mixture.

TABLE I

SUPPRESSION OF MOLYBDENUM INTERFERENCE WITH EDTA

(In each case 0.1 μg Se was added; 3.0 ml of digestion mixture and 5.0 ml of 2,3-diaminonaphthalene were used)

0.1 *M* EDTA added (ml)	1.0	1.5	2.0	2.5	3.0
Peak height (arbitrary units)	None	46	43	42	43

Recovery studies

Preliminary experiments were designed to test the possible loss of selenium during the digestion procedure. It is well known that acid digestion mixtures must incorporate perchloric acid in order to maintain oxidizing conditions and prevent losses of selenium[10,18,21,32]. Cummins *et al.*[33] utilized a molybdenum(VI) catalyst in a mixture of sulfuric and perchloric acids for the digestion of selenium-containing samples. This catalyst greatly improves the digestion efficiency. However, unless care

is taken, charring occurs and selenium is lost; this can be prevented by adding nitric acid to the mixture[21,34].

In the present work, a nitric–sulfuric–perchloric acid digestion mixture and the molybdenum catalyst were used, and a digested sample of Moni-Trol (previously determined to be free of selenium) containing 0.1 μg of added selenium, yielded a chromatographic peak height of 32 units; an undigested 0.1-μg selenium standard recorded a peak height of 34 units. The digestion could be carried out in 20–25 min, and no charring of the samples occurred when the recommended procedure was followed and oxidizing conditions were maintained throughout. The results (Table II) indicate that losses of selenium during the digestion procedure are small, and that for samples containing 0.2 μg of added selenium, the peak heights are twice those containing 0.1 μg of added selenium. This indicates also that the recovery is constant over the range of selenium concentrations measured.

TABLE II

DETERMINATION OF LOSSES OF SELENIUM DURING THE DIGESTION PROCESS BY THE RECOMMENDED PROCEDURE

Sample	*Moni-Trol added (ml)*	*Selenium added (μg)*	*Peak height (arbitrary units)*
A	0	0	0
B	1.0	0.1	32
C	1.0	0.1	31
D	1.0	0.2	32[b]
E	1.0	0.2	30[b]
F[a]	0	0.1	34
G[a]	0	0.1	34

[a] Undigested standards.
[b] Measured at one-half attenuation of A, B, C, F and G.

Sensitivity

Preliminary work indicated that the electron-capture was extremely sensitive to the selenium complex. In experiments designed to establish detection limits and linear range, 0.01 μg of selenium as its complex could be detected when extracted into 0.1 ml of hexane with 5 μl of this injected into the gas chromatograph; the detector response was linear over the 0.01–0.1 μg range when $\log[I_B/I_B - I_s]$, where I_B is the background current and I_s the sample peak current, was plotted against micrograms of selenium. These quantities represent the total amount of selenium in the samples which is extracted into the hexane. The smallest amount of selenium actually injected into the gas chromatograph therefore was only 0.0005 μg. A linear calibration graph was also obtained for 0.1–1.0 μg selenium extracted into 1 ml of hexane with 1 μl of this injected.

Reproducibility

The reproducibility of the method was established simultaneously with the study of losses of selenium during the digestion process (Table II). Results of duplicate determinations of digested and undigested samples at various concentrations

TABLE III

COMPARISON OF RESULTS BY NEUTRON ACTIVATION ANALYSIS AND GAS CHROMATOGRAPHY

Materials analyzed	*Selenium content determined ($\mu g\ ml^{-1}$)*		*Source of sample*
	N.a.a.	*G.c.*	
(A) Serum	0.44	0.52	Serum pooled from 20 individu
(B) Serum	0.46	0.40	Same as (A)
(C) Serum	0.39	0.36	Same as (A)
(D) Plasma	0.32	0.26	Plasma pooled from 20 individu
(E) Plasma	0.36	0.38	Plasma from blood bank (A-)
(F) Plasma	0.94 (E+0.5 p.p.m.)	1.41 (E+1.0 p.p.m.)	Plasma from blood bank (A-)

of selenium are summarized in Table II. For the concentrations of selenium (submicrogram amounts) and conditions studied, the present method is very reproducible. Also, duplicate determinations of 2 ml of normal human serum yielded arbitrary peak heights of 34 and 33 units, respectively (attenuation one-tenth that used for the study in Table II).

Analysis of samples (biological and environmental)

The accuracy of the present method was determined by analyzing human blood serum and blood plasma samples from a variety of sources, by the present gas-chromatographic method and by neutron activation analysis. The results (Table III) show excellent correlation between the two methods for all samples studied. Serum and plasma samples were pooled from 20 individuals, and a 1-ml aliquot of the pooled specimen was taken for gas-chromatographic analysis while 2 ml was taken for neutron activation analysis.

Sometimes, extraneous chromatographic peaks occurred between 0.3 and 1.2 min with serum samples, but these did not interfere with the selenium peaks. The extraneous peaks may have been associated with decomposition products of old reagent solutions.

Few data on the selenium content of human fluids are available for comparison. Dickson and Tomlinson[35] determined the selenium content of the whole blood, plasma, and cells of over 250 individuals in Canada by neutron activation analysis. The mean concentrations were 0.18, 0.14 and 0.24 p.p.m. in whole blood, plasma, and cells, respectively. Burk *et al.*[36] reported similar levels for an adjacent N.E. location in the United States. Allaway *et al.*[37] analyzed 210 human blood samples obtained from blood banks in 19 American cities, and found a mean selenium concentration of 0.21 p.p.m. There was no pronounced association between selenium concentration and the age of donors. Significantly higher selenium concentrations were obtained for certain areas, such as South Dakota and Wyoming, but the differences were less pronounced than those in locally produced food. Bowen and Cawse[38] in England found a range of 0.26–0.37 p.p.m. selenium in human blood with a mean of 0.32 p.p.m. These values compare with our mean level of 0.38 p.p.m. in serum (range 0.26–0.52 p.p.m.). The present method possesses the sensitivity to determine much smaller concentrations.

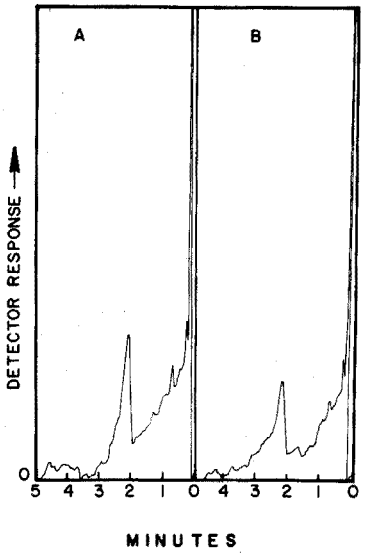

Fig. 3. Determination of selenium in urine. (A) Selenium standard (0.1 μg Se extracted into 0.1 ml of hexane). (B) Urine sample (10 ml of digested urine extracted with 0.1 ml of hexane).

The gas-chromatographic method was extended to include samples from other sources. Urine samples collected over a 24-h period were made 1 *M* in nitric acid to prevent losses of selenium[39]. The urine (10 ml) was digested in the usual manner, and the selenium allowed to react with 2,3-diaminonaphthalene for the 2-h period, after which it was extracted into 0.1 ml of hexane. Figure 3 illustrates the chromatogram of the complex obtained when 1 μl of the hexane extract was injected into the gas chromatograph; also shown is the chromatogram for a 0.1-μg selenium standard. The chromatogram represents *ca.* 0.07 μg of selenium in the urine extract, which is equivalent to 0.007 p.p.m. in the urine sample studied; this figure corresponded to 10 μg of selenium excreted per day in the urine.

The concentration of selenium in raw untreated river water was also determined. This study was performed in conjunction with chemists at the Kentucky State Water Pollution Control Laboratory in an effort to develop a rapid method suitable for the analysis of selenium in natural waters. Several liters of raw river water were collected from the Ohio River at Covington, Ky., and immediately transferred to the laboratory. Several amounts of the water (1.0, 2.0, 3.0, 4.0 and 5.0 ml) were analyzed by the present method, but selenium was found to be absent in all samples. Also, no selenium was found when the river water was concentrated 100-fold (1 l evaporated to 10 ml and analyzed). Hence, the concentration of selenium in the water appeared to be less than 0.01 μg l^{-1} or 0.00001 p.p.m.

The procedures recommended here are for submicrogram quantities of selenium. Extractions of greater amounts may be performed with larger volumes of hexane.

Determination of selenium(IV) with other aromatic o*-diamines*

Experiments were conducted to determine the sensitivity of other piaselenol

derivatives to electron-capture detection.

Nakashima and Toei[40] have proposed a gas-chromatographic procedure for selenium by electron-capture detection of 5-chloropiaselenol and 4,5-dichloropiaselenol. They reported the latter as being three times more sensitive than the former, owing to the added chlorine; the minimal amount of selenium detectable was about 0.04 μg as the 5-chloropiaselenol. More recently, Shimoishi and Toei[41] reported the gas-chromatographic determination of selenium with 4-nitro-*o*-phenylenediamine as the reagent. They determined trace amounts of selenium in pure sulfuric acid as the 5-nitropiaselenol, and reported concentrations in the sulfuric acid as 10^{-6}–10^{-5}%. They did not report a detection limit, but did report that the sensitivity is superior to that of 5-chloro- or 4,5-dichloropiaselenol. Shimoishi[42] used this reagent also for the determination of selenium in pure tellurium. No investigations of interferences were reported in either of these studies.

The work of Nakashima and Toei was confirmed in the present study and it was determined that the 4,5-dichloropiaselenol exhibits approximately the same sensitivity as the selenium–2,3-diaminonaphthalene complex. However, difficulty was experienced in preparing solutions of 5-chloro- and 4,5-dichloro-*o*-phenylenediamine, because of the impurities encountered in the commercial products. Attempts to recrystallize the compounds did not prove successful in eliminating the difficulty. It appeared that the reagents would not be stable for any appreciable time. The present method possesses the advantage of using a standard selenium reagent which is well characterized and readily available in pure form.

The authors wish to thank Cecil Webb for permission to use facilities at the Kentucky State Department of Health. R. A. Nadkarni performed the neutron activation analyses.

SUMMARY

Selenium(IV) is reacted with 2,3-diaminonaphthalene at pH 2 to form the well established complex, which is extracted into hexane. An aliquot of the hexane layer is analyzed gas chromatographically with an electron-capture detector. As little as $5 \cdot 10^{-10}$ g of selenium could be detected; 0.01 μg of selenium could be determined in a sample by extracting into 0.1 ml of hexane and injecting a 5-μl aliquot of the extract. The method was applied to the determination of physiological amounts of selenium in human blood and urine. Averages of 0.38 p.p.m. and 0.007 p.p.m. selenium were found in blood and urine, respectively. River water samples were also analyzed. Complete analysis time for a single sample is less than 3 h, including time for digestion of the sample and 2 h for formation of the complex.

RÉSUMÉ

Le sélénium(IV) réagit avec le diamino-2,3-naphtalène à pH 8.0. Le complexe formé peut être extrait par l'hexane. Une partie aliquote de la couche hexane est analysée par chromatographie gazeuse, avec détecteur à capture électronique. On peut déceler ainsi $5 \cdot 10^{-10}$ g de sélénium et doser 0.01 mg de sélénium dans un échantillon, par extraction dans 0.1 ml d'hexane et injection d'une aliquote d'extrait

de 5 ml. Cette méthode a été appliquée au dosage de quantités physiologiques de sélénium dans le sang et l'urine; 0.38 p.p.m. et 0.007 p.p.m. de sélénium ont été trouvés respectivement dans le sang et l'urine. Des échantillons d'eau de rivière ont également été analysés. La durée d'une analyse complète, comprenant temps de digestion et formation du complexe, ne dépasse pas 3 h.

ZUSAMMENFASSUNG

Selen(IV) wird mit 2,3-Diaminonaphthalin bei pH 2 zu einem wohldefinierten Komplex umgesetzt, der mit Hexan extrahiert wird. Ein aliquoter Anteil der Hexanphase wird gas-chromatographisch unter Anwendung eines Elektroneneinfang-Detektors analysiert. $5 \cdot 10^{-10}$ g Selen konnten nachgewiesen werden; 0.01 μg Selen konnten in einer Probe bestimmt werden, indem mit 0.1 ml Hexan extrahiert und ein 5 μl-Anteil des Extraktes injiziert wurde. Die Methode wurde auf die Bestimmung von physiologischen Mengen Selen in menschlichem Blut und Urin angewendet. Mittelwerte von 0.38 p.p.m. und 0.007 p.p.m. Selen wurden in Blut bzw. Urin gefunden. Flusswasser-Proben wurden ebenfalls analysiert. Die gesamte Analysendauer für eine einzige Probe ist geringer als 3 h, einschliesslich der Zeit für die Behandlung der Probe und 2 h für die Bildung des Se–DAN-Komplexes.

REFERENCES

1 K. W. Franke and E. P. Painter, *J. Nutr.*, 10 (1935) 599.
2 A. Shrift, *Amer. J. Bot.*, 41 (1954) 223, 345.
3 K. Schwarz and C. M. Foltz, *J. Amer. Chem. Soc.*, 79 (1957) 3292.
4 I. D. Desai and M. L. Scott, *Arch. Biochem. Biophys.*, 110 (1965) 309.
5 R. C. Dickson and A. L. Tappel, *Lab. Manage.*, Oct. 1969, p. 15.
6 G. D. Christian and F. J. Feldman, *Atomic Absorption Spectroscopy. Applications in Agriculture, Biology, and Medicine*, Wiley–Interscience, New York, 1970.
7 Assoc. Off. Agr. Chem., *Official Methods of Analysis*, 9th Ed., 1960, p. 86.
8 Assoc. Off. Agr. Chem., *Official Methods of Analysis*, 9th Ed., 1960, p. 330.
9 Amer. Public Health Assoc., *Standard Methods for the Estimation of Water, Sewage and Industrial Water*, New York, 11th Ed., 1961, p. 219.
10 D. N. Fogg and N. T. Wilkinson, *Analyst*, 81 (1956) 525.
11 M. N. Rudra and S. Rudra, *Curr. Sci.*, 21 (1952) 229.
12 C. L. Newberry and G. D. Christian, *J. Assoc. Off. Agr. Chem.*, 48 (1965) 322.
13 J. Hoste, *Anal. Chim. Acta*, 2 (1948) 402.
14 K. Cheng, *Anal. Chem.*, 28 (1956) 1738.
15 C. A. Parker and L. G. Harvey, *Analyst*, 86 (1961) 54.
16 K. Strenge, *Arch. Gewerbepathol. Gerwerbehyg.*, 16 (1958) 588; *Chem. Abstr.*, 55 (1961) 239f.
17 P. F. Lott, P. Cukor, G. Moriber and J. Solga, *Anal. Chem.*, 35 (1963) 1159.
18 F. B. Cousins, *Aust. J. Biol.*, 38 (1960) 11.
19 F. B. Cousins and I. M. Cairney, *Aust. J. Agr. Res.*, 12 (1961) 927.
20 J. H. Watkinson, *Anal. Chem.*, 32 (1960) 981.
21 G. D. Christian, E. C. Knoblock and W. C. Purdy, *J. Assoc. Off. Agr. Chem.*, 48 (1965) 877.
22 D. A. Griffin, *Anal. Chem.*, 41 (1969) 462.
23 H. Ariyoshi, M. Kiniwa and K. Toei, *Talanta*, 5 (1960) 112.
24 O. Hinsberg, *Ber.*, 22 (1899) 866.
25 K. Schwarz, *Nutr. Rev.*, 18 (1960) 193.
26 W. Mertz and K. Schwarz, *Proc. Conf. Physiological Aspects of Water Quality*, Washington, D.C., Sept. 8–9, 1960.

27 K. P. McConnell, *1961 Int. Conf. on Modern Trends in Activation Analysis, College Station, Texas, Dec. 15–16.*
28 J. W. Young and G. D. Christian, *Anal. Chem.*, in press.
29 W. H. Allaway and E. E. Cary, *Anal. Chem.*, 36 (1964) 1359.
30 J. H. Watkinson, *Anal. Chem.*, 38 (1966) 92.
31 C. A. Parker and L. G. Harvey, *Analyst*, 87 (1962) 558.
32 T. T. Gorsuch, *Analyst*, 84 (1959) 259.
33 L. M. Cummins, J. L. Martin, G. W. Magg and D. D. Magg, *Anal. Chem.*, 36 (1964) 382.
34 R. K. Simon, G. D. Christian and W. C. Purdy, *Amer. J. Clin. Pathol.*, 49 (1968) 207, 733.
35 R. C. Dickson and R. H. Tomlinson, *Clin. Chim. Acta*, 16 (1967) 311.
36 R. F. Burk, Jr., W. N. Pearson, R. F. Wood and F. Viteri, *Amer. J. Clin. Nutr.*, 20 (1967) 723.
37 W. H. Allaway, J. Kubota, F. Losee and M. Roth, *Arch. Environ. Health*, 16 (1968) 342.
38 H. J. M. Bowen and P. A. Cawse, *Analyst*, 88 (1963) 721.
39 A. G. Faulkner, E. C. Knoblock and W. C. Purdy, *Clin. Chem.*, 7 (1961) 22.
40 S. Nakashima and K. Toei, *Talanta*, 15 (1968) 1475.
41 Y. Shimoishi and K. Toei, *Talanta*, 17 (1970) 165.
42 Y. Shimoishi, *Bull. Chem. Soc. Jap.*, 44 (1971) 3370.

Analytica Chimica Acta, 65 (1973) 139–145

PULSED COLUMN REDOX TECHNIQUES WITH FLEXIBLE FOAM FILLINGS

T. BRAUN and A. B. FARAG

Institute of Inorganic and Analytical Chemistry, L. Eötvös University, Muzeum krt. 4/B, Budapest 8 (Hungary)

(Received 20th November 1972)

Many methods are available for the reduction of metal ions in their higher valency states[1]. In recent years, attention has been directed to the use of non-metallic reducing agents in columns. Reduction of some metal ions by tetrachlorohydrobenzoquinone held on Kel-F powder (polytrifluorochloroethylene) was suggested by Cerrai and Testa[2] and studied also by Belcher *et al.*[3]. In a recent communication, Braun *et al.* suggested the application of flexible polyurethane foam as an improved support for chloranil (tetrachloro-*p*-benzoquinone) in column operation. Quantitative reduction of cerium(IV), vanadium(V) and iron(III) was obtained with the proposed foam-filled columns at room temperature and at relatively high flow-rates, especially in the case of cerium(IV) reduction. When a temperature of 35° was applied, it was possible to use higher flow-rates in the case of the reduction of vanadium(V) and iron(III).

In comparison with Kel-F powder, the application of polyurethane foam allowed the use of relatively high flow-rates, yet it is still necessary to minimize the time required for the reduction operation, in order to be more suitable for routine analysis.

In the present investigation, a new rapid method is described for the reduction of Ce(IV), V(V) and Fe(III), by making use of the special flexible character of polyurethane foam. The method depends upon packing the foam material, after loading with chloranil, in a syringe (pulsed column); after several pulses in a solution of ascorbic acid, the chloranil is reduced to tetrachlorohydrobenzoquinone. If this syringe is allowed to pulse in a solution of the metal ion in its higher valency state, the metal ion is reduced to the lower one. This is due to the redox reaction between the oxidized form of the metal ion in solution and tetrachlorohydrobenzoquinone loaded on the foam material.

EXPERIMENTAL

Reagents and materials

All reagents used were of standard analytical purity unless otherwise mentioned. "Pure" grade chloranil was recrystallized from chlorobenzene or by sublimation under vacuum. Flexible polyurethane foam, a polyether of open cell-type, was supplied by the North Hungarian Chemical Works, Sajóbábony, Hungary.

Iron, vanadium, cerium and ascorbic acid solutions were standardized by the known standard methods[5].

Apparatus

10-ml and 20-ml all-glass syringes (*i.e.* without any metal connection) were used.

Column preparation

Polyurethane foam was loaded with chloranil by two methods. In the first method the foam material was washed three times with acetone and dried at 80°; 3 g of the dried foam material was mixed with 50 ml of a chlorobenzene solution containing 1 g of chloranil, in a glass dish which was kept in a drying oven at *ca.* 80°. The solvent was gradually removed by mixing the foam material with a glass rod until a swollen foam remained with little excess of the solvent. The loaded foam was dried between two sheets of filter paper to remove excess of chloranil solution. The foam material was then packed in the syringe, gentle pressure being applied with a glass rod. Ascorbic acid (20 ml of 0.2 *N*) was used for the reduction of the chloranil held on the polyurethane foam by releasing and pressing (pulsing) the glass plug of the syringe several times, with the glass tip of the syringe in the ascorbic acid solution. The syringe was operated in a manner that allowed the external solution to enter or leave the syringe at a flow-rate of 60–100 ml min^{-1}.

The second method of foam loading was the same as described previously[4]; the loaded foam material was then packed and treated as described above.

Procedures

Determination of cerium(IV). The foam syringe was washed three times by pulsing with 5-ml aliquots of 1 *M* sulphuric acid, with the syringe tip in the acid solution. Cerium(IV) sulphate solution (5 ml) was placed in a 100-ml beaker and the syringe was allowed to pulse several times (usually 5 pulses). The syringe was then washed three times with 5-ml aliquots of 1 *M* sulphuric acid by successively sucking in the acid solution and ejecting it into the same beaker which contained the reduced cerium. The syringe filling was then reduced by allowing it to pulse in a known excess amount of ascorbic acid solution. The syringe was washed three times with 5-ml aliquots of distilled water. The combined eluate was titrated with standard iodine solution. The amount of cerium(IV) reduced was considered to be equivalent to the difference between the original quantity of ascorbic acid used and that determined after reduction. Usually, the flow-rates of the solution which entered or left the syringe ranged from 60 to 100 ml min^{-1} by releasing or pressing the glass plug of the syringe.

Determination of vanadium(V) and iron(III). The procedure for the determination of vanadium(V) was exactly the same as described for cerium(IV).

For the determination of iron(III), the same procedure was followed, but 0.03 *M* hydrochloric acid solution was used instead of sulphuric acid to wash the syringe before and after reduction.

RESULTS AND DISCUSSION

The analytical application of the redox system consisting of tetrachlorohydrobenzoquinone held on flexible polyurethane foam in column operation was previously investigated[4]. In addition to the advantageous hydrodynamic properties of the

foam-filled columns, it was reported that the reduction of cerium(IV), vanadium(V) and iron(III) can be carried out quantitatively at room temperature and at relatively high flow-rates. The reduction rates of vanadium(V) and iron(III) were found to depend greatly on temperature. At 35°, it was possible to use the foam column at moderately higher flow-rates without affecting the quantitativeness of the reduction.

The main aim of the present study was to exploit the application of the chloranil–foam system in syringes for analytical purposes by effecting the reduction simply by pulsing. The pulsed column principle depends mainly on the flexible character of open-cell plastic foams (*e.g.*, polyurethane), which is not found in any other kind of inert supports, and on the rapid reaction between the metal ion in solution and the redox reagent on the foam surface.

In general, pressing the glass plug of a pulsed column packed with chloranil-loaded foam produces a compression of the foam material. If the tip of the column (syringe) is kept in a given solution and the plug is released gradually, the solution will go into the column and the foam material will return to its original volume. The repetition of this process allows the external solution to come into contact with the redox reagent several times. This will result in a reaction between the metal ion in solution and the redox reagent on the foam.

In order to translate this simple process into a satisfactory procedure for the quantitative reduction of some metal ions, a detailed study of various factors had to be carried out.

Effect of the number of pulses on the reduction efficiency of the pulsed column

As previously demonstrated[4], polyurethane foam holds chloranil in fine crystals when the solvent of the chloranil solution is evaporated gradually and completely. It was also mentioned[4] that the reaction between the ions tested and the redox reagent is better when the latter is held on the foam material in a finely divided state (small crystals). This suggested the use of solvated loaded-foam (*i.e.* without complete evaporation of the solvent), in order to achieve a more homogeneous reaction between the metal ion in solution and the redox solution

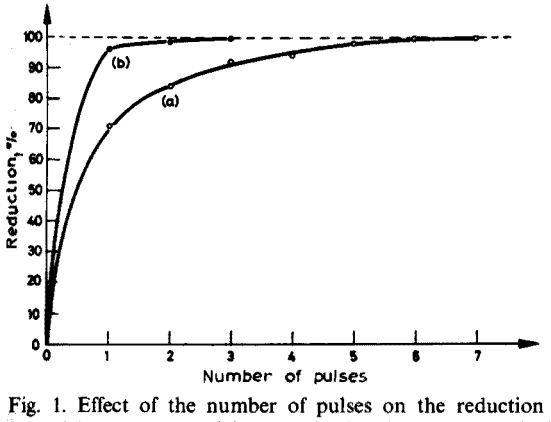

Fig. 1. Effect of the number of pulses on the reduction efficiency of the pulsed column. (a) With 2 g of loaded foam; (b) with swollen foam. Cerium(IV) sulphate concentration 0.005 *M*; volume of the solution 5 ml; at room temperature.

loaded on the foam. In this case the foam is loaded not with small chloranil crystals, but swollen by a solution of the redox reagent in chlorobenzene.

The effect of the number of pulses on the percentage reduction of cerium(IV) was examined with both the swollen foam (containing chloranil solution) and the dry loaded foam (containing small chloranil crystals) under otherwise the same experimental conditions. The reduction efficiency of the pulsed column packed with swollen foam material was found to be better than that of the column packed with dry foam (Fig. 1). In the case of the swollen foam, complete reduction of cerium(IV) was obtained after three pulses, while in the case of the dry foam, complete reduction was only obtained after six pulses. These results recommend the use of the swollen foam material in further investigations.

Effect of temperature on the break-through capacity of the pulsed column

To examine the redox capacity of the pulsed column for cerium(IV), break-through experiments were carried out at room temperature and after preheating the solution before reduction to *ca.* 80°. Aliquots of a 0.1 *M* solution of cerium(IV) sulphate were reduced by the pulsed column successively with a constant number of pulses (5 pulses). After washing three times with 5-ml aliquots of 1 *M* sulphuric acid, the combined eluate, after each reduction process, was titrated with 0.02 *N* sodium thiosulphate in the presence of excess of potassium iodide. Plots of the percentage of reduced cerium against the volume of cerium(IV) sulphate solution used are shown in Fig. 2. It is clear from the curves given that the break-through capacity curve obtained in the case of preheating the solution before reduction was sharper than that obtained at room temperature. Moreover, the capacity obtained up to the break-through point was very dependent on the temperature of the external solution. At room temperature it was 242.6 mg of cerium(IV), while in case of preheating the solution it was 606.5 mg.

The percentage of metal ion reduced by the pulsed column (for 5 pulses) varied

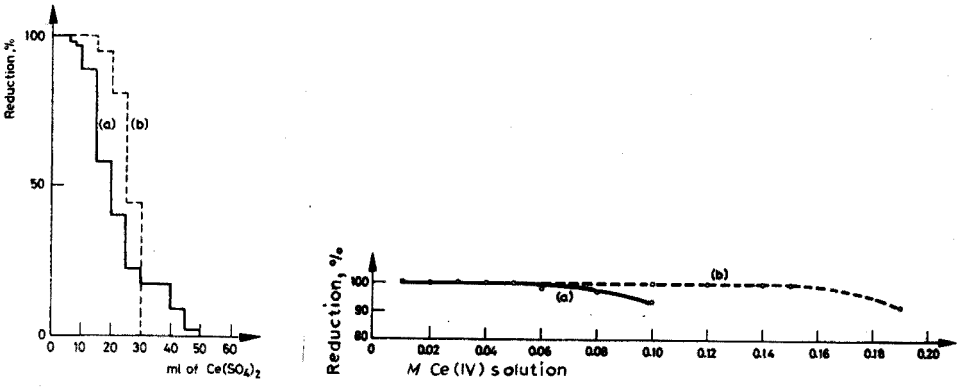

Fig. 2. Break-through capacity curves for cerium(IV). (a) At room temperature; (b) after preheating the solution to *ca.* 80°. Weight of the swollen foam 2 g; cerium(IV) sulphate concentration 0.1 *M*.

Fig. 3. Effect of the concentration of the cerium(IV) sulphate on the efficiency of the redox pulsed column. (a) At room temperature; (b) after preheating the solution to *ca.* 80°. Number of pulses 5; volume of the solution 10 ml.

considerably with temperature and with the original concentration of the external solution, all other parameters remaining constant. Figure 3 shows the amount of cerium(IV) reduced at different concentrations of cerium(IV) at room temperature and at *ca.* 80°. It is clear from the curves that at room temperature complete reduction of 10 ml of cerium(IV) solution was obtained up to a concentration of 0.06 *M* (curve a); but when the cerium(IV) solution was previously warmed to *ca.* 80°, quantitative reduction was possible up to 0.15 *M* cerium(IV).

In the case of vanadium(IV), the reduction of 10 ml of ammonium vanadate at room temperature was quantitative only in the concentration range 0.001–0.004 *M*. Concentrations higher than 0.004 *M* gave incomplete reduction. This may be due to the same reason as described before[4]. However, when the solution was preheated to *ca.* 80°, quantitative reduction was obtained even for concentrations as high as 0.12 *M* (Fig. 4).

The same temperature effect was observed in the reduction of iron(III) (Fig. 5).

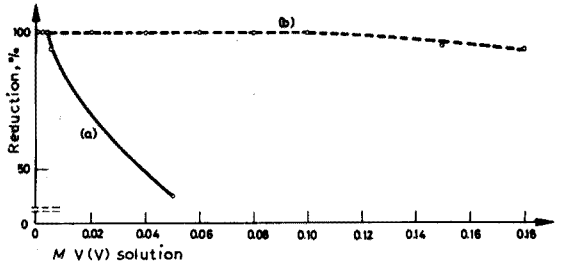

Fig. 4. Effect of the concentration of ammonium vanadate solution on the reduction efficiency of the pulsed column. (a) At room temperature; (b) after preheating the solution to *ca.* 80°. Number of pulses 5; volume of the solution 10 ml.

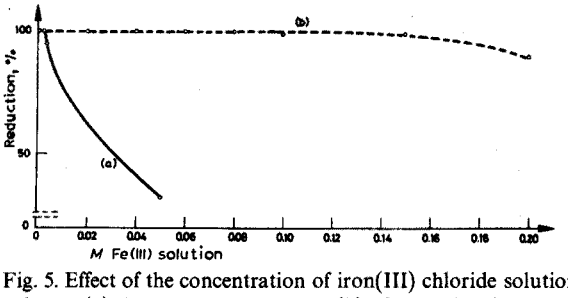

Fig. 5. Effect of the concentration of iron(III) chloride solution on the reduction efficiency of the pulsed column. (a) At room temperature; (b) after preheating the solution to *ca.* 80°. Number of pulses 5; volume of the solution 10 ml.

Generally, preheating the solution containing the metal ion before reduction increases the efficiency of the pulsed column.

Application of the foam pulsed column for the determination of cerium(IV), vanadium(V) and iron(III) gave quantitative results. It was also possible to make a further measurement of the amount of ion reduced by means of the "memory"[3,4] of the pulsed column. The results are shown in Table I. The average relative error was $\pm 2.2\%$ for different concentrations of the three metal ions. The pulsed column

TABLE I

DETERMINATION OF CERIUM(IV), VANADIUM(V) AND IRON(III) BY THE PULSED COLUMN TECHNIQUE

Element	*Eluting solution*	*Temp. of the metal ion soln. (°)*	*Metal ion (mg)*		*Error (%)*	*Average (%)*	*Total average error (%)*
			Taken	*Found*			
Ce^{4+} [a]	1 *M* H_2SO_4	Room temp.	6.87	6.67	−2.9		
	1 *M* H_2SO_4	Room temp.	6.87	6.87	0.0		
	1 *M* H_2SO_4	Room temp.	13.75	13.54	−1.5	±1.8	
	1 *M* H_2SO_4	Room temp.	13.75	13.54	−1.5		
	1 *M* H_2SO_4	Room temp.	20.62	21.02	+1.9		
	1 *M* H_2SO_4	Room temp.	20.62	20.01	−3.0		
V^{5+} [b]	1 *M* H_2SO_4	*ca.* 80	1.95	1.89	−4.1		
	1 *M* H_2SO_4	*ca.* 80	1.95	1.99	+1.9		
	1 *M* H_2SO_4	*ca.* 80	3.91	3.81	−2.8	±2.9	+2.2
	1 *M* H_2SO_4	*ca.* 80	3.91	3.74	−4.2		
	1 *M* H_2SO_4	*ca.* 80	5.86	5.67	−3.2		
	1 *M* H_2SO_4	*ca.* 80	5.86	5.91	+0.9		
Fe^{3+} [c]	0.03 *M* HCl	*ca.* 80	5.31	5.41	+1.9		
	0.03 *M* HCl	*ca.* 80	5.31	5.41	+1.9		
	0.03 *M* HCl	*ca.* 80	10.65	10.81	+1.5	+0.9	
	0.03 *M* HCl	*ca.* 80	10.65	11.08	+4.1		
	0.03 *M* HCl	*ca.* 80	15.98	16.08	+0.6		
	0.03 *M* HCl	*ca.* 80	15.98	16.21	+1.5		

[a] Elution with 1 *M* sulphuric acid. Cerium(IV) solution at room temperature.
[b] Elution with 1 *M* sulphuric acid. Vanadium(V) solution at 80°.
[c] Elution with 0.03 *M* hydrochloric acid. Iron(III) solution at 80°.

technique with flexible foam fillings may be applied to other chromatographic techniques, such as reversed phase and ion exchange.

SUMMARY

The analytical utility of chloranil-loaded polyurethane foam in a syringe column was investigated. A rapid method for the determination of micro and semimicro amounts of cerium(IV), vanadium(V) and iron(III) by means of this redox "pulsed" column has been developed. The effects of number of pulses, temperature and concentration of metal ion in solution on the reduction efficiency of the proposed pulsed column were critically studied. Analyses for different concentrations of Ce(IV), V(V) and Fe(III) were successfully carried out with an average relative error of ±2.2%.

RÉSUMÉ

On examine les possibilités analytiques d'un remplissage de colonne redox à pulsation avec une mousse polyuréthane chargée de chloranile. On a mis au point une méthode rapide pour le dosage de micro- et semimicroquantités de

cérium(IV), de vanadium(V) et de fer(III). L'influence de divers paramètres est examinée. L'erreur relative moyenne est de $\pm 2.2\%$.

ZUSAMMENFASSUNG

Die analytische Anwendbarkeit von mit Chloranil beladenem Polyurethan-Schaum in einer Kolben-Kolonne wurde untersucht. Eine schnelle Methode für die Bestimmung von Mikro- und Halbmikromengen Cer(IV), Vanadin(V) und Eisen(III) mit Hilfe dieser "gepulsten" Redox-Kolonne wurde entwickelt. Der Einfluss der Pulsanzahl, der Temperatur und der Metallionenkonzentration in der Lösung auf die Reduktionswirkung der vorgeschlagenen Kolonne wurde kritisch untersucht. Der mittlere relative Fehler bei der Bestimmung verschiedener Konzentrationen von Ce^{4+}, V^{5+} und Fe^{3+} betrug $\pm 2.2\%$.

REFERENCES

1 See, *e.g.* I. M. Kolthoff and R. Belcher, *Volumetric Analysis*, Vol. III, Interscience, New York, 1957.
2 E. Cerrai and C. Testa, *Anal. Chim. Acta*, 28 (1963) 205.
3 R. Belcher, J. R. Majer and G. A. H. Roberts, *Talanta*, 14 (1967) 1245.
4 T. Braun, A. B. Farag and A. Klimes-Szmik, *Anal. Chim. Acta*, 64 (1973) 71.
5 I. Vogel, *Quantitative Inorganic Analysis*, Longmans, London, 3rd Ed., 1961.

Analytica Chimica Acta, 65 (1973) 147–153

INTERMEDIATE STORAGE TECHNIQUE IN ORGANIC MICROANALYSIS*

PART II. DETERMINATION OF SULPHUR

H. TRUTNOVSKY and ALFY B. SAKLA**

Medical Chemistry Institute and Pregl Laboratory, University of Graz, A 8010 (Austria)

(Received 22nd November 1972)

In studies made to extend the application of the intermediate storage technique, which has already been described for the determination of halogens[1], to the determination of sulphur in organic compounds, some unexpected results were obtained, before a final procedure could be developed. It is well known from several publications that oxides of sulphur react to form silver sulphate with silver in an oxidizing atmosphere. This reaction has been widely used for the determination of sulphur by gravimetric (Stragand and Safford[2]) and titrimetric (Zinneke[3]) methods and also for the removal of sulphur in the determination of carbon and hydrogen. The reaction proceeds with sufficient speed at temperatures of about 500°. Different preparations of silver have been recommended.

In contrast to silver halides, silver sulphate may react with hydrogen to yield various reduction products:

$$Ag_2SO_4 + 5\ H_2 \rightarrow 2\ Ag + 4\ H_2O + H_2S \quad (1)$$

$$Ag_2SO_4 + 2\ H_2 \rightarrow 2\ Ag + 2\ H_2O + SO_2 \quad (2)$$

Thermodynamically both reactions should proceed readily, reaction (1) being preferred. Takeuchi *et al.*[4] claimed that in their trace determination of sulphur the reduction would produce hydrogen sulphide. Accordingly, it was surprising that in our own experiments mostly sulphur dioxide was evolved.

A thorough investigation to clarify this discrepancy was therefore started. The intention was to find a method which could be used without any modification for the determination of sulphur and halogens or even for simultaneous determinations.

For these experiments various preparations of silver were reduced at different temperatures. To permit rapid setting of any desired silver temperature, a special furnace with minute heat capacity and an electronic temperature control circuit, which also actuated the solenoid valves, was developed. These devices, which are described below, also proved very convenient for routine work.

EXPERIMENTAL

Apparatus

The combustion tube and the general setup were the same as for the

* Dedicated to Prof. Dr. Th. Leipert on the occasion of his 70th birthday.

** Present address: Microanalytical Unit, Faculty of Science, Cairo University, Giza, Egypt.

halogen determination[1]. The silver furnace and the electronic control unit are shown in Figs. 1 and 2, respectively. The low voltage (12 V, 10 A) furnace permits high heating and cooling rates, the stability of temperature within the tube being $\pm 5°$. The electronic circuit permits independent setting of the temperature for the oxygen and hydrogen periods, the intermediate nitrogen time of 1 min being prolonged if the second temperature takes longer to attain. The same is applicable for the second nitrogen time which follows each hydrogenation before

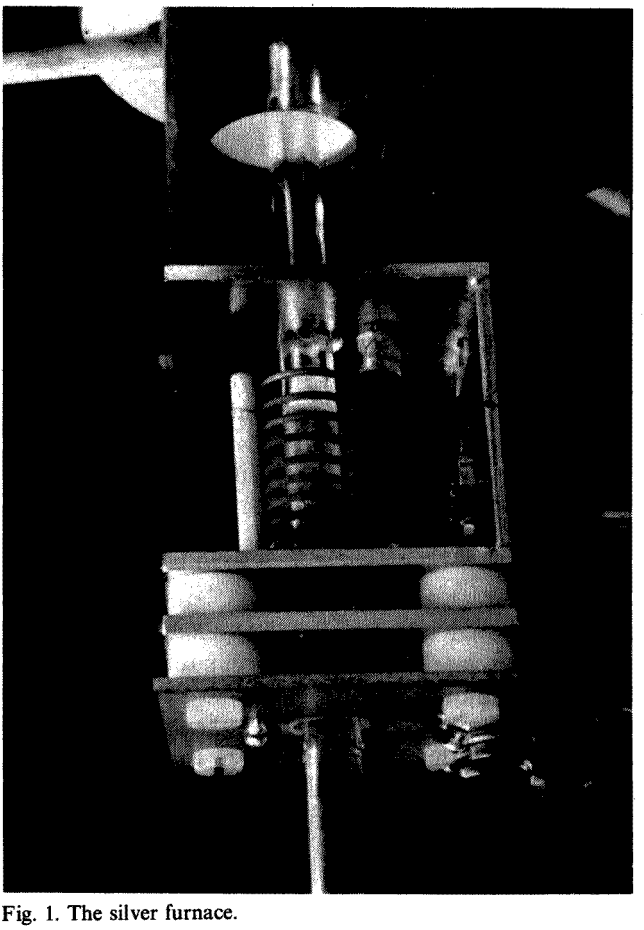

Fig. 1. The silver furnace.

a new analysis can be started. The hydrogenation time can be set digitally to 0–1–3–...–17 min. The whole program begins by starting the movable furnace, during whose travel the gas flow is switched to oxygen; restarting the movable furnace before the full cycle has been executed does not admit a new flow of oxygen but merely interrupts the program. As soon as the movable burner stops again, the program continues. Thus no operating error except closing the nitrogen line can cause the simultaneous presence of oxygen and hydrogen within the combustion tube with its dangerous possibilities.

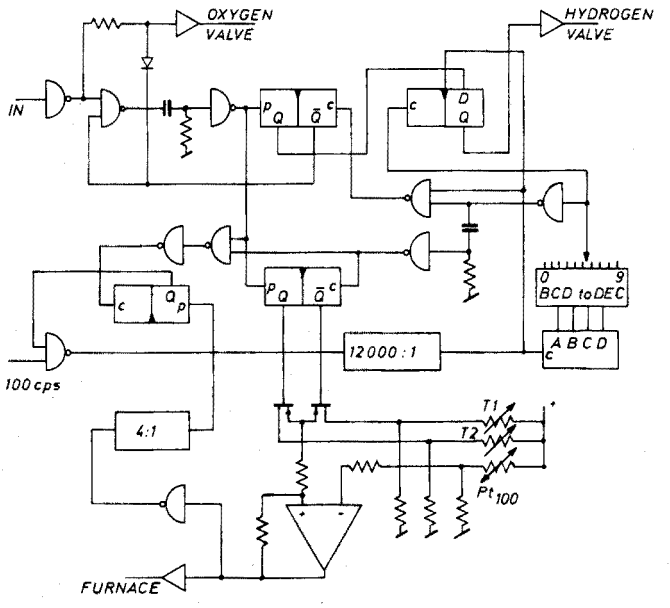

Fig. 2. Electronic control unit. In is low during the travel of the movable furnace.

Types of silver used

The following kinds of silver were used:

1. Silver wire as used for the C, H determination.
2. Silica gel impregnated with 10% (w/w) silver.
3. Silica gel impregnated with 10% silver and 5% platinum.
4. Silver with 5% alumina as described by Pechaneč and Horáček[5].
5. Silver filings, grain size 0.3 mm.
6. Silver powder (5 μm grain size) on pumice.
7. Electrolytic silver needles as described by Mitsui and Sato[6].

All these different brands of silver were used as a 5-mm long layer in the narrow part of the combustion tube. The absorption temperature was 500°, and the gas flow rates for oxygen, nitrogen, and hydrogen were 50, 50, and 40 ml per min, respectively.

Preliminary studies

When used in the analysis of sulphonal, the silver wire, silver filings, and silver powder did not quantitatively absorb the oxides of sulphur. To ensure complete reaction, not only had the length of the silver layer to be increased, but also a reduction of the oxygen flow was necessary. This adversely affected the combustion within the empty tube. The other preparations absorbed all oxides of sulphur, even in the case of samples up to 8 mg.

The reduction was carried out at different temperatures. The resulting hydrogen sulphide was absorbed in 0.1 *M* sodium hydroxide and titrated as described by Binkowski and Wrónski[7]. The sulphur dioxide was determined from separate samples by absorption in dilute hydrogen peroxide and titration with

barium perchlorate (standardized against 0.01 *M* sulphuric acid) as described by Fritz and Yamamura[8]; most, if not all, of the hydrogen sulphide passed through the absorption solution without oxidation, and could be detected with lead acetate paper in the emergent gas in this case. The results of these experiments with silver containing 5% alumina are shown in Fig. 3; all preparations containing a carrier behaved similarly. The preparations consisting of pure silver quantitatively produced sulphur dioxide. Not even traces of hydrogen sulphide could be observed up to 550°.

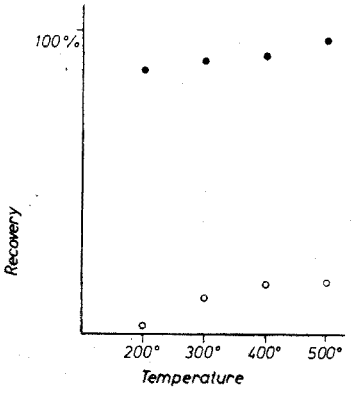

Fig. 3. Recovery rates for sulphur at different temperatures of reduction. (○) Recovery as H_2S, (●) total recovery.

When hydrogen sulphide was evolved, the recovery of sulphur was always less than 100%, probably because of the reaction

$$2\ H_2S + SO_2 \rightarrow 2\ H_2O + 3S \qquad (3)$$

within the absorbing liquid. It could be proved that all the sulphur was released during the hydrogenation step by passing the gas through strong bromine water, thus oxidizing all the sulphur to sulphuric acid, evaporating this solution twice nearly to dryness, and then performing the sulphate titration. The sulphur values were correct but this method is rather inconvenient.

The fact that hydrogen sulphide was produced only when material other than silver was present in the storage layer, leads to the conclusion that reaction (2) does not really proceed and that the hydrogen sulphide is the product of a secondary reaction

$$SO_2 + 3\ H_2 \rightarrow H_2S + 2\ H_2O \qquad (4)$$

which is catalysed by the surface of the silver carrier. This hypothesis is supported by the fact that a layer of 5% platinum on silica gel behind a layer of electrolytic silver needles also caused the appearance of hydrogen sulphide in the effluent gas.

Procedure

From those findings the use of electrolytic silver needles was adopted and the following conditions proved to be excellent for routine work:

(*a*) gas flow, 50 ml of oxygen, 50 ml of nitrogen, and 40 ml of hydrogen per minute;

(*b*) silver temperature, 500° during the combustion, 450° during the reduction;

(*c*) a combustion time of 3 min (60 mm travel of the movable furnace at a speed of 20 mm min^{-1}) and a reduction time of 5 min.

The apparatus and combustion were as described for the determination of halogen; the tightly packed 5-mm silver layer consisted of electrolytic silver needles. The sulphur dioxide was absorbed in a 100-ml Erlenmeyer flask containing 5 ml of water and 0.5 ml of hydrogen peroxide through which the gas was bubbled. Care should be taken to prevent any condensation of moisture around the silver layer because this would cause the formation of sulphur trioxide mists which cannot be absorbed. The final determination was carried out by adding 20 ml of ethanol and a few drops of thorin solution and titrating with a 0.01 *M* solution of barium perchlorate. The blank was zero.

RESULTS AND DISCUSSION

Some results obtained by this method are shown in Table I. As the conditions for the sulphur and for the chlorine determination are the same, a simultaneous titration can easily be effected by first titrating sulphur with a very small amount of indicator, and then adding 0.5 ml of 0.5 *M* nitric acid and diphenylcarbazone indicator and titrating with 0.005 *M* mercury(II) perchlorate.

TABLE I

RESULTS OBTAINED FOR STANDARD COMPOUNDS

Compound	*% Sulphur*		*Deviation (%)*
	Found	*Calculated*	
Sulphonal	28.10	28.09	+0.01
	28.12		+0.03
	28.05		−0.04
	28.27		+0.18
	28.14		+0.05
S-Benzylthi-	15.74	15.82	−0.08
uronium chloride	15.76		−0.06
	15.74		−0.08
Phenylthiourea	20.91	21.07	−0.16
	20.83		−0.24
	20.89		−0.18
Dibenzyldisulphide	26.16	26.03	+0.13
	26.19		+0.16
	26.07		+0.04
Sulphamic acid	32.95	33.03	−0.08
	33.03		0.00
	32.79		−0.24
	32.92		−0.09
	33.07		+0.04
	33.16		+0.13

Some results of this determination are shown in Table II. A simultaneous determination of sulphur and bromine would be possible if the time of hydrogenation was increased but results would be affected by the unfavourable conversion factor for bromine; an iodometric finish would necessitate the evaporation of the ethanol after the sulphur determination. Therefore bromine and iodine are better determined in separate samples. The method has shown excellent results in routine work without any difficulties. The only possible source of error noticed so far is a leakage of the hydrogen valve. If even small amounts of hydrogen leak into the nitrogen and oxygen flows, a ring of sulphuric acid forms behind the silver layer and the results would be low. In this case the solenoid valve should be serviced and the sulphuric acid be removed by heating.

TABLE II

RESULTS FOR S-BENZYLTHIURONIUM CHLORIDE

	Calculated	*Found*	*Deviation*
%S	15.82	15.75	−0.07
		16.00	+0.18
		16.04	+0.22
%Cl	17.49	17.52	+0.03
		17.44	−0.05
		17.77	+0.28

The authors wish to express their thanks to Ögussa Ltd., Vienna, for some samples of silver and to Mrs. G. Biheller for the careful performance of several hundred test analyses.

SUMMARY

A method for the microdetermination of sulphur in organic compounds by means of combustion in a flow of oxygen is described. The oxides of sulphur are absorbed and stored on a small silver layer. After completion of the combustion, the oxygen is replaced first by nitrogen and secondly by hydrogen which liberates the sulphur as sulphur dioxide and regenerates the silver layer. The sulphur dioxide can be easily absorbed by dilute hydrogen peroxide and determined by any convenient method.

RÉSUMÉ

On décrit une méthode pour le microdosage du soufre dans des substances organiques, par combustion dans un courant d'oxygène. Les oxydes de soufre sont absorbés sur argent. Après combustion totale l'oxygène est remplacé d'abord par l'azote, puis par l'hydrogène; ce dernier libère le dioxyde de soufre et régénère la couche d'argent. Le dioxyde de soufre est facilement absorbé par le peroxyde d'hydrogène dilué et dosé par une méthode habituelle.

ZUSAMMENFASSUNG

Ein Verfahren zur Mikrobestimmung von Schwefel in organischen Verbindungen durch Verbrennung im Sauerstoffstrom wird beschrieben. SO_2 und SO_3 werden in einer kurzen Silberschicht absorbiert und gespeichert. Nach Beendigung der Verbrennung wird der Sauerstoff zuerst durch Stickstoff und dieser durch Wasserstoff verdrängt, welcher die Silberschicht regeneriert, und Schwefel als Schwefeldioxid in Freiheit setzt. Das Schwefeldioxid kann leicht in verdünnter Wasserstoffperoxidlösung absorbiert und nach einer geeigneten Methode bestimmt werden.

REFERENCES

1 H. Trutnovsky and A. B. Sakla, *Anal. Chim. Açta*, 59 (1972) 285.
2 G. L. Stragand and H. W. Safford, *Anal. Chem.*, 21 (1949) 625.
3 F. Zinneke, *Z. Anal. Chem.*, 132 (1951) 175.
4 T. Takeuchi, J. Fujishima and Y. Wakayama, *Mikrochim. Acta*, (1965) 635.
5 V. Pechaneč and J. Horâček, *Mikrochim. Acta*, (1966) 357.
6 T. Mitsui and H. Sato, *Mikrochim. Acta*, (1956) 1603.
7 J. Binkowski and M. Wrónski, *Mikrochim. Acta*, (1971) 429.
8 J. S. Fritz and S. S. Yamamura, *Anal. Chem.*, 27 (1955) 1461.

Analytica Chimica Acta, 65 (1973) 155–162

IMPROVED LINEAR TITRATION PLOTS FOR POTENTIOMETRIC PRECIPITATION AND STRONG ACID–STRONG BASE TITRATIONS

C. McCALLUM* and D. MIDGLEY**

Chemistry Department, The University, Glasgow G12 8QQ (Scotland)

(Received 16th October 1972)

The end-point in potentiometric titrations is normally obtained from a plot of the e.m.f. against the volume of titrant added, despite the fact that this may not be identical to the equivalence point[1]. For a non-isovalent precipitation titration, *i.e.*, one in which the precipitate is of the form A_iB_j, where $i \neq j$, the point of inflexion does not necessarily coincide even approximately with the equivalence point[2]. Gran's method of linear titration plots[3], based on Sørensen's earlier work[4], provides a better means of determining the equivalence point, but is inexact in that it takes no account of the solubility of the precipitate (or of the equivalent in strong acid–strong base titrations, the autoprotolysis of water), nor is allowance made for changes in activity coefficients during the titration.

The solubility of the precipitate causes the Gran function to curve in the region of the equivalence point, the curvature becoming more pronounced as the solubility increases. When very dilute solutions are used, the same effects are evident even with quite insoluble precipitates, *e.g.*, the silver–chloride titration of Kolthoff and van Berk[5]. For the same reasons, the end-point in the conventional step-curve titration becomes less sharp. In order to improve the discrimination, titrations have been performed at reduced temperature[6] or with the addition of a solvent of low dielectric constant[7]. By derivation from the charge and mass balance equations, we have obtained functions that allow for the solubility of the precipitate and have been used by Gardner and Paterson[8] in the titration of small amounts of chloride ion leached from ion-exchange membranes. By a similar process Ingman and Still[9] have developed a function that corrects for hydrolysis in the titration of a weak monobasic acid with a strong base, and Johansson[10] has also made this correction.

An alternative approach to non-ideal Gran functions is that of Anfält *et al.*[11], who, having first analysed the titration curves by means of the program HALTAFALL, developed a number of Gran functions for the titration of fluoride with lanthanum or thorium. Each function represents the dominant reaction under the conditions used and is applied to a group of data from a particular part of the titration curve. These functions are not general in application and do not allow for the solubility of the precipitate, nor are they always linear, or, when

* Present address: Chemistry Department, The University, Whiteknights Park, Reading RG6 2AD (England).

** Present address: Central Electricity Research Laboratories, Kelvin Avenue, Leatherhead, Surrey (England).

linear, always accurate. A similar combination of HALTAFALL and Gran titrations has been proposed for weak acid–strong base titrations[1,2].

The effect of changes in activity coefficients on the Gran function as a titration proceeds has hitherto been neglected or else minimized by means of a constant ionic medium. Adding high concentrations of inert electrolyte may, unless rigorous purification has been undertaken, introduce sufficient impurity to bias the result, especially if the unknown concentration is low. Activity corrections can be applied satisfactorily by means of iteration and we have written an ALGOL program that calculates linear functions, taking account of both the solubility of the precipitate and activity coefficients for systems in which side reactions, such as the formation of soluble metal complexes and ligand protonation, are negligible. The differences between these functions and Gran functions and the ranges in which these differences are significant, are discussed below.

THEORY

V_0 ml of a solution of a salt, AP_a, are titrated with a solution of a salt, B_qQ, of concentration m molar. The charges on the ions A, P, B and Q are $+a$, -1, $+1$ and $-q$ respectively. For convenience, charges are omitted from ionic symbols. The reaction is:

$$qAP_a + aB_qQ = aqB + aqP + A_qQ_a$$

The solubility product is

$$K_s = \{A\}^q\{Q\}^a \tag{1}$$

From the condition for electroneutrality,

$$a[A] - q[Q] = [P] - [B] \tag{2}$$

If A is the indicator ion, combining equations (1) and (2), and deriving the concentrations of the non-reacting species P and B from the mass-balance equations, we obtain:

$$\frac{a\{A\}}{f_A} - \frac{q}{f_Q}(K_s\{A\}^{-q})^{1/a} = [P] - [B] = qm(v_e - v)/(V_0 + v)$$

where f_A and f_Q are the activity coefficients of A and Q respectively, v is the volume of solution added and v_e is the volume added at the equivalence point. A plot of the function

$$F = (V_0 + v)\left(\frac{\{A\}}{f_A} - \frac{r}{f_Q} \cdot K_s^{1/a} \cdot \{A\}^{-r}\right)$$

where $r = q/a$, is linear with slope $-rm$ and intercept v_e on the v-axis. The function F is equally valid on both sides of the equivalence point, unlike the Gran case, where two functions are necessary. The same function serves for strong acid–strong base titrations, where A is the hydrogen ion, Q the hydroxide ion and K_s the autoprotolysis constant for water.

Comparison of the F and Gran functions

Since the Gran function involves less calculation than the F function, its use is convenient in many cases and it is therefore desirable to know how accurate it is. Variations in activity coefficients are dealt with below and for the purposes of this comparison it is convenient to neglect them. The function F' is defined as follows:

$$F' = (V_0+v)([\mathrm{A}]-r \cdot K_s^{1/a} \cdot [\mathrm{A}]^{-r})$$

If the indicator ion, A, is in excess, the Gran function is

$$G = (V_0+v)[\mathrm{A}]$$

and if the counter-ion, Q, is in excess, it is

$$G' = (V_0+v)[\mathrm{Q}] = (V_0+v)[\mathrm{A}]^{-r} K_s^{1/a}$$

When A is in excess, the condition for good agreement is that the ratio F':G be greater than some limit, D, where $D<1$, *i.e.*, $[\mathrm{A}]^{r+1} > r \cdot K_s^{1/a}/(1-D)$. When Q is in excess, the condition is that $-F'$:$rG' > D$, *i.e.*, $[\mathrm{A}]^{r+1} < r(1-D)K_s^{1/a}$. In each case the percentage error is $100(1-D)$. The area of applicability of the Gran function can therefore be related to the concentration of the indicator ion and hence to the e.m.f. Examples of the ranges of concentration of indicator ion in which the Gran and F functions differ by more than 0.1% are given in Table I for various charge types and solubility products. If the range of $-\log[\mathrm{A}]$ for a difference of 0.1% is $X-Y$, that for a difference of 1% is given by $(X+\Delta)-(Y-\Delta)$. Values of Δ are also given in Table I.

TABLE I

RANGES OF $-\log[\mathrm{A}]$ FOR WHICH THE GRAN AND F FUNCTIONS DIFFER BY MORE THAN 0.1%

q	a	$-\log K_s$			Δ
		14	*10*	*6*	
1	1	5.5–8.5	3.5–6.5	1.5–4.5	0.5
2	2	2.0–5.0	1.0–4.0	0.0–3.0	0.5
2	1	3.5–5.6	2.2–4.3	0.9–2.9	0.33
1	2	2.6–6.7	1.5–5.6	0.2–4.3	0.66
2	3	1.1–4.8	0.3–4.0	−0.5–3.2	0.6
3	2	1.5–4.0	0.7–3.2	−0.1–2.4	0.4

The difference between the Gran and F functions is illustrated in Fig. 1 for the case $q=a=1$ and $K_s = 10^{-4}$. The conventional $-\log[\mathrm{A}]$ step curve is also shown for comparison.

Effect of an error in the solubility product

Use of the F function demands a knowledge of the value of the solubility product, K_s. If the available value, L_s, is in error, the Gran function may be superior to the F function. When the indicator ion A is in excess, the following function may be defined (again neglecting activity coefficients),

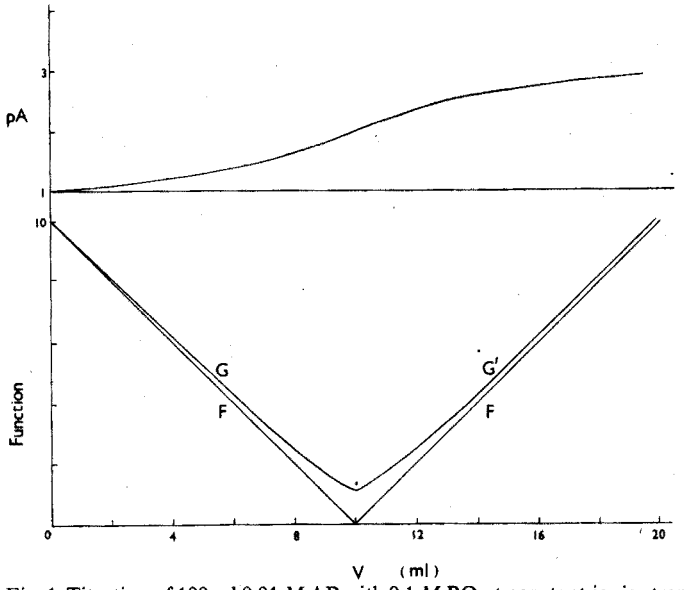

Fig. 1. Titration of 100 ml 0.01 *M* AP with 0.1 *M* BQ at constant ionic strength: $K_s(AQ) = 10^{-4}$ mol^2 l^{-2}; pA = $-\log[A]$; $G = (V_0+v)[A]$; $G' = (V_0+v)[Q]$; $F = (V_0+v)([A][Q])$; v = volume of titrant added. After the equivalence point the F function is shown reflected in the V-axis.

$$E = (V_0+v)([A]-r[A]^{-r}L_s^{1/a})$$

The functions F', G and G' are defined as above. The Gran function is better than the E function if $|G-F'| < |E-F'|$, *i.e.*, if $L_s > 2^a K_s$.

When the counter-ion is in excess, the Gran function is better if

$$|-rG'-F'| < |E-F'|, \textit{ i.e.}, \text{ if } L_s < K_s/2^a.$$

It follows that the Gran function can be better than the E function on only one side of the equivalence point, and only then if the assumed solubility product is considerably in error. The higher the charge on the indicator ion, the more likely it is that the E function is superior to the Gran function.

The effect of neglecting activity coefficients

The effect of neglecting activity coefficients when they are not kept constant, is illustrated for the case of the titration of a strong monobasic acid with a strong monoacidic base. Neglecting activity coefficients, we obtain the function

$$F'' = (V_0+v)(\{H\}-\{OH\}) = fF$$

where f is the mean activity coefficient for a 1:1 electrolyte. Plots of F and F'' have a common intercept on the v-axis, and in assessing the F'' function it is desirable to know its deviation from linearity, *i.e.*, the variation in activity coefficients as the titration proceeds.

Before the equivalence point the total number of ions in solution is constant, neglecting the effects of autoprotolysis, and the ionic strength is affected only by the degree of dilution. For an addition of v ml, the ionic strength is given by

$$I = mv_e/(V_0+v)$$

If the activity coefficients, f_1 and f_2, corresponding to additions v_1 and v_2 are not to differ by more than a predetermined amount, then

$$-\log(f_1/f_2) \leqslant R \tag{3}$$

where R is a discrimination factor and $v_2 > v_1$. The range, $\delta = v_2 - v_1$, within which condition (3) is satisfied can be calculated simply, if the activity coefficient for a 1:1 electrolyte is expressed as

$$-\log f = AI^{\frac{1}{2}}/(1+I^{\frac{1}{2}}) \tag{4}$$

Substituting eqn. (4) in eqn. (3), we obtain by rearrangement

$$\delta \leqslant \left[\left\{\frac{1}{V_x^{\frac{1}{2}}+(mv_e)^{\frac{1}{2}}} - \frac{R}{A(mv_e)^{\frac{1}{2}}}\right\}^{-1} - (mv_e)^{\frac{1}{2}}\right]^2 - V_x$$

where $V_x = V_0 + v_1$. Values of δ corresponding to $R = 5 \cdot 10^{-4}$ and $R = 5 \cdot 10^{-3}$ are given in Table II for some typical titration conditions. The above discriminations are equivalent to changes of *ca.* 0.1% and 1%, respectively, in the activity coefficient.

TABLE II

ADDITION OF TITRANT FOR ACTIVITY COEFFICIENT VARIATIONS OF 0.1 AND 1% FOR A 1:1 ELECTROLYTE

V_x (ml)	v_e (ml)	m (M)	$v < v_e$		$v > v_e$	
			δ^a (ml)	δ^b (ml)	δ^a (ml)	δ^b (ml)
100	10	1	1.1	—[c]	0.1	1.2
100	10	0.1	2.4	—[c]	0.4	3.2
100	10	0.01	—[c]	—[c]	0.7	9.6
25	10	0.1	0.35	4.0	0.2	2.7
10	1	1	0.1	—[c]	0.01	0.1
10	1	0.1	0.23	—[c]	0.04	0.3

[a] $R = 5 \cdot 10^{-4}$.
[b] $R = 5 \cdot 10^{-3}$.
[c] The activity coefficient does not change by the prescribed amount before the equivalence point.

After the equivalence point, the ionic strength is given by

$$I = mv/(V_0+v)$$

Since the titrant is more concentrated in base than the test solution at the equivalence point, we have the condition

$$\log(f_1/f_2) \leqslant R$$

which after substitution and rearrangement as above gives

$$\delta \leqslant (V_x - v_1\theta^2)/(\theta^2-1)$$

where

$$\theta = \left[\frac{R}{Am^{\frac{1}{2}}} + \frac{1}{(V_x/v_1)^{\frac{1}{2}} + m^{\frac{1}{2}}}\right]^{-1} - m^{\frac{1}{2}}$$

Values of δ corresponding to $R = 5 \cdot 10^{-4}$ and $R = 5 \cdot 10^{-3}$ are given in Table II for some typical titration conditions when $v_1 = v_e$, *i.e.*, at the point where the activity coefficients are changing most rapidly. The effect of neglecting activity coefficients is the same for both Gran and F functions.

Calculation of the F function

Calculation of the F function is greatly facilitated by the use of an electronic computer and an ALGOL program has been written for use with the English Electric–Leo–Marconi KDF.9 computer. The best straight line through the titration points is determined by the method of least squares. If the ionic strength changes during the course of a titration, the activity coefficients can be calculated iteratively. Initially, the ionic strength is approximated by $I = uV_0/(V_0+v)$, where u is an estimate of the sample concentration obtained from the conventional step curve or from previous experience or from a guess. Iteration proceeds until successive results agree to within 0.1%. Activity coefficients are calculated from the equation

$$-\log f_z = Az^2(I^{\frac{1}{2}}/(1+BaI^{\frac{1}{2}}) - bI)$$

where A and B are the Debye–Hückel parameters and a and b are adjustable parameters to be supplied to the program.

Provision is also made in the program for calculating the Gran function, with or without activity corrections.

DISCUSSION

The tendency of the Gran function to deviate from linearity increases as the solubility product of the precipitated species increases, as the charge on the indicator ion increases, and as the ratio of the charge on the indicator ion to the charge on the counter-ion increases, as may be seen in Table I. The Gran function can be made to yield the equivalence point by extrapolation of the straight part of the curve, but the further the line has to be extrapolated, the greater the uncertainty in the equivalent volume; the choice of the linear portion may not be easy and will involve an element of discretion by the analyst. Curvature in the Gran plot before the equivalence point leads to an overestimate of the equivalent volume of titrant and hence of the concentration of the sample. After the equivalence point the error is in the opposite sense. It can be seen from Fig. 2 that the two Gran functions (before and after the equivalence point) intersect at the equivalence point itself. In order to obtain an unknown equivalence point from curved Gran plots, it is desirable to have the points arranged as symmetrically as possible about the point of intersection and to have a sufficient number of points to define the curves properly. It should be noted that the Gran curves in Fig. 2, being expressed in terms of the concentration of either the indicator ion or the counter-ion, are normalized, unlike conventionally calculated Gran functions. Normalization is necessary if the intersection method is used.

If activity coefficients are neglected and the F' function is used, the plot will

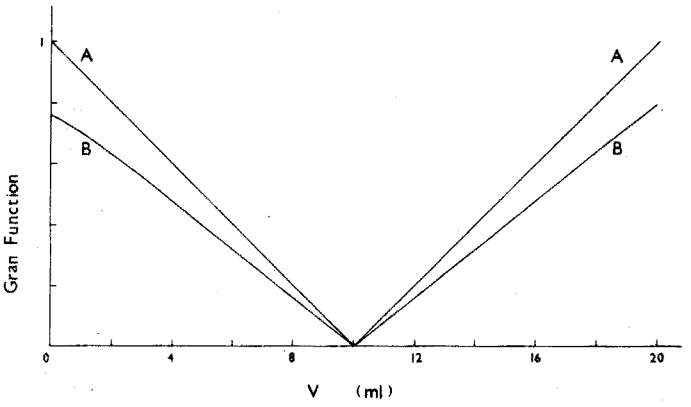

Fig. 2. Titration of 10 ml of 0.1 *M* strong acid with 0.1 *M* strong base: Gran plots with, (A), and without, (B), activity corrections.

still intersect the *v*-axis at the equivalence point, but may be curved. Curvature in the plot before the equivalence point leads to an overestimate of the equivalent volume of titrant and after the equivalence point to an underestimate. Neglecting activity coefficients in the Gran functions produces the same trends. The effects are not of the same magnitude before and after the equivalence point, the difference increasing as the ratio of the ionic strength of the titrant to the ionic strength of the sample increases. It is possible that the curvature observed by Jagner and Årén[13] in the Gran function for silver chloride precipitation is caused, at least in part, by activity effects arising from changes in the ionic strength and dilution of a mixed aqueous–organic solvent.

Compared with the Gran function, the *F* function involves more calculation per datum, but when the Gran function is curved, fewer points are needed to define the linear *F* function. Use of the *F* function requires a knowledge of the appropriate solubility product and of the calibration of the electrode. Good analytical procedure demands that the latter be known in any case.

In the automatic analysis of titration data by means of an electronic computer, the *F* function has the advantage of being continuous, with no need for grouping data from different parts of the titration curve. Moreover, its linearity enables the equivalence point to be calculated from a straight line which has been determined from all the data by the method of least squares, without extrapolation or omission of data at the operator's discretion.

For strong acid–strong base titrations, the *F* function offers no significant advantage over the Gran function, since K_s, *i.e.*, the autoprotolysis constant for water, is so small that deviations from linearity are negligible. Many ion-selective electrodes are now available and the range of ion combination reactions suitable for potentiometric titration methods is increasing. Use of the *F* function extends this range still further by removing restrictions caused by the magnitude of the solubility product.

SUMMARY

Gran plots have limitations caused by neglecting the effects of the auto-

protolysis of water in acid–base titrations or of the solubility of the precipitate in precipitation titrations. Gran plots are compared with a linear function which takes account of the above factors; the concentration ranges in which Gran plots show deviations from linearity are calculated for different reactions. The effect of neglecting activity coefficients is also discussed.

RÉSUMÉ

Les courbes de titrage potentiométrique de Gran sont limitées par les effets d'autoprotolyse de l'eau, lors des titrages acide–base et par la solubilité du précipité dans les titrages par précipitation. On compare les courbes de Gran avec une fonction tenant compte de ces effets. Les limites de concentration dans lesquelles les courbes de Gran montrent des erreurs sont données pour plusieurs réactions. On examine également l'influence des coefficients d'activité sur les deux fonctions.

ZUSAMMENFASSUNG

Bei der Methode von Gran entstehen Fehler, wenn bei potentiometrischen Säure–Base-Titrationen die Autoprotolyse von Wasser und bei Fällungstitrationen die Löslichkeit des Niederschlags vernachlässigt werden. Die Auftragungen nach Gran werden mit einer linearen Funktion verglichen, die die genannten Faktoren berücksichtigt. Die Konzentrationsbereiche, in denen Gran-Auftragungen Abweichungen von der Linearität zeigen, werden für verschiedene Reaktionen berechnet. Der durch Vernachlässigung der Aktivitätskoeffizienten bedingte Einfluss wird ebenfalls diskutiert.

REFERENCES

1 L. Meites and J. A. Goldman, *Anal. Chim. Acta*, 29 (1963) 472.
2 J. N. Butler, *Ionic Equilibrium*, Addison-Wesley, Mass., 1964, p. 189.
3 G. Gran, *Analyst*, 77 (1952) 661.
4 P. Sørensen, *Kem. Maanedsbl.*, 32 (1951) 73; ref. in ref. 3.
5 I. M. Kolthoff and L. H. van Berk, *Z. Anal. Chem.*, 70 (1927) 369.
6 M. J. Smith and S. E. Manahan, *Anal. Chim. Acta*, 48 (1969) 315.
7 J. W. Ross and M. S. Frant, *Anal. Chem.*, 41 (1969) 967.
8 C. R. Gardner and R. Paterson, in *Diffusion Processes*, Proc. Thomas Graham Memorial Symposium, University of Strathclyde, 1969, Gordon and Breach, London, 1970.
9 F. Ingman and E. Still, *Talanta*, 13 (1966) 1431.
10 A. Johansson, *Analyst*, 95 (1970) 535.
11 T. Anfält, D. Dyrssen and D. Jagner, *Anal. Chim. Acta*, 43 (1968) 487.
12 D. Dyrssen, D. Jagner and F. Wengelin, *Computer Calculations of Ionic Equilibria and Titration Procedures*, Wiley, London, 1968.
13 D. Jagner and K. Årén, *Anal. Chim. Acta*, 52 (1970) 491.

Analytica Chimica Acta, 65 (1973) 163–170

POTENTIOMETRIC TITRATION OF SOME AZOLES IN NON-AQUEOUS SOLUTION

STIG VEIBEL and L. B. KUZNETZOWA*

Department of Organic Chemistry, Technical University, DK-2800 Lyngby (Denmark)

(Received 26th November 1972)

Many substances belonging to the azole class of 5-membered heterocyclic compounds are found among natural products or are prepared for pharmaceutical purposes, as dyes, or as analytical reagents[1]. Fast and reliable methods for the determination of such compounds are therefore important.

Most azoles show protolytic activity but this is not sufficiently pronounced to allow their titration in aqueous solution. In some non-aqueous solvents the protolytic properties are enhanced and the titration of imidazoles, imidazolidines, and pyrazolines in anhydrous acetic acid, propionic acid, or N,N-dimethylformamide has been reported[2–7]

As the basic properties usually are more pronounced than the acidic, perchloric acid in anhydrous acetic acid is most frequently used as titrant. In anhydrous acetic acid the following autoprotolysis will take place:

$$2\,CH_3COOH \rightleftarrows CH_3COOH_2^+ + CH_3COO^- \qquad (1)$$

the equilibrium constant[9] being $10^{-12.6}$.

On addition of perchloric acid this equilibrium is forced over to the right:

$$CH_3COO^- + HClO_4 \rightarrow CH_3COOH + ClO_4^- \qquad (2)$$

the actual titrant thus being $CH_3COOH_2^+$.

With imidazole as example the reaction is:

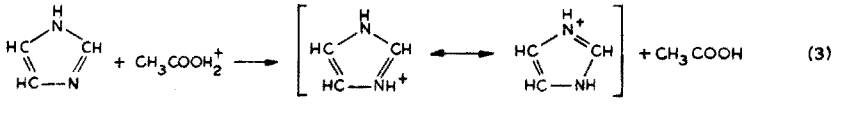

(3)

the imidazolium ion being stabilized by resonance.

Obviously when the base, B, to be titrated is stronger than the acetate ion, a levelling effect as shown in eqn. (4) will take place:

$$B + CH_3COOH \rightleftarrows BH^+ + CH_3COO^- \qquad (4)$$

which means that in such cases it is the acetate ion which is titrated according to eqn. (1) with the equilibrium going to the left. When the titration is carried out potentiometrically, the titration curves of all bases stronger than the acetate ion will be nearly identical, whereas for bases weaker than the acetate ion the curves

* On leave from the Mendeleev Institute for Chemical Technology, Moscow.

will be differently situated in the mV/pK_a diagram[8]; from the half-neutralization potentials the relative basic strengths may be estimated, the pK_a values showing a linear dependence on the half-neutralization potential, following the Henderson equation:

$$pK_{a(x)} = pK_{a(standard)} + (E_{standard} - E_x)/0.059 \quad (5)$$

According to Remick[9], pK_b for the acetate ion in anhydrous acetic acid is 6.58, hence pK_a is 6.02.

When pK_a values in aqueous solution are known for two members of a series of compounds of similar structure (*e.g.* substituted anilines), it has been found that the Henderson equation is followed[6,8,11] but that the slope of the straight line is not the same for all types of compounds and for all types of solvents. When the value 0.059 is used for unknown types, it is, therefore, only the relative value of the basic strength which is determined, and when values are calculated for aqueous solutions, they are only rough approximations.

Imidazolium halides cannot be titrated with perchloric acid in anhydrous acetic acid, because the halide ion is too weak a base to take up a proton in this solvent. Pifer and Wollish[12] have shown that when a solution of mercury(II) acetate in anhydrous acetic acid is added to a solution of a substituted ammonium halide in anhydrous acetic acid, acetate ions are quantitatively substituted for halide ions:

$$2\,BH^+ + 2\,X^- + Hg(CH_3COO)_2 \rightarrow 2\,BH^+ + 2\,CH_3COO^- + HgX_2 \quad (6)$$

As both mercury(II) acetate and mercury(II) halide are completely undissociated, the titration of the acetate ions liberated is then possible. The titration of some substituted imidazolium halides dissolved in acetic anhydride is possible with perchloric acid in anhydrous acetic acid without addition of mercury(II) acetate.

Anhydrous acetic acid is an amphiprotic solvent, though with more pronounced acidic than basic properties. Substituted imidazoles, too, may exhibit basic as well as acidic properties, although the basic properties are more pronounced. Compared with water as solvent, anhydrous acetic acid will enhance the basic properties of weak bases.

Another amphiprotic solvent is methanol, but this proved to be less suitable for the titration of substituted imidazoles than anhydrous acetic acid. It is, on the other hand, an excellent solvent for the titration of substituted imidazolium halides with tetrabutylammonium hydroxide.

Ethers are protophilic solvents. Comparable with ethers is sulpholane, tetrahydrothiophene-S-dioxide, which has been recommended by Morman and Harlow[13] because the potential jump at the neutralization point is much higher than in anhydrous acetic acid. In this solvent, both the titration of substituted imidazoles as bases with perchloric acid in anhydrous acetic acid, and the titration of substituted imidazolium halides with tetrabutylammonium hydroxide in benzene/-methanol were found to be possible.

In the protophilic solvent dimethylformamide a few of the imidazoles investigated could be titrated as acids with tetrabutylammonium hydroxide; the titration of substituted imidazolium halides as acids was also possible.

As shown in Table I, the pK_a values of most of the substituted azoles studied are so close to each other that a differentiating titration of their mixtures

is not possible. Such titrations require a difference between the pK_a values of at least about 2. Some differentiating titrations are, however, possible.

EXPERIMENTAL

Samples

Most of the compounds studied are listed in Table I.

TABLE I

TITRATION OF SUBSTITUTED IMIDAZOLES AND IMIDAZOLIUM CHLORIDES

(Medium, anhydrous acetic acid; titrant, perchloric acid in anhydrous acetic acid)

Compound no.	*Compound*	$pK_a(H_2O)$	*Half-neutralization potential (mV)*	*Accuracy (%)*	$pK_a(CH_3COOH)$
1	Imidazole	6.95	−330	0.2	6.52
2	1-Methylimidazole	7.25	−320	1.0	6.73
3	2-Methylimidazole	7.86	−321	0.2	6.72
4	1,2-Dimethylimidazole	—	−314	1.0	6.82
5	2-Phenylimidazole	6.39	−332	0.3	6.54
6	1-Benzylimidazole	—	−331	0.2	6.53
7	2-Methyl-2-imidazoline	—	−313	2.7	6.85
8	1-Ethoxycarbonylmethyl-2-methyl-5-nitroimidazole	—	−462	0.2	4.34
9	2-Aminobenzothiazole	—	−379	0.2	5.74
10	3-Amino-1,2,4,triazole	—	−371	0.2	5.87
11	4-Amino-1,2,4-triazole	—	−386	0.2	5.62
12	Pyrazole	2.53	−449	0.1	4.55
13	Sodium acetate	4.75	−362	0.1	6.02[a]

[a] Indicated by Remick[9].

Most of these substances were commercial products, the purity of which was confirmed by m.p.'s in agreement with the values recorded in the literature. 1-Ethoxycarbonylmethyl-2-methyl-5-nitroimidazole and 1-ethoxycarbonylmethyl-2-methylimidazolium chloride were prepared by one of us (S.V.) and gave correct elemental analysis within 0.4%. Compounds 9–11 were kindly placed at our disposal by lic. techn. M. Begtrup.

Solvents

As solvents were used anhydrous acetic acid, acetic anhydride, methanol, sulpholane or dimethylformamide. Their purity was checked by conventional methods as indicated *e.g.* by Kreshkov *et al.*[10], and for sulpholane as indicated by Morman and Harlow[13].

Titrants

As titrants were used 0.1 *M* perchloric acid in anhydrous acetic acid, 0.1 *M* perchloric acid in dioxan, or 0.1 *M* tetrabutylammonium hydroxide in benzene/methanol(4/1)[14]. The actual normality was determined by titration of

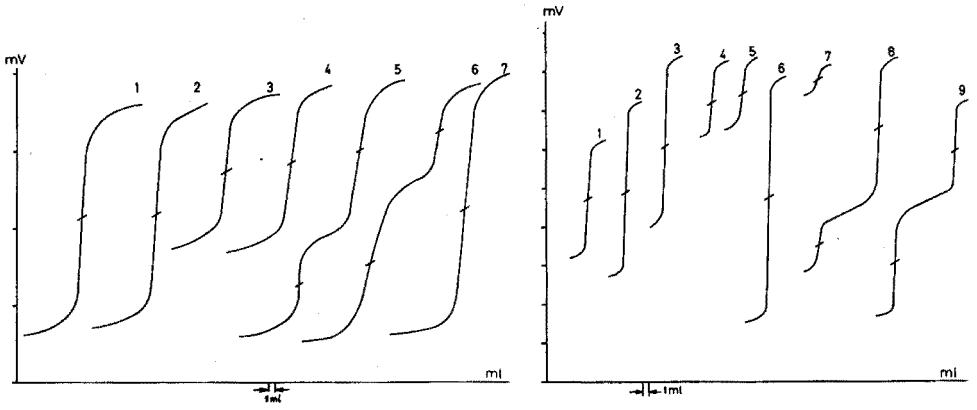

Fig. 1. Titration curves of some imidazole derivatives. Solvent, anhydrous acetic acid; titrant, perchloric acid. Only the parts near the neutralization point are shown. (1) Imidazole, 1-methylimidazole, 2-methylimidazole, 1,2-dimethylimidazole, 2-phenylimidazole and 2-benzylimidazole; these curves were practically identical near the neutralization point. (2) 2-Methyl-2-imidazoline. (3) 1-Ethoxycarbonylmethyl-2-methyl-5-nitroimidazole. (4) Pyrazole. (5) Mixture of imidazole and pyrazole. (6) Mixture of imidazole and 1-ethoxycarbonyl-2-methyl-5-nitroimidazole. (7) Pilocarpinium chloride (solvent, acetic anhydride; titrant, perchloric acid).

Fig. 2. Titration curves of some imidazole derivatives. Solvent, sulpholane; titrant, perchloric acid in dioxan. (1) Imidazole. (2) 2-Methylimidazole. (3) 2-Phenylimidazole. (4) Pyrazole. (5) 1-Ethoxycarbonylmethyl-2-methyl-5-nitroimidazole. (6) 2-Methyl-2-imidazoline. (7) 2-Benzylimidazolium chloride. (8) Mixture of 2-methylimidazole and 2-phenylimidazole. (9) Mixture of 2-methyl-2-imidazoline and 2-methylimidazole.

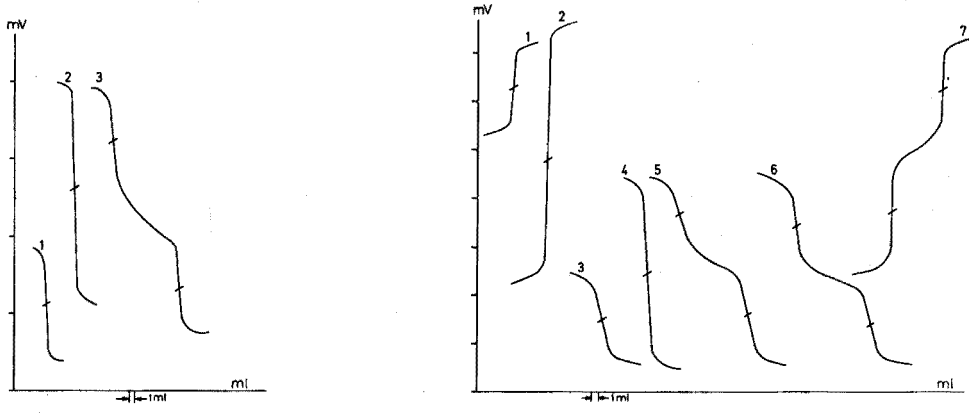

Fig. 3. Titration curves of substituted imidazolium chlorides. Solvent, sulpholane; titrant, tetrabutylammonium hydroxide. (1) 2-Benzylimidazolium chloride. (2) Pilocarpinium chloride. (3) Mixture of pilocarpinium chloride and 2-benzylimidazolium chloride.

Fig. 4. Titration curves of some imidazole derivatives in methanol.
Perchloric acid titrant: (1) Imidazole. (2) 2-Methyl-2-imidazoline. (7) Mixture of 2-methylimidazole and 2-methyl-2-imidazoline.
Tetrabutylammonium hydroxide titrant: (3) 2-Benzylimidazolium chloride. (4) 1-Ethoxycarbonyl-2-methylimidazolium chloride. (5) Histidine dihydrochloride. (6) Mixture of 2-benzylimidazolium chloride and pilocarpinium chloride.

potassium hydrogenphthalate (perchloric acid) or benzoic acid (tetrabutylammonium hydroxide).

Potentiometric titrations

For the titrations a Radiometer pH-meter 28 and a glass/calomel electrode assembly were used. The calomel electrode was filled with a saturated solution of potassium chloride in water.

The sample (*ca.* 1 meq) was dissolved in 25 ml of solvent and the titration was carried out with magnetic stirring. The readings on the potentiometer were plotted against the amount of titrant added.

With anhydrous acetic acid as solvent, a visual titration to a crystal violet end-point was possible.

RESULTS AND DISCUSSION

The results obtained are given in Tables I–VI and Figs. 1–4.

All the compounds investigated required 1 equivalent of acid. For 2-

TABLE II

TITRATION OF SUBSTITUTED IMIDAZOLIUM CHLORIDES

((a) In anhydrous acetic acid after addition of mercury(II) acetate; (b) in acetic anhydride without addition of mercury(II) acetate. Titrant, perchloric acid in anhydrous acetic acid)

Substance	*Accuracy (%)*	
	a	*b*
2-Benzyl-2-imidazolium chloride	0.2	0.9
1-Ethoxycarbonylmethyl-2-methylimidazolium chloride	0.9	0.2

TABLE III

TITRATION OF SUBSTITUTED IMIDAZOLES AND IMIDAZOLIUM HALIDES IN SULPHOLANE WITH PERCHLORIC ACID IN DIOXAN

Compound	*Half-neutralization potential (mV)*	*Accuracy (%)*
Imidazole	−70	0.1
1-Methylimidazole	−59	1.0
2-Methylimidazole	−11	0.5
1,2-Dimethylimidazole	+16	1.0
2-Phenylimidazole	−143	0.3
1-Benzylimidazole	−89	0.2
2-Methyl-2-imidazoline	+233	0.5
1-Ethoxycarbonylmethyl-2-methyl-5-nitroimidazole	−422	0.1
Pilocarpinium chloride	−484	0.7
2-Benzyl-2-imidazolium chloride	−486	0.2
1-Ethoxycarbonylmethyl-2-methylimidazolium chloride	−490	1.0
Pyrazole	−402	0.5

TABLE IV

TITRATION OF SUBSTITUTED IMIDAZOLIUM CHLORIDES IN SULPHOLANE WITH TETRABUTYLAMMONIUM HYDROXIDE IN BENZENE/METHANOL(4/1)

Compound	*Half-neutralization potential (mV)*	*Accuracy (%)*
Pilocarpinium chloride	−15	0.5
2-Benzyl-2-imidazolium chloride	+189	0.4
1-Ethoxycarbonylmethyl-2-methylimidazolium chloride	−14	0.1

TABLE V

DIFFERENTIATING TITRATION OF SOME SUBSTITUTED IMIDAZOLES AND IMIDAZOLIUM CHLORIDES

Substances	*Accuracy (%)*
a. In anhydrous acetic acid with perchloric acid in anhydrous acetic acid	
1+8[a]	0.4 and 0.9
1+12	1.0 and 2.0
b. In sulpholane with perchloric acid in dioxan	
3+5	3 and 1.8
3+7	2.7 and 0.9
c. In sulpholane with tetrabutylammonium hydroxide in benzene/methanol	
Pilocarpinium chloride + 2-benzyl-2-imidazolium chloride	1.0 and 1.0

[a] Numbers refer to compounds in Table I.

TABLE VI

HALF-NEUTRALIZATION POTENTIALS FOR SOME SUBSTITUTED PYRAZOL-5-ONES

(Titrated (a) with tetrabutylammonium hydroxide (solvent, methanol) and (b) with perchloric acid (solvent, anhydrous acetic acid))

Substance	*Half-neutralization potential (mV)*	
	a	*b*
3-Methyl-4-propylpyrazol-5-one	243	167
3-Methyl-4-ethylpyrazol-5-one	233	164
3-Methyl-4-allylpyrazol-5-one	216	164
3-Methylpyrazol-5-one	198	151
3-Methyl-4-phenylpyrazol-5-one	190	183

aminobenzothiazole, 3-amino-1,2,4-triazole and 4-amino-1,2,4-triazole, an uptake of 2 protons might be expected, but as they are a sort of amidines, the cation formed after uptake of 1 proton is stabilized by resonance, *e.g.*:

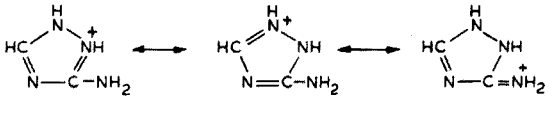

In another series of titrations the acidic and basic properties of some substituted pyrazol-5-ones were compared. Their relative basic strengths had previously been determined by titration with perchloric acid in anhydrous acetic acid. Now the pyrazol-5-ones were titrated in methanolic solution with tetrabutylammonium hydroxide in benzene/methanol. In Table VI, the pyrazol-5-ones are arranged in decreasing order of the half-neutralization potential when titrated with tetrabutylammonium hydroxide (column 2); the half-neutralization potentials when the pyrazol-5-ones were titrated with perchloric acid are indicated in column 3. It can be seen that the variations in acidic and basic strength do not follow any well defined trend.

Thanks are due to the Governments of the U.S.S.R. and Denmark for a grant under the Cultural Agreement between the two countries which made the stay of L.B.K. in Denmark possible.

SUMMARY

The titration of some substituted azoles in non-aqueous solution has been studied and their relative basic strengths determined. Differentiating titration of mixtures of substituted imidazoles is only possible when one of the imidazoles is substituted with a powerful electronegative substituent, *e.g.* a nitro group. Azolium halides may be titrated with perchloric acid in anhydrous acetic acid after addition of mercury(II) acetate, or dissolved in acetic anhydride without addition of mercury(II) acetate; dissolved in methanol, they may be titrated as acids with tetrabutylammonium hydroxide in benzene/methanol. The acidic and basic properties of some substituted pyrazol-5-ones have been compared.

RÉSUMÉ

Une étude est effectuée sur le titrage de quelques azoles substitués, en solution non-aqueuse. Leur force basique relative est déterminée. Un titrage sélectif de mélanges d'imidazoles substitués n'est possible que dans le cas où l'un des imidazoles possède un substituant fortement électronégatif, tel que le groupe nitro. On procède par titrage à l'aide d'acide perchlorique, dans l'acide acétique glacial ou dans l'anhydride acétique. Le titrage comme acide peut se faire dans le méthanol, au moyen de l'hydroxyde de tétrabutylammonium dans le mélange benzène/méthanol. Les propriétés acides et basiques de quelques pyrazolones-5 ont été déterminées.

ZUSAMMENFASSUNG

Einige substituierte Azole wurden in nicht-wässeriger Lösung titriert und die relativen Basenstärken bestimmt. Eine differenzierende Titration von Mischungen substituierter Imidazole ist nur möglich, wenn eins der Imidazole stark elektronegativ substituiert ist, z.B. mit einer Nitrogruppe. Azoliumhalogenide lassen sich nach Zugabe von Quecksilber(II)-acetat mit Perchlorsäure in Eisessig titrieren. In Essigsäureanhydrid-Lösung ist die Zugabe von Quecksilber(II)-acetat nicht notwendig. In methanolischer Lösung lassen sich die Azoliumhalogenide mit Tetrabutylammoniumhydroxid in Benzol/Methanol titrieren. Die sauren und basischen Eigenschaften einiger 5-Pyrazolone wurden verglichen.

REFERENCES

1 A. R. Katritzky and J. M. Lazowski, *The Principles of Heterocyclic Chemistry*, Methuen, London, 1967.
2 C. Hennart and E. Merlin, *Chim. Anal. (Paris)*, (1958) 264.
3 C. Hennart and G. Berteleau, *Ind. Chim. Belg.*, 32 (1967) 893.
4 H. W. Wanzlich and W. Löchel, *Chem. Ber.*, 86 (1953) 1463.
5 S. Veibel and I. G. K. Andersen, *Anal. Chim. Acta*, 15 (1956) 15.
6 S. Veibel, K. Eggersen and S. C. Linholt, *Acta Chem. Scand.*, 6 (1952) 1066.
7 S. Veibel, K. Eggersen and S. C. Linholt, *Acta Chem. Scand.*, 8 (1954) 768.
8 H. F. Hall, *J. Amer. Chem. Soc.*, 52 (1930) 5115.
9 A. E. Remick, *Electronic Interpretation of Organic Chemistry*, Wiley, New York, 1949.
10 A. P. Kreshkov, L. N. Bykova and N. A. Kazaryan, *Acid–Base Titration in Non-Aqueous Solutions*, Khimiya, Moskow, 1967.
11 J. S. Fritz, *Anal. Chem.*, 25 (1953) 408.
12 C. W. Pifer and E. G. Wollish, *Anal. Chem.*, 24 (1952) 300.
13 H. Morman and G. A. Harlow, *Anal. Chem.*, 39 (1967) 1869.
14 R. H. Cundiff and P. C. Markunas, *Anal. Chem.*, 28 (1956) 792.

Analytica Chimica Acta, 65 (1973) 171–176

THE DETERMINATION OF SILVER IN ORES BY ANODIC STRIPPING VOLTAMMETRY

P. PETÁK

Ore Research Institute

and F. VYDRA

J. Heyrovský Institute of Physical Chemistry and Electrochemistry, Czechoslovak Academy of Sciences, Prague 1 (Czechoslovakia)

(Received 18th November 1972)

In recent years, various attempts have been made to replace the classical fire assay technique for the determination of silver in ores by a more convenient, rapid and simple method. Several photometric methods have been reported but all such procedures have failed in industrial laboratories, mainly because of the necessity of separating interfering elements; the separation is time-consuming, and the use of uncommon reagents is often necessary.

In this paper, a simple method for the determination of trace amounts of silver in ores is presented. Basically, the method consists of stripping voltammetry of silver at a rotating glassy carbon electrode. Stripping voltammetry of silver at a stationary electrode has been studied by Monien *et al.*[1], who used various types of carbon as the electrode material. Stripping voltammetry of silver at a rotating glassy carbon electrode has been reported by Kopanica and Vydra[2], who determined silver in the presence of copper. Temmerman and Verbeek[3] determined silver in cadmium. An a.c. technique has also been used for the determination of silver in copper[4].

For the determination of silver in ores, silver is separated by extraction; the presence of high concentrations of interfering metal ions can lead to their co-extraction. In the proposed method, silver was extracted with dithizone[5], or was separated on a silica gel column as its ammine complex[6].

EXPERIMENTAL

Apparatus

An OH-102 polarograph (Radelkis, Hungary) and a rotating disk electrode were used. The disk electrode was prepared from a glassy carbon rod (Le Carbon Lorraine, France) fixed in a Teflon tube, and was rotated at 2300 rev min^{-1}. The tip of the saturated calomel reference electrode was placed close to the disk electrode. Before each measurement, the electrode surface was polished with metallographic paper 5/0 (SIA, Switzerland).

Reagents

All solutions were prepared from p.a. chemicals and twice-distilled water. For the dissolution of ores with minimal silver content, Suprapur (Merck) acids were used.

Dithizone was dissolved in carbon tetrachloride and purified by extracting twice with dilute ammonia solution (1 + 100). The aqueous phase was separated, filtered and neutralized with (1 + 1) hydrochloric acid. The precipitated dithizone was then extracted again with carbon tetrachloride.

Silica gel was prepared as described by Pitra[7]. The gel (pore size 85 Å and particle size 0.15–0.20 mm) activated at 120° was used in a column 100 mm high with an internal diameter of 16 mm. The pH of the silica was adjusted to the required value by washing with the following buffer solution.

Buffer solution. Dissolve 60 g of ammonium nitrate in water, add 350 ml of ammonia, and dilute the solution to 1 l with water.

Procedures

Dissolution of sample and separation with dithizone. To 2 g of sample in a teflon beaker, add 10 ml of nitric acid (d. 1.40) and 10 ml of hydrofluoric acid (40%). After dissolution of the material at room temperature, transfer the beaker to a sand bath and evaporate almost to dryness. Add 10 ml of perchloric acid (d. 1.68) and 10 ml of hydrofluoric acid and repeat the evaporation. Cool, add 5 ml of hydrofluoric acid and repeat the evaporation once or twice to remove all the silica. Cool and add hot water; after dissolution, transfer the solution to a 100-ml volumetric flask, cool and dilute to 100 ml with water.

To a portion of this solution containing 0.5–10 μg of silver, add 3 ml of 0.25 *M* EDTA and neutralize with ammonia to pH 4.8. Transfer the solution to a separatory funnel and add 10 ml of a 0.01% solution of dithizone in carbon tetrachloride; after the extraction, the organic phase should be greenish in colour. Separate the phases and back-extract the silver from the organic phase three times with 10, 10 and 5 ml of 1 *M* hydrochloric acid. Transfer the aqueous (acidic) phase to a 100-ml beaker and dilute to 50 ml with 1 *M* hydrochloric acid. Before the electrolysis, remove any droplets of carbon tetrachloride, because they may cause breaking of the circuit when they come in contact with the electrode surface. After complete separation of carbon tetrachloride, deaerate the solution for 10 min with pure nitrogen. Insert the electrodes, rotate the glassy carbon electrode and start the electrolysis at −0.6 V for a fixed time. During the electrolysis, nitrogen should flow through the cell above the solution to prevent contamination by air. After the electrolysis, start the potential scan at a rate of 30 mV s^{-1} without disconnecting the electrodes, and record the anodic dissolution curve of silver. The peak corresponding to the dissolution of silver has maximal current at a potential of +0.05–+0.09 V. For calculation of the result, use a calibration curve.

Dissolution of sample and separation on silica. For the analysis of ore concentrates (with the exception of lead sulphide concentrates), ores rich in silver and converter copper, it is advantageous to separate silver by sorption on silica.

Dissolve 0.5–1.0 g of the sample in a (30 + 5 + 1) mixture of hydrofluoric (40%), perchloric (d. 1.68) and nitric acid (d. 1.40) in a teflon beaker. Evaporate nearly to dryness, redissolve the residue in the acid mixture and evaporate once more. After cooling, dissolve the residue in 20 ml of hot water and transfer to a 100-ml volumetric flask. Add 10 ml of 10% (w/v) tartaric acid solution and 15 ml of 0.25 *M* EDTA, adjust the pH with ammonia to 8.0–8.5, and dilute to 100 ml with water. To a suitable portion of this solution, add 10 ml of buffer solution and let the solution

flow through the silica column, prepared as described above, at a flow rate of 2 ml min^{-1}. Wash the column with diluted (1+9) buffer solution, and elute silver with 100 ml of 0.1 *M* nitric acid. Deaerate the sample solution for 10 min with nitrogen and carry out the electrolysis step as described above. After electrolysis, remove the beaker with the analyzed solution (without disconnecting the circuit) and insert the electrodes into an identical beaker containing a deaerated solution of 0.1 *M* hydrochloric acid. Immediately start the stripping step by an anodic potential shift and record the dissolution curve of silver. For calculation of the results, use a calibration curve prepared as described with standard silver solutions.

RESULTS AND DISCUSSION

The influence of the base electrolyte

A study of the influence of the base electrolyte showed that the stripping analysis for silver was more sensitive in acidic media. The optimal acidity for the pre-electrolysis step was 1 *M*, whereas sharp peaks of maximal height were obtained when the silver deposit was stripped into a 0.1 *M* hydrochloric acid solution. Good results were also obtained when silver was stripped into solutions of sulphuric acid, but in nitric and perchloric acids, the corresponding peaks were too broad.

In the analysis of ores with very low silver contents, silver was first separated by extraction with dithizone and, for the back-extraction of silver into the aqueous phase, a mixture containing 0.03 *M* hydrochloric acid and 20% sodium chloride was advantageous, because traces of copper and mercury remained in the organic phase[5]. This mixture was also suitable for the electrolysis and stripping steps of the analysis.

Concentration dependence

In a study of the stripping voltammetry of silver on stationary carbon electrodes, Brainina *et al.*[8] found that the dependence of the maximal anodic current on the amount of silver deposited on the electrode was given by two lines of different slopes. The line corresponding to low amounts of silver (10^{-7} *M* silver(I) in solution) had a smaller slope than the line corresponding to higher amounts of silver (10^{-6}–10^{-5} *M* silver(I) in solution). In the present study, the above dependence was followed with the rotating glassy carbon electrode. The results obtained showed only one line even at silver concentrations as low as 10^{-7} *M* (Fig. 1). Moreover, the dependence of the maximal anodic current on the concentration of silver in the solution was a straight line over the concentration range $5 \cdot 10^{-8}$–$1 \cdot 10^{-5}$ *M* Ag. At a stationary electrode, this dependence was a straight line only over a narrow concentration interval (Fig. 2). These results suggested that the mechanism of the deposition of the layers of silver on the electrode depends on whether or not the electrode is rotated. With the rotating electrode, the thickness of the deposit appeared to have no influence on the mechanism of the deposition and stripping processes studied. For practical application, the rotating electrode was superior, because only one calibration graph was necessary, and because the results obtained were more reproducible than those with a stationary electrode.

The content of silver in ore concentrates lies in the range 50–1000 g ton^{-1} and therefore the proposed method for the determination of silver was tested mainly for the upper content limit. The use of 1 *M* hydrochloric acid as the base electrolyte

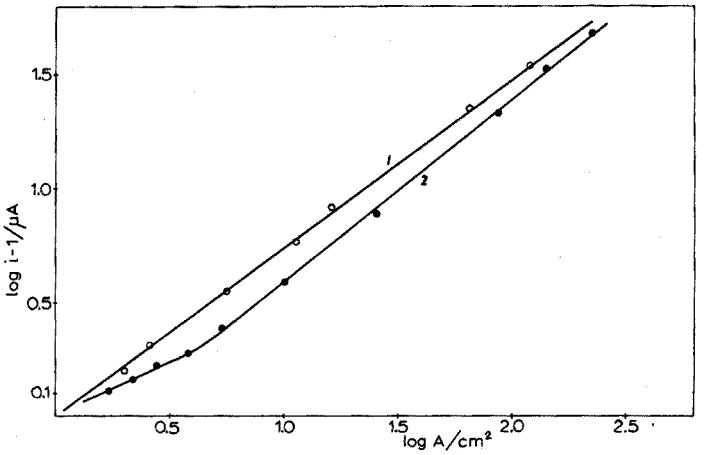

Fig. 1. Dependence of the maximal anodic current of silver on the amount present on the glassy carbon electrode. (1) Rotating electrode; (2) stationary electrode. Solutions: 0.1 M $KNO_3 + x$ M $AgNO_3 + HNO_3$ (pH 2, $x = 2 \cdot 10^{-7} - 1 \cdot 10^{-5}$). Scan rate 30 mV s^{-1}; $U_{el.} = -0.2$ V *vs.* S.C.E.

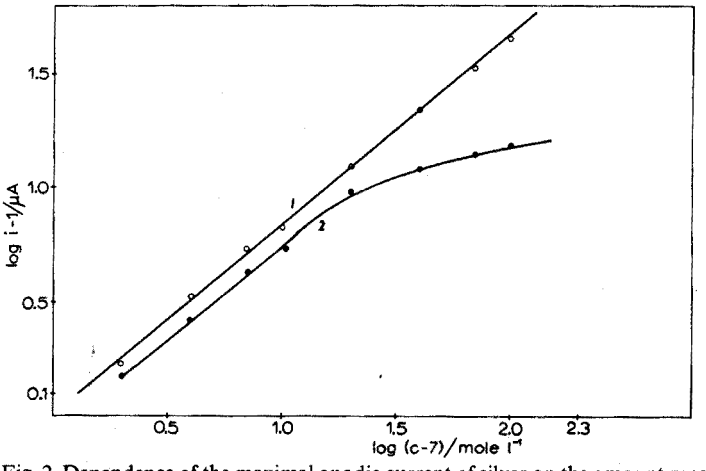

Fig. 2. Dependence of the maximal anodic current of silver on the amount present in solution. (1) Rotating electrode; (2) stationary electrode. Solutions: 0.1 M $KNO_3 + x$ M $AgNO_3$ (pH 2, $x = 2 \cdot 10^{-7} - 1 \cdot 10^{-5}$). Scan rate 30 mV s^{-1}; $U_{el.} = -0.2$ V *vs.* S.C.E.

for the electrolysis step allowed the determination of a maximum of $4 \cdot 10^{-6}$ M silver. At higher concentrations of silver, the dependence of the peak heights on the amount of silver in solution was not linear, owing to the value of the solubility product of silver chloride. When nitric acid was used as the base electrolyte for the electrolysis step and hydrochloric acid as the electrolyte for the stripping step, it was possible to determine $1 \cdot 10^{-5}$ M silver. The lowest measurable concentration was $5 \cdot 10^{-8}$ M silver.

Separation of silver

Before the determination, silver had to be separated from interfering elements.

As mentioned above, silver was separated by extraction at pH 4.8 in the presence of EDTA with a 0.01% solution of dithizone in carbon tetrachloride. After separation of the phases, the organic phase was extracted three times with 1 *M* hydrochloric acid, to return the silver to the aqueous phase. When the organic phase was extracted with two 10-ml portions of 1 *M* hydrochloric acid for 1 min each time, 15 μg of silver could be back-extracted.

When the material analyzed (ores, concentrates) contained high amounts of copper, the separation of silver on a silica column[6] was advantageous. An excess of EDTA was added to the acidic sample solution, the pH was adjusted to 8.0 and finally ammoniacal buffer solution was added. When the sample solution contained metal ions which did not form stable complexes with EDTA, tartaric acid was also added. The resulting solution was passed through the silica column. When the sample contained high amounts of calcium and aluminium, these elements were adsorbed together with silver but did not interfere with the determination. Similarly, traces of iron(III) could also be adsorbed in the form of the hydroxocomplex, but did not interfere. For the determination of silver in ores containing low amounts of silver (less than 50 g ton^{-1}), the separation of silver by extraction is recommended because of the limited capacity of silica.

The results obtained by the proposed methods are in good agreement with the fire-assay technique (Table I).

TABLE I

COMPARISON OF STRIPPING VOLTAMMETRY AND FIRE ASSAY

Sample	*Ag found (g ton^{-1})*		*Deviation (%)*
	Stripping	*Fire assay*	
Sb ore	6.2	7.0	12.9
Cu concentrate	248.0	265.0	6.3
Zn concentrate	323.0	350.0	8.5
Converter Cu	369.0	370.0	0.3

In the case of antimony ores, silver was separated by extraction; in the case of copper and zinc concentrates, silver was separated by sorption on silica. The sample of converter copper was dissolved in nitric acid and, after addition of EDTA and ammonia, silver was separated on a silica column. In this case, a large amount of EDTA had to be added for complete complexation of copper (copper–ammine complexes are adsorbed on silica).

SUMMARY

Stripping voltammetry at a rotating glassy carbon electrode is proposed for the determination of silver in ores. The ores or concentrates are dissolved in suitable acid mixtures, and silver is separated either by extraction with dithizone in carbon tetrachloride, or by adsorption on silica from ammoniacal buffered solution and subsequent elution with 0.1 *M* nitric acid. The results obtained with stationary and

rotating glassy carbon electrodes are discussed. Stripping voltammetry and fire assay give results in reasonably good agreement.

RÉSUMÉ

Une méthode voltammétrique "strippante" anodique est proposée pour le dosage de l'argent dans les minerais. Les minerais ou les concentrés sont dissous dans un mélange d'acides approprié. L'argent est séparé soit par extraction au moyen de dithizone dans le tétrachlorure de carbone; soit par absorption sur silice et élution par l'acide nitrique 0.1 *M*. Les résultats sont examinés, ils correspondent bien à ceux obtenus avec les méthodes habituelles.

ZUSAMMENFASSUNG

Für die Bestimmung von Silber in Erzen wird inverse Voltammetrie an einer rotierenden Glascarbonelektrode vorgeschlagen. Nach Auflösung der Erze oder Konzentrate in geeigneten Säuregemischen wird das Silber abgetrennt, indem es entweder mit Dithizon in Tetrachlorkohlenstoff extrahiert oder an Kieselsäure aus ammoniakalischer gepufferter Lösung adsorbiert und anschliessend mit 0.1 *M* Salpetersäure eluiert wird. Die bei stationären und rotierenden Glascarbonelektroden erhaltenen Ergebnisse werden diskutiert. Die durch inverse Voltammetrie und durch dokimastische Analyse erhaltenen Ergebnisse stimmen recht gut überein.

REFERENCES

1 H. Monien, H. Specker and K. Zinke, *Z. Anal. Chem.*, 225 (1967) 347.
2 M. Kopanica and F. Vydra, *J. Electroanal. Chem.*, 31 (1971) 175.
3 E. Temmerman and F. Verbeek, *Anal. Chim. Acta*, 58 (1972) 263.
4 F. Vydra, M.Štulíková and P. Peták, *J. Electroanal. Chem.*, 40 (1972) 99.
5 G. H. Morrison and H. Freiser, *Solvent Extraction in Analytical Chemistry*, J. Wiley, New York, 1957.
6 F. Vydra, *Talanta*, 10 (1963) 753.
7 J. Pitra, *Chem.Listy*, 56 (1962) 495.
8 Kh. Z. Brainina, N. F. Zacharchuk, D. P. Synkova and I. G. Judelevich, *J. Electroanal. Chem.*, 35 (1972) 165.

Analytica Chimica Acta, 65 (1973) 177–187

THE ADSORPTION OF CORYPALLINE AND RELATED COMPOUNDS ON A PYROLYTIC GRAPHITE ELECTRODE

ROBERT D. BRAUN and JOHN T. STOCK

Department of Chemistry, University of Connecticut, Storrs, Conn. 06268 (U.S.A.)

(Received 26th October 1972)

The simple isoquinoline alkaloid corypalline (I; 7-hydroxy-6-methoxy-N-methyl-1,2,3,4-tetrahydroisoquinoline) and certain related compounds readily undergo electrolytic oxidative coupling in aqueous[1–4] and in acetonitrile[4–6] solutions, to give dimer-type products such as (II) and (III). If a graphite electrode that has been

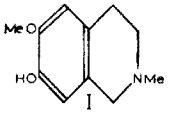

I

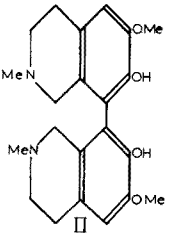

II

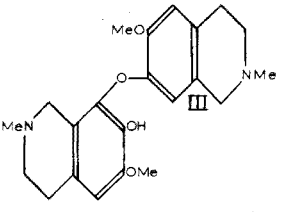

III

dipped into an acetonitrile solution of one of these isoquinoline compounds is rinsed, transferred to acetonitrile containing a suitable supporting electrolyte and anodized, a current that decays with time is obtained. Presumably, this current is caused by the oxidation of isoquinoline compound that has been adsorbed on the surface of the electrode. In fact, Bobbitt *et al.*[5] have postulated that the stereoselective, stereospecific oxidative coupling of 1-methylcorypalline in acetonitrile solution occurs through adsorption of the reacting molecules on the surface of the graphite electrode. The present work is a study of the behavior of corypalline and two of its relatives at a pyrolytic graphite electrode and a semi-quantitative assessment of adsorption effects.

EXPERIMENTAL

Reagents

Corypalline (I), isocorypalline (6-hydroxy-7-methoxy-N-methyl-1,2,3,4-tetrahydroisoquinoline) and 1-methylcorypalline and their dimer-type products were prepared by methods developed by Bobbitt *et al.*[1–5,7,8]. Methylene blue (Allied Chemical and Dye Corp.) was twice recrystallized from acetone. Acetonitrile (Aldrich Chemical Co.) and tetraethylammonium perchlorate (TEAP; Eastman) were used as received.

Equipment

The 6-mm diameter pyrolytic graphite electrodes were prepared as described

by Turner and Elving[9]. When required, the electrodes were resurfaced by careful application of fine-grade sandpaper.

Constant-temperature ($t \pm 0.1°$) runs were made in a water-jacketted cell.

Cyclic voltammograms were recorded by a Beckman Electroscan. A Leeds and Northrup Type E Electrochemograph was used to record slow-scan voltammograms and current–time curves. All potentials are with respect to the saturated calomel electrode.

Beckman models B and DB-GT spectrophotometers, with 1-cm cells, were used to obtain absorption spectra.

RESULTS

Voltammetry

Although the effect can be minimized by continuous electrode activation, certain corypalline-type compounds give distorted and time-dependent current–voltage curves at a rotating platinum electrode[10,11]. Electrode deactivation can be alleviated by working in a TEAP–acetonitrile medium. In fact, high yields of dimer-type products (*e.g.* II) are obtainable by passing a quantity of electricity that corresponds to a one-electron oxidation of the starting material[4].

The fact that the dimers are known to be capable of undergoing further oxidation (*e.g.*, to IV, or to higher polymers) is in line with the cyclic voltammograms in 0.1 *M* TEAP in acetonitrile shown by corypalline, isocorypalline, and 1-methylcorypalline. At a scan rate of 200 mV s^{-1}, all three compounds show an anodic peak A in the region 0.45–0.55 V. A second peak (or incipient peak) B occurs between 1.20 and 1.25 V. There are indications of a third peak, C, at a potential of *ca.* 1.55 V.

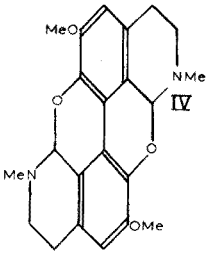

IV

On the reverse scan there is no cathodic current that might be attributed to the reduction of products formed near peak C. However, cathodic wave B and peak or wave A are probably the counterparts of anodic peaks B and A, respectively. Decreasing the scan rate has the general effect of decreasing the difference between the potentials of an anodic peak and its cathodic counterpart. The electrode processes associated with these peaks therefore show significant irreversibility[12]. The reaction mechanisms associated with the various waves are now being studied. However, wave A is almost certainly associated with the reaction $I \rightarrow I^+ + e$.

In the electrolytic preparation of the various dimer-type compounds, the anode potential is kept low[4–6]. The essential *electrode* reaction is that associated with peak A. However, the actual products isolated from the *overall* reaction are also governed by the *chemical* reactions undergone by the radical, *e.g.*, I^+. In TEAP–

acetonitrile, corypalline and 1-methylcorypalline give mainly the type II or carbon–carbon linked dimers at a graphite-felt anode, while the product obtained from isocorypalline is mainly an oxygen-linked dimer[4].

Multi-sweep cyclic voltammetry in the limited range 0–0.6 V and at a freshly resurfaced graphite electrode, of 1 m*M* corypalline in 0.1 *M* TEAP in acetonitrile gave the successive peak A currents 20.2, 19.0, 18.8, 18.7, and 18.6 μA, respectively. The marked difference between the first-scan current and that observed in subsequent scans also occurred when isocorypalline or 1-methylcorypalline replaced corypalline.

The multiple-peak curves given by corypalline and related compounds at the high scan rates normally employed in cyclic voltammetry are not obtained when these compounds are examined by the slow-scan (typically about 5 mV s^{-1}) technique. A single wave that begins at *ca.* +0.2 V is obtained on slowly scanning corypalline in aqueous borax solution[2]. The behavior of corypalline in 0.1 *M* TEAP in acetonitrile is similar, but the wave begins at, or close to, a potential of zero. Under slow-scan conditions, the carbon–carbon coupled compound II gives a wave that covers approximately the same voltage range as the wave given by corypalline itself. No potential could be found at which corypalline, but not compound II, gave an anodic wave. However, the wave given by II is considerably smaller than that given by a similar concentration of corypalline.

Current–time studies

A freshly resurfaced electrode was immersed for a given time in an unstirred saturated solution of corypalline (*ca.* 0.019 *M*) in acetonitrile. After rinsing with 0.1 *M* TEAP in acetonitrile solution, the electrode was transferred to another portion of this solution, a potential of +0.45 V was applied, and the current–time curve was recorded. The circuit was then opened while the recorder chart was rewound to the original "time" zero, and then a second current–time curve was recorded immediately. Similar pairs of runs were made for other immersion times, the electrode being resurfaced before the commencement of each pair of runs. In these experiments, the area between each pair of current–time curves was assumed to measure the oxidation of corypalline adsorbed by the electrode during its immersion in the solution of this compound. Similar runs were made with a saturated solution of isocorypalline (*ca.* 0.036 *M*). These preliminary experiments showed that the apparent adsorption increased rapidly with time for short immersion times, and then increased more slowly for times greater than *ca.* 1 h. However, adsorption was still increasing after immersion times of more than 12 h. In order to examine other factors, an immersion time of 1 h was adopted unless otherwise specified.

A problem encountered early in the current–time measurements was the temporary change in electrode response brought about by the resurfacing operation. This was suspected because of the peculiar results obtained during the repetitive cyclic voltammetry of corypalline solutions. Using a freshly resurfaced electrode, the first anodic voltammetric sweep was stopped at +0.50 V, and a current–time curve was recorded at this potential. The area under this current–time curve was noticeably larger than the corresponding areas obtained from subsequent runs that were made without resurfacing the electrode. The presence of corypalline is not the prime cause of this effect, because TEAP–acetonitrile solution (*i.e.*, the medium

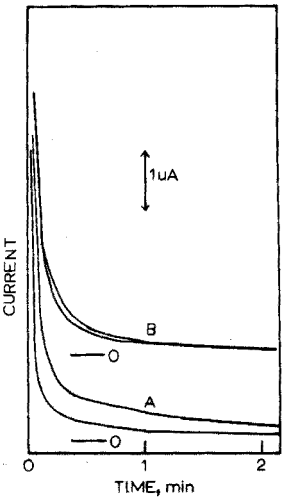

Fig. 1. Current–time curves ($E = +0.45$ V) after soaking electrode for 5 min in acetonitrile. (A) Anodic prepolarization: upper curve, electrode freshly resurfaced; lower curve, electrode not resurfaced. (B) as A, but no prepolarization.

used in most of the present work) or even acetonitrile alone, gave results analogous to those obtained with corypalline solutions. The upper curve of each of the pairs shown in Fig. 1 was obtained by soaking the freshly resurfaced electrode in acetonitrile for 5 min, then transferring the electrode to 0.1 *M* TEAP in acetonitrile and at once recording a current–time curve at a potential of +0.50 V. A repetition of this sequence without resurfacing the electrode gave the lower curve in each of the pairs. During the soaking periods associated with the pair of curves A, the graphite electrode was maintained at +0.05 V with respect to a platinum electrode that was also immersed in the acetonitrile. The actual potential of the graphite electrode fell from *ca.* +0.6 V to *ca.* +0.3 V during the 5-min period. Curves B were obtained when the graphite electrode was soaked on open circuit. It is therefore the act of anodizing that causes the response of the graphite electrode to shift significantly from the response given to it by the act of resurfacing. This is the probable cause of the decrease in peak height observed in multi-sweep voltammetry.

Measurement of the adsorption of corypalline and its relatives on a graphite electrode requires that clean (*i.e.*, resurfaced) graphite be presented to the solution. Although open-circuit conditions can be used during the immersion or soaking period, the measurement of the isoquinoline compound picked up by the electrode requires anodic conditions.

Blank runs in 0.1 *M* TEAP–acetonitrile solution were performed as follows. The freshly resurfaced electrode was placed in a portion of this solution. A potential of +0.45 V was then applied and the current–time curve was recorded. After re-opening the circuit for a period sufficient for the rewinding of the recorder chart, the recording was repeated. This allowed the area between the two curves to be calculated. Ten pairs of runs, carried out with each of four electrodes gave the mean "medium effects" and standard deviations: electrode (1) 18.0 ± 3.8; (2) 13.7 ± 2.5; (3) 11.8 ± 2.7; (4) 16.5 ± 3.3 μC, respectively.

The current–time curves for the actual adsorption measurements were obtained in a similar manner. However, the freshly resurfaced electrode was placed in the adsorbate solution and allowed to equilibrate for 1 h. The electrode was then rinsed with a jet of 0.1 *M* TEAP in acetonitrile, briefly immersed in another portion of this solution, rinsed again, and then at once transferred to the electrolysis cell, which contained 50 ml of 0.1 *M* TEAP in acetonitrile. The two current–time curves were then recorded in succession as described. A typical pair of curves is shown in Fig. 2.

Figure 3 shows the effect of concentration upon the apparent adsorption of the various isoquinoline compounds. The center of each circle is placed at the mean of three determinations in each case. Where larger than represented by the diameter of the circle, the standard deviation is indicated by the length of the vertical line. Table I lists similar data for methylene blue, obtained in the same general manner as those for the isoquinoline compounds. However, the measurements were made by recording reduction current–time curves at a potential of −0.50 V.

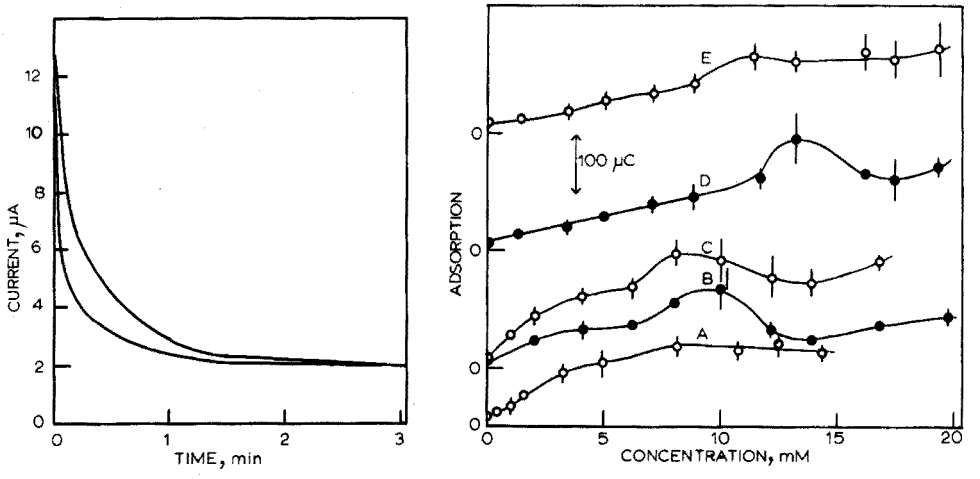

Fig. 2. Pair of current–time curves obtained after soaking electrode in 1 m*M* corypalline solution for 1 h.

Fig. 3. Effect of concentration on apparent adsorption. Temperature, 23.0°–26.4°. (A) Corypalline, electrode 2; (B) isocorypalline, electrode 3; (C) isocorypalline, electrode 2; (D) 1-methylcorypalline, electrode 3; (E) 1-methylcorypalline, electrode 4.

The effect of temperature on the apparent adsorption at constant initial concentration is shown in Fig. 4. During the observations on isocorypalline, which were made in order of increasing temperature (curve B), a crack was found in the mounting of the electrode after a very high current had been observed at 60°. The electrode was remounted, then the observations were repeated in order of decreasing temperature (curve C).

Absorption spectra of methylene blue

The adsorption of methylene blue on graphite and other solids, and, consequently, the properties of this dyestuff in solution, have been extensively studied. Unless the concentration is very low, the predominant form of methylene blue in

TABLE I

ADSORPTION OF METHYLENE BLUE ON FOUR DIFFERENT GRAPHITE ELECTRODES

Concentration $\cdot 10^4$ *M*	*Adsorption* (μC)[a]			
	1[b]	*2*	*3*	*4*
0[c]	116±32	134±20	137±33	144±24
0.05	60±12	89±6	81±1	86±11
0.10	70±12	78±3	62±4	76±8
0.28	100±10	119±15	105±12	101±15
0.38	110±8	105±3	136±11	142±11
0.59	132±2	158±11	138±29	140±19
0.69	129±10	162±6	168±6	167±10
0.84	649±55	538±123	544±76	552±57
0.94	779±113	652±141	589±112	444±59
1.06	525±94	529±54	586±122	523±99
9.75	296±91	463±138	349±94	308±94
31.3	258±38	230±8	275±46	316±47
53.6	353±56	370±73	395±26	357±67
92.3	360±91	357±101	298±45	289±54
111	321±30	319±53	325±27	288±21
158	312±53	357±38	294±30	297±30
193	374±28	371±62	411±51	381±34

[a] Means of 3 runs and standard deviations. Temperature, 23.0°–26.2°.
[b] This electrode was used in preliminary investigations of the isoquinoline compounds, but not in the subsequent runs with these compounds.
[c] Means of 10 runs and standard deviations.

aqueous solution is a dimeric aggregate[13–16]. There is evidence for trimer formation when the concentration is at least 0.06 *M*[17]. Aqueous solutions of methylene blue show two spectral maxima in the visible region. The monomeric form absorbs light at 655–665 nm, while the dimeric form absorbs at 590–605 nm[13,14,16,18].

Curve A of Fig. 5 shows the absorption spectrum of 10^{-5} *M* methylene blue in acetonitrile. The two maxima, at 595 nm and 645 nm respectively, are at positions close to those observed in aqueous solutions. It is therefore reasonable to assume that these maxima indicate the presence of both monomeric and dimeric methylene blue in the acetonitrile solution. The single peak of curve B, obtained at a higher concentration of methylene blue in acetonitrile, occurs at *ca.* 616 nm, and is presumably caused by the overlapping of the peaks that are separately visible at lower concentrations. Estimated monomer:dimer peak-height ratios are 1.98:1.00 at a concentration of 10^{-5} *M*, and 1.04:1.00 when the concentration is 10^{-4} *M*.

DISCUSSION

Giles *et al.*[19] have presented a compact classification of the general shapes that adsorption isotherms may take. Isotherms that exhibit maxima appear to be given only by solutes that undergo pronounced association in solution[15]. Giles *et al.*[15] found that the isotherm for graphite powder–aqueous methylene blue shows a

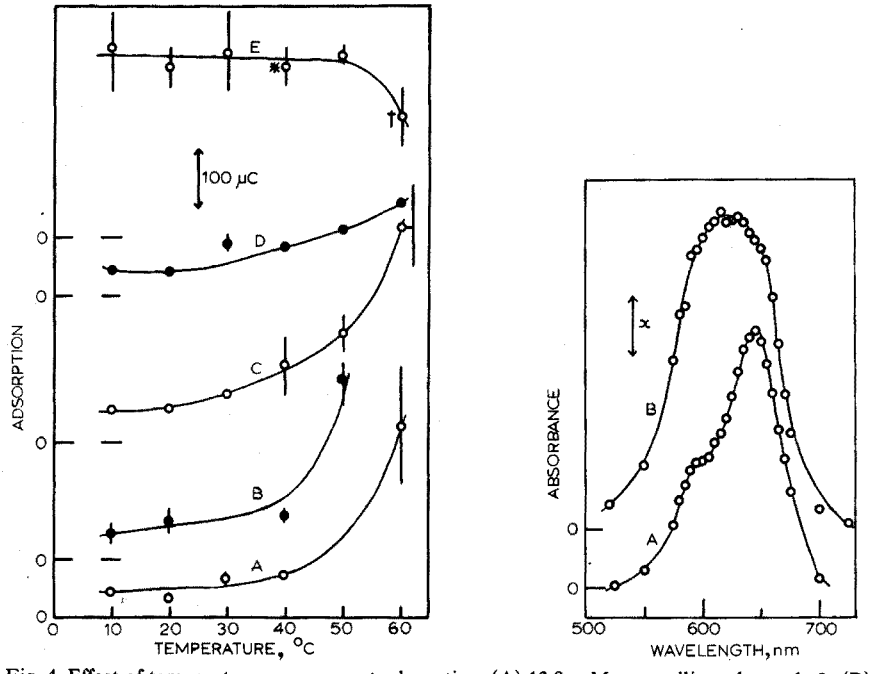

Fig. 4. Effect of temperature on apparent adsorption. (A) 13.9 m*M* corypalline, electrode 3; (B) 14.0 m*M* isocorypalline, electrode 2; (C) as B, but electrode remounted; (D) 14.0 m*M* 1-methylcorypalline, electrode 4; (E) 5.44 m*M* methylene blue, electrode 4; (*) 5 runs; (†) 4 runs.

Fig. 5. Absorption spectra of methylene blue in acetonitrile. (A) $1.07 \cdot 10^{-5}$ *M*, $x = 0.1$; (B) $1.07 \cdot 10^{-4}$ *M*, $x = 0.4$.

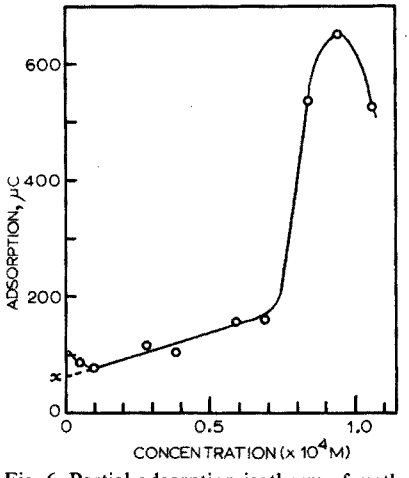

Fig. 6. Partial adsorption isotherm of methylene blue on electrode 2.

pronounced maximum at a concentration of *ca.* 0.1 m*M*. The results in Table I and in Fig. 6 demonstrate that the isotherm for pyrolytic graphite–methylene blue in acetonitrile also exhibits a maximum in the same concentration region.

Except at high dilution, methylene blue is adsorbed from aqueous solution in its dimeric form, *i.e.*, as two layers[15,20]. Adsorption occurs with the rings of the dye molecule flat on the surface of the graphite adsorbant, occupying an area, A_m, which is best equated to the area of the smallest enclosing rectangle[15,16,20].

An inspection of models indicates that although the molecules of the three isoquinoline compounds and of methylene blue have similar widths and similar depths, the length of the methylene blue molecule is greater by a factor of *ca.* 1.2. The approximate dimensions of the methylene blue molecule[21] are $16 \times 8 \times 4$ Å^3. If A_c is the area occupied by one molecule of corypalline or of its relatives, the ratio A_m/A_c will depend on the orientation of corypalline on the graphite surface. Obviously, the approximate values of this ratio will be 1.2, 2.4, or 4.0, corresponding to an orientation that is flat-on, edge-on, or end-on respectively.

The value of this ratio can also be calculated from the relationship $A_m/A_c = 4Q_c/Q_m$, where Q_c and Q_m are the adsorptions, expressed in μC, of isoquinoline compound and of methylene blue, respectively, at the peaks of their adsorption isotherms. Q_c and Q_m are, of course, measured at the same electrode. The factor of four arises from the assumed two-layer adsorption of methylene blue from acetonitrile solution and from the non-identical electron transfers involved in the measurements of Q_c and Q_m. Methylene blue undergoes a two-electron reduction[22], while the principal source of current in the case of corypalline is a one-electron oxidation.

In order to evaluate Q_c and Q_m, corrections must be applied to the apparent peak adsorption values. A correction for the "medium effect" must first be considered. The average correction for all runs made on the isoquinoline compounds is *ca.* 14 μC. This is less than one standard deviation of the average of the peak heights for those compounds (Fig. 3). The corresponding correction for the runs on methylene blue is less straightforward. Here the "medium effect" is not only large, but appears to pass through a minimum in the presence of traces of methylene blue. This phenomenon occurred in all runs with all four electrodes. The correction for methylene blue that is given in Table II was obtained as follows. The initial portion of each methylene blue isotherm was plotted, as shown by the example in Fig. 6. Intercept x, which was used as correction, was then obtained by linear extrapolation of the portion of the isotherm that lies in the concentration range $0.1 \cdot 10^{-4}$ to $0.6 \cdot 10^{-4}$ M.

TABLE II

CALCULATION OF A_M/A_C FROM PEAK ADSORPTION VALUES

Compound	*Electrode*	*Peak adsorption (μC)*						$A_M/A_C = 4Q_C/Q_M$
		Isoquinoline cpd.			*Methylene blue*			
		Obsd.	*Corr.*[a]	Q_C	*Obsd.*	*Corr.*	Q_M	
Corypalline	2	139	21	118	652	62	590	0.80
Isocorypalline	2	195	16	179	652	62	590	1.21
Isocorypalline	3	133	16	117	589	62	527	0.89
1-Me-corypalline	3	190	13	177	589	62	527	1.34
1-Me-corypalline	4	133	13[b]	120	552	69	483	1.00

[a] Correction obtained as discussed in text.

[b] Not measured. The value obtained with electrode 3 was used.

At a fixed potential of +0.45 V, the one-electron oxidation current of corypalline will be augmented by the further oxidation of any of the product, the carbon–carbon coupled compound II, that remains absorbed on the electrode. To assess the maximum augmentation likely to be encountered, adsorption measurements of a 1.05 m*M* (nearly saturated) solution of compound II were made in the same manner as used for corypalline and the related compounds. The mean value found was 21.3 ± 6.5 μC. Deduction of the sum of this value and of the blank value, 13.7 ± 2.5 μC, from the observed adsorption peak value, 139 μC, of corypalline at electrode 2, gives a Q_c value of 104 μC. At the same electrode, the corrected Q_m value is 590 μC. The ratio $A_m/A_c = 4Q_c/Q_m$ is thus 0.71. Similar measurements were made at electrodes 2 and 3 with solutions of the oxygen-linked dimer of isocorypalline and of the carbon-linked dimer of 1-methylcorypalline. The results are summarized in Table II.

Two alternative but extreme methods of utilizing the apparent peak adsorption values of methylene blue should be considered. One is to deduct the *entire* "medium effect", or blank, while the other is to ignore the "medium effect" completely. The average value of A_m/A_c then becomes 1.21 or 0.94, respectively, instead of 1.05, which applies to the results given in Table II. All three averages are much closer to the value of 1.2, proposed for flat-on orientation of the adsorbed isoquinoline compound, than to the values proposed for edge-on or end-on adsorption.

Although there is no obvious evidence that corypalline or its relatives are adsorbed in the two-layer mode adopted by methylene blue, this possibility should be considered. The ratio A_m/A_c should then be equal to *twice* Q_c/Q_m, *i.e.*, to *ca.* 0.5. This does not check with any of the values proposed for the various orientations that the adsorbed isoquinoline molecule might assume.

Adsorption from solution is usually exothermic, so that adsorption normally increases as the temperature is lowered. In the temperature range 10–40°, the adsorption of methylene blue thus follows the general rule, although the temperature coefficient is small. The marked decrease in adsorption when the temperature is raised to 50° is opposite to the behavior exhibited by all three isoquinoline compounds (Fig. 4). Increased adsorption of these compounds at high temperatures could result from additional exposure of graphite by solvent attack on the mounting cement. However, the positive temperature coefficient appears to be real, because it was not eliminated by remounting the electrode and repeating the runs in order of decreasing temperatures (Fig. 4, curve C). Rise in adsorption with temperature has been observed with certain dyes that are aggregated in solution. The explanation given is that the solute is partially dissociated on adsorption[23]. If this explanation also holds for the behavior of corypalline and its relatives, then the likelihood of their adsorption in a dimeric form would seem to be small.

This work was carried out with the partial support of the National Science Foundation (Grant GP-30574X). We thank Professor J. M. Bobbitt for supplies of the isoquinoline compounds, and for many helpful discussions.

SUMMARY

Anodic current–time curves have been used to study the adsorption, from TEAP–acetonitrile solution, of corypalline (7-hydroxy-6-methoxy-N-methyl-1,2,3,4-

tetrahydroisoquinoline), isocorypalline (6-hydroxy-7-methoxy-N-methyl-1,2,3,4-tetrahydroisoquinoline), and 1-methyl-corypalline. A comparison with analogous cathodic current–time curves obtained with methylene blue leads to the conclusion that, on a pyrolytic graphite electrode, these isoquinoline compounds are adsorbed in a "flat-on" configuration. This conclusion is in harmony with the postulation that the known steroselective, stereospecific oxidative coupling of 1-methylcorypalline occurs through the adsorption of the reacting molecules on the electrode surface.

RÉSUMÉ

Une étude est effectuée à l'aide des courbes courant anodique–temps pour déterminer l'adsorption de corypalline, et de composés dérivés, sur une électrode de graphite pyrolytique. Une comparaison est faite avec des courbes analogues, courant cathodique–temps, obtenues avec le bleu de méthylène. On arrive à la conclusion que la réaction stéréosélective et stéréospécifique d'oxydation de la méthyl-1-corypalline se produit par adsorption des molécules réagissantes sur la surface de l'électrode.

ZUSAMMENFASSUNG

Anodische Strom–Zeit-Kurven wurden aufgenommen zur Untersuchung der Adsorption von Corypallin (7-Hydroxy-6-methoxy-N-methyl-1,2,3,4-tetrahydroisochinolin), Isocorypallin (6-Hydroxy-7-methoxy-N-methyl-1,2,3,4-tetrahydroisochinolin) und 1-Methyl-corypallin aus TEAP-Acetonitril-Lösung. Ein Vergleich mit analogen kathodischen Strom–Zeit-Kurven, die mit Methylenblau erhalten werden, führt zu dem Schluss, dass an einer pyrolytischen Graphitelektrode diese Isochinolinverbindungen in einer "flat-on"-Konfiguration adsorbiert werden. Dies stimmt mit der Annahme überein, dass die bekannte stereoselektive, stereospezifische oxydative Kopplung von 1-Methyl-corypallin bei der Adsorption der reagierenden Moleküle an der Elektrodenoberfäche auftritt.

REFERENCES

1 J. M. Bobbitt, J. T. Stock, A. Marchand and K. H. Weisgraber, *Chem. Ind. (London)*, (1966) 2127.
2 G. F. Kirkbright, J. T. Stock, R. D. Pugliese and J. M. Bobbitt, *J. Electrochem. Soc.*, 116 (1969) 219.
3 J. M. Bobbitt, K. H. Weisgraber, A. S. Steinfeld and S. G. Weiss, *J. Org. Chem.*, 35 (1970) 2884.
4 J. M. Bobbitt, H. Yagi, S. Shibuya and J. T. Stock, *J. Org. Chem.*, 36 (1971) 3006.
5 J. M. Bobbitt, I. Noguchi, H. Yagi and K. H. Weisgraber, *J. Amer. Chem. Soc.*, 93 (1971) 3551.
6 J. M. Bobbitt and R. C. Hallcher, *Chem. Commun.*, (1971) 543.
7 J. M. Bobbitt, J. M. Kiely, K. L. Khanna and R. Ebermann, *J. Org. Chem.*, 30 (1965) 2247.
8 J. M. Bobbitt, D. N. Roy, A. Marchand and C. W. Allen, *J. Org. Chem.*, 32 (1967) 2225.
9 W. R. Turner and P. J. Elving, *Anal. Chem.*, 37 (1965) 207.
10 J. T. Stock, *Microchem. J.*, 15 (1970) 564.
11 J. T. Stock, *Anal. Chem.*, 43 (1971) 289.
12 R. N. Adams, *Electrochemistry at Solid Electrodes*, Dekker, New York, 1969, p. 148.
13 E. Rabinowitch and L. F. Epstein, *J. Amer. Chem. Soc.*, 63 (1941) 69.
14 P. Mukherjee and A. K. Ghosh, *J. Phys. Chem.*, 67 (1963) 193.
15 C. H. Giles, L. A. Easton, R. B. McKay, C. C. Patel, N. B. Shah and D. Smith, *Trans. Faraday Soc.*, 62 (1966) 1963.

16 A. L. Thakkar, W. L. Wilham and G. Zagrafi, *J. Pharm. Sci.*, 59 (1970) 1466.
17 E. Braswell, *J. Phys. Chem.*, 72 (1968) 2477.
18 M. J. Blandamer, J. A. Brivati, M. F. Fox, M. C. R. Symons and G. S. P. Verma, *Trans. Faraday Soc.*, 63 (1967) 1850.
19 C. H. Giles, T. H. McEwan, S. N. Nakhwa and D. Smith, *J. Chem. Soc.*, (1960) 3973.
20 C. H. Giles, *J. Amer. Chem. Soc.*, 9 (1969) 759.
21 J. W. Galbraith, C. H. Giles, A. G. Halliday, A. S. A. Hassan, D. C. McAllister, N. Macaulay and N. W. MacMillan, *J. Appl. Chem.*, 8 (1958) 416.
22 R. H. Wapshall and I. Shain, *Anal. Chem.*, 39 (1967) 1527.
23 C. H. Giles, J. J. Greczek and S. N. Nakhwa, *J. Chem. Soc.*, (1961) 93.

Analytica Chimica Acta, 65 (1973) 189–197

AN AMMONIUM ION-SPECIFIC ELECTRODE

JOSEPH G. MONTALVO, JR

Department of Analytical Chemistry, Gulf South Research Institute, 5010 Leroy Johnson Drive, P.O. Box 26500, New Orleans, La. 70186 (U.S.A.)

(Received 17th November 1972)

Electrode sensors have been developed which are capable of determination of the enzyme urease[1,2] and its substrate urea[3,4]. The urease enzyme sensor was made by coupling the substrate urea to the active surface of a cationic electrode responsive to ammonium ion, a product of the urea–urease reaction. The electrode was covered with a layer of cellophane which trapped a thin layer of urea solution between the glass sensing bulb and the membrane. When the electrode was dipped into a solution containing urease, the urea which diffused out of the cellophane membrane reacted with urease (which cannot diffuse through the membrane) to produce ammonium ion at the membrane surface. The buildup of an ammonium ion activity gradient caused diffusion of the ion back to the electrode, where it was sensed. The urea sensor was made by immobilizing the enzyme urease over a glass cationic electrode. When this electrode was dipped into a solution containing urea, the urea diffused into the immobilized urease layer and reacted with the enzyme to produce ammonium ion, which was detected by the cationic electrode.

Application of the above principles of operation to detect enzymes and substrates in body fluids via the production of ammonium ion have been hampered by the lack of selectivity of the available cationic (monovalent) glass electrodes for ammonium ion in the presence of sodium and potassium.

Work has been directed in these laboratories to develop a specific ammonium ion electrode which can operate at or near physiological pH values. The basic principle has been to attempt to increase the selectivity of the available cationic glass electrodes for ammonium ion by coupling the glass electrode to an appropriate thin polymer membrane. Various membrane-wrapped cationic electrode systems which utilize ionic (ion-exchange) and non-ionic (gas-permeable) membranes, are being investigated.

In the present paper, the complete lack of response of a gas-permeable membrane cationic electrode to potassium and sodium ion (at representative clinical levels) and the response to ammonium ion are illustrated by noting the response when the electrode is dipped into various solutions.

EXPERIMENTAL

Reagents

All chemicals were of reagent grade unless stated otherwise. All solutions were prepared in 0.5 *M* TRIS buffer. Only the chloride salts of ammonium, sodium and

potassium were employed. Type IV urease (Sigma Chemical Co., 3.53 units mg^{-1}) was used. One unit will produce 1 mg of ammonia nitrogen from urea in 5 min at pH 7.0 and 30°.

Instrumentation and electrodes

A Corning research pH meter was used to measure the potential. The hydrophobic ammonia-permeable membrane placed over the glass cationic electrode dictated the position of the reference electrode with respect to the ammonia-permeable membrane, otherwise the observed potential could be due in part to an electric potential across the ammonia-permeable membrane. This unwanted potential was excluded from the observed potential by placing the reference electrode (a glass pH electrode) via a small plastic tubing containing electrolyte, between the glass surface of the electrode and the ammonia-permeable membrane. The internal reference electrode was connected to the reference electrode terminal and the membrane-wrapped cationic electrode connected to the indicating electrode terminal on the pH meter. The Beckman 39137 monovalent-cationic electrode was used. The pH meter was operated in the mV mode. The recorder terminals of the pH meter were connected to a Sargent mV recorder. The sensitivity of the recorder was adjusted so that 1 mm = 1 mV.

Preparation of thin ammonia-permeable membranes

Thin ammonia-permeable membranes of silicone–polycarbonate (Type XD-7 powder, G. E. Company), collodion (23% solution, Curtin Chemical Co.), and 40% leucine–60% methionine were prepared. A carbon dioxide silastic membrane (Instrumentation Lab, Inc.) was also used.

The silicone–polycarbonate powder (1.5 g) was dissolved in 25 ml of cyclohexanone and cast over water as follows. A large oblong pyrex dish was filled with water. The surface of the water was wiped clean by pulling a sheet of tissue paper slowly across the entire length of the pyrex dish. Another sheet of tissue paper was placed over the water leaving about $\frac{1}{2}$ in space between the tissue paper and a narrow side of the dish. A little of the polymer solution was poured over this space. The tissue paper was pulled slowly over the surface of the water. The polymer solution spread and formed a very thin film.

Thin collodion membranes were cast over glass plates. Glass plates were cleaned with chromic acid before casting. A single layer of masking tape (100 μm thick) was laid on opposite sides of the glass plate. A little of the 23% collodion solution was poured on the plate, and then spread evenly over the plate with a flat edge of glass pulled over the masking tape. The resultant thin film was allowed to dry for 4 min at room temperature, chilled in ice-cold water for 14 min, removed from the glass plate and blotted dry with tissue paper. The film was examined under a low-power lens for holes, soaked for 2 h in cold distilled water, and then soaked for 2 h in ice-cold buffer.

Thin 40% leucine–60% methionine membranes were prepared and donated by Dr. E. Klein and Mr. J. Smith of GSRI.

Membrane thickness was measured by the interference fringes technique.

Procedures

The ammonium ion-specific electrode was prepared as follows. The Beckman

cationic electrode was mounted upside down. Two "O" rings were placed over the stem of the electrode: the first, 2 in below the active surface of the electrode, and the other 0.5 in below the active surface of the electrode. Two microplastic tubings (i.d. 0.034 in, o.d. 0.050 in) were positioned under the "O" rings and on opposite sides of the glass bulb. The tubings extended 1 mm over the glass sensing bulb. The tubing tips were held in place tightly against the bottom of the glass bulb with cotton string. Masking tape was wrapped around the stem of the electrode to prevent movement of the tubings under the "O" rings. A 2×2 in piece of 10-μm cellophane was covered with a piece of 150-μm nylon netting of the same size. The coverings were placed over the electrode (with the nylon as the outer covering) and held in place over the glass bulb with another "O" ring positioned just below the active surface of the glass bulb. The electrode was carefully inspected with a low-power lens to insure that the tips of both micro tubings were still protruding 1 mm over the glass bulb, which is enough to insure that both cellophane and nylon netting cover the tips of the tubings.

Excess of membrane and netting material were cut flush with the "O" ring; coverings were sealed to the glass electrode with RTV-11 sealant (General Electric Company).

The Beckman electrode, complete with coverings as described above, was dipped under the silicone–polycarbonate film (which was cast on water) and raised from the water. The silicone–polycarbonate film was held in place over the nylon netting by virtue of its ability to cling to the netting.

The electrodes wrapped with collodion and leucine–methionine were prepared as described above, except that the collodion film was placed between the cellophane and nylon netting layers. The electrode wrapped with carbon dioxide silastic membrane was prepared in a similar fashion, except that the silastic membrane was used in place of the nylon netting.

Variation of the spacers (coverings) between the glass sensing bulb and the ammonia-permeable membrane resulted in a range of distances (13–160 μm) between the glass and ammonia-permeable membrane. The coverings under this membrane served not only as spacers, but also as a reservoir for internal filling solution. The spacers allowed the gas-permeable membrane to be tightly wrapped over the electrode while preventing complete extrusion of the internal filling solution. The volume of the internal solution was about 25 μl when the spacer thickness was 160 μm.

The ammonium ion-specific electrode, complete with membrane coverings and buffer-electrolyte inlet and outlet tubings, was then ready to be connected to the reference electrode and potentiometer.

The exposed tip of one of the tubings was connected to a 2-ml syringe mounted against the cationic electrode. The exposed tip of the other tubing was connected to an inlet tube of a roller pump (Holter Company). The syringe, filled with buffer-electrolyte, provided electrical contact with the reference electrode; the roller pump applied gentle suction to the membrane trap over the electrode, which forced the buffer in the trap over the electrode and removed air bubbles. The buffer-electrolyte pumped out of the electrode system was discarded.

TRIS buffer (1 ml of 0.5 *M*) was placed in the syringe. The reference electrode (a standard pH sensing glass electrode) was placed in the syringe. The roller pump was turned on, the pumping rate adjusted to 10 μl min^{-1}, and pumping continued

TABLE I

EFFECT OF VARIATION OF AMMONIA-PERMEABLE MEMBRANE

Membrane	*Membrane thickness (μm)*	*Buffer-electrolyte trap, thickness (μm)*	*Temp. (°)*	*Buffer pH*	*Test sample*	*Observations*	
						Time for steady-state potential (min)	*Time of observation[a] (min)*
50% Silicone–50% polycarbonate copolymer	11	160	25	9.0	0.01 *M* NH_4Cl	12	—
					0.01 *M* KCl	—	12
	2.4	160	25	9.0	0.01 *M* KCl	—	25
	~1	160	37	8.5	0.001 *M* NH_4Cl	15	—
			22	8.5	0.001 *M* NH_4Cl	19	—
					0.001 *M* KCl	—	15
	~1	160	37	8.0	0.001 *M* NH_4Cl	18.5	—
				8.0	0.001 *M* NH_4Cl	21	—
CO_2 silastic	65	13	25	9.0	0.01 *M* NH_4Cl	—	20
40% Leucine–60% methionine	0.8	75	25	9.0	0.0833 *M* KCl	—	17
					0.0833 *M* NH_4Cl	Response still increasing after 11 min	
Collodion	~8	150	25	7.3	0.07 *M* KCl	—	19
					0.1 *M* NaCl	—	19
					0.0833 *M* urea	—	19
					25 mg urease	—	19
					0.0833 *M* urea plus 25 mg urease	19	
					0.001 *M* NH_4Cl	19	

[a] The time given here is the duration of time in which no potential response was observed for the added cation.

until the space between the Beckman cationic electrode and membrane trap had been completely flushed with the buffer. This procedure was done with the electrode suspended upright in the air and not in water so that any leaks could be quickly detected. The ammonium ion-specific electrode was then dipped in the test solution and the roller pump turned off.

All measurements were carried out in a thermostated cell at 22–37°. The Teflon bar stirring the 50 ml of test solution, buffered with 0.5 *M* TRIS (pH 7.3–9.0) was tuned to an appropriate speed such that only a small vortex was observed in the test solution. Unless otherwise stated, the pH of the sample (test) solution was exactly the same as the pH of the buffer-electrolyte trap between the glass electrode and gas-permeable membrane.

After the buffer potential had been recorded for a few minutes, the test cation (NH_4^+, Na^+, or K^+) was added to the test solution with a Hamilton microsyringe from 0.5 *M* stock solutions. The potential *vs.* time curve was recorded for periods up to 25 min. The electrode was then placed in an automatic electrode washer (miniature pipet washer) and the potential was monitored until a low level of ion concentration was obtained in the membrane trap over the electrode. The membrane trap could also be flushed out after a run by turning on the roller pump for a few minutes at 10 μl min^{-1}.

The electrical resistance of the electrode system was quite high and noise spikes were occasionally observed. However, with due care the system was entirely functional.

RESULTS AND CONCLUSIONS

Equal pH values of test solution and buffer-electrolyte trap

Table I summarizes the experimental results obtained with various ammonia-permeable membranes, at different temperatures, and at different pH values; all the data shown in Table I were obtained with the pH of the test solution equal to the pH of the buffer-electrolyte trap over the glass surface of the cationic electrode. The rate of response of the indicating electrode depended on the temperature and pH of the test solution and on the ammonia permeability of the membrane, which was impermeable to sodium and potassium ions.

The variation of the steady-state response to ammonium ion *vs.* the pH and temperature of the test solution indicates a mechanism in which the dissolved ammonia in the test solution and not the ammonium ion permeates the polymeric membrane. Figure 1 shows an illustration of the chemistry involved in this electrode. The driving force for ammonia transport through the gas-permeable membrane is the partial pressure of the ammonia, P_{NH_3}, which is proportional to the aqueous ammonia concentration:

$$P_{NH_3} = K[NH_3]_{aqueous}$$

where K = Henry's law constant. As the temperature is increased, the partial pressure of the dissolved ammonia also increases. When the ammonium ion-specific electrode is place in a test solution containing ammonium ion, there is an equlibrium between the ammonia and ammonium ion depending on the pH of the solution. The partial pressure of the ammonia in the test solution results in the gas dissolving

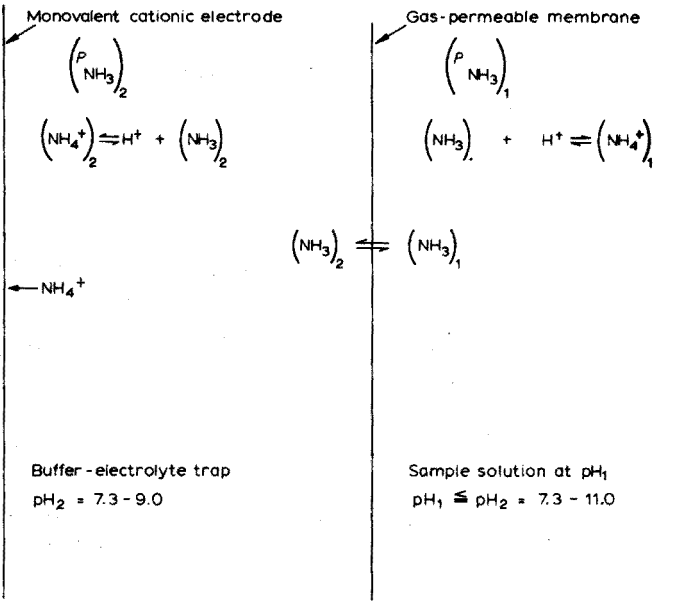

Fig. 1. Chemistry of ammonium ion-specific electrode.

in the membrane on the test solution side, diffusing through the membrane under the influence of the pressure difference, then coming out of the membrane on the low-pressure side (the buffer-electrolyte trap over the glass electrode). The diffusion of ammonia across the membrane continues until, at equilibrium:

$$(P_{NH_3})_2 = (P_{NH_3})_1$$

The ammonia in the buffer-electrolyte trap is also in equilibrium with the monovalent cationic species:

$$NH_3 + H^+ \rightleftharpoons NH_4^+$$

The relative amount of ammonia and ammonium ion is determined by the solution pH. The ammonium ion diffuses to the surface of the cationic electrode where it is sensed.

The ammonia gas transport mechanism was observed with the collodion, leucine–methionine, and silicone–polycarbonate membranes.

The lack of response of this electrode to sodium and potassium ions is due to the fact that the characteristics of the gas-transport membranes studied do not allow the transport of these ions across the membrane. The permeability of a gas-transport membrane to a particular gas depends on the solubility multiplied by the rate of diffusion. The solubility of sodium and potassium in the membranes studied is very, very low; therefore, no transport of these ions can occur.

Most of the investigations were performed with the silicone–polycarbonate membrane. Figure 2 shows the response times for ammonium ion with the silicone–polycarbonate membrane over the gas-sensing tip of the electrode. A steady-state response to ammonium ion was obtained at pH 8.5 in 18.0 min and at pH 8.0 in

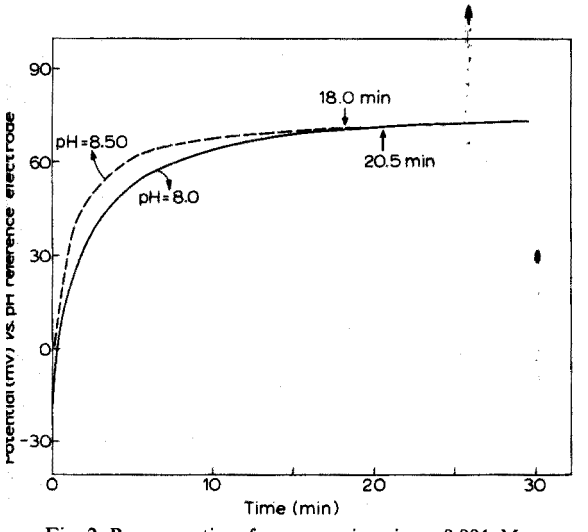

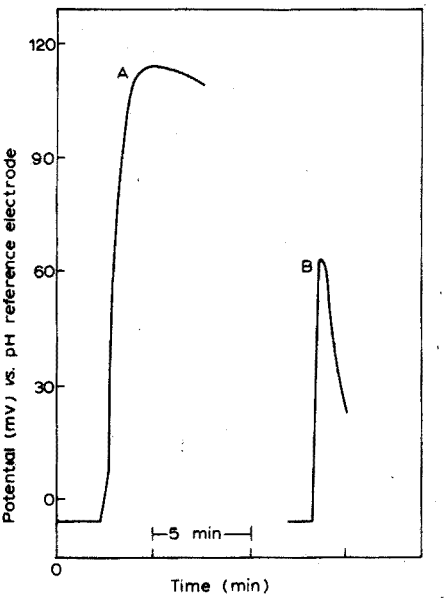

Fig. 2. Response time for ammonium ions. 0.001 *M* ammonium chloride at 37°. $E_{\frac{1}{2}}$ = 0.6 min at pH 8.5, and 1.2 min at pH 8.0.

Fig. 3. Ammonium ion response curves concurrent with pH stripping of ammonia from test solution at pH 11.0 and 25°. (A) Electrode suspended in air above test solution; (B) electrode dipped in test solution.

20.5 min (at 37°) for 0.001 *M* ammonium chloride. At these mildly basic conditions the fraction of the total ammonium ion concentration added to the solution which exists as ammonia is 5.3% at pH 8.0 and 15.2% at pH 8.5. At pH 7.5. and 7.0 the percent ammonia would be 1.75% and 0.56%, respectively (calculated from the appropriate equilibrium constant). In the response studies with the silicone–polycarbonate membrane over the Beckman cationic electrode, the same steady-state potential response was obtained for a given ammonium ion concentration with and without the silicone–polycarbonate membrane over the electrode. From this data, the linear range of the ammonium ion-specific electrode to ammonium ion was essentially the same as for the uncoated cationic electrode. The linear range was from about $5.5 \cdot 10^{-4}$ to 0.1 *M* NH_4^+.

The response of the electrode to the urea–urease reaction (Table I) is noteworthy. The electrode did not respond to either 0.07 *M* KCl, 0.1 *M* NaCl, 0.0833 *M* urea, or 25 mg of urease in 19 min. However, a steady-state ammonium ion response was obtained with added 0.0833 *M* urea and 25 mg of urease in 19 min. Clearly, coupling a cationic glass electrode with a hydrophobic ammonia gas-permeable membrane resulted in an electrode specific for ammonium ion in the presence of sodium and potassium. However, the equilibrium response time is still far from ideal. No attempt was made in this study to optimize the equilibrium response times; the study was concerned solely with experimental verification of the applicability of the gas-transport mechanism at or near physiological pH values where the ratio of NH_3 to NH_4^+ ion concentration is about 0.01.

To optimize the equilibrium response times to ammonium ion at physiological pH values, it is necessary to: (*a*) reduce the thickness of the buffer-electrolyte membrane trap over the glass electrode, and (*b*) to optimize the gas permeability of the ammonia membrane by varying its composition and thickness. These experiments are presently under way.

More rapid potentiometric determination of ammonium ion in the presence of sodium and potassium ion with the present ammonium ion-specific electrode is possible by initial rate measurements. In fact, ammonium ion can be determined in less than 1 min at pH 8.0, and in 1 min at pH 7.5 by computing the initial rate of change in the potential, which is proportional to the ammonium ion concentration. Note that the values for the half-response potential in Fig. 2 are 0.6 min at pH 8.5, and 1.2 min at pH 8.0.

pH of test solution less than pH of buffer-electrolyte trap

In the work described above, the pH of the buffer-electrolyte trap over the electrode was identical to that of the test solution. Because the gas-transport membrane permits only ammonia and not ammonium ion to diffuse across the membrane, the electrode can be made much more sensitive to ammonium ion than could be detected by the Beckman electrode alone. A theoretical study predicted that this could be done simply by changing the pH in the test solution, pH_1, so that

$$pH_1 < pH_2$$

where pH_2 is the pH of the buffer-electrolyte trap. At equilibrium (and $pH_1 < pH_2$) the activities of ammonia on both sides of the ammonia-permeable membrane would be equal, but the activity of ammonium ion would be less in the test solution than in the buffer trap over the electrode. The net result is a preconcentration of ammonium ion over the electrode surface, which should continue until the buffer capacity in the buffer-electrolyte trap is overcome. Figure 3 shows experimental verification of this theory. Ammonia solution was added to distilled water until the pH was 11.0. Curve A was obtained with the ammonium ion-specific electrode suspended in air over the stirred solution. Curve B was obtained with the same solution except that the electrode was dipped into the solution. In both cases there was a rapid rise of the potential as the ammonium concentration built up in the buffer electrolyte trap; eventually the buffer capacity of the solution in the membrane trap was overcome as the ammonia continued to diffuse into the trap and the potential peaked and became more negative.

Research was supported by National Institutes of Health research grants No. S01-FR-05672 and No. GM-17929-01, and -02.

SUMMARY

An ammonium ion-specific electrode was prepared by coupling a hydrophobic ammonia-permeable membrane to a Beckman monovalent cation electrode. At physiological pH values the ratio of ammonia to ammonium ion is only 0.01, yet the gas-transport mechanism is still operable; an electrode designed on this principle was able to detect ammonium ion produced via the urea–urease reaction.

The electrode can be operated in an air stream or in an aqueous medium. The electrode can also be used in an ultra-sensitive mode by pH stripping of ammonia from the test solution.

RÉSUMÉ

Une électrode ionique spécifique ammonium a été préparée par couplage d'une membrane perméable ammoniac-hydrophobe et d'une électrode Beckman à cation monovalent. Aux valeurs de pH physiologiques le rapport ammoniac/ammonium n'est que de 0.01. Une telle électrode permet de déceler l'ion ammonium formé dans la réaction urée–uréase.

ZUSAMMENFASSUNG

Eine ammoniumionenspezifische Elektrode wurde hergestellt, indem eine hydrophobe ammoniakdurchlässige Membran mit einer einwertigen Beckman-Kationenelektrode verbunden wurde. Bei physiologischen pH-Werten ist das Verhältnis Ammoniak: Ammoniumion nur 0.01, jedoch ist der Gastransportmechanismus noch wirksam; eine nach diesem Prinzip entwickelte Elektrode konnte Ammoniumion, das über die Harnstoff–Urease-Reaktion erzeugt wird, nachweisen. Die Elektrode kann in einem Luftstrom oder in einem wässrigen Medium benutzt werden. Die Elektrode kann ebenfalls bei einer ultraempfindlichen Methode verwendet werden, indem das Ammoniak aus der Probenlösung nach Einstellung des pH-Wertes entfernt wird.

REFERENCES

1 J. G. Montalvo, Jr., *Anal. Biochem.*, 38 (1970) 357.
2 J. G. Montalvo, Jr., *Anal. Chem.*, 41 (1969) 2093.
3 G. G. Guilbault and J. G. Montalvo, Jr., *Anal. Lett.*, 2 (1969) 283.
4 G. G. Guilbault and J. G. Montalvo, Jr., *J. Amer. Chem. Soc.*, 92 (1970) 2533.

Analytica Chimica Acta, 65 (1973) 198–201

SHORT COMMUNICATION

$Eu(fod)_3$ for the determination of the *cis–trans* composition of methyl elaidate–oleate by n.m.r. spectroscopy*

DOUGLAS B. WALTERS and ROBERT J. HORVAT

Animal Products Laboratory, Richard B. Russell Research Center, USDA, ARS, Athens, Ga. 30604 (U.S.A.)

(Received 24th July 1972)

A rapid, novel method of determining the *cis–trans* composition of unsaturated fatty acid methyl esters by means of n.m.r. spectroscopy and the recently discovered shift reagent, $Eu(fod)_3$, is described. This technique has some advantages over previously described methods. The standard infrared method[1] requires two measurements, an iodine value and a *trans*-concentration, obtained by using the 970 cm^{-1} band. The Raman technique[2] requires sophisticated instrumentation methods and specialized knowledge. The gas chromatographic method[3] and the n.m.r. mercury adduct procedure[4] necessitate time-consuming formation of derivatives.

Our method is simple, rapid, nondestructive and it gives *cis–trans* ratios directly, from which standard calibration curves can be prepared. As Schaumberg[4] noted three features favor an n.m.r. method rather than the standard i.r. method. First, signals representing both the *cis* and *trans* compounds can be observed directly; second, signal intensities are linearly related to solution concentrations; and finally, the method is not restricted to cases where two protons are located at the double bond. However, unlike Schaumberg's method, the proposed method does not require lengthy preparation of derivatives.

Since the initial report[5] that large, selective shifts are induced by n.m.r. shift reagents, numerous papers have described the use of these reagents for characterization of n.m.r. spectra of complex organic molecules, and for identification of *cis–trans* mixtures other than unsaturated esters[6,7]. Successful application of $Eu(fod)_3$ [tris-(1,1,1,2,2,3,3-heptafluoro-7,7-dimethyloctadione)europium(III)] to esters of unsaturated fatty acids[8] led us to choose this shift reagent.

The *cis–trans* composition of unsaturated fatty ester mixtures is of interest for several reasons: (*a*) nutritional studies have indicated that *trans* isomers may not be nutritionally equivalent to the naturally occurring *cis* isomers[9]; (*b*) animal studies have indicated that blood-clotting time is altered when *trans* isomers are substituted for *cis* isomers[10]; (*c*) subtle molecular structural changes often account for major flavor changes[11]; and (*d*) when fat or oil is partially hydrogenated, mixtures of *cis* and *trans* unsaturated acids are obtained[12], so that oxidative stability studies are of interest.

* Presented in part at the 163rd National American Chemical Society Meeting, Boston, Mass., April, 1972.

The *cis* and *trans* isomers, methyl oleate (I) and methyl elaidate (II), represent a good model system and were used throughout this study.

I

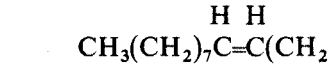

II

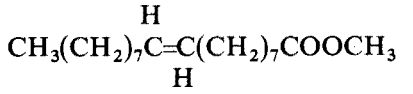

Experimental

Spectra were obtained with a Varian HA-100 n.m.r. spectrometer at an ambient probe temperature of 30°. Calibrations were made with a Hewlett-Packard Model 5244L electronic frequency counter, and chemical shifts were measured relative to tetramethylsilane. Line positions are estimated to be accurate to ± 0.5 Hz. The instrument was tuned for each sample to compensate for changes in the magnetic field from the paramagnetic metal present. Methoxy singlets were integrated by means of Schaumberg's peak-height method[5].

Methyl oleate and methyl elaidate were obtained from the Hormel Institute of the University of Minnesota, and certified >99% pure. This was verified by gas chromatography, thin-layer chromatography, and infrared analysis in this laboratory.

$Eu(fod)_3$ (Norell Chemical Company)* was stored over P_2O_5 to ensure dryness. Carbon tetrachloride (Matheson, Coleman, and Bell) was spectroquality grade.

Spectra were obtained of 0.2–0.5 *M* solutions of these substrates in carbon tetrachloride to which increments of $Eu(fod)_3$ were added.

Results and discussion

Figure 1A shows the n.m.r. spectrum of a 70.81:29.19 mole% mixture of methyl oleate and methyl elaidate, respectively, in carbon tetrachloride. All the individual absorbances coincide and it is not possible to distinguish *cis* and *trans* configurations, as noted by others[1-3]. When 0.0508 g of $Eu(fod)_3$ was added to this solution (Fig. 1B), all peaks were selectively shifted downfield, the magnitude of the induced shift being dependent upon the amount of $Eu(fod)_3$ added. After addition of $Eu(fod)_3$, the *cis* methoxy singlet shifted 4.97 p.p.m. downfield and the *trans* methoxy singlet, 5.02 p.p.m. downfield. These two peaks were separated enough from one another and from other proton absorbances to provide unique signals representing each of the components of this mixture (Fig. 2).

Since line shapes for the two methoxy signals are symmetrically similar, peak-height measurements are linearly related to concentration, and were used to determine the *cis–trans* ratio[4]. Table I shows the results of mole% *cis–trans* ratios found by n.m.r., compared to the actual values calculated by weight. Excellent agreement was found.

Caution must be used when this technique is used, to ensure that enough $Eu(fod)_3$ is added to shift the methoxy peaks in a manner to obtain a unique

* Reference to company or product name in this article does not imply approval or recommendation by the USDA.

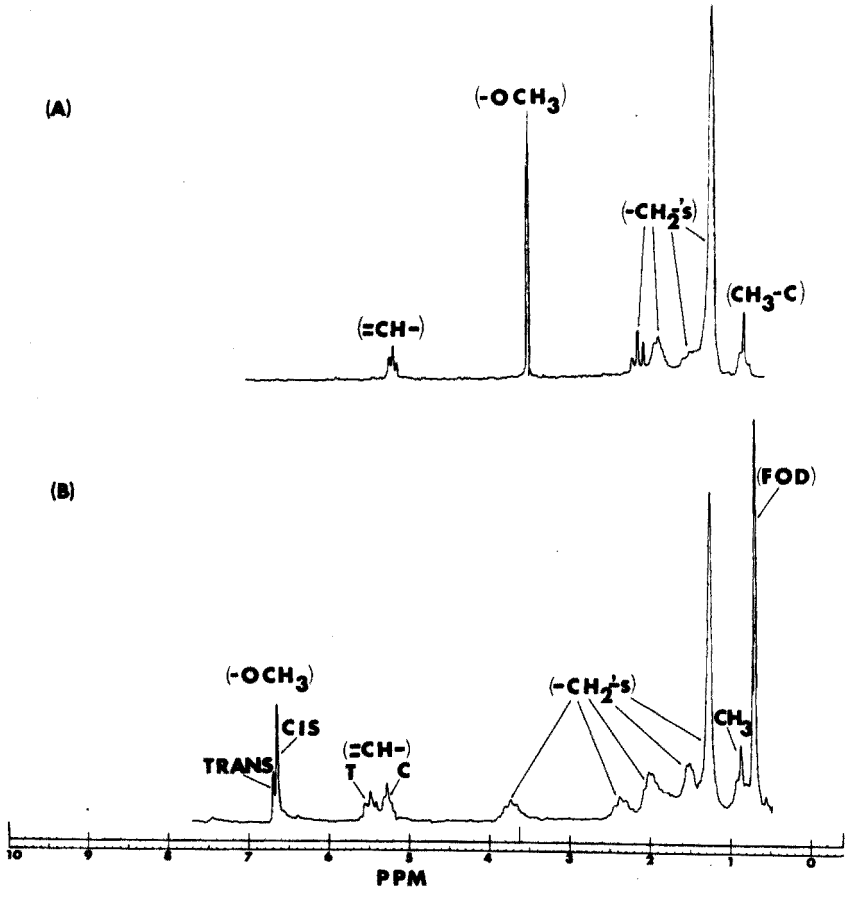

Fig. 1. N.m.r. spectrum of a 70.81:29.19 mole% mixture of methyl oleate and methyl elaidate in CCl_4. (A) Before addition of $Eu(fod)_3$; (B) after addition of 0.0508 g of $Eu(fod)_3$.

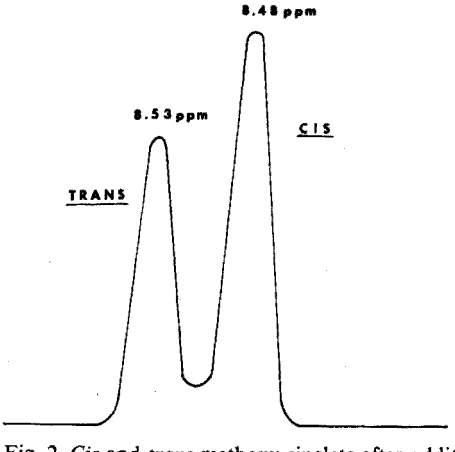

Fig. 2. *Cis* and *trans* methoxy singlets after addition of $Eu(fod)_3$.

TABLE I

ACTUAL *cis:trans* MOLE% BY WEIGHT AND BY n.m.r. METHOD

Actual cis:trans mole % by weight	*Cis:trans mole% found by n.m.r.*	*Δ mole%*
17.32:82.68	16.07:83.93	1.25
30.36:69.64	29.02:70.98	1.34
62.72:37.28	62.67:37.33	0.05
70.81:29.19	69.70:30.30	1.11
87.99:12.01	87.76:12.24	0.23

absorbance for each. However, if too much shift reagent is added, broadening occurs and the peaks are no longer separated enough to allow accurate integration. For the 0.2–0.5 *M* solutions used in this study, the optimal range for added $Eu(fod)_3$ was 60–80 mg.

The authors are indebted to Dr. L. H. Keith and the Southeast Water Laboratory, E.P.A., for the use of the n.m.r. spectrometer for completion of this work. The technical assistance of Miss Fredda Gillen is also greatly appreciated.

REFERENCES

1 *Amer. Oil Chem. Soc. Official and Tentative Methods*, 3rd Ed., Revised to 1970.
2 G. F. Bailey and R. J. Horvat, *J. Amer. Oil Chem. Soc.*, in press.
3 E. A. Emken, *Lipids*, 6 (1971) 686.
4 K. Schaumberg, *Lipids*, 5 (1970) 505.
5 C. C. Hinckley, *J. Amer. Chem. Soc.*, 91 (1969) 5160.
6 H. G. Richey, Jr. and F. W. Von Rein, *Tetrahedron Lett.*, (1971) 3781.
7 K. Stensio and U. Ahlin, *Tetrahedron Lett.*, (1971) 4729.
8 D. Swern and J. P. Weinberg, *J. Amer. Oil Chem. Soc.*, 48 (1971) 371.
9 P. G. Rand and F. W. Quackenbush, *J. Nutr.*, 87 (1965) 489.
10 G. Raccuglia and O. S. Privett, *Lipids*, 5 (1970) 85.
11 R. Teranishi, P. Issenberg, I. Hornstein and E. I. Wick, *Flavor Research, Principles and Techniques*, Marcel Dekker, New York, 1971, p. 282.
12 S. Koritala, *J. Amer. Oil Chem. Soc.*, 47 (1971) 269.
13 K. Schaumberg and H. J. Bernstein, *Lipids*, 3 (1968) 193.

Analytica Chimica Acta, 65 (1973) 202–205

SHORT COMMUNICATION

The mass spectra of dithizone and some related compounds

P. A. ALSOP and H. M. N. H. IRVING

Department of Inorganic and Structural Chemistry, University of Leeds, Leeds LS2 9JT (England)

(Received 12th December 1972)

In connection with X-ray studies of the crystalline structure of solid dithizone (diphenylthiocarbazone, 3-mercapto-1,5-diphenylformazan, I), its S-methyl derivative (II) and its reduction product diphenylthiocarbazide (III), the mass spectra of authentic samples were measured and compared with those of the aliphatic analogue (IV).

$PhN{=}N\cdot C(SH){=}N\cdot NHPh$ or $PhN{=}N\cdot C(SCH_3){=}N\cdot NHPh$ (II)

$PhN{=}N\cdot CS\cdot NH\cdot NHPh$ (I) $PhNH\cdot NH\cdot CS\cdot NH\cdot NHPh$ (III)

$(CH_3)_2N\cdot NH\cdot CS\cdot NH\cdot N(CH_3)_2$ (IV)

The mass spectra are shown in Fig. 1 and can be rationalized as follows.

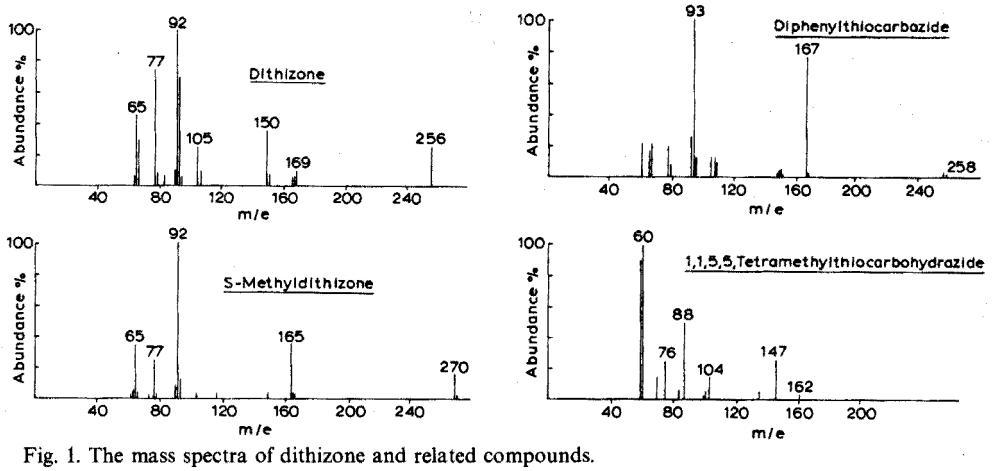

Fig. 1. The mass spectra of dithizone and related compounds.

Dithizone

The following splitting scheme accounts for the principal peaks.

The fragmentation of $m/e=256$ to 150 and $m/e=256$ to 93 are supported by metastable peaks at m/e 87.9 and 33.8, respectively[2]. Fragments of m/e 169, 168

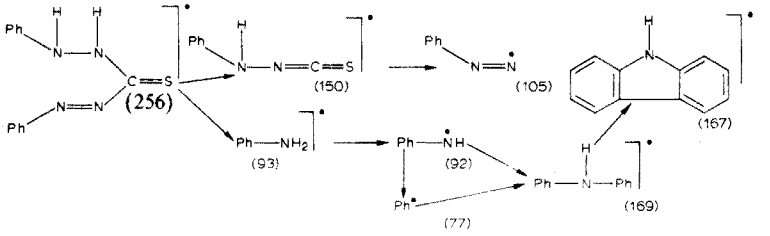

and 167 could not be accounted for by any expected splitting or likely impurities and must therefore be due to a rearrangement. Accurate mass determinations gave the following results:

m/e found	*Empirical formula*	*m/e calculated*[3]
169.088 7	$C_{12}H_{11}N$	169.089 1
168.080 6	$C_{12}H_{10}N$	168.081 3
167.073 7	$C_{12}H_9N$	167.073 5
	$C_7H_9N_3S$	167.051 7

It was therefore concluded that the 169-*m/e* peak is due to diphenylamine, Ph_2NH, and the 167-*m/e* peak to carbazole. This is supported by the mass spectra of the primary dithizonates of copper, nickel and cobalt described below (*cf.* Fig. 2). Das *et al.*[4] have demonstrated unambiguously that the sequence $Ph \cdot CH_2 \cdot CO \cdot NPh_2$ (V) → Ph_2NH → carbazole represents a possible route in the stepwise fragmentation of this amide (V) and have suggested a detailed mechanism. Diphenylamine is also known to be converted into carbazole on photolysis[5].

S-Methyldithizone (II)

The fragmentation follows a similar pattern though the formation of diphenylamine and carbazole appear to be inhibited. The following scheme accounts for the principal peaks:

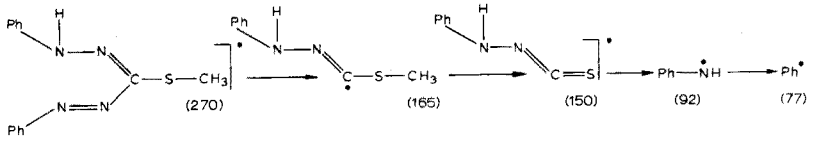

Diphenylthiocarbazide (III)

The two principal fragments are accounted for by the following scheme:

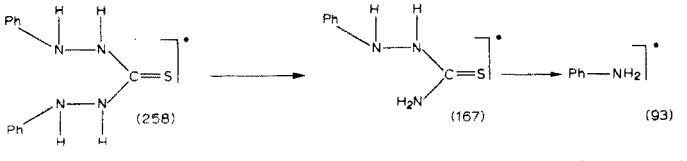

Other fragments found in the spectrum of dithizone are far less abundant.

1,1,5,5-Tetramethylthiocarbohydrazide (IV)

The splitting pattern is due mainly to the successive removal of methyl

groups. The following scheme accounts for all the principal peaks and confirms the structure of this aliphatic analogue of diphenylthiocarbazide (III).

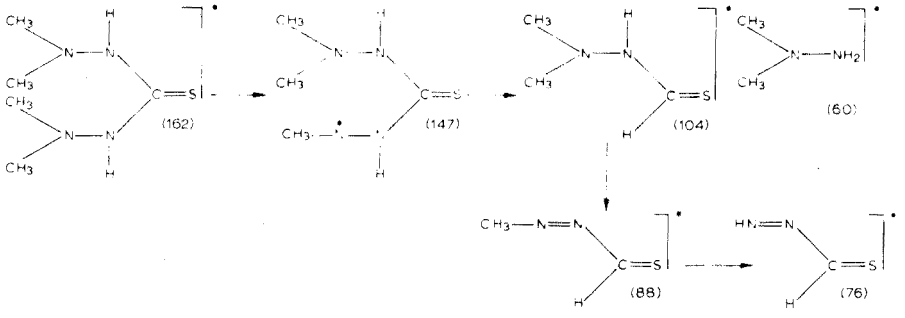

Primary dithizonates

The mass spectra of the primary dithizonates of copper(II), nickel(II) and cobalt(III) shown in Fig. 2 were measured at the minimal temperature required to give a sufficient ion current. The determination was originally carried out in the hope of obtaining the molecular weights of these very insoluble chelate complexes. All three chelate complexes afforded very similar spectra and gave no evidence of the molecular peaks. A common feature of interest is the presence of peaks at $m/e = 169$, 168 and 167 as in that of dithizone; these are due again to the formation and rearrangement of diphenylamine. In the spectrum of $Co(HDz)_3$ where the base peaks are due to the fragments $C_6H_5^+$ (77), C_6H_5–$\dot{N}H$ (92) and $C_6H_5 \cdot NH_2$ (93),

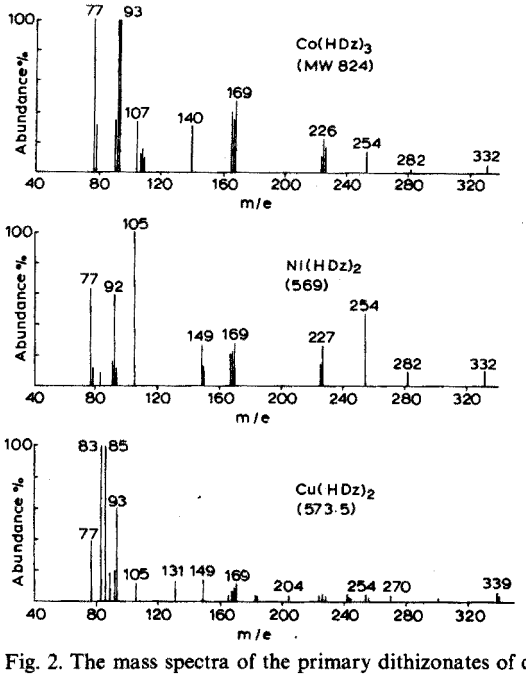

Fig. 2. The mass spectra of the primary dithizonates of copper(II), nickel(II) and cobalt(III).

the peak for $m/e = 169$ amounts to no less than 50% of the base peak, an abundance which seems unusually large for a rearrangement product. It is tempting to suppose that the process

$$C_6H_5^{\cdot} + C_6H_5 \cdot \dot{N}H \rightarrow (C_6H_5)_2NH$$

is catalysed by cobalt (and to a lesser extent by nickel) ions, so that this process is more efficient than in the mass spectra of the copper complex or with dithizone itself.

Experimental

Dithizone(I), diphenylthiocarbazide(III) and S-methyldithizone(II) were prepared by published methods and rigorously purified. 1,1,5,5-Tetramethylthiocarbohydrazide(IV) was prepared by replacing phenylhydrazine by N,N-dimethylhydrazine in the usual preparation of dithizone by Fischer's method. It formed a white crystalline solid (m.p. 148° dec.) soluble in chloroform but lacking chelating properties. Its identity is completely confirmed by the mass spectrum.

All mass spectra were measured on an AEI MS9 mass spectrometer. Metal complexes were prepared by standard methods[6] and isolated by slow evaporation of their solutions in chloroform after drying over anhydrous magnesium sulphate. In view of the controversy over the oxidation state of the metal in the cobalt complex and concerning its stoichiometry[6,7], the sample was analysed and found to conform to the tris-chelate. Found: C, 56.7; H, 3.9; N, 20.0%. Calc. for $Co(HDz)_3$: C, 56.8; H, 4.0; N, 20.4%. Calc. for $Co(HDz)_2$: C, 54.8; H, 3.9; N, 19.7%.

REFERENCES

1 P. A. Alsop, H. M. N. H. Irving and others, to be published shortly.
2 J. H. Beynon, R. A. Saunders and A. E. Williams, *Tables for Metastable Transitions for Use in Mass Spectrometry*, Elsevier, London, 1965.
3 J. H. Beynon and A. E. Williams, *Mass and Abundance Tables for Use in Mass Spectrometry*, Elsevier, London, 1963.
4 K. G. Das, P. T. Funke and A. K. Bose, *J. Amer. Chem. Soc.*, 86 (1964) 3729.
5 K. H. Grellmann, G. M. Sherman and H. Linschitz, *J. Amer. Chem. Soc.*, 85 (1963) 1881.
6 L. S. Meriwether, E. C. Breitner and N. D. Colthup, *J. Amer. Chem. Soc.*, 87 (1965) 4448.
7 J. F. Duncan and F. G. Thomas, *J. Chem. Soc.*, (1960) 2814 and refs. therein.

Analytica Chimica Acta, 65 (1973) 206–209

SHORT COMMUNICATION

The rapid determination of tungsten in ores and concentrates by atomic absorption spectrometry

B. F. QUIN and R. R. BROOKS

Department of Chemistry, Biochemistry and Biophysics, Massey University, Palmerston North (New Zealand)

(Received 21st November 1972)

The upsurge in the world demand for tungsten has resulted in an intensifying search for this element in countries such as New Zealand, and there is an increasing need for rapid methods for analysing ores and concentrates.

The colorimetric method of Quin and Brooks[1] has a high productivity for the analysis of soils, stream sediments, low-grade ores and vegetation, and in the past year approximately 2,000 analyses have been carried out in the authors' laboratory. However, the analysis of tungsten ores by this technique was less satisfactory, as the analyses often had to be repeated several times using progressively smaller aliquots of the sample solution until the absorbance reading fell in the range of the standard curve. Besides seriously reducing productivity, the large percentage volumetric error caused by taking small aliquots decreased the reproducibility of the method.

A further problem encountered in the analysis of ores by the colorimetric procedure was the tendency for tungsten in high-grade samples to precipitate out of the concentrated hydrochloric acid leach solution as tungstic acid. It was therefore decided to investigate the use of atomic absorption spectrometry for the analysis of tungsten ores and concentrates. Previous procedures involve time-consuming solvent extraction[2] or pH adjustment[3], and neither of these methods is capable of a productivity greater than 35 samples per man-day.

The method reported below involves dissolution of the sample with a mixture of concentrated hydrofluoric and nitric acids, evaporation to dryness, redissolution of the residue with a small volume of 0.5 *M* potassium hydroxide, and determination of tungsten by conventional atomic absorption spectrometry.

Experimental

Equipment. The atomic absorption measurements were carried out with a Varian Techtron AA5 atomic absorption spectrophotometer under the conditions listed below.

Source: ASL hollow-cathode lamp. *Lamp current:* 20 mA. *Wavelength:* 255.1 nm. *Slit width:* 0.15 mm. *Burner:* Techtron AB40 or AB50.

Gas mixture: nitrous oxide, flow rate 7.5 scale units (15 p.s.i.); acetylene, flow rate 8.0 scale units (16 p.s.i.), red cone 2 cm high.

Scale expansion was needed only for samples containing less than 10% WO_3.

Standard tungsten solutions. Dissolve 6.30 g of tungsten trioxide (99.9%) in hot 0.5 *M* potassium hydroxide, and make up to 500 cm^3 with this alkali. This gives a solution containing 10,000 p.p.m. (1%) tungsten in solution. From this prepare solutions containing 7500, 5000, 2000, 1000, 500, 200 and 100 p.p.m. by diluting with 0.5 *M* potassium hydroxide.

Digestion of the sample. Digest 0.2-g samples of ore or concentrate in polypropylene beakers over a boiling water bath with 10 cm^3 of a (1+1) mixture of hydrofluoric (40%, AR) and nitric (s.g. 1.42, AR) acids.

When samples have evaporated to dryness (2–3 h), add 10 cm^3 of 0.5 *M* potassium hydroxide and continue heating for 20 min. Transfer solution and any residue to a 10-cm^3 centrifuge tube, washing in with distilled water. Make up to 10 cm^3 with distilled water and centrifuge for 2 min at 5000 rev min^{-1}.

Atomic absorption determination of tungsten. For routine analysis, standards comprising 100, 200, 500, 1000, 2000, 5000, 7500 and 10,000 p.p.m. tungsten in 0.5 *M* potassium hydroxide were used. Under optimal instrumental conditions a solution containing 10,000 p.p.m. tungsten gave an absorbance of 0.50 when no scale expansion was used. A typical calibration curve is shown in Fig. 1.

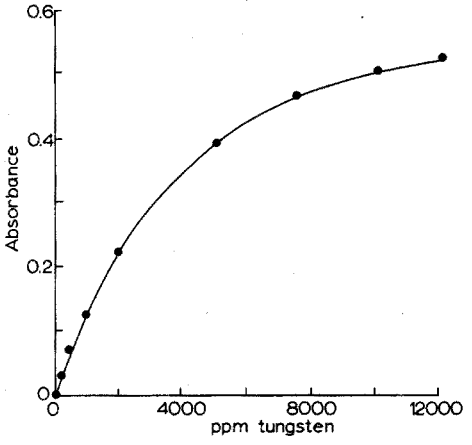

Fig. 1. Standard curve for tungsten.

TABLE I

RECOVERY OF TUNGSTEN TRIOXIDE ADDED TO LOW-GRADE ORE

WO_3 added (mg)	*WO_3 recovered[a] (mg)*	*Range (mg)*	*Coefficient of variation (%)*
0	1.0	0.9–1.1	±8.5
50	50.9	49.0–53.5	±3.6
100	100.8	99.9–102.0	±0.9
150	150.2	148.5–152.3	±1.2

[a] Mean of 4 determinations.

Results and discussion

Recovery of tungsten. Table I shows the results of replicate analyses of a low-grade ore to which known amounts of tungsten trioxide had been added. Recovery was complete within the precision of the method.

Method of digestion. The tungsten ores scheelite ($CaWO_4$), wolframite ($[Fe, Mn]WO_4$) and tungstite (WO_3) are all soluble in hydrofluoric acid, and during the digestion any silica present is volatilized, resulting in a complete breakdown of the silicate lattice. As the last of the acid is volatilized, the tungsten is reprecipitated as yellow tungstic acid, $WO_3 \cdot H_2O$, irrespective of the original ore type. This compound, while being rather insoluble in acids other than hydrofluoric acid, is readily soluble in alkali, and the addition of 10 cm^3 of 0.5 *M* potassium hydroxide achieves this dissolution in a matter of minutes. Smaller concentrations (down to 0.2 *M*) can be used provided that longer heating is used, but a concentration 0.5 *M* was considered to offer the best compromise between speed and economy.

The addition of the alkali causes other metals such as iron, manganese and aluminium to precipitate but the excellent recovery results (Table I) show that no tungsten is lost by occlusion in this precipitate.

Reproducibility and accuracy of the method. Table II summarizes analytical data for tungsten in synthetic samples and in selected samples of scheelite and wolframite ores. Coefficients of variation reported for each sample show that the reproducibility is more than adequate for the requirements of a method for the routine analysis of ores and concentrates.

TABLE II

ANALYTICAL DATA FOR REPLICATE DETERMINATIONS OF TUNGSTEN IN SYNTHETIC STANDARDS AND ORE SAMPLES

Sample[a]	*No. of analyses*	*Mean (% WO_3)*	*Range (% WO_3)*	*Coefficient of variation (%)*
A (29.0% WO_3)	4	29.4	29.0–29.7	±1.3
B (10.0% WO_3)	4	10.1	9.7–10.4	±3.4
C (4.8% WO_3)	4	4.9	4.7–5.0	±3.0
D (0.48% WO_3)	4	0.50	0.48–0.52	±3.5
Scheelite ore, Westland	6	9.6	9.3–9.7	±3.1
Scheelite ore, Marlborough	6	40.7	39.0–42.6	±2.5
Wolframite ore, Westland	6	27.6	27.1–28.1	±1.3

[a] Synthetic standards (A, B, C, D) by courtesy of A. G. Fricker, Otago University, New Zealand.

Sensitivity. Although the original requirement was only for a method capable of analysing ores containing more than 1% WO_3, the sensitivity of the method is much better than this and concentrations as low as 200 p.p.m. in the original sample can be determined. These low concentrations necessitate such a high scale expansion that the absorbance reading from the potassium hydroxide becomes significant, but this is easily corrected for by running a blank. In any case, if this degree of sensitivity were required, it would be more suitable to use the lowest possible concentration of potassium hydroxide (0.2 *M*).

Interferences. A hydrogen hollow-cathode lamp was used to check interferences from metals such as calcium, iron, manganese, and aluminium in the samples analysed. In no instance was significant interference found, and it is concluded that correction need only be made for the potassium, and then only when high scale expansion is being used.

Productivity. The inherent simplicity of the method lends itself to a high analysis rate, and a figure of 100 samples per man-day can be easily achieved.

Conclusions. It is concluded that, in terms of reproducibility, recovery and particularly productivity, this method represents a significant improvement over existing atomic absorption and colorimetric procedures for the determination of tungsten in ores and concentrates.

REFERENCES

1 B. F. Quin and R. R. Brooks, *Anal. Chim. Acta*, 58 (1972) 301.
2 P. D. Rao, *At. Absorpt. Newsl.*, 9 (1970) 131.
3 E. Keller and M. L. Parsons, *At. Absorpt. Newsl.*, 9 (1970) 92.

Analytica Chimica Acta, 65 (1973) 210–212

SHORT COMMUNICATION

Die Bestimmung von Neodym in neodymdotierten Yttrium–Aluminium–Granat-Kristallen mittels Atomabsorptions-Spektralanalyse*

K.-H. KÖNIG und P. NEUMANN

Anorganische Chemie, Chemische Institute, Johann-Wolfgang-Goethe-Universität, Robert-Mayer-Strasse 7–9, Frankfurt am Main (Deutschland)

(Eingegangen den 6. Dezember 1972)

Bei der Züchtung von neodymdotierten Yttrium–Aluminium–Granat-Kristallen (Nd-YAG) interessierte der Gehalt an Neodym der Züchtungsprodukte. Als bequeme Methode bietet sich hier die Atomabsorptions-Spektralanalyse an[1–3], da Neodym nach einem Borat-Aufschluss ohne vorherige Abtrennung bestimmt werden kann[4]. Als Standard wird eine Neodym-Konzentrationsreihe benutzt, die die gleiche Zusammensetzung wie die Analysenlösung besitzt. Die Eichkurve für die Standardneodymlösung (30–80 μg Nd ml^{-1}) verläuft linear. Da jedoch im Bereich der Nachweisgrenze des Neodyms gearbeitet wird, sind bei der Bestimmung folgende Punkte zu beachten.

Die Bestimmung muss in einer brenngasreichen Flamme (Acetylen–Lachgas) erfolgen, bei der sich sehr schnell Kohlenstoff am Brennerschlitz abscheidet, sodass die Flammenbedingungen nur sehr schwierig konstant gehalten werden können und die Einzelwerte einer Messung stark streuen können. Deshalb wurde für die Neodymbestimmungen jeweils sofort im Anschluss an eine Messung der Probe eine Standardlösung gemessen. Für jedes Paar dieser Messungen wird der Neodymgehalt bezogen auf den jeweiligen Extinktionswert der Standardlösung berechnet. Dieses Verfahren wird mehrmals wiederholt, aus den dabei erhaltenen Einzelwerten der Mittelwert gebildet und das Analysenergebnis berechnet (vgl. Tabelle I). Im vorliegenden Fall wurde eine Standardlösung mit 50 μg Nd ml^{-1} benutzt.

Für die Standardlösung ergibt sich eine Empfindlichkeit von 32 μg Nd ml^{-1} (1% Absorption) und 22 μg Nd ml^{-1} als Nachweisgrenze, wenn diese als diejenige Konzentration definiert wird, die ein doppelt so grosses Signal wie der Rauschpegel von Spitze zu Spitze zeigt. Das Rauschen betrug $\pm$0.00075 Extinktionseinheiten. Die Angaben von Empfindlichkeit und Nachweisgrenze beziehen sich wohlgemerkt nicht auf wässrige Neodymlösungen, sondern auf die benutzten Standard-Neodymlösungen.

Versuche mit Soda–Borax-Aufschlüssen[4] ergaben für die Standards zwar günstigere Empfindlichkeiten und damit auch bessere Nachweisgrenzen, jedoch war die Linearität der Eichkurven schlechter.

* Ein Projekt des Sonderforschungsbereiches Festkörperspektroskopie Darmstadt–Frankfurt, gefördert durch Sondermittel der Deutschen Forschungsgemeinschaft.

TABELLE I

MESSERGEBNISSE

	Probe 1		*Probe 2*	
	Messung	*Probe in % vom Standard*	*Messung*	*Probe in % vom Standard*
Probe	0.00525	91.2	0.00300	80.0
Standard[a]	0.00575		0.00375	
Probe	0.00500	87.0	0.00275	81.5
Standard[a]	0.00575		0.00338	
Probe	0.00400	86.5	0.00275	78.6
Standard[a]	0.00462		0.00350	
Probe	0.00500	90.8	0.00175	77.8
Standard[a]	0.00550		0.00225	
Probe	0.00500	87.0	0.00225	81.7
Standard[a]	0.00575		0.00275	
Mittelwert in Bezug auf den Standard		88.5±2.1%		79.9±1.6%
Gehalt der Probelösung (μg Nd ml^{-1})		44.3±0.9		40.0±0.7

[a] Der Standard enthält 50 μg Nd ml^{-1}.

Experimenteller Teil

Geräte und Messbedingungen. Die Messungen wurden mit einem Spektrometer vom Typ SP 90, einem Konzentrationswandler SP 45 und einem Schreiber SP 20 (Pye Unicam) ausgeführt.

Die benutzte Acetylen–Lachgasflamme soll Brenngasüberschuss (*ca.* 3.8 l min^{-1} bei 1 atm C_2H_2 und *ca.* 5 l min^{-1} bei 2 atm N_2O) besitzen, sodass die Höhe der roten Reduktionszone mindestens 50 mm beträgt, bei einer Brennerhöhe von 0.75 cm.

Die Hohlkathodenlampe (Pye Unicam) wird mit 10 mA betrieben und die Messungen erfolgen bei 489.7 nm mit 0.1 mm Spaltbreite. Der Quarzglasprismenmonochromator besitzt bei 550 nm eine lineare Dispersion von 78 nm mm^{-1}. Durch die 12-fache Skalendehnung (einmalige Nullpunktunterdrückung am SP 90 und Bereich 0–0.1 am SP 45) ist es vorteilhaft mit Dämpfungsstufe 4 zu arbeiten (Ansprechzeit am Schreiber: 4 s).

Arbeitsvorschriften. 250 mg des auf Analysenfeinheit gemahlenen und getrockneten YAG werden mit je 1 g Lithiumcarbonat und Lithiumtetraborat im Platintiegel 4 Std. im elektrischen Muffelofen bei 1000° geschmolzen. Anschliessend wird die erstarrte Schmelze auf dem Wasserbad in 60 ml *ca.* 1 *N* Schwefelsäure gelöst. Die Lösung wird in einem 100 ml-Messkolben mit Wasser aufgefüllt. Zur Messung werden aliquote Teile mit dem gleichen Volumen Wasser verdünnt.

Standardlösungen. Die Standardneodymlösungen enthalten 0.1 *N* Salzsäure

und 1 g Nd l^{-1}. Daraus werden durch Verdünnen mit Wasser Lösungen mit 60, 100 bzw. 150 μg Nd l^{-1} hergestellt.

Für die Vergleichsmessungen werden jeweils gleiche Volumina dieser Lösungen mit einer Lösung gemischt, die in 100 ml die Aufschlusssubstanz von 250 mg nichtdotiertem gemahlenem Granatpulver enthält, das wie oben beschrieben aufgeschlossen wurde. Die Standardlösungen enthalten somit die gleiche Matrix wie die Analysenlösung und 30, 50 bzw. 75 μg Nd ml^{-1}.

LITERATUR

1 V. G. Mossotti und V. A. Fassel, *Spectrochim. Acta*, 20 (1964) 1117.
2 W. Slavin, *Atomic Absorption Spectroscopy*, Wiley–Interscience, New York, 1968.
3 B. Welz, *Atomabsorption*, Verlag Chemie, Weinheim, 1972.
4 W. Grosskreuz, D. Schultze und T.-K. Wilke, *Z. Anal. Chem.*, 232 (1967) 278.

Analytica Chimica Acta, 65 (1973) 213–215

SHORT COMMUNICATION

Spectrophotometric determination of traces of ruthenium with *o*-tolidine

RAÚL S. DE PABLO
Diamond Shamrock Corporation, P.O. Box 348, Painesville, Ohio (U.S.A.)
(Received 20th October 1972)

o-Tolidine is known to react with free chlorine, gold(III), osmium tetroxide, ruthenium salts, tungstates, etc.[1,2], but it has not been applied to the determination of ruthenium *via* its reaction with ruthenium tetroxide. This procedure is less sensitive than the catalytic cerium–arsenic method[3], but is more sensitive than any of the following methods: thiourea, diphenylthiourea, dithiooxamide, diphenylthiosemicarbazide, *o*-phenanthroline, *p*-nitrosodimethylaniline[3].

Experimental

Apparatus. Microgram amounts of ruthenium were readily distilled from a 200-ml all-glass Claisen flask in a stream of air; the all-glass sidearm of the flask was placed into a test tube in an ice-bath. Before use, the apparatus was washed with hot cleaning mixture (15 g of potassium dichromate dissolved in about 500 ml of concentrated sulfuric acid) followed by a water rinse and a steam cleaning. Otherwise, traces of organic impurities might reduce the ruthenium tetroxide and lead to low results. The joints of the distillation apparatus should not be lubricated.

A Beckman B spectrophotometer was used with 5-cm cells.

o-Tolidine solution. Suspend 0.200 g of pure *o*-tolidine dihydrochloride in about 100 ml of distilled water, add 30 ml of concentrated hydrochloric acid, dissolve, make up to 200 ml and mix well. Prepare fresh daily. This solution should be colorless.

Ruthenium standard solution. Pure ruthenium trichloride hydrate is analyzed for total ruthenium *via* reduction under hydrogen or atomic absorption. Weigh the proper amount, dissolve in 2 *M* hydrochloric acid, make up to the desired volume, and calculate the exact concentration. By dilution, prepare another solution containing 1 p.p.m. of ruthenium.

Procedure. Treat the sample so as to bring all the ruthenium into solution[4]. Transfer an aliquot (containing not more than 10–12 μg Ru) to a beaker. Add sufficient concentrated hydrochloric acid to react with any nitrate present (if any was used) and to leave an excess of 20–25 ml. Add sufficient (1 + 1) sulfuric acid to transform all the salts into neutral sulfates and to leave an excess of 5–7 ml of the concentrated acid. Mix well, heat to fumes of sulfur trioxide without boiling, and fume for 4–5 min. Cool to room temperature. Carefully transfer all the solution to the distillation apparatus. Dilute to about 80–100 ml. Add 0.2–0.3 g of ammonium cerium(IV) sulfate without leaving any particles stuck to the walls. Place 10 ml

of *o*-tolidine solution and 10 ml of water in the receiver test tube, mix, cool to about 0–+5° with an ice bath, start a flow of clean air (3–4 bubbles s^{-1}), heat the flask solution to the boiling point and boil for about 25–30 s after the sidearm of the distillation flask becomes hot. Remove the receiver tube, make up to 50 ml and mix well. Wait for 5 min after boiling begins and determine the absorbance at 430 nm in 5-cm cells *versus* water. Run a calibration curve by the same procedure, using aliquots of the standard solution.

Results

Beer's law was obeyed over the range 0–10.8 μg Ru. The reagent blank was *ca.* 0.010 absorbance units. The sensitivity according to Sandell[3] was about 10^{-3} μg cm^{-2}.

Under the recommended conditions, osmium was the only likely interfering element. The results obtained with various concentrations of osmium are shown in Table I. With osmium, the absorbance increased after the specified 5-min period, whereas the absorbance caused by ruthenium began to decrease slowly (Table II). When osmium is added as the tetroxide, most is eliminated in the fuming step; but, when it is added as potassium osmate or potassium chlorosmate, most or all remains in the system. If desired, the osmium may be separated by some suitable procedure[3,4].

TABLE I

INFLUENCE OF OSMIUM IN ABSENCE OF RUTHENIUM

Os added (μg)	*Added as*	*Ru found (μg)*
9,000	OsO_4	0.5
100	K_2OsO_4	0.2
500	K_2OsO_4	0.4
700	K_2OsO_4	0.6
1,000	K_2OsO_4	0.8
3,200	K_2OsO_4	2.0
2,090	K_2OsCl_6	< 1.0
6,640	K_2OsCl_6	13.0

TABLE II

VARIATION OF THE ABSORBANCE OF THE OSMIUM AND RUTHENIUM COLORS WITH TIME

1000 μg Os as K_2OsO_4		*11.7 μg Ru*	
Time (min)	*Absorbance*	*Time (min)*	*Absorbance*
5	0.10	5	1.21
15	0.19	10	1.20
30	0.35	15	1.18
45	0.48	26	1.14
60	0.59	35	1.10
80	0.77	54	1.04

Discussion

This reaction seems to involve the oxidation of *o*-tolidine by ruthenium tetroxide, with simultaneous reduction of ruthenium(VIII) to one or more lower valences. This mechanism is supported at least in part by the fact that the absorption curve of the yellow compound obtained coincides in shape and absorption maximum with that obtained from *o*-tolidine oxidized by other reagents like sodium hypochlorite, in the absence of ruthenium (Fig. 1).

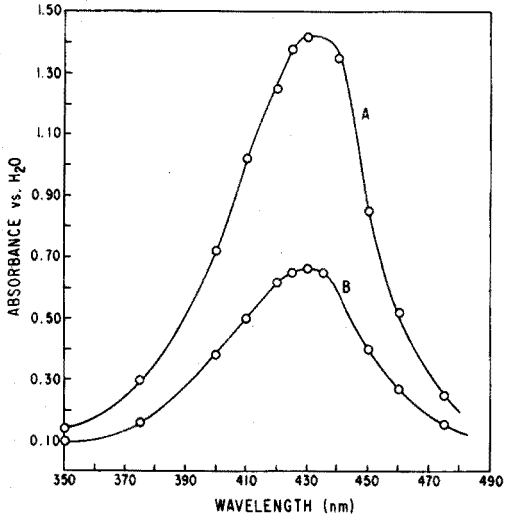

Fig. 1. Spectral absorption curves. (A) 15.8 μg sodium hypochlorite in 50 ml solution; (B) 6.3 μg ruthenium in 50 ml solution.

REFERENCES

1 W. B. Pollard, *Analyst*, 44 (1919) 94; *Bull. Inst. Min. Metall.*, 223 (1923).
2 See, *e.g.* K. Kodama, *Methods of Quantitative Inorganic Analysis*, Wiley–Interscience, New York, 1963.
3 E. B. Sandell, *Colorimetric Determination of Traces of Metals*, Interscience, New York, 3rd Ed., 1959.
4 F. E. Beamish, *The Analytical Chemistry of the Noble Metals*, Pergamon Press, Oxford, 1966, p. 156.

Analytica Chimica Acta, 65 (1973) 216–219

SHORT COMMUNICATION

o-Hydroxythiobenzhydrazide—a selective reagent for the spectrophotometric determination of ruthenium

S. C. SHOME and P. K. GANGOPADHYAY
Department of Chemistry, Presidency College, Calcutta-12 (India)
(Received 17th November 1972)

Very many organic reagents[1] have been employed for the spectrophotometric determination of ruthenium(III). 1,4-Diphenylthiosemicarbazide[2] and 2,4-diphenylthiosemicarbazide[3] have been used for the determination of ruthenium as chloroform-extractable complexes in the presence of considerable amounts of osmium. Recently, Sur and Shome[4] suggested thiosalicylamide for the gravimetric and spectrophotometric determination of the metal. However, no previous analytical method seems to allow the determination of ruthenium in the presence of the other platinum metals.

In the work described here, the analytical properties of *o*-hydroxythiobenzhydrazide ($HO \cdot C_6H_4CS \cdot NH \cdot NH_2$) were studied. The reagent was found to be very sensitive for the colorimetric determination of ruthenium(III). Further, the compound seems to be unique in the sense that it is suitable for the determination of microamounts of the metal in the presence of large amounts of other platinum metals.

o-Hydroxythiobenzhydrazide in hot solution forms a purple complex with ruthenium(III), which is only partially extractable in chloroform but is completely soluble in 20% ethanol. For quantitative development of the colour, the optimal acidity ranges between 3.0 *M* and 9.0 *M* in hydrochloric acid. The aqueous ethanolic solution of the complex shows maximal absorbance at 540 nm and Beer's law is obeyed over the range 0.44–8.8 μg Ru ml^{-1}.

The reagent forms coloured complexes with several other metals such as copper, iron, vanadium, titanium, molybdenum, selenium, tellurium, gold, platinum, osmium and rhodium. Studies on the determination and separation of these elements are in progress.

Experimental

Apparatus. A Unicam spectrophotometer SP 500 model with 1-cm silica cells was used for the absorbance measurements. All the pH measurements were made with a Cambridge pH meter (Bench model).

Preparation and properties of o-hydroxythiobenzhydrazide. *o*-Hydroxythiobenzhydrazide may be prepared as follows[5]. Dissolve 10 ml of salicylaldehyde (freshly distilled) in 30 ml of ethanol and heat to *ca.* 60°. Add 44 ml of

ammonium polysulphide with vigorous shaking. Boil for 10 min, cool to room temperature and filter. Transfer the filtrate to a separatory funnel, cover with ether and acidify with ice-cold (1:1) hydrochloric acid. Extract the free *o*-hydroxydithiobenzoic acid formed into ether. Wash the dark brown ether layer several times with ice-cold brine and back-extract with several 5-ml portions of 10% hydrazine hydrate solution. The volume of the combined extract should not exceed 50 ml, because of the high solubility of *o*-hydroxythiobenzhydrazide in water. After 30 min just acidify the solution with acetic acid and extract with ether. Recrystallize the *o*-hydroxythiobenzhydrazide obtained by evaporation of ether from tepid water. The pure compound melts at 101–102°.

o-Hydroxydithiobenzhydrazide is appreciably soluble in water and highly soluble in ethanol, benzene, chloroform and various other organic solvents. It is insoluble in petroleum ether. Acids and very dilute alkali have no action on the compound. The reagent should be stored in the dark, preferably below 15°.

Ruthenium solution. Dissolve a known quantity of ruthenium(III) chloride in, and make up to volume with, water containing a little hydrochloric acid to prevent hydrolysis. Standardize the solution by the hydrolytic precipitation method[6]. Prepare weaker solutions by proper dilution with water containing a little hydrochloric acid.

Other standard solutions of different metals used to study the effect of diverse ions were prepared by dissolving weighed quantities of their salts separately in distilled water of dilute hydrochloric acid. Solutions of anions were prepared by dissolving the respective alkali metal salts in water. All the chemicals used were of A.R. grade.

Procedure. Place a measured amount of ruthenium(III) chloride solution in a 25-ml Erlenmeyer flask and make the solution 6.0–8.0 *M* with concentrated hydrochloric acid. Add a measured quantity of alcoholic 0.01 *M* *o*-hydroxythiobenzhydrazide solution. Heat on a boiling water bath for 25–30 min. Cool and transfer quantitatively to a 25-ml volumetric flask with a mixture of water, ethanol and hydrochloric acid, so that the final solution is *ca.* 6.0 *M* with respect to hydrochloric acid and 20% with respect to ethanol. Measure the absorbance at 540 nm against an appropriate reagent blank.

Results and discussion

Absorbance curves. The absorbance spectra of the ruthenium–hydroxythiobenzhydrazide complex in 20% ethanol–6.0 *M* hydrochloric acid media are shown in Fig. 1.

Effect of acidity. The most suitable acidity for the complete development of the complex was determined by adjusting the pH with varying amounts of 10% sodium acetate solution and dilute hydrochloric acid. The absorbances of different solutions were measured at 540 nm against appropriate reagent blanks. The pH of the final solutions was then remeasured. The complex began to form at pH 5.5 and colour development was complete at acidities between 1.0 *M* and 9.0 *M* in hydrochloric acid. The colour was stable in 3.0–9.0 *M* hydrochloric acid for more than 24 h; below 3.0 *M* the complex decomposed very slowly with formation of a black precipitate. However, reproducible results could be obtained in 1.0–3.0 *M* hydrochloric acid if the absorbance was measured within 6 h.

Effect of diverse ions. In the study of the effect of diverse ions, the

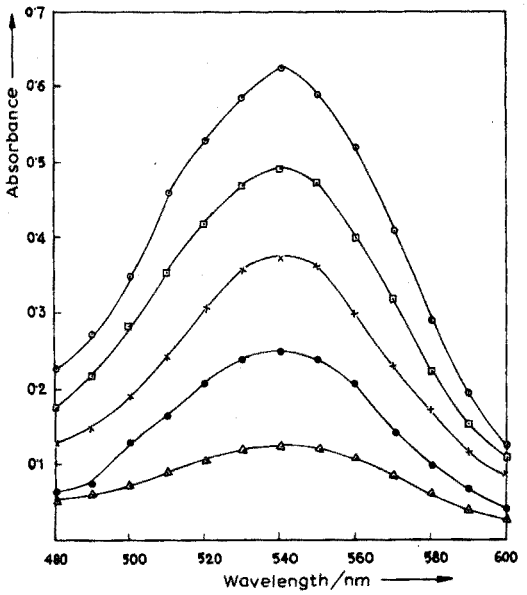

Fig. 1. Absorbance curves for ruthenium-*o*-hydroxythiobenzhydrazide complex. [Ru(III)]: (△) 0.88 μg ml^{-1}. (●) 1.76 μg ml^{-1}. (×) 2.64 μg ml^{-1}. (⊡) 3.52 μg ml^{-1}. (⊙) 4.40 μg ml^{-1}.

standard ruthenium(III) chloride solution containing 109.4 μg of the metal was mixed with a solution of the required metal ion and the acidity was adjusted to 6.0–8.0 *M* with hydrochloric acid. An excess of 0.01 *M* reagent solution was added and the above procedure was then applied. In the presence of copper(II) and iron(III), prior reduction of the metal ions with sulphurous acid was necessary. Table I shows the concentrations of foreign ion that caused an error of less than 2%.

TABLE I

EFFECT OF DIVERSE IONS IN THE DETERMINATION OF RUTHENIUM(III)

(Ruthenium taken = 109.4 μg)

Ion added	*Amount tolerated (μg)*	*Ion added*	*Amount tolerated (μg)*
Ti^{4+}	2000	Re^{7+}	2000
V^{5+}	2000	Os^{6+}	1500
Cr^{3+}	3000	Ir^{3+}	2000
Mn^{2+}	3000	Pt^{4+}	2000
Fe^{3+} [a]	1500	Hg^{2+}	2000
Co^{2+}	1000	Au^{3+}	2000
Ni^{2+}	3000	Tl^{3+}	2000
Cu^{2+} [a]	2000	U^{6+}	2000
Zn^{2+}	5000	Mo^{6+}	1000
Ga^{3+}	5000	W^{6+}	1000
Rh^{3+}	2000	Pd^{2+}	5000
Cd^{2+}	5000	In^{3+}	5000

[a] Prior reduction with sulphurous acid.

Effect of concentration of the reagent. The ruthenium complex was developed fully when the reagent to metal ratio was 15 or more; ruthenium-(III) was reduced to the divalent state by the reagent before complex formation. For this reason, the empirical formula of the complex could not be determined by the mole-ratio method.

Molar absorptivity, sensitivity and optimal concentration. The molar absorptivity was found to be 13,750. The sensitivity of the colour reaction in aqueous ethanol was 0.007 $\mu g\ cm^{-2}$ according to Sandell's notation[7]. The optimal range of concentration of ruthenium (absorbances between 0.2 and 0.7) was 1.4–4.9 $\mu g\ ml^{-1}$.

Accuracy and precision. The relative mean error and the coefficient of variation of the method were found to be 0.48% and 0.85%, respectively.

The authors thank Dr. H. R. Das for helpful discussion.

REFERENCES

1 F. E. Beamish, *Talanta*, 12 (1965) 789.
2 T. Hara and E. B. Sandell, *Anal. Chim. Acta*, 23 (1960) 65.
3 W. Geilmann and R. Neeb, *Z. Anal. Chem.*, 152 (1956) 96.
4 K. Sur and S. C. Shome, *Anal. Chim. Acta*, 48 (1969) 149.
5 K. A. Jensen and C. Pedersen, *Acta Chim. Scand.*, 15 (1961) 1097.
6 R. Gilchrist, *Natl. Bur. Stand. J. Res.*, 3 (1929) 993.
7 E. B. Sandell, *Colorimetric Determination of Traces of Metals*, Interscience, New York, 1959, p. 83.

Analytica Chimica Acta, 65 (1973) 220–222

SHORT COMMUNICATION

Dosage colorimétrique des stéroïdes acétyléniques à l'aide des ions Ag^+

M. RIZK, J. J. VALLON et A. BADINAND

Laboratoire de Chimie Analytique, U.E.R. des Sciences Pharmaceutiques, 8, Avenue Rockefeller, Lyon 8° (France)

(Reçu le 28 novembre 1972)

Les éthinyl-stéroïdes sont une classe de composés d'une grande importance pharmaceutique: principes actifs de la plupart des contraceptifs oraux, ils sont habituellement analysés par spectrophotométrie ultra-violette combinée avec une séparation chromatographique[1,2], ou par colorimétrie de la même manière que les stéroïdes en général. Cependant, la plupart de ces méthodes ne sont pas spécifiques du groupement éthinyl (–C≡CH) qui est le groupement fonctionnel de cette famille de composés.

Pour la détermination des dérivés acétyléniques monosubstitués, la réaction la plus simple est celle avec les métaux et principalement avec l'argent[3]:

$$R\text{–}C{\equiv}CH + Ag^+ \rightleftharpoons RC{\equiv}CAg + H^+ \qquad (1)$$

L'acétylure d'argent formé est précipité, mais en présence d'ions argent(I) en excès, le précipité est redissous:

$$R\text{–}C{\equiv}CH + 2\,AgNO_3 \rightleftharpoons RC{\equiv}CAg \cdot AgNO_3 + HNO_3 \qquad (2)$$

Le principe de cette réaction (2) a été utilisé originellement par Görög[4] pour doser des éthinyl-stéroïdes par titration de l'acide nitrique formé avec une solution standard d'hydroxyde de sodium en présence de pyridine et de thymol-phtaléine comme indicateur. Ou bien, cet acide est titré par potentiométrie avec la solution alcaline en milieu tétrahydrofuranne[5].

Le but de ce travail était de mettre au point une méthode rapide basée sur le même principe et utilisant une petite quantité d'éthinyl-stéroïde de l'ordre de 1 mg; l'addition d'une solution d'ammoniaque diluée déplace la réaction (1) à droite et l'acétylure d'argent est précipité en présence des ions Ag^+ en excès. Ce précipité peut être filtré sur un verre fritté, G4, ou centrifugé; l'argent en excès dans le filtrat peut être dosé colorimétriquement par la méthode à la dithizone[6].

Matériel et méthodes

Stéroïdes. Norethistérone, acétate de norethistérone, lynostéronol, éthinyl-oestradiol, mestranol, norethynodrel.

Courbe d'étalonnage de Ag^+. Diluer dans l'eau à 25 ml, 1 ml d'une solution de nitrate d'argent (0.1‰, p/v). Mélanger dans des ampoules à décantation 0.5,

1, 1.5 ml de cette solution (équivalent à 20, 40, 60 μg de nitrate d'argent) avec 10 ml d'eau et 1 ml d'acide sulfurique 2 *M*; extraire en ajoutant des fractions de 5 ml d'une solution chloroformique de dithizone (0.001%, p/v), agiter vigoureusement pendant 1 min; extraire jusqu'à apparition de la coloration jaune-vert qui indique l'extraction totale de Ag^+ (présence d'un excès de dithizone). Les extraits chloroformiques sont lavés avec 5 ml d'acide sulfurique 0.05 *M*, puis avec des fractions de 5 ml d'une solution ammoniacale dans l'eau (1/1000), jusqu'à ce que la solution de lavage n'ait plus la couleur jaune.

Diluer les solutions chloroformiques de dithizonate d'argent à 20 ml avec du chloroforme dans des fioles jaugées; mesurer l'absorbance de chacune à 472 nm et tracer la courbe d'étalonnage (la coloration suit la loi de Beer).

Dosage du stéroïde. Transférer 1 ml d'une solution alcoolique de stéroïde équivalent à 1 mg dans une fiole jaugée de 25 ml; on ajoute d'abord 4 gouttes d'une solution ammoniacale dans l'eau (1/25), puis 1.5 ml de la solution aqueuse 0.1% de nitrate d'argent (= 1.5 mg $AgNO_3$), agiter le mélange et abandonner environ 5 min. Compléter au volume avec de l'eau distillée, agiter et filtrer sur verre fritté, G4. Rejeter les premiers 5 ml du filtrat.

Mesurer exactement 0.5 ml du filtrat clair dans une ampoule à décantation et procéder au dosage de l'argent en excès avec la même méthode que précédemment.

En se reportant à la courbe d'étalonnage, on obtient la quantité d'argent en excès; on peut alors calculer la quantité d'argent équivalent à l'éthinyl-stéroïde par soustraction de la quantité totale de nitrate d'argent ajoutée:

1 mg de nitrate d'argent équivaut à: 1.827 mg de mestranol, 2.004 mg d'acétate de norethistérone, 1.756 mg de norethistérone, 1.756 mg de norethynodrel, 1.723 mg de lynostéronol, 1.715 mg d'éthinyl-oestradiol.

Résultats et discussion

Cette méthode d'analyse a été d'abord appliquée à des quantités semblables de stéroïdes, par exemple, à 1 ml de solution alcoolique d'acétate de norethistérone $3 \cdot 10^{-3}$ *M* (environ 1 mg). On ajoute 1, 2, 3 ml de solution $3 \cdot 10^{-3}$ *M* de nitrate d'argent; la réaction n'est pas équimoléculaire et, par suite, la précipitation complète de l'acétylure d'argent n'est obtenue que lorsque la quantité de nitrate d'argent ajoutée en excès est triple de celle du stéroïde, c'est-à-dire 3 ml d'$AgNO_3$ $3 \cdot 10^{-3}$ *M* (Tableau I).

Des essais ont été faits avec des quantités de stéroïde inférieures à 1 mg; le précipité formé est dans un état colloïdal et ne peut pas être filtré parfaitement.

TABLEAU I

INFLUENCE DE L'EXCÈS DE $AgNO_3$ SUR LES RÉSULTATS DU DOSAGE DE L'ACÉTATE DE NORETHISTÉRONE[a]

Acétate de norethistérone $3 \cdot 10^{-3}$ *M* (ml)	1.0	1.0	1.0	1.0	1.0	1.5	2.0
$AgNO_3$ $3 \cdot 10^{-3}$ *M* (ml)	1.0	1.5	2.0	3.0	4.0	5.0	6.0
Récupération (%)	72	82	96.5	100.5	98.5	95.5	98.0

[a] Moyenne de trois essais.

TABLEAU II

DOSAGE DE DIVERS STÉROÏDES ACÉTYLÉNIQUES

Stéroïdes	*Récupération (%)*	*Erreur (%)*
Acétate de norethistérone	102	±2
	98	
	98	
Norethistérone	97.8	±1.4
	99.6	
	98.5	
Norethynodrel	98.0	±1.8
	98.5	
	98.0	
Lynostéronol	99.4	±2.5
	103.4	
Mestranol	98.4	±1.6
	98.4	
Ethinyl-oestradiol	97.5	±3.8
	104.5	
	104.7	

En conséquence, la méthode n'est valable que pour des quantités de plus de 1 mg de stéroïde.

Comparée avec notre méthode (Tableau II), la méthode de Görög[4] basée sur le même principe, ne s'applique qu'à des quantités de stéroïde supérieures à 10 mg. En outre, le point final observé n'est pas net, de sorte que l'erreur est voisine de ±8% pour des quantités de 10 mg. L'erreur est voisine de ±1.5% pour des quantités de 30 mg. La méthode de la Pharmacopée Britannique n'est applicable, elle aussi, qu'à des quantités de l'ordre de 200 mg de stéroïde.

Le Tableau II montre les résultats obtenus pour les différents éthinyl-stéroïdes présents généralement dans les contraceptifs oraux.

BIBLIOGRAPHIE

1 G. R. Keay, *Analyst*, 93 (1968) 28.
2 S. Klein, A. E. James et M. M. Tuckerman, *J. Amer. Pharm. Assoc., Sci. Ed.*, 49 (1960) 314.
3 N. D. Cheronis et T. S. Ma, *Organic Functional Group Analysis*, Wiley–Interscience, New York. 1964, p. 385.
4 S. Görög, *Acta Chim. Acad. Sci. Hung.*, 47 (1966) 1.
5 *British Pharmacopeia*, 1968, p. 664.
6 E. B. Sandell, *Colorimetric Metal Analysis*, Interscience, New York, 3e Ed., 1959, p. 816.

Analytica Chimica Acta, 65 (1973) 223–226

SHORT COMMUNICATION

Determination of thorium in titanium and zirconium concentrates

P. PAKALNS

Australian Atomic Energy Commission, Research Establishment, Lucas Heights, N.S.W. 2232 (Australia)

(Received 23rd October 1972)

Arsenazo-III is a sensitive and selective reagent for spectrophotometric determination of thorium, but high concentrations of titanium(IV) and zirconium(IV) cause serious interference[1] which prevents direct application of arsenazo-III to the determination of thorium in titanium and zirconium concentrates.

A simple separation of thorium before its determination with arsenazo-III has been reported[2] in which iron, uranium, zirconium and other metal ions are removed by extraction with Alamine-336 (a long-chain tertiary amine) from 9 *M* hydrochloric acid. Unfortunately, most of the titanium remains in the aqueous phase with thorium, and despite modifications[2] to the arsenazo-III method the amount of titanium that can be tolerated in the sample is severely limited.

Aliquat-336, a long-chain quaternary amine, was found to be much more efficient than Alamine-336 for the extraction of titanium(IV) from hydrochloric acid media (87% extraction from 10 *M* hydrochloric acid) and its use allows thorium to be determined in rutile and titanium concentrates. In addition, the extraction coefficient of 150 for zirconium from 10 *M* hydrochloric acid is sufficiently high for most of the zirconium to be extracted into the organic phase. The remaining traces of zirconium can be masked with oxalic acid.

Reagents

Aliquat-336 solution, 10%. Add 10 ml of Aliquat-336 (tricaprylmethylammonium chloride, General Mills Chemical Division, Kankakee, Ill) and 6 ml of nonanol to 84 ml of white spirit and mix. Cyclohexane may be used instead of white spirit.

White spirit (s.g. 0.776, i.b.p. 148°, f.b.p. 196°, aromatics 19, aniline point 54°; Shell Co. of Aust. Ltd) was used. Other kerosene grades such as heating kerosene and Shellsol-T cannot be used because a third phase is formed giving lower extraction coefficients for titanium.

Arsenazo III solution and thorium solutions the same as described previously[2].

Recommended procedure

Transfer 5.00 ml of sample solution (6 *M* in hydrochloric acid) to a 50-ml separating funnel. Add 15.00 ml of 12 *M* hydrochloric acid and mix. Add 20 ml of 10% Aliquat-336 solution and shake for 2 min. Allow the phases to separate and

continue as recommended previously[2]. A second extraction may be required, see Results and discussion. The absorbance of a blank carried through the extraction procedure was negligible.

Sample preparation

Weigh 0.5 g of concentrate sample (−200 mesh) into a 50-ml platinum crucible. Add 2.5 g of sodium peroxide and mix. Sinter at 480±20° for 1 h. Dissolve the sinter in 150 ml of water and boil the solution for 15 min. Cool. Filter through a fast 12.5-cm filter paper (Whatman 541). Wash the precipitate with 50 ml of 2% sodium hydroxide solution, then dissolve it in 60 ml of hot 8 *M* hydrochloric acid. Boil the solution until the volume is reduced to 45 ml. Cool. Transfer it into a 50-ml volumetric flask and dilute to the mark with 6 *M* hydrochloric acid. Continue as in the Recommended procedure.

Results and discussion

The extraction coefficients E_a° for titanium extracted by Alamine-336 in diethylbenzene and Aliquat-336 in diethylbenzene–tridecanol from 10 *M* hydrochloric acid have been reported as 10^{-2} and 1, respectively[3]. Solvents such as white spirit, household kerosene, Shellsol-T, cyclohexane, and toluene were investigated as diluents for Aliquat-336. It was found that white spirit and cyclohexane were suitable diluents only after they were modified with nonanol to prevent the separation of the amine chloride salt from the diluent as a third liquid phase at high chloride concentrations. Toluene could be used as a diluent without modification, but high and non-reproducible blanks were obtained when more than 5-ml aliquots were taken for the spectrophotometric determination of thorium, and the E_a° of 1.4 is too low for efficient extraction of titanium.

The extraction coefficient of 6.7 for titanium extracted with 10% Aliquat-336–6% nonanol in white spirit from 10 *M* hydrochloric acid (Table I) is high enough to eliminate any titanium interference when concentrates containing not more than 15% of titanium are analysed for thorium. Second extractions with

TABLE I

EXTRACTION COEFFICIENT E_a° FOR TITANIUM AND ZIRCONIUM USING ALIQUAT-336 EXTRACTANT

HCl (M)	*10% Aliquat-336 in toluene*		*10% Aliquat-336 in 6% nonanol–white spirit*	
	E_a° *of titanium*[a]	E_a° *of zirconium*[b]	E_a° *of titanium*[a]	E_a° *of zirconium*[b]
9	0.45	100	1.9[c]	44[d]
10	1.4	150	6.7[c]	150[e]

[a] 1.5 mg of titanium.
[b] 30 mg of zirconium.
[c] The same value was obtained with cyclohexane diluent.
[d] $E_a^\circ = 22$ for cyclohexane diluent.
[e] $E_a^\circ = 100$ for cyclohexane diluent.

fresh 10%-Aliquat-336–6% nonanol solution will allow thorium to be determined in rutile and mineral concentrates which are higher in titanium. The saturation capacity is 100 mg of titanium per 20 ml of extractant.

Zirconium interferes slightly in the spectrophotometric procedure and 700 μg of zirconium produces a colour equivalent to 1 μg of thorium (20 μg of zirconium = 0.001 absorbance in 4-cm cells). However, when sample aliquots containing as much as 30 mg of zirconium are separated by solvent extraction with 10% Aliquat-336–6% nonanol in white spirit, the aqueous phase contains only 200 μg of zirconium which, for a 10-ml aliquot in the spectrophotometric method, will produce an absorbance of only 0.005. Double extraction completely eliminates the interference of zirconium. The extraction coefficient for zirconium with cyclohexane as diluent is smaller than with white spirit (Table I).

Rare earths interfere slightly and an error equivalent to 1 μg of thorium is given by 370 μg Y, 250 μg Ce(IV), 100 μg La and 450 μg Lu.

TABLE II

DETERMINATION OF THORIUM IN TITANIUM AND ZIRCONIUM CONCENTRATES AND ZIRCONIUM METAL AND SALTS

Material	*Th (p.p.m.)*
90% zircon plus garnet, rutile and tourmaline[a]	1040
Zircon flour	149
Zircon product, uncalcined	221[b]
Zircon product, calcined ceramic	183
Heavy mineral concentrate[c]	320
Rutile, sample 1	44[b]
Rutile, sample 2	38
Ilmenite	41
Magnetite–ilmenite	80
$ZrOCl_2 \cdot 8\ H_2O$ (AR)[d]	20
$Zr(NO_3)_4$(comm.)[d]	23
$Zr(SO_4)_2$(comm.)[d]	46
Zircaloy II[e]	191

[a] Titanium 1.1%.
[b] Standard additions of 5 μg of thorium were made before extraction and the recoveries were 100 ± 2%.
[c] Rutile 35%, zircon 34%, ilmenite 23%, garnet 4%, chrome 2.4%, monazite 0.4%, black magnetic zircon 0.4%.
[d] 30 mg of metal used for extraction.
[e] 0.5 g metal dissolved in 1 ml 40% HF + 8 ml 4.5 *M* H_2SO_4. Fumed and diluted to 50 ml with water. A 3-ml aliquot and 17 ml of 12 *M* HCl were used for extraction.

Results of thorium determinations on various materials containing titanium and zirconium are shown in Table II. The standard deviation of the results obtained on twelve portions of rutile sample 2 (38 p.p.m. Th) was ±2.6 p.p.m. Th. The variation in absorbance for thorium standards (1–10 μg) carried through the recommended procedure was less than ±0.005.

REFERENCES

1 S. B. Savvin, *Talanta*, 8 (1961) 673.
2 P. Pakalns, *Anal. Chim. Acta*, 58 (1972) 463.
3 F. G. Seeley and D. J. Crouse, *J. Chem. Eng. Data*, 11 (1966) 424.

Analytica Chimica Acta, 65 (1973) 227–230

SHORT COMMUNICATION

Determination of isonicotinic acid hydrazide in pharmaceutical preparations

P. V. KRISHNA RAO, G. BALA BHASKARA RAO and R. SAMBASIVA RAO
Department of Chemistry, Andhra University, Waltair (India)
(Received 10th November 1972)

Isonicotinic acid hydrazide (Isoniazid) is an extremely valuable antitubercular agent in chemotherapy. Most of the titrimetric[1–13] and colorimetric[14–17] procedures reported in the literature have received little attention, because the commonly used excipients interfere. The hydrazino group is susceptible to oxidation, and most titrimetric procedures are based on this property. Titration with potassium bromate[3] is considered to be the best method, although Kuhni *et al.*[9] stated that titration with 0.05 *N* potassium bromate gave results that were 0.5% high. Gowda and Gopala Rao[18] proposed sodium vanadate for the indirect oxidimetric determination of isoniazid, claiming advantages over the iodimetric and bromometric methods. Recently, a potentiometric assay of isoniazid based on titration of standard vanadium(V) solution in 0.75–2.0 *N* orthophosphoric acid medium in presence of osmium tetroxide, was reported[19]. Under the conditions used, all the hydrazino-nitrogen was stoichiometrically liberated, but a direct potentiometric titration of isoniazid with vanadate was impracticable because of unstable potentials.

In continuation of this work, it was found that a direct titration of isoniazid alone and in presence of the commonly used excipients in pharmaceutical preparations, was possible with vanadium(V) in phosphoric acid medium even in the absence of osmium tetroxide, provided that a photometric procedure was adopted. With the proposed method, there is no interference from oxalic acid and chromium-(III), which interfered in the potentiometric method. The advantages of photometric titration procedures have been described by Underwood[20] and Headridge[21].

Experimental

Equipment. A Klett–Summerson photoelectric colorimeter with a rectangular glass cell (2 × 4 × 8 cm) and a red filter (maximum transmission 660 nm) was used. Stirring was provided by a stream of carbon dioxide from an inlet tube placed in a corner of the cell.

Sodium vanadate solution. Approximately 0.1 *M* sodium metavanadate was prepared by boiling AnalaR ammonium metavanadate with a slight excess of sodium carbonate, and standardized against Mohr's salt which in turn was standardized against AnalaR potassium dichromate.

Isonicotinic acid hydrazide (Isoniazid) solution. A 0.025 *M* solution was prepared from a U.S.P. grade material which had been twice recrystallized from

water and dried at 110°. The solution was stored in an amber coloured bottle and standardized by the bromate method[3].

The orthophosphoric acid used (p.a., Merck) was found to be relatively free from other reducing impurities. All other chemicals were of analytical-reagent grade. All solutions were prepared in deionized water.

Recommended procedure. Transfer 2–10 ml (7–35 mg) of isoniazid solution to the optical cell. Add 8–16 ml of syrupy orthophosphoric acid and dilute to 30 ml. Allow to cool to room temperature and place the cell in the colorimeter. Titrate with standard 0.1 *M* sodium vanadate, adding small aliquots from a microburette and mixing the solutions well. Measure the colour of the vanadium(IV) formed 1 min after stopping the passage of carbon dioxide. Multiply the dial readings of the colorimeter (absorbance $\times 500$) by the factor $(V+v)/V$ where V is the volume of the reaction mixture and v is the volume of titrant added each time, to account for the dilution effect on the absorbance readings. Plot the corrected dial readings against the volume of sodium vanadate solution. A typical titration curve is shown in Fig. 1. The point of intersection corresponds to the amount of vanadate consumed for the stoichiometric oxidation of isonicotinic acid hydrazide to isonicotinic acid and nitrogen.

Interferences. Starch, dextrin, dextrose, gum acacia and oxalic acid do not interfere even when present in 50-fold (weight) amounts.

Application to the analysis of pharmaceutical preparations. The reliability of the new method in the assay of isoniazid in tablets was tested by comparing the results obtained with those by the official B.P. method[22].

Dissolve three 300-mg tablets (Nydrazid, Isonex or Isokin, from Squibb Pharmaceuticals, Dumex Pharmaceuticals or Warner Hindustan Ltd, respectively) in deionized water and filter through a G4 sintered glass crucible. Make up the filtrate to 250 ml. Titrate aliquots as in the recommended procedure.

Results and discussion

Representative results from a large number of titrations for the determination

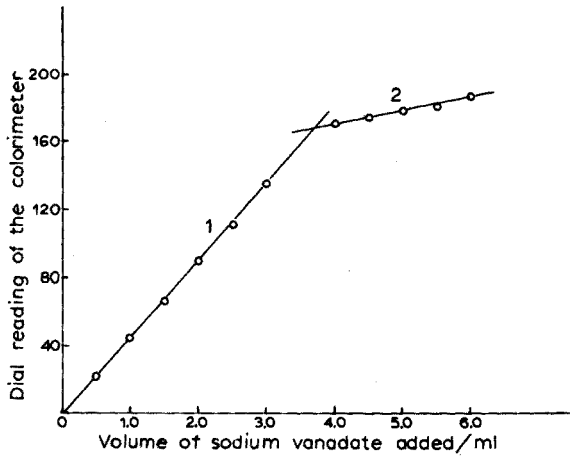

Fig. 1. Photometric titration of isoniazid with sodium vanadate at 660 nm.

TABLE I

TITRIMETRIC DETERMINATION OF ISONIAZID WITH VANADIUM(V)

Isoniazid (mg)	Taken	7.32	12.67	22.56	31.85
	Found	7.25	12.76	22.45	31.72

TABLE II

ASSAY OF ISONIAZID IN PHARMACEUTICAL PREPARATIONS

Tablet	*Amount of isoniazid found (wt.%)*	
	B.P. method	*Proposed method*
Nydrazid	98.95	99.00
	98.47	99.00
	99.44	99.58
	99.90	99.97
Isonex	99.98	99.10
	99.96	99.30
	99.91	99.25
	99.99	99.28
Isokin	97.02	96.65
	97.34	96.65
	97.46	97.79
	97.59	97.05

of isoniazid alone and in presence of excipients by the recommended procedure are given in Tables I and II. It can be seen that this titration of isoniazid can be carried out with an error permissible in any photometric procedure. The use of phosphoric acid as the medium affords a rapid direct titration, which was found to be not feasible in sulphuric, hydrochloric or perchloric acid media. The results in Table II show that the new method can be applied to the routine analysis of isoniazid in pharmaceutical preparations with results similar to those by the official titrimetric method.

Two of us (G.B.B.R. and R.S.R.) thank, respectively, the University Grants Commission and the Council of Scientific and Industrial Research, India, for the award of research fellowships. We are also grateful to Prof. G. Gopala Rao for his helpful suggestions and keen interest in this work.

REFERENCES

1 E. A. Haugas and B. W. Mitchell, *J. Pharm. Pharmacol.*, 4 (1952) 687.
2 J. Vulterin, *Collect. Czech. Chem. Commun.*, 28 (1963) 1391.
3 J. Vulterin and J. Zyka, *Chem. Listy*, 48 (1954) 1745.
4 J. Zyka, *Chem. Listy*, 48 (1954) 1754.
5 J. Vulterin, *Thesis*, Charles University, Prague, 1961.
6 J. Laszlovszky, *Acta Pharm. Hung.*, 30 (1960) 101.
7 P. Spacu and G. Teodorescu, *Rev. Chim. Bucur.*, 8 (1957) 42.

8 F. Jancik, O. Cinkova and J. Korbl, *Collect. Czech. Chem. Commun.*, 24 (1959) 2695.
9 E. Kuhni, M. Jacob and H. Grossglauser, *Pharm. Acta Helv.*, 29 (1954) 233.
10 A. Berka and J. Zyka, *Chem. Listy*, 50 (1956) 314.
11 M. Z. Barakat and M. Shaker, *Analyst*, 91 (1966) 466.
12 J. A. C. Van Pinxteren and M. E. Verloop, *Pharm. Weekbl. Ned.*, 99 (1964) 1125.
13 M. B. Devani and C. J. Shishoo, *J. Pharm. Sci.*, 59 (1970) 90.
14 Naito, Takio, H. Shirai and N. Oda, *Bull. Nagoya City Univ. Pharm. Sch.*, 3 (1955) 34.
15 B. Brettoni, *Arch. Ital. Sci. Farmacol.*, 2 (1955) 227.
16 G. Machek, *Sci. Pharm.*, 24 (1956) 11.
17 H. Erlenmeyer and S. Fallab, *Experientia*, 8 (1952) 298.
18 H. S. Gowda and G. Gopala Rao, *Z. Anal. Chem.*, 165 (1959) 36.
19 P. V. Krishna Rao and G. Bala Bhaskara Rao, *Analyst*, 96 (1971) 712.
20 A. L. Underwood, *Anal. Chem.*, 26 (1954) 1322.
21 J. B. Headridge, *Talanta*, 1 (1958) 293.
22 *The British Pharmacopeia*, Pharmaceutical Press, London, 1963, p. 429.

Analytica Chimica Acta, 65 (1973) 231–235

SHORT COMMUNICATION

Titration of arsenic(III) with cerium(IV) sulphate in presence of diphenylamine-type indicators

MURALIKRISHNA GANDIKOTA and G. GOPALA RAO
Department of Chemistry, Andhra University, Waltair (India)
(Received 16th November 1972)

The revival of diphenylamine and its derivatives as redox indicators for cerium(IV) titrations may need some excuse. The use of ferroin in the titration of arsenic(III) with cerium(IV) sulphate as described by Willard and Young[1] is not very satisfactory. The titration cannot be made accurately at room temperature because of the slowness of the reduction of ferriin (oxidized ferroin) by arsenic(III) near the equivalence point; hence the titration should be done at room temperature until this difficulty is experienced and then the mixture must be heated to 50° before the titration is continued. Even at this temperature the titration must be done slowly. The temperature cannot be too high because of the risk of dissociation of the ferroin complex, and if the temperature falls to 45° during titration, the mixture must be reheated.

Ferroin does not function quite satisfactorily even in the procedure of Gleu[2] who proposed that the titration be done in 0.5 *M* sulphuric acid with osmium tetroxide as catalyst. It is of interest to note that ferriin is not reduced by arsenic(III) alone; in the presence of the osmium catalyst only a faint red color appears, but as soon as a drop of cerium(IV) solution is added, the deep red color of ferroin appears. Obviously, the osmium-catalysed cerium(IV)–arsenic(III) reaction induces the reduction of ferriin by arsenic(III). Thus there is a need for a reversible indicator which does not require so much care as ferroin. It has been found in these laboratories that the Willard and Young and Gleu procedures prove troublesome to inexperienced students. We have, therefore, carried out an extensive investigation on the use of diphenylamine, diphenylbenzidine, diphenylaminesulphonic acid, and N-phenylanthranilic acid in this titration, and established conditions for their successful use in the accurate titration of arsenic(III) by cerium(IV) sulphate in sulphuric acid media.

The molar absorptivity of the oxidation product of diphenylamine has been recently reported[3] as 45,000 l mol^{-1} cm^{-1}, a value much higher than that of ferroin, 11,000 l mol^{-1} cm^{-1} as determined by Moss *et al.*[4]. In the proposed titration a very small amount of diphenylamine (0.2 ml of 0.005 *M* (*ca.* 0.1%) solution) was found to give a vivid blue-violet color at the end-point to 50 ml of the titration mixture. This indicates that in titrations with 0.1 *M* solutions of cerium(IV) sulphate, the indicator correction is small. In the past some investigators have used

unnecessarily high concentrations of the indicator in titrations of iron(II) with potassium dichromate, which led to such difficulties as high indicator corrections, formation of green colors, etc. In the present method, the end-point color was found to be stable for more than 30 min, and it could be reversed to and fro a number of times. Diphenylamine could also be used in the reverse titrations. The oxidation of diphenylamine to blue-violet diphenylbenzidine by cerium(IV) was very rapid, but the reduction of the blue oxidation product by arsenic(III) was slow. However, it was observed that this reaction was markedly catalysed by traces of iodine, iodide, and iodate. The use of iodine did not necessitate any correction, whereas iodide involved a positive correction and iodate a negative correction. Iodine monochloride did not prove satisfactory.

When 0.5 ml of the catalyst mixture was used per 50 ml, the reduction of the oxidized indicator was not sufficiently rapid for a quick titration; 1–2 ml was adequate. Higher amounts created difficulty in locating the end-point. As the iodine catalyst was left in the mixture in the same condition as originally taken, no correction for the catalyst was necessary.

Experimental

Reagents. A 0.1 *N* solution of arsenic(III) was prepared by dissolving AnalaR arsenic trioxide in 0.6 *M* sodium hydroxide solution, making slightly acidic (*ca.* 0.15 *M*) with sulphuric acid, and making up to the desired volume. It was standardized with 0.1 *M* potassium permanganate by Bright's[5] procedure. The weight purity and the assay purity agreed to within $\pm 0.1\%$.

A 0.1 *M* cerium(IV) sulphate solution in 0.5 *M* sulphuric acid was prepared and standardized by the method of Willard and Young[6].

The catalyst mixture was prepared by mixing 20.8 ml of 0.1 *M* potassium iodide and 4.16 ml of 0.1 *M* potassium iodate in a 250-ml volumetric flask and diluting to the mark; 1 ml of this solution was found to be satisfactory for 50 ml of titration mixture.

Indicator solutions. 0.1% solutions of diphenylamine and diphenylbenzidine were prepared in concentrated sulphuric acid free from traces of nitric acid. A 0.1% solution of barium diphenylamine sulphonic acid was prepared in water. A 0.2% solution of N-phenylanthranilic acid was prepared as described by Bishop and Crawford[7]. For 50 ml of titration mixture, 0.1 ml of the N-phenylanthranilic acid solution and 0.2 ml of the other indicator solutions were found to give vivid color changes at the end-points. With these amounts of indicators, the indicator corrections were negligible for 0.1 *N* solutions. Table I gives the indicator corrections for higher amounts of indicators.

Procedure. Treat 5–9 ml of arsenic(III) solution with sulphuric acid to give an overall acidity of 1–4 *N* when diluted to 50 ml. Add 1.0 ml of the catalyst mixture and the indicator solution. Titrate with 0.1 *M* cerium(IV) sulphate solution at the usual speed, except in the case of barium diphenylamine sulphonate where a wait of 10 s between drops is necessary for the last 0.2 ml of the oxidant. Representative results are presented in Table II.

Interferences. Iron(III) (0.2–2.0 meq), nickel(II) (0.2–1.0 meq), cobalt(II) (0.2–2.0 meq), copper(II) (0.2–1.0 meq) and manganese(II) (0.5–2.0 meq) did not interfere.

TABLE I

INDICATOR CORRECTIONS IN THE TITRATION OF ARSENIC(III) WITH CERIUM(IV) SULPHATE

Indicator	*Amount of indicator (ml of 0.1% solution)*	*Indicator correction (ml of 0.1 M Ce(IV))*
Diphenylamine	1.0	0.08
	0.5	0.04
	0.2	Negligible
Barium diphenylamine sulphonic acid	0.4	0.02
	0.2	Negligible
N-Phenylanthranilic acid	0.2	0.02
	0.1	Negligible

TABLE II

TITRATION OF ARSENIC(III) WITH CERIUM(IV) SULPHATE

Indicator	*Arsenic(III) (meq)*		*Indicator*	*Arsenic(III) (meq)*	
	Taken	*Found*		*Taken*	*Found*
Diphenylamine	0.5999	0.5990	Barium diphenylamine sulphonic acid	0.5000	0.5000
	0.7197	0.7197		0.6198	0.6198
	0.8098	0.8110		0.6998	0.7008
	0.8300	0.8299		0.8999	0.8999
	0.8999	0.8999	N-Phenylanthranilic acid	0.4200	0.4206
	0.9099	0.9099		0.4977	0.4977
Diphenylbenzidine	0.5218	0.5218		0.6097	0.6098
	0.6977	0.6985		0.8299	0.8308
	0.7998	0.7998			
	0.8999	0.8999			

Reverse titrations. Excellent results were obtained in the titration of cerium(IV) with arsenic(III) if the diphenylamine indicator was added when most of the yellow color of the cerium(IV) had disappeared. The color change at the end-point was blue violet to very light yellow which was due to the iodine catalyst. The volume of arsenic(III) solution added had to be corrected by adding 0.02 ml of 0.1 *N* solution. When diphenylamine was added from the start, the volume of arsenic(III) had to be corrected by subtraction of 0.04 ml of 0.1 *N* solution. In this case, the color change was from light green to very light yellow.

Titrations of 0.01 N solutions of arsenic(III). More dilute (0.01 *N*) solutions of arsenic(III) could be accurately titrated with 0.01 *M* solutions of cerium(IV) sulphate in the presence of 0.2 ml of 0.1% diphenylamine, provided that an indicator correction of 0.2 ml of 0.01 *M* cerium(IV) sulphate was deducted.

Titrations of arsenic(III) in hydrochloric acid medium. Willard and Young[8] stated that diphenylamine was not satisfactory in the titration of arsenic(III) with cerium(IV) sulphate, without giving details. When titrations were done in 3.6 *M* hydrochloric acid with 5 ml of iodine monochloride solution as catalyst—the

conditions used by Willard and Young—it was observed that the reduction of oxidized indicator was slow towards the end-point requiring a wait of 20 s between drops. Moreover the results were not reproducible. Reducing the amount of iodine monochloride solution to 2 ml greatly decreased the speed of reduction of the oxidized indicator. Titrations carried out in 1 *M* and 2 *M* hydrochloric acid with varying amounts of iodine monochloride were also unsatisfactory. Titrations were carried out in 1 *M* and 2 *M* hydrochloric acid with the iodate–iodide catalyst, but the results were again irreproducible. Evidently diphenylamine is unsatisfactory as a redox indicator for the titration of arsenic(III) in hydrochloric acid medium. Success with this indicator is due to the use of sulphuric acid as the medium and iodine as catalyst.

Differential titration of iron(II) and arsenic(III). It was observed that iron(II) and arsenic(III) could be titrated in the same solution in sulphuric acid medium if 2–3 ml of syrupy phosphoric acid was added per 50 ml of the titration mixture. After the iron(II) end-point, 1 ml of the catalyst mixture was added and the titration completed. The volume of cerium(IV) between the first and second end-points corresponded to arsenic(III). However, the second end-point required a negative correction of 0.03 ml of 0.1 *M* cerium(IV) solution to give an accurate assay of the arsenic(III). Table III gives some typical results.

TABLE III

DIFFERENTIAL TITRATION OF IRON(II) AND ARSENIC(III)

Amount of iron(II) (meq)		*Amount of arsenic(III) (meq)*	
Taken	*Found*	*Taken*	*Found*
0.5999	0.5999	0.2000	0.2000
0.7997	0.7997	0.3000	0.2998
0.9997	1.0007	0.4997	0.5003
1.1990	1.1990	0.5599	0.5606
1.4000	1.4020	0.5999	0.6010
1.6000	1.6020	0.6998	0.7008

Conclusion

Diphenylamine, diphenylbenzidine, barium diphenylaminesulphonate, and N-phenylanthranilic acid are satisfactory as indicators in titrations of arsenic(III) with cerium(IV) sulphate if a suitable catalyst is used. Compared with ferroin, these indicators possess the advantages of giving vivid color changes at the end-point, and ease of titration even in inexperienced hands. The indicator corrections are negligible with 0.1 *M* cerium(IV) sulphate solution. The colors of the oxidized indicators are stable for a long time and the indicator actions are reversible.

REFERENCES

1 H. H. Willard and P. Young, *J. Amer. Chem. Soc.*, 55 (1933) 3260.
2 K. Gleu, *Z. Anal. Chem.*, 95 (1933) 305.

3 E. Bishop and L. G. Hartshorn, *Analyst*, 96 (1971) 26, 36.
4 M. L. Moss, M. G. Mellon and G. P. Smith, *Ind. Eng. Chem., Anal. Ed.*, 14 (1942) 931.
5 H. A. Bright, *Ind. Eng. Chem., Anal. Ed.*, 9 (1937) 577.
6 H. H. Willard and P. Young, *J. Amer. Chem. Soc.*, 50 (1928) 1322.
7 E. Bishop and A. B. Crawford, *Analyst*, 74 (1949) 365.
8 H. H. Willard and P. Young, *J. Amer. Chem. Soc.*, 50 (1928) 1375.

Analytica Chimica Acta, 65 (1973) 236–239

SHORT COMMUNICATION

Determination of mercaptans by titration with lead tetraacetate

KRISHNA K. VERMA and SAMEER BOSE

Department of Post-Graduate Studies and Research in Chemistry, University of Jabalpur, Jabalpur, M.P. (India)

(Received 24th October 1972)

A rapid and precise titrimetric method for the determination of mercaptans is described. In anhydrous acetic acid medium, mercaptans are oxidized by lead tetraacetate to disulfides[1], according to the reaction:

$$2RSH + Pb(OAc)_4 \rightarrow RSSR + Pb(OAc)_2 + 2HOAc$$

Tomiček and Valcha[2] have already referred to this reaction, and Suchomelova and Zyka[3] used it for titration of a few mercaptans.

The reaction is immediate and its end-point may be determined visually with quinalizarin as indicator[2], the color changing from red to blue. In potentiometric titrations, the equivalence point is shown by a large potential change (about 250 mV for 0.05 ml of a 0.05 *M* lead acetate solution); the potential at the inflexion is in the region of 400 mV *vs.* S.C.E. A large number of mercaptans can be determined by this method.

Experimental

Reagents and apparatus. Lead tetraacetate solution (0.05 *M*) was prepared by dissolving *ca.* 23.0 g of acetic acid-soaked tetraacetate salt[4] in 1 l of anhydrous acetic acid; it was standardized iodimetrically[5]. Most of the mercaptans were gifts from Evans Chemetics, New York, U.S.A. Some samples were prepared and purified[6] by the authors.

Potentiometric titrations were performed with Toshniwal titration potentiometer type CL 06, equipped with a fiber-type saturated calomel electrode and a bright platinum electrode. For visual indication 5–10 drops of a 0.2% solution of quinalizarin (1, 2, 5, 8-tetrahydroxyanthraquinone) in anhydrous acetic acid was used.

Visual procedure. Weigh the sample containing 0.1–1.0 mmole of mercaptan into a 100-ml Erlenmeyer flask containing 15 ml of solvent and add about 0.5 ml of quinalizarin solution to make the solution orange-red. Titrate with 0.05 *M* lead tetraacetate solution from a 10-ml microburet, to a blue color.

Potentiometric procedure. Weigh the sample containing 0.1–1.0 mmole of mercaptan into a 100-ml beaker containing 40 ml of solvent and titrate potentiometrically with 0.05 *M* lead tetraacetate, using a platinum indicating electrode and a

saturated calomel reference electrode. The point of equivalence is shown by a large potential jump.

Choice of titration solvents. Anhydrous acetic acid is the medium of choice for oxidimetry with lead tetraacetate; also, it is an excellent solvent for all types of mercaptans and their disulfides. Ethanol reacts with tetraacetate and gives high results. A mixed solvent of acetic acid with methanol can be used in all proportions. Acetic acid–benzene, acetic acid–toluene and acetic acid–petroleum ether solvents containing less than 60% (v/v) of hydrocarbon may be used without causing precipitation. Water, if present, should not exceed 6% of the total solvent.

Results

Quantitative results for the visual titration of several mercaptans are given in Table I. As a check, mercaptans were determined by independent methods and the values agreed within analytical precision with those obtained by lead(IV) titration. The results obtained by potentiometric titration agreed with the visual indicator results within ±0.2%.

TABLE I

DETERMINATION OF MERCAPTANS WITH QUINALIZARIN INDICATOR

Compound	*Purity (%)*			
	Present method[a]	*Av. deviation* ±	*Comparison method*	
o-Mercaptobenzoic acid	99.8	0.3	99.5	Hg^{2+} titration[7]
3-Mercaptopropionic acid	100.0	0.0	99.7	Hg^{2+} titration[7]
2-Mercaptopropionic acid	96.4	0.3	96.6	Iodimetry[8]
2-Diethylaminoethanethiol hydrochloride	98.1	0.1	98.1	Iodimetry[8]
2-Butanethiol	97.2	0.2	97.1	Iodimetry[8]
Toluene-α-thiol	98.8	0.3	98.5	Iodimetry[8]
Mercaptoacetic acid	80.1	0.2	80.3	Iodimetry[8]
1-Butanethiol	90.5	0.3	90.5	Iodimetry[8]
Allylthiol	93.2	0.4	93.0	Acetylation[9]
Mercaptosuccinic acid	99.3	0.5	99.1	Hg^{2+} titration[7]
1-Pentanethiol	80.0	0.4	88.2	Iodimetry[8]
2-Mercaptobenzoxazole	98.1	0.0	98.0	Titrated as acid with NaOH

[a] Six determinations.

In the titration of some mercaptans, *e.g.*, mercaptoacetic and mercaptosuccinic acid, a white precipitate appears. It dissolves rapidly near the equivalence point and does not affect the titration or the end-point. In such cases, addition of an extra 10 ml of the solvent is recommended. Under the described conditions of titration, mercaptosuccinic acid yields low results, but this is prevented by using 3% hydrochloric acid solution in anhydrous acetic acid as the medium. Hydrochloric acid and the mercaptan should be present in a molar ratio of about 2:1.

TABLE II

INTERFERENCES

Mercaptan titrated	*Compound added*	*Molar ratio added compd./ RSH*	*RSH recovery (%)*[a]
Toluene-α-thiol	Sulfur	29:1	100.0
	Potassium cyanide[b]	6:1	100.2
	Sulfosalicylic acid	4:1	99.7
	Bromobenzene	53:1	100.2
1-Pentanethiol	Methylacrylate[c]	9:1	100.0
	Thiophene	18:1	100.2
1-Butanethiol	Acetone	31:1	99.7
	Isobutyl methyl ketone	30:1	100.0
	Diethylsulfone	15:1	99.7
	Diphenyl disulfide	36:1	99.8
3-Mercaptopropionic acid	Diacetone alcohol[d]	7:1	100.4
	Diphenyl sulfide	28:1	100.1
2-Mercaptopropionic acid	Maleic acid	3:1	100.2
	Sodium chloride	3:1	100.1
o-Mercaptobenzoic acid	Carbon disulfide	77:1	99.2
	Formic acid	158:1	100.0
	o-Dichlorobenzene	81:1	100.0
	Acrylonitrile[e]	138:1	100.0
	Cinnamic acid	6:1	100.3
	Urea	15:1	100.3

[a] Average of 2 determinations; % recovery takes into account the previously determined purity of sample (Table I).
[b] Molar ratio 25:1 gives 1.5% high results.
[c] Molar ratio 40:1 gives 3% high results.
[d] Molar ratio 57:1 gives 2% high results.
[e] Molar ratio 321:1 gives 1.5% low results.

Interferences

In Table II, results for the determination of mercaptans in the presence of several interfering compounds are given. The interferences studied included compounds that interfere in existing methods, and compounds that contain other sulfur-containing functional groups. The visual indicator method was used in the determinations. Iodide, bromide, sulfide ions and thiocarbonyl compounds interfere seriously. The color change observed was indistinct for samples containing, in addition to the mercaptan function, groups sensitive to oxidation with lead tetraacetate; examples are 2-mercaptoethylammonium chloride, cysteine, 2-mercaptobenzimidazole, etc.

We are grateful to Evans Chemetics, New York, N.Y., for generous gifts of most of the mercaptan samples and to Dr. B. P. Sinha for timely help.

REFERENCES

1 L. Field and J. E. Lawson, *J. Amer. Chem. Soc.*, 80 (1958) 838.
2 O. Tomiček and J. Valcha, *Chem. Listy*, 44 (1950) 283.

3 L. Suchomelova and J. Zyka, *J. Electroanal. Chem.*, 5 (1963) 57.
4 R. E. Oesper and C. L. Deasy, *J. Amer. Chem. Soc.*, 61 (1939) 972.
5 A. Berka, J. Vulterin and J. Zyka, *Newer Redox Titrants*, Pergamon Press, Oxford, 1965, p. 78.
6 A. I. Vogel, *A Text-book of Practical Organic Chemistry*, Longmans, London, E.L.B.S. Ed., 1968, p. 197.
7 J. S. Fritz and T. A. Palmer, *Anal. Chem.*, 33 (1961) 98.
8 J. W. Kimball, R. L. Kramer and E. E. Reid, *J. Chem. Soc.*, 43 (1921) 1199.
9 G. H. Schenk and J. S. Fritz, *Anal. Chem.*, 32 (1960) 987.

Analytica Chimica Acta, 65 (1973) 240–244

SHORT COMMUNICATION

Electrochemical study of a heterogeneous copper(II)-selective electrode; study of selectivity and potential stability

J. PICK, K. TÓTH and E. PUNGOR
Institute for General and Analytical Chemistry, Technical University, Budapest (Hungary)
(Received 6th November 1972)

The selectivity of ion-selective membrane electrodes, their life time and the stability of the electrode potential are important factors in the use of these electrodes. No detailed investigations dealing with the life time of membrane electrodes, *i.e.* the changes in the membrane potential values during pretreatment and application of the electrodes, have yet been reported in literature.

The selectivity constant is a function of the reciprocal of the equilibrium constant of the exchange reaction taking place on the membrane surface. It provides a measure of the amount of interfering ions in the presence of which the primary ion can still be measured with sufficient accuracy. Pungor *et al.* have studied the selectivity problems of precipitate-based membrane electrodes. They suggested a function describing the electrode potential value when the solution to be measured contains ions other than the primary ions[1–3].

Experimental

Reagents. All chemicals used in the measurements were of *pro analysi* grade (Reanal, Budapest). The stock solutions were prepared by weighing and standardized by appropriate classical analytical methods.

Apparatus. An expanded-scale precision pH-meter (Model OP 205, Radelkis, Budapest) and a TTT1c Radiometer automatic titrator were used for the measurements. A saturated calomel electrode (Model OP 810, Radelkis, Budapest) was used as reference electrode. As indicator electrode the silicone-rubber membrane copper(II)-selective electrode[4] was used.

Results and discussion

Life time. In studies of the copper(II)-selective membrane electrode, the electrode function was investigated for three conditions: (*a*) in the first period of pretreatment in a reducing medium (Fig. 1); (*b*) in prolonged use (Fig. 2); and (*c*) on soaking the electrode in 1 *M* copper(II) sulphate (Fig. 3).

As can be seen from Fig. 1, the electrode responds to copper(II) even without pretreatment. However, stable and reproducible potentials were achieved only by pretreating the electrodes in a reducing medium, *e.g.* in 10^{-2} *M* ascorbic acid solution. For the formation of an equilibrium ratio of copper(I):copper(II) on the

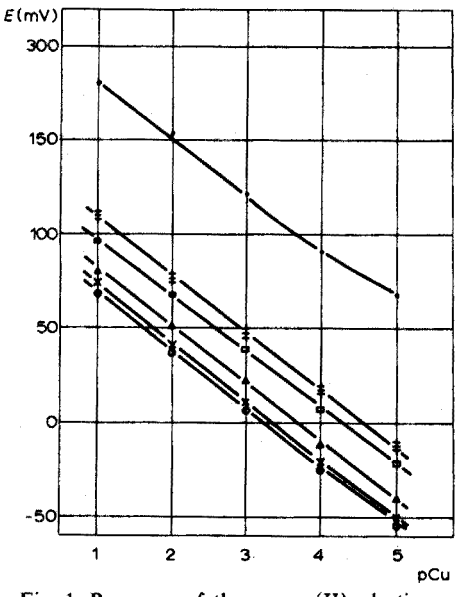

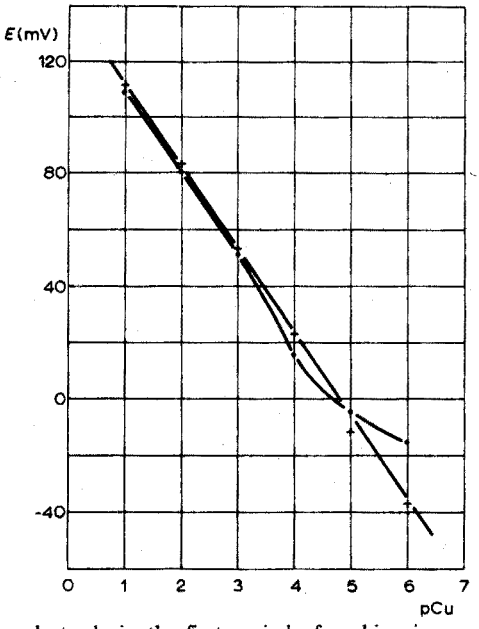

Fig. 1. Response of the copper(II)-selective membrane electrode in the first period of soaking in a reducing medium. Time, t, of measurement: (●) 0, (≠) 72-n, (□) 48, (▲) 36, (×) 25, (○) 1.5 h.

Fig. 2. Life-time investigations. t=(+) 1 day, (●) 3 months.

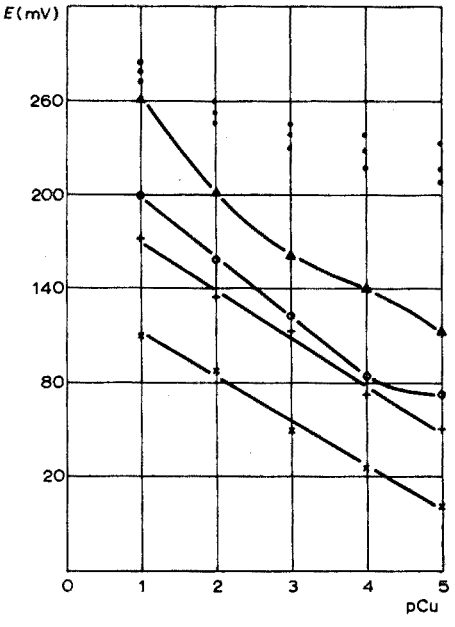

Fig. 3. Soaking in 1 M copper(II) sulphate solution. Time, t, of measurement: (×) 0, (+) 1, (○) 2, (▲) 3, (●) 30 days.

surface of the freshly prepared (or dry) electrode, 2–3 days were required. Curves of potential *vs.* pCu during the pretreatment are shown in Fig. 1.

The changes in the electrode function were then examined during frequent use. A significant decay in the electrode response occurred only after 3 months (Fig. 2).

Figure 3 shows the changes in the response to copper(II) of a freshly prepared electrode which was soaked between measurements in 1 *M* copper sulphate solution. In this case, the life time of the electrode was shorter, being only about three weeks (Fig. 3). This change was, however, reversible; when the electrode was placed into a reducing medium, *E vs.* pCu curves analogous to those in Fig. 1 were again recorded.

Selectivity. Two methods were applied. In the direct method, the electrode potential was determined in a series of solutions containing copper ions at a constant concentration (10^{-5} *M* Cu^{2+}) and interfering ions at varied concentrations (10^{-5} *M*–$8 \cdot 10^{-1}$ *M* Me^{2+}). The ionic strength was adjusted with potassium nitrate to a constant value in every series. The selectivity constant was calculated from the point of intersection obtained by the extrapolation of the two linear portions of the *E vs.* $pa_{Me^{2+}}$ curve.

In the indirect method, the solution containing copper(II) and interfering

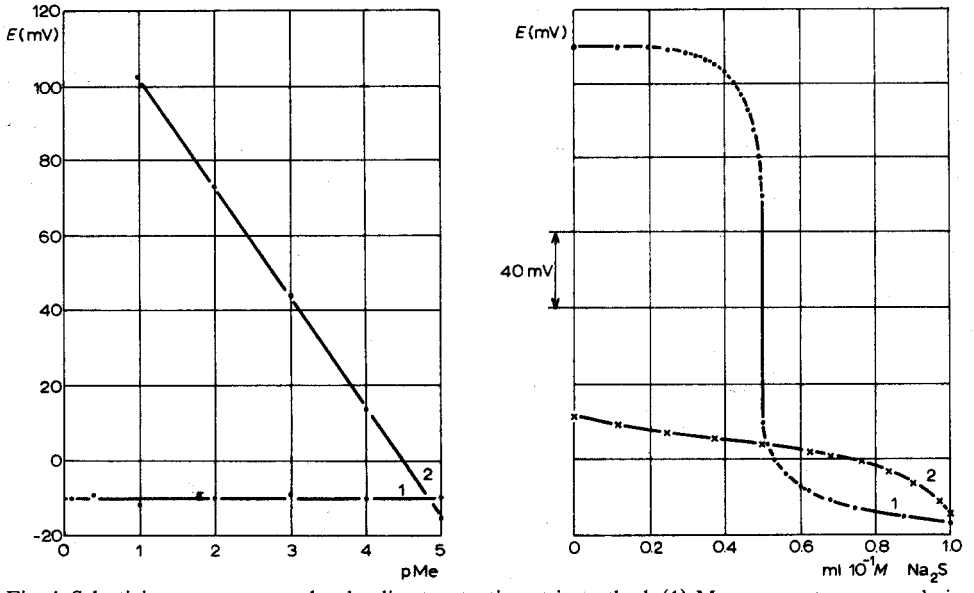

Fig. 4. Selectivity measurements by the direct potentiometric method. (1) Measurements were made in solutions containing 10^{-5} *M* Cu^{2+} and varying concentrations of cadmium(II). (2) Calibration curve for copper(II)

Fig. 5. Selectivity measurements by the indirect potentiometric method. Curve (1) was recorded for both the following solutions: (a) 5 ml 10^{-2} *M* Cu^{2+} + 5 ml 10^{-2} *M* Cd^{2+} + 1 ml 1 *N* H_2SO_4; (b) 5 ml 10^{-2} *M* Cu^{2+} + 5 ml dist. water + 1 ml 1 *N* H_2SO_4. Curve (2) was recorded for both the following solutions: (a) 5 ml dist. water + 5 ml 10^{-2} *M* Cd^{2+} + 1 ml 1 *N* H_2SO_4; (b) 10 ml dist. water + 1 ml 1 *N* H_2SO_4.

(Me^{2+}) ions in identical concentrations was titrated potentiometrically at pH 1 with an aqueous solution of sodium sulphide. The selectivity constant was calculated from the concentration data at the coprecipitation point.

The selectivity of the copper(II)-selective membrane electrode was studied in the presence of the following ions: Pb^{2+}, Cd^{2+}, Zn^{2+}, Co^{2+}, Ni^{2+} and Mn^{2+}. There was no detectable difference between the effects of these diverse ions. The results with cadmium(II) are given as an example (Figs. 4 and 5).

The results obtained in these experiments indicated that the electrode response does not depend on the presence of the other ions; the electrode behaved as if only copper(II) ions were present in the solution. In the direct measurements there was no interference in the investigated activity ratios.

By calculation from the potential jump in the potentiometric titration at the end-point, the change in the copper ion exponent was $\Delta pCu \approx 8.55$; accordingly, $pK_{CuMe} \geqslant 8.55$.

However, metal cations forming less soluble sulphide precipitates than copper sulphide, such as Ag^{+}, Hg^{2+} and Bi^{3+}, interfered with the electrode function. These ions interfered by transforming the membrane surface and so destroying the reversibility of the electrode. Investigations were made as to whether the surface still responded to copper(II). Results are given for the example of mercury(II) ions. After pretreatment and calibration, the copper(II)-selective electrode was soaked in a 1 *M* mercury(II) sulphate solution: the response of the electrode to copper ions ceased after 24 h, and a quasi-stable potential was obtained in copper calibration solutions. However, the value of this quasi-stable potential became more and more positive as the electrode was soaked in 1 *M* mercury(II) sulphate solution for a longer period of time, and finally became quite stable in copper(II) solutions.

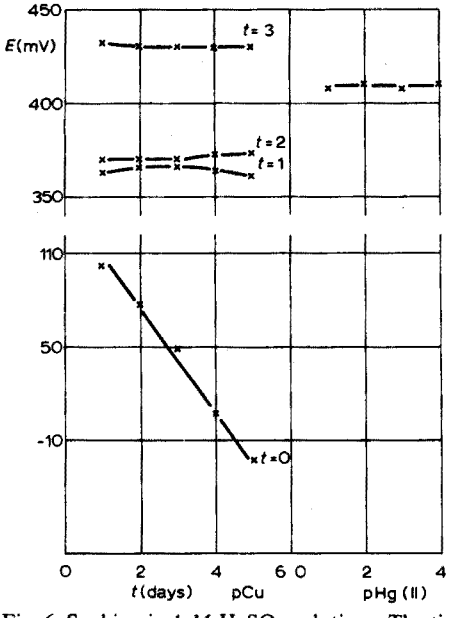

Fig. 6. Soaking in 1 *M* $HgSO_4$ solutions. The time of soaking, *t*, is given in days.

A series of measurements in mercury(II) solutions showed that the new transformed surface layer did not respond to mercury(II) ions (Fig. 6).

REFERENCES

1 E. Pungor, *Anal. Chem.*, 39 (1967) 28A.
2 E. Pungor and K. Tóth, *Anal. Chim. Acta*, 47 (1969) 291.
3 E. Schmidt and E. Pungor, *Magy. Kem. Foly.*, 77 (1971) 397.
4 J. Pick, K. Tóth and E. Pungor, *Anal. Chim. Acta*, 61 (1972) 169.

Analytica Chimica Acta, 65 (1973) 245–247

SHORT COMMUNICATION

Diagramme potential/pO^{2-} de l'uranium dans l'eutectique LiCl–KCl fondu

G. LANDRESSE* et G. DUYCKAERTS

Laboratoire de Chimie Analytique et Nucléaire, Université de Liège au Sart Tilman, B-4000 Liège (Belgique)

(Reçu le 11 décembre 1972)

Les diagrammes d'équilibre potentiel redox/pO^{2-} (où $pO^{2-} = -\log[O^{2-}]$), préconisés par Trémillon[1] dans le cas où, en sels fondus, des solutés existent sous forme de complexes oxyde, présentent autant d'intérêt que les diagrammes potentiel/pH dans le cas des solutions aqueuses; en effet, ils donnent d'une part une vue d'ensemble sur les domaines de stabilité des différents états d'oxydation d'un élément dans un solvant donné et permettent d'autre part la prévision des réactions chimiques.

Dans le cas particulier de l'uranium dissous dans les chlorures fondus, Molina[2] et Ishino[3] ont publié un diagramme E/pO^{2-} sur lequel ne se trouve pas l'uranium(V). Les travaux d'Adams *et al.*[4,5] et les nôtres[6,7] ayant montré l'existence et la stabilité de UO_2(V) dans les chlorures fondus, il nous a semblé intéressant de revoir le diagramme E/pO^{2-} de l'uranium en tenant compte des différents états d'oxydation, 0, III, IV, V et VI dans l'eutectique LiCl–KCl à 450°.

Molina[2] donne les valeurs des produits de solubilité des oxydes UO_2 et UO_3. Pour une solution telle que: $[U^{3+}] = [U^{4+}] = [UO_2^+] = [UO_2^{2+}] = 10^{-2}$ M, on a

$$L_{UO_3} = [UO_2^{2+}][O^{2-}] = 10^{-4.6}$$
$$[O^{2-}] = (10^{-4.6}/10^{-2}) = 10^{-2.6}$$

La précipitation de UO_3 a lieu pour $pO^{2-} \leqslant 2.6$.

$$L_{UO_2} = [U^{4+}][O^{2-}]^2 = 10^{-9}$$
$$[O^{2-}] = (10^{-9}/10^{-2})^{\frac{1}{2}} = 10^{-3.5}$$

La précipitation de UO_2 a lieu pour $pO^{2-} \leqslant 3.5$.

Le potentiel normal du couple UO_2^{2+}/UO_2 a été déterminé par Hill *et al.*[8]. Sa valeur est égale à -0.584 V dans l'eutectique LiCl–KCl à 450°[9].

Dans le même solvant à la même température, la valeur du potentiel normal du couple UO_2^{2+}/UO_2^+ est égale à -0.41 V[10]. D'autre part, les potentials normaux de couples U^{4+}/U^{3+} et U^{3+}/U^+ valent[11,12] respectivement -1.521 et -2.557 V. Tous ces potentiels sont rapportés au système de référence $Cl_2/2Cl^-$ et les compositions sont en moles par litre. En appliquant la relation:

* Chargé de Recherches du Fonds National Belge de la Recherche Scientifique.

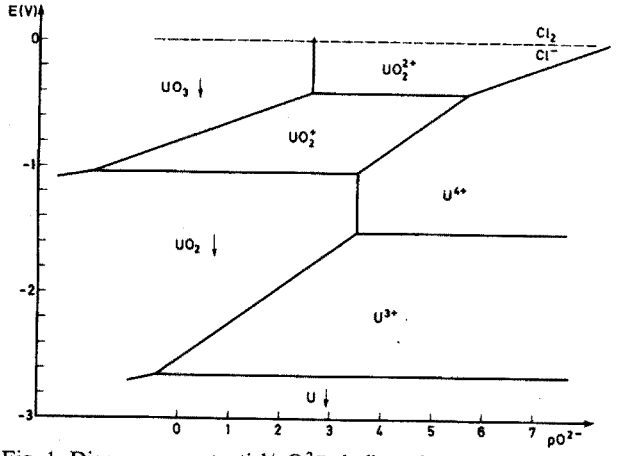

Fig. 1. Diagramme potentiel/pO^{2-} de l'uranium dans l'eutectique LiCl–KCl à 450°. $[U^{3+}]=[U^{4+}]=[UO_2^+]=[UO_2^{2+}]=10^{-2}$ *M*.

$$E^0_{UO_2^{2+}/UO_2} = (E^0_{UO_2^{2+}/UO_2^+} + E^0_{UO_2^+/UO_2})/2$$

on obtient la valeur du potentiel normal du couple UO_2^+/UO_2 soit -0.758 V.

Ces valeurs permettent de tracer le diagramme de la Figure 1.

La réaction de dismutation de UO_2(V) en présence de HCl

$$2UO_2^+ + n\ HCl \rightleftharpoons UO_2^{2+} + U^{4+} + 2\ W + n\ Cl^-$$

(*W* représentant OH^-, H_2O et H_3O^+ et *n* prenant respectivement les valeurs 2, 4 et 6) est prévisible à partir de ce diagramme. En effet, si on traite par HCl un bain de chlorures fondus contenant des ions oxydes, ceux-ci vont se transformer successivement selon les réactions

$$O^{2-} + HCl \rightleftharpoons OH^- + Cl^-$$

$$OH^- + HCl \rightleftharpoons H_2O + Cl^-$$

$$H_2O + HCl \rightleftharpoons H_3O^+ + Cl^-$$

ce qui revient à diminuer la concentration en O^{2-}, c'est-à-dire à augmenter pO^{2-}. Dans ces conditions, UO_2^+ doit se dismuter en UO_2^{2+} et U^{4+}. La réaction est réversible, car en éliminant HCl, on diminue le pO^{2-} du bain et on retombe dans le domaine de stabilité de UO_2^+. La réaction d'amphotérisation n'a pas lieu au départ de UO_2^{2+} et U^{4+} car le pO^{2-} du milieu est trop élevé; par contre, en présence d'eau, cette réaction se produit.

Si l'on veut préparer de l'UO_2 par réduction cathodique d'un bain d'uranyle dans LiCl–KCl, on peut constater, par le diagramme, qu'en partant d'un bain de UO_2^{2+} à haut pO^{2-}, la réduction en U^{4+} libère des ions oxydes qui diminuent progressivement pO^{2-} et rapidement cet U^{4+} disparaît par amphotérisation et se transforme en UO_2^+; lorsque pO^{2-} devient suffisamment faible, la réduction peut se faire directement suivant la voie $UO_2^{2+} \rightarrow UO_2^+ \rightarrow UO_2\downarrow$.

Enfin, on peut aussi comprendre, d'après ce diagramme, que UO_2^{2+} puisse être réduit partiellement par les chlorures du bain, surtout si l'on fait le vide qui élimine au fur et à mesure le chlore formé.

Nous remercions l'Institut Interuniversitaire des Sciences Nucléaires et le Fonds National de la Recherche Scientifique pour l'intérêt constant apporté à nos travaux et le soutien financier accordé à notre laboratoire.

BIBLIOGRAPHIE

1 B. Trémillon, *Rev. Chim. Miner.*, 3 (1966) 767.
2 R. Molina, *Bull. Soc. Chim. Fr.*, (1961) 1184.
3 T. Ishino, *J. Electrochem. Soc. Jap.*, 34 (1966) 133.
4 M. D. Adams, D. A. Wenz et R. K. Steunenberg, *J. Phys. Chem.*, 67 (1963) 1939.
5 D. A. Wenz, M. D. Adams et R. K. Steunenberg, *Inorg. Chem.*, 3 (1964) 989.
6 G. Landresse, *Anal. Chim. Acta*, 56 (1971) 29.
7 G. Landresse et G. Duyckaerts, *Anal. Chim. Acta*, 57 (1971) 214; 58 (1972) 369; 59 (1972) 101, 261.
8 D. L. Hill, J. Perano et R. A. Osteryoung, *J. Electrochem. Soc.*, 107 (1960) 698.
9 L. Martinot et G. Duyckaerts, *Bull. Soc. Chim. Belg.*, 78 (1969) 495.
10 L. Martinot, communication personelle, 1971.
11 F. Caligara, L. Martinot et G. Duyckaerts, *Bull. Soc. Chim. Belg.*, 77 (1968) 77.
12 F. Caligara, L. Martinot et G. Duyckaerts, *Bull. Soc. Chim. Belg.*, 76 (1967) 211.

Analytica Chimica Acta, 65 (1973) 248

ANNOUNCEMENT

Prize Biochemical Analysis

A prize of DM 10.000,— is donated from Boehringer, Mannheim, and is awarded every two years at the conference "Biochemische Analytik" in Munich for outstanding work in the field of biochemical analysis.

The donation will take place during the 1974 conference between 23 and 26 April. One paper or several papers concerning one theme, either published or accepted for publication between 1st October 1971 and 30th September 1973 may be sent in triplicate before 15th November 1973 to Prof. Dr. Dr. Ivar Trautschold, Secretary of the Prize "Biochemical Analysis", Medizinische Hochschule Hannover, 3 Hannover-Kleefeld, Karl Wiechert Allee 9.

Analytica Chimica Acta, 65 (1973) 249–252

BOOK REVIEWS

Annual Reports on Analytical Atomic Spectroscopy, 1971, Vol. 1, Edited by D. P. Hubbard, Society for Analytical Chemistry, London, xi + 204 pp., price £5.00.

Atomic spectroscopy is the basis of one of the most interesting and rapidly expanding areas of analytical chemistry. It embraces atomic emission, absorption and fluorescence spectrophotometry in all their various guises. In step with the rapid development, the number of papers has increased greatly, until, in 1971, 1092 items were published. This first Annual Report lists all of these publications, and gives a comprehensive but readable account of their contents.

The book is essentially in three parts. The first (43 pp.) is a description of the advances in instrumentation, such as light sources, atomizing and/or excitation systems (flames, arcs and sparks, plasmas, furnaces, etc.), optics, detector systems, data processing, complete instruments, and ancillary equipment. The second (86 pp.) deals with methodology, beginning with sample preparations and method evaluation, and continuing with applications to various types of sample (metals, petroleum products, refractories, medical and environmental samples, minerals, agricultural samples and chemicals). Each of these last sections includes an extensive tabulation, listed by element, of essential details of the published methods. The third part (74 pp.) contains a useful list of new books (9) and review articles (27) relevant to analytical atomic spectroscopy and a complete list of 1971 papers as well as an author index.

This volume is a model example for an annual report of this type. It has been produced quickly, but the text shows no evidence of haste. It is well written, accurately produced, and, as is often unusual in a book of this type, eminently readable. Anyone concerned with analytical atomic spectroscopy and related topics will find it an essential reference work to have close at hand.

A. Townshend (Birmingham)

Environmental Mercury Contamination, Edited by R. Hartung and B. D. Dinman, Ann Arbor Science Publishers Inc., Ann Arbor, 1972, Distributed by J. Wiley and Sons, ix + 349 pp., price £9.40.

This book consists of papers presented to an international conference on environmental mercury contamination held at Ann Arbor, Michigan in October 1970. The volume is divided into four sections: the occurrence of mercury in the environment; methods of analysis; environmental dynamics of mercury; and biological effects of mercury compounds.

Apart from a short paper on the levels of mercury in fish in Minimata Bay and a review paper on the sources and uses of mercury, the major portion of

Section I is devoted to the results of the analysis of fish, sediments, wild life, plankton etc. in the rivers and waters of the Great Lakes area. The greater part of Section II is taken up by a review paper dealing with the analysis of mercury and its compounds (7 pages of text and 32 pages of references). The remaining seven short papers report some analyses made of fish, birds and biological tissue by gas chromatography, neutron activation analysis and flameless atomic absorption techniques.

Section III has a good paper on the assessment of factors regulating the movement of mercury through aquatic food chains, and reports some laboratory and field studies made on the distribution of mercury in soils. Section IV, by far the biggest, covers such topics as dose–response relationship, biotransformation of organomercurials, subclinical effects of mercury intoxication and biological reactions and pathological changes in humans exposed to organomercurials (an account of the Minimata incident).

Considering the quality of the paper, printing and layout the book is an expensive purchase at £9 per copy. The book may be useful to the chemist who wishes to get a broad background to the subject of mercury and the environment, but will be of little use to the active workers in the fields covered by the above sections.

G. Topping (Aberdeen)

Organometallic Compounds. Methods of Synthesis, Physical Constants and Chemical Reactions, Vol. 3, First Supplement, Edited by M. Dub, Springer-Verlag, Berlin, 2nd Ed., 1972, xxi+613 pp., price Clothbound DM 78,20; US $24.80.

This volume covers methods of synthesis, physical constants and chemical reactions of the compounds of arsenic, antimony and bismuth, which have been published during the period 1965–1968. It bears ample testimony to the increasing importance of organometallic chemistry. The output of chemical literature has increased to such an extent that this four-year supplement includes almost three-quarters as many references as the main volume contained for the period 1937–1964. The coverage is thorough and includes numerous patents and articles from Soviet journals obtained from the U.S.S.R. National Public Library for Science and Technology. This supplement is arranged in the same manner as the main volume, with identical classification numbers. In addition to method of synthesis, etc., as mentioned above, biological properties and uses have been included. Pharmacological activities and medicinal uses have not, however, been covered. The format of the book is good and the production is of the usual high standard. Whilst it will be useful to have this book (and other supplements) available for reference, it has to be remembered that the latest reference is 4 years old. With an ever-increasing volume of literature in this field, steps will have to be taken to see that the next supplement is not even further behind.

E. J. Forbes (Birmingham)

Pharmaceutical Applications of Thin-layer and Paper Chromatography, Edited by Karel Macek, Elsevier Publishing Company, Amsterdam, 1972, xvi+743 pp., price DFl 250.00 ($78.25).

The first nine chapters are concerned with general methodology. The remainder of the book is concerned with applications, the drugs being classified according to their pharmacodynamic properties rather than their chemical constitution, although some sub-chapters are classified in this way, *e.g.*, those concerned with phenothiazines, barbiturates and sulphonamides.

Macek (Chapter 2) gives an excellent introduction to the techniques of t.l.c. and paper chromatography (p.c.), and the beginner will find here all he needs to know to make good practical progress. The more experienced worker will find many useful references, and possibly some new ways of applying these techniques.

Hais (Chapter 3) is concerned with radioactive compounds and illustrates well the use of t.l.c. and p.c. in biochemistry and pharmacology to identify the actual compounds in which radioisotopes end up in living systems. Janák (Chapter 4) also shows the potentialities of combining flat-bed chromatographic techniques with other techniques, in this case with column chromatography and gas chromatography. Székely (Chapter 5) is concerned with the use of i.r. spectroscopy and mass spectrometry after a chromatographic separation.

The general use of t.l.c. and p.c. for the identification of organic compounds is discussed critically by Macek (Chapter 6). The approach to the problem is discussed in detail and is illustrated by a scheme of analysis to distinguish between 161 nitrogen-containing drugs. Smaller chapters by Macek (Chapters 7–9) deal with documentation of chromatograms, laboratories for t.l.c. and p.c., and the tasks of t.l.c. and p.c.

The application of t.l.c. and p.c. to synthetic drugs, which has received scant attention in other texts, is covered extensively by Macek (Chapter 10). Steroids are covered separately by Lisboa (Chapter 11), and the remaining special chapters deal with cardiac glycosides and their genins (Nover), saponins (Hiller and Woitke), peptide and protein hormones (Rábek), alkaloids (Macek), vitamins (Katsui), antibiotics (Betina), plant extracts (Luckner), and auxiliary compounds such as antioxidants, colouring matters, preservatives, excipients and artificial sweeteners (Davídek). This, the major part of the book, is excellently set out, tabulated and referenced, so that information of practical use can be found readily and the original papers consulted where necessary to obtain further information.

This is an excellent book. The layout, conciseness and style make it enjoyable to read and use. Laboratories concerned with the t.l.c. and p.c. of pharmaceuticals will benefit from having a copy readily available.

A. G. Fogg (Loughborough)

PUBLICATIONS RECEIVED

NATIONAL BUREAU OF STANDARDS PUBLICATIONS

J. Paul Cali, J. Mandel, L. Moore and D. S. Young, *Standard Reference Materials: A Referee Method for the Determination of Calcium in Serum*, NBS Spec. Publ. 260-36, May 1972, 136 pp., price $ 1.25.

C. H. Page and P. Vigoureux, *The International System of Units (SI)*, NBS Spec. Publ. 330, 1972 Ed., April 1972, 45 pp., price 30 cent.

H. L. Wagner, *Standard Reference Materials: Comparison of Original and Supplemental SRM 705, Narrow Molecular Weight Distribution Polystyrene*, NBS Spec. Publ. 260-33, May 1972, 30 pp., price 35 cent.

A. F. Clark, V. A. Deason, J. G. Hust and R. L. Powell, *Standard Reference Materials: The Eddy Current Decay Method for Resistivity Characterization of High-Purity Metals*, NBS Spec. Publ. 260-39, May 1972, 53 pp., price 55 cent.

American National Standard: Radiation Safety for X-ray Diffraction and Fluorescence Analysis Equipment, American National Standards Institute Subcommittee N43-1, NBS Handbook 111, June 1972, 20 pp., price 30 cent.

J. C. Richmond and J. J. Hsia, *Standard Reference Materials: Preparation and Calibration of Standards of Spectral Specular Reflectance*, NBS Spec. Publ. 260-38, May 1972, 57 pp., price 60 cent.

K. D. Mielenz and K. L. Eckerle, *Design, Construction and Testing of a New High-Accuracy Spectrophotometer*, NBS Tech. Note 729, June 1972, 60 pp., price 60 cent.

The above publications can be ordered from the Superintendent of Documents, U.S. Government Printing Office, Washington, D.C. 20402. Orders from outside the U.S.A. should include an added 25% of price to cover mailing costs.

A new indispensable work of reference in Inorganic Chemistry

COMPREHENSIVE INORGANIC CHEMISTRY

6000 pages (approx) 245mm(9⅝")x168mm(6⅝")

- The most modern and authoritative standard reference work and literature guide to Inorganic Chemistry

Compiled under the editorial control of

J C Bailar *Jr* **H J Emeléus** *FRS*
† Sir Ronald Nyholm *FRS* **A F Trotman-Dickenson**

- Written by 71 of the world's most eminent research workers, industrial practitioners and teachers in chemistry.
- Easy retrieval – each volume has an individual subject index and the fifth volume contains a master index to the entire work.

ıtributors:—

/ Abel *PhD, DSc, FRIC*
Adams *MA, DPhil*
hrland *PhD*
Aylett *MA, PhD*
V Bagnall *DSc, FRIC*
Banister *PhD*
artlett *DSc*
Beumel *Jr PhD*
M Bevan *PhD*
Bradley *PhD, DSc*
rown *PhD, DSc*
H Clark *PhD, DSc, FRIC*
Cockett *BSc*
Connor *PhD*
avis *BSc, PhD*
f Dell *BSc, PhD*
A Dove *MA, PhD*
Downs, *MA, PhD*
S H Eberle *PhD*
E A V Ebsworth *DSc, FRIC*
D A Everest *PhD, FRIC, AMINN*
R D Goodenough *BSc*
J C Green *PhD*
M L H Green *BSc, PhD*
N N Greenwood *PhD, ScD, FRIC*
W P Griffith *PhD, DSc*
P Hagenmuller *DSc*
W A Hart *PhD*
A K Holliday *DSc, FRIC*
G Hughes *BSc, PhD*
B F G Johnson *BSc, PhD*
K Jones *PhD*
C Keller *PhD*
R D W Kemmitt *PhD*
D L Kepert *PhD*
J A Lee *BSc, PhD*
J O Liljenzin tekn *Dr*
S E Livingstone *DSc, FSTC*
K M MacKay *PhD*
P G Mardon *MA*
J A C Marples *MA*
A G Massey *DSc*
G W C Milner *DSc, FRIC, AInstP*
T Moeller *PhD*
D Nicholls *PhD, ARIC*
T A O'Donnell *PhD, DSc*
R D Peacock *PhD, DSc*
G Phillips *ARIC*
P E Potter *BSc, PhD*
P Powell *MA, DPhil, FRCO*
J E Prue *MA, DPhil*
E G Rochow *PhD*
C L Rollinson *BSc, PhD*
J Rydberg *DSc*
M Schmidt *PhD*
B L Shaw *BSc, PhD*
W Siebert *BSc, PhD*
F O Sladky *PhD*
K C Smith *BSc, FRIC*
J D Smith *MA, PhD*
V A Stenger *DSc*
N R Thompson *BSc, PhD*
P Thornton *BSc, PhD*
A D F Toy *PhD*
N I Tucker *BSc, PhD*
J J Turner *MA, PhD, FRIC*
R C Vickery *DSc*
K Vrieze *PhD*
K Wade *PhD, DSc*
S M Walker *BSc, PhD*
T P Whaley *PhD*

blication Price £165.00/$388.50.

ease write to address most convenient for a full colour enty page descriptive brochure.

blished by **Pergamon Press Ltd, Headington Hill Hall, ford OX3 0BW**
ıtributed in the Western hemisphere by Compendium blishers, Maxwell House, Fairview Park, Elmsford NY 523, USA

See overleaf for summary of Contents

Special Issue of the

Journal of Radioanalytical Chemistry:
CHEMICAL ANALYSIS BY CHARGED PARTICLE BOMBARDMENT

Contents:

Postcard

Elsevier Sequoia SA

P.O. Box 851

CH-1001 Lausanne

Switzerland

(Continued from page 4 of cover)

CONTENTS

(continued on inside page of cover)